Université du Québec
Institut National de la Recherche Scientifique
Centre Énergie Matériaux Télécommunications

Capacity and Performance Analysis of Advanced Relay-Assisted Communication Systems

Par
Imène Trigui

Thèse présentée pour l'obtention
du grade de philosophiae doctor (Ph.D.)

Président du jury	Charles Despins Prompt-Québec
Examinateur	Wessam Ajib UQAM
Examinateur	Salama Ikki Université Lakehead
Directeur de recherche	Sofiène Affes INRS-EMT
Codirecteur de recherche	Alex Stéphenne Ericsson Canada

Remerciements

Je tiens, tout d'abord, à remercier mon directeur de recherche Dr. Sofiène Affes d'avoir supervisé cette thèse. Je lui dois ma profonde reconnaissance pour son soutien continu et ses précieux conseils qui m'ont permis de réaliser une recherche de qualité dans le domaine des télécommunications.

Mes vifs remerciements vont également à mon co-directeur Dr. Alex Stéphenne, pour sa disponibilité et son soutient infaillible tout au long de mes études.

Je remercie aussi Dr. Charles Despins qui m'a fait l'honneur de présider le jury, ainsi que Dr. Wessam Ajib et Dr. Salama Ikki qui ont accepté d'évaluer ce travail.

Je ne voudrais pas oublier de remercier le conseil de recherches en sciences naturelles et en génie (CRSNG) d'avoir financé cette thèse. Ceci m'a permis de me concentrer er de m'épanouir dans mes études et ma recherche.

J'aimerais également exprimer ma gratitude à toute l'équipe du "Wireless Lab" pour l'ambiance chaleureuse qui règne dans notre groupe et pour tous les débats passionnés et discussions instructives qu'on a eus au cours de ces années.

Je souhaite aussi remercier mes chers parents pour leurs amour et encouragement qui m'ont permis d'aller de l'avant dans les moments les plus difficiles.

Enfin, un très grand merci à mon très cher époux et collègue Slim Zaidi pour son soutien, sa patience et sa présence réconfortante à mes cotés tout au long de mes études. Un très grand merci aussi à mon rayon de soleil Yassin qui n'a cessé d'illuminer notre vie depuis sa naissance.

Table des matières

Liste des figures

Résumé

Afin de faire face à l'explosion du volume de trafic des données prévue dans les années à venir, les futurs systèmes de communication 5G devront être capables de délivrer des débits extrêmement élevés et sans précédent. Puisque les technologies actuelles ne sont pas en mesure de supporter de tel débits, des changements radicaux dans le paradigme des communications sans fil doivent être envisagés. Plusieurs nouvelles technologies capables d'assurer de tels performances ont heureusement émergé, au cours de la dernière décennie, et sont présentement considérées comme candidates pour les futurs standards. Parmi ces technologies, on trouve les communications coopératives, telles que le relayage, la formation de voie collaborative, etc., les systèmes MIMO, incluant ceux appelés massifs (i.e., à très grands nombres d'antennes) et ceux à multi-utilisateurs et la radio cognitive (RC).

Il est cependant claire qu'afin d'assurer une interaction harmonieuse et une coexistante durable entre ces nouvelles technologies dans les réseaux sans fil du futur, on doit bien comprendre leurs propriétés et assimiler leurs comportments. Ceci passe forcément par une analyse rigoureuse et une étude approfondie des performances de ces systèmes dans des environnements réels. Dans cette thèse, les performances d'une multitude de systèmes de communication combinant ces nouvelles technologies sont étudiées dans des conditions réelles.

D'abord, on étudie les performances d'un système avec relayage à sauts multiples, où les données transmises par une source passent par plusieurs relais avant d'atteindre leurs destination, en presence d'un évanouissement Nakagami-m. Une méthode unifiée pour le calcul du taux d'erreur a permis d'établir une connexion, jusqu'ici inconnue, entre la probabilité d'erreur relative à différentes modulations et la fonction Lauricella. Les effets des interférences co-canal et du bruit sur ces systèmes sont ensuite examinés en considérant un nombre arbitaire de sauts et d'interférents. Grâce à de nouvelles transformations d'intégrale, le principe de découplge obtenu a permis l'évaluation des performances du plusieurs scénarios et environnements de propagation

en termes de capacité érgodique.

Enfin, des systèmes MIMO avec relayage à double sauts sont considérés. Une nouvelle transformation novatrice d'intégrale, appelée la transformation de la fonction génératrice de moment complémentaire (FGMC), est proposée comme un outil universel de calcul de la capacité érgodique de ces systèmes en présence non seulement des interférences co-canal mais aussi du bruit. En plus, un scénario mettant en évidence l'interaction de la technologie RC avec ce genre de système est étudié en détails. La capacité érgodique et le taux d'erreur dans ce contexte RC sont analysés grâce à différentes expressions analytiques de leurs valeurs exactes et asymptotiques. Par ailleurs, la transformation FGMC proposée s'est avérée être aussi efficace pour des systèmes beaucoup plus complexes. En effet, elle a permis le calcul et l'analyse de la capacité érgodique des systèmes MIMO multi-utilisateurs avec relayage employant un ordonnancement opportuniste et opérant en présence d'évanouissement de Rayleigh et des interférences co-canal. L'analyse de ce système à large échelle concrétise des observations populaires, jusqu'ici intuitives ou obtenues empiriquement, à l'aide de formules analytiques élégantes et très perspicaces.

Introduction

La communication sans fil est entrain d'atteindre, de nos jours, une véritable apogée fulgurante non seulement en termes d'avancées technologiques, mais aussi d'accessibilité à une portion de plus en plus large de la population. En effet, ce domaine, qui connaît une évolution des plus frénétiques, ne cesse d'envahir notre quotidien et de changer notre manière de vivre, travailler et même d'interagir. De plus en plus de technologies sont promues chaque jour par les opérateurs et industriels visant à fournir à des usagers extrêmement exigeants, de nouveaux services et médias avec une qualité et fiabilité irréprochables.

Les systèmes de communication sans fil les plus répondus sont incontestablement les systèmes de communication mobiles dont la première génération (1G) a été déployée en 1980. Exploitant pour la première fois la structure cellulaire de la couverture, ces systèmes ont permis l'amélioration de la capacité du réseau ainsi que le support de la mobilité. La deuxième génération (2G), appelée "Global System for Mobile Communication-GSM", n'a été déployée qu'en 1990. Ces systèmes ont effectué les tout premiers pas dans la transmission de données ouvrant ainsi la porte à une nouvelle aire de communication sans fil où de nouveaux services, tel que la navigation web, le téléchargement, le "streaming" des vidéos et les services bancaires en ligne, ont fait leurs apparition.

Cependant, l'utilisation de ces services a augmenté significativement le trafic des donnés dans les réseaux (2G) qui n'étaient plus en mesure, à l'époque, de satisfaire toutes les exigences des usagers. Offrant un débit allant jusqu'à 2 Mbps grâce à la technique d'accès multiple par répartition en codes à large bande, "wideband code division multiple access-CDMA", les systèmes de troisième générations (3G) sont apparus pour répondre à la forte demande de trafic des données. Cette demande n'a pas cessé d'augmenter depuis et a même forcé la migration vers les systèmes de quatrième génération (4G), communément connus sous le nom de "Long-Term Evolution-LTE Advanced". Ce standard, qui a été défini par un groupe d'associations de

télécommunications appelé 3GPPP, a exploité les techniques les plus avancées, tel que la transmission multi-antennes, la transmission et réception coordonnées à travers des points multiples, le relayage, etc., afin d'atteindre des débits avoisinant le 1 Gbps. L'avancée impressionnante réalisée par les systèmes 4G ne sera cependant pas suffisante pour faire face à l'explosion du volume de trafic des données prévue dans les années à venir. Ce déluge de données sans précédent sera, en fait, causé par la forte croissance du nombre d'appareils connectés sur le réseaux (téléphones intelligents, tablettes, etc.), d'une part, et le partage des vidéos à très haute définition via surtout les médias sociaux tel que YouTube et Facebook, d'autre part. Les prévisions suggèrent qu'en 2020 le trafic par consommateur augmentera jusqu'à 20 fois le trafic actuel. Visant à satisfaire cette exigence, des études sur les systèmes de cinquième génération (5G) futurs ont été récemment entamées par des industriels et groupes de recherche. Elles ont démontré que ces systèmes devront non seulement incorporer les différentes technologies d'accès radio (WIFI, 3G, LTE/LTE-A, 5G) mais aussi, exploiter la bande de fréquences millimétriques jusqu'ici inutilisée.

Paralèllement, les réseaux locaux sans fil, developpés pour des communications à courte portée, n'ont cessé eux aussi de prendre de l'ampleur. Ces réseaux sont, en fait, destinés à des communications à haut débit entre des usagers stationnaires ou des piétons dans des petites zones géographiques, notamment des résidences, des bureaux, un compus universitaire ou un aéroport. D'un autre côté, ces systèmes opèrent sur des bandes de fréquences non octroyées et, par conséquent, une contrainte sur leurs puissances de transmission est souvent imposée, afin de minimiser l'interférence entre des réseaux co-existants sur la même bande. La famille de protocoles IEEE 802.11 régit ce type de réseaux qui offrent des débits atteignant les 54 Mbps.

Motivations

Néanmoins, obtenir des hauts débits sur des canaux sans fil tout en maintenant un taux d'erreur acceptable n'est pas toujours évident. En effet, contrairement aux communications filaires, les communications sans fil font face à des défis majeurs qui rendent laborieuses toute transmission fiable et rapide. Parmi ces défis, on trouve les interférences et l'évanouissement du canal ("fading") qui peuvent sévèrement atténuer le signal transmis dégradant ainsi la qualité de la transmission. Un autre défi d'importance égale à ces derniers est la gestion efficace des ressources (puissance, spectre, etc.) qui permet un partage équitable entre plusieurs usagers.

Il a été démontré que l'évanouissement du canal peut être surmontée par l'implementation de techniques de diversité visant à fournir à la destination plusieurs copies du même message passant par des canaux statistiquement indépendants. Ce gain de diversité peut être obtenu en utilisant la transmission à entrées et sorties multiples ("multiple-input multiple-output") MIMO. En exploitant les antennes implémentées à la source et à la destination, les systèmes MIMO sont capables d'augmenter le débit et la fiabilité de la communication sans avoir recours à du spectre et/ou de la puissance additionnels ; des resources très coûteuses dans le contexte des communications sans fil. À cause de la petite taille des récents dispositifs sans fil, l'implementation de plusieurs antennes s'avère malheureusement impossible. Dans un tel cas, le concept de communications cooperatives pourrait être envisagé afin de surmonter le problème de l'évanouissement du canal. Ce concept consiste en la transmission du même message à partir de différents dispositifs munis d'une seule et unique antenne créant ainsi une sorte de transmission MIMO virtuelle qui fournit un gain de diversité. En plus, la communication cooperative présente un autre avantage qui est l'extension de la couverture. En effet, lorsque la communication directe entre une source et une destination est impossible à cause de la grande distance qui les sépare, les messages pourront être délivrés via d'autres terminaux partenaires en modes multi-sauts.

Généralement appelé relayage, ce type de communication cooperative a été introduit par van der Meulen en 1968. Ses performances ont été étudiées par Cover et El Gamal qui ont développé plusieurs stratégies de relayage. Les systèmes de communication avec relayage ont suscité depuis l'intérêt de la communauté scientifique et plusieurs autres stratégies de relayage ont été proposées dans la littérature. Ces stratégies peuvent être classées comme suit : non-dégénérative et dégénérative. Parmi les stratégies non-dégénératives, on trouve l'amplification-puis-transmission (AT) qui consiste en l'amplification du signal reçu au niveau du relais qui transmet ensuite le signal résultant vers la destination. Cette stratégie a été introduite et étudiée dans le contexte des communications cooperatives par Lanemann. D'un autre côté, la stratégie non-dégénérative la plus utilisée est le décodage-puis-transmission (DT) qui a été suggérée originalement par El Gamal. En utilisant DT, le relai décode le signal reçu afin de reconstituer le message original puis, ré-encode ce dernier avant de le transmettre à la destination. Une autre stratégie non-dégénérative existe dans la littérature, mais elle y est beaucoup moins adoptée ; c'est la compression-puis-transmission (CT). Avec cette stratégie, une quantification du signal reçue est réalisée au niveau du relai qui encode les échantillons obtenus puis transmet le message résultant

à la destination.

Cependant, il est claire qu'on ne pourra malheureusement pas profiter pleinement des avantages de ces technologies émergentes de MIMO et de relayage sans une utilisation optimale ou du moins efficace du spectre disponible. Le problème majeur avec cette resource est que toute la bande de fréquence est exclusivement allouée à des services spécifiques destinés à des usagers particuliers, appelés usagers primaires (UP)s. De plus, aucune utilisation d'autres usagers non-autorisés, appelés usagers secondaires (US)s, n'est permise. Une récente étude de la commission fédérale des communications ("*Federal Communications Commission-FCC*") a d'ailleurs démontré que le spectre actuel est largement sous-utilisé dans les dimensions temporelle et géographique. Par exemple, des mesures prises dans les villes de New York et de Washington ont révélé que les maximums d'occupation du spectre y sont seulement de 13.1% et 35%, respectivement. Visant à améliorer la gestion du spectre disponible afin d'assurer son utilisation optimale, la radio cognitive (RC), introduite par Mitola en 1999, permet aux USs de partager la même bande de fréquence exploitée par les UPs sans pour autant diminuer la qualité de service perçue par ces derniers.

Une compréhension des propriétés et du comportement de toutes ces nouvelles technologies est cependant indispensable pour assurer une conception optimale des futures systèmes de communication sans fil. Cette thèse fournit, à ce titre, une analyse rigoureuse et une étude approfondie des performances des systèmes de communication combinant ces technologies et opérant dans des conditions réelles.

Structure de la Thèse et Contributions

Le reste de cette thèse est organisé comme suit. Au Chapitre 2, quelques notions fondamentales des communications sans fil sont introduites. Au Chapitre 3, les performances des systèmes de communication à sauts multiples sont analysées. Les Chapitres 4 et 5 sont consacrés à l'étude des effets des interférences co-canal et du bruit sur ces systèmes. Au Chapitre 6, l'étude des systèmes avec relayage est réalisée dans un contexte RC. Le Chapitre 7 examine les performances d'un système MIMO avec relayage à double sauts en présence d'interférence co-canal et le Chapitre 8 analyse les effets du contexte multi-usagers avec un ordonnancement opportuniste sur ces systèmes.

En particulier, le Chapitre 3 considère des systèmes de communication à sauts multiples. De tels systèmes permettent, en fait, l'amélioration des performances des réseaux cellulaires ou ad hoc ainsi que l'extension de leurs couverture. On a proposé pour la première fois des nouvelles solutions pour la forme intégrale infinie impliquant le produit de fonctions de Bessel. Ces solutions ont été d'une grande utilité dans l'évaluation de la probabilité d'erreur de ces système en considérant un nombre arbitraire de relais à gains variables subissant un évanouissement Nakagami-m. Les formules obtenues ont permis d'établir une connexion, jusqu'ici inconnue, entre la probabilité d'erreur relative à de différentes modulations et la fonction Lauricella. Dans le cas spécial où m est un multiple impair de un et demi, des expressions plus simples de la probabilité d'erreur impliquant les fonctions hypergéométriques de Gauss ont été obtenues.

Malgré leur importance, les résultats obtenus dans la première contribution ne tiennent pas compte de l'existence des interférences co-canal. Causées principalement par la réutilisation intense des fréquences, les interférences co-canal affectent aussi la capacité des systèmes avec relayage et peuvent même entraîner une dégradation plus sévère de leurs performances. Aux Chapitres 4 et 5, des modèles flexibles sont proposés pour fournir une analyse traitable et suffisamment précise du débit moyen réalisé par les systèmes à sauts multiples en présence d'interférences co-canal. Les modèles obtenus se sont avérés suffisamment flexibles pour être exploités avec différentes distributions de l'évanouissement (incluant l'évanouissement composite) et techniques de diversité au niveau de chaque saut. Contrairement aux anciens résultats, nos expressions sont valides avec n'importe quel nombre d'interférants et n'importe quels paramètres d'évanouissement. Les expressions de la capacité érgodique exacte et de sa forme réduite dans le cas de haut SNR ont été présentés sous des formes élégantes et aisément interpretables.

Les résulats susmentionnés sont généralisés au Chapitre 6 dans le contexte RC. Dans ce chapitre, on fournit une expression analytique et précise des différentes mesures de performances du système dans un contexte RC avec approche "underlay".

Le Chapitre 7 examine l'impact des interférences co-canal sur la capacité des systèmes MIMO à double sauts subissant un évanouissement de Rayleigh. Le résultat principal consiste en une formule générique et flexible basée sur la MGF qui peut être facilement adaptée à des différents types d'évanouissement, techniques de diversité et configuration d'interférences.

Les systèmes considérés dans tous les travaux mentionnés ci-dessus sont à un seul et unique usager. Plusieurs études ont, cependant, démontré que les systèmes à plusieurs usagers peuvent

eux aussi bénéficier du relayage. Dans ce contexte, la conception et l'analyse des performances de systèmes MIMO multi-utilisateurs avec relayage employant un ordonnancement opportuniste et opérant en présence d'évanouissement de Rayleigh et des interférences co-canal sont effectuées au Chapitre 8.

Le Chapitre 9 expose toutes ces observations en guise de conclusion et présente des perspectives futures des travaux accomplis.

Chapitre 1

Quelques Notions Fondamentales

1.1   Systèmes de communication sans fil

Dans cette section, le système de communication sans fil est défini et les éléments qui le composent sont décrits. La fonction primaire d'un tel système est le transfert d'informations entre une source donnée et une destination à travers un canal sans fil. Pour assurer cette fonction, certaines étapes ou sous-fonctions sont généralement réalisés au niveau de l'émission et de la réception. La Figure 1.1 illustre le schéma en blocs d'un système de communication avec toutes ses sous-fonctions. D'après cette figure, avant sa transmission, le message passe en premier par un encodeur source. Durant cette étape, le message est converti en une séquence de bits et la redondance est éliminée. Après l'encodage source, le message est crypté afin de prévenir la lecture de son contenu par un tiers non autorisé rendant, ainsi, la communication plus sécurisée. Ensuite vient le codage canal qui vise à améliorer la fiabilité de la communication par l'introduction de la redondance dans le message. Cette redondance sert, en fait, à la detection et la correction d'éventuelles erreurs survenant lors de la propagation du message dans le canal sans fil. Enfin, la dernière étape c'est la modulation qui consiste à convertir les séquences de bits en un signal ("wavefront") adapté au canal de la transmission. Comme illustré dans la Figure 1.1, côté récepteur, le message passe par ce même processus mais inversé afin de récupérer sa version originale. Dans le reste de ce chapitre, on désigne par s le symbole modulé de puissance $P_s = \mathrm{E}\{|s|^2\}$ transmis par la source et par y le symbole reçu par le récepteur. La relation entre s et y peut être définie comme suit :

$$y = hs + n, \tag{1.1}$$
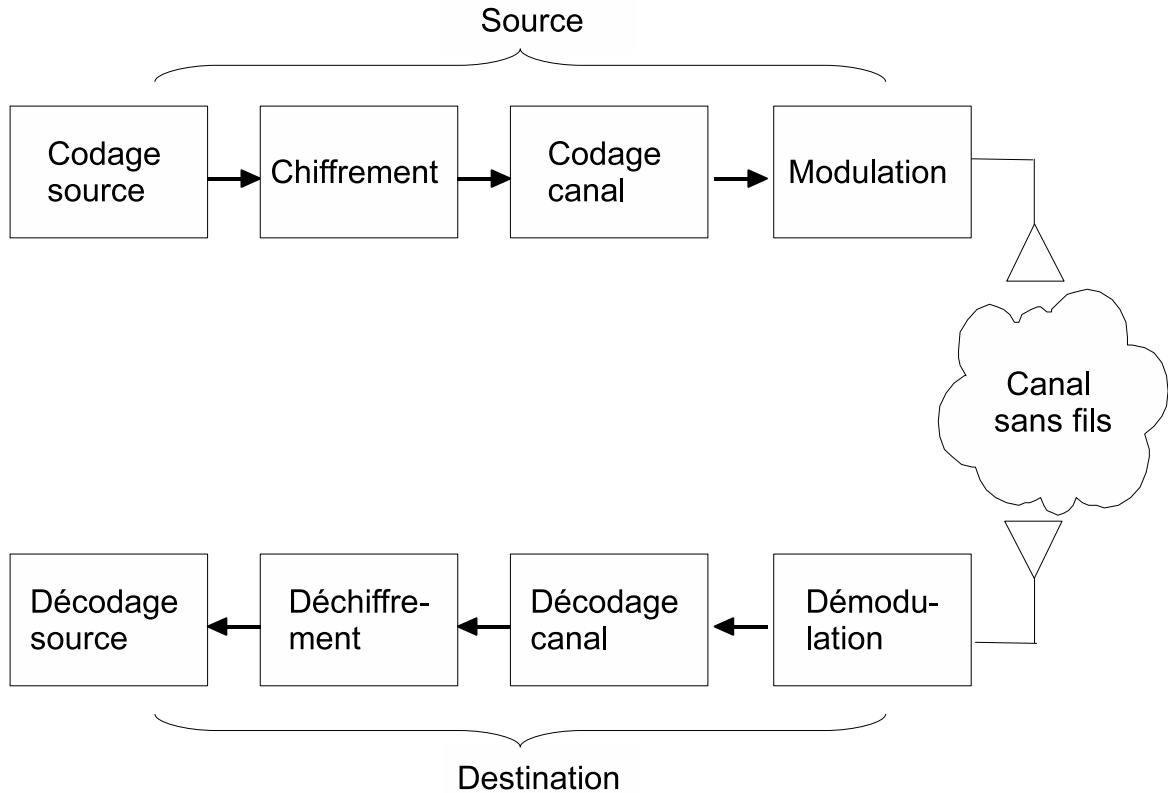
FIGURE 1.1 – Schéma en blocs d'un système de communication sans fil.

où n est un bruit blanc additive Gaussien (BBAG) généralement modélisé comme une variable aléatoire (VA) Gaussienne complexe, symétrique et circulaire de variance σ^2, c-à-d $n \overset{d}{=} \mathcal{CN}(0, \sigma^2)$, et h est un coefficient du canal sans fil qui sera amplement détaillé dans la partie suivante.

1.1.1 Le canal sans fil : caractéristiques et performance

Un canal sans fil est un canal caractérisé par la variation de l'attenuation d'un signal qui s'y propage. Communément appelé évanouissement (''*fading*''), ce phénomène peut varier non seulement au cours du temps mais aussi d'une fréquence à une autre ; ce qui rend sa modélisation mathématique rigoureuse très complexe si toutefois possible. Pour cette raison, le phénomène d'évanouissement est généralement caractérisé par ses propriétés statistiques afin de simplifier toute étude et analyse de performances des systèmes de communication sans fil. Notons que plusieurs modèles statistiques de l'évanouissement existent dans la littérature et que les plus connus et utilisés seront détaillés plus tard dans cette section. Ces modèles sont souvent catégorisés

suivant le type de l'évanouissement encouru pendant la propagation du signal qui peut être soit un évanouissement à grande échelle ("*large-scale fading*") soit à petite échelle ("*small-scale fading*"). Le premier est dû à

- *L'atténuation ("pathloss")* : c'est l'affaiblissement que subit l'onde radio en parcourant la distance entre la source et la destination. Ce phénomène est causé par la dispersion de la puissance de l'onde dans toutes les directions de sorte que seulement une partie de sa puissance est reçue à la destination.
- *Ombrage ("shadowing")* : il est causé par la présence entre la source et la destination d'obstacles relativement grands tels que des immeubles, des collines, etc.. Ces derniers occasionnent la détérioration de la qualité du signal même lorsque ces terminaux sont proches.

tandis que le second est dû aux

- Multi-trajets ("multipath") : Pendant sa propagation, l'onde peut subir des réflexions, diffractions et/ou diffusions et atteindre ainsi la destination à travers de multiples trajets. Chaque trajet est caractérisé par ses propres délai et phase et peut donc interférer sur les autres trajets.

Bien que plusieurs modèles statistiques de l'évanouissement existent dans la littérature, dans cette thèse on se limite aux modèles suivants :

Évanouissement de Rayleigh

L'évanouissement de Rayleigh est un des modèles les plus utilisés dans la littérature grâce à sa simplicité et sa précision, spécialement dans les environnements de multi-trajets où aucune ligne de mire ("*line-of-sight*") directe n'existe entre la source et la destination. L'amplitude d'un canal Rayleigh est distribuée selon la loi suivante :

$$p(r) = \frac{2r}{\Omega} \exp\left(-\frac{r^2}{\Omega}\right), \quad r \geq 0, \tag{1.2}$$

où $\Omega = \mathrm{E}\{r^2\}$.

Évanouissement Nakagami-m

L'évanouissement Nakagami-m est un modèle plus générale que l'évanouissement de Rayleigh. La distribution de l'amplitude d'un canal Nakagami est donnée comme suit

$$p(r) = \frac{2m^m r^{2m-1}}{\Omega^m \Gamma(m)} \exp\left(-\frac{mr^2}{\Omega}\right), \quad r \geq 0, \tag{1.3}$$

où $m \geq 1/2$ est le paramètre de l'évanouissement. On peut facilement observer que (1.3) se réduit à (1.2), quand $m = 1$. Le modèle de l'évanouissement de Rayleigh est ainsi un cas particulier de l'évanouissement Nakagami-m.

Évanouissement Nakagami-m / Ombrage Log-Normal

La loi composite Nakagami-m/log-normal fut introduite pour les environnements présentant des évanouissements de type Nakagami-m en présence d'ombrage log-normal. L'inconvénient de ce modèle est que la distribution qui en résulte est sous la forme d'une intégrale, ce qui rend énormément difficile tout étude de performances des systèmes de communication opérant sur ces canaux. Afin de palier à ce problème, nous nous intéressons dans cette thèse à un autre modèle de canal composite plus simple à étudier. L'amplitude de ce canal suit la distribution K donnée par

$$p(r) = \frac{2\left(\frac{\lambda m}{\Omega}\right)^{\frac{\beta+1}{2}}}{\Gamma(m)\Gamma(\lambda)} r^{\beta-1} K_\alpha\left(2\sqrt{\frac{\lambda m}{\Omega} r^2}\right), \quad r \geq 0, \tag{1.4}$$

où $\alpha = \lambda - m$ et $\beta = \lambda + m - 1$.

Les modèles susmentionnés serviront par la suite à l'étude de l'impact du phénomène de l'évanouissement sur les performances des systèmes de communication sans fil. Deux mesures de performances sont souvent adoptées dans la littérature dans le contexte des communications sans fil : la capacité de Shannon et le taux d'erreur symbole ("symbol error rate") (TES). Le premier mesure le débit maximal de communication fiable, sans erreur, qu'un canal est capable d'assurer, tandis que le second indique le pourcentage des symboles erronés pendant une période de transmission. Ce dernier est en fait obtenu en divisant le nombre de symboles mal décodés ou non décodés par le nombre total de symboles transmis. Le TES peut aussi être interprété différemment comme le taux de succès en symboles de la communication entre la source et la destination. Il est généralement donné par la somme de plusieurs termes impliquant la Fonction d'erreur complémentaire ou la Fonction-Q. Dans les prochains chapitres, on va montrer que les

effets du phénomène de l'évanouissement sur les performances des systèmes de communication sans fil peuvent être facilement décrits et mieux compris à l'aide de ces mesures de performances, dont les expressions seront mises sous des formes élégantes et aisément interpretables.

Par ailleurs, il a été observé que l'impact de l'évanouissement sur les performances de ces systèmes est étroitement lié à l'interrelation entre la durée du symbole (DS) transmis et le temps de cohérence (TC) du canal, pendant lequel ce dernier est considéré constant. Deux cas se présentent alors : TC est plus large que DS ou l'inverse. Dans le permier cas, on parle d'évanouissement lent ("slow fading") alors que dans le second, on parle d'évanouissement rapide ("fast fading").

1.1.2 Évanouissement lent

On parle d'évanouissement lent lorsque la puissance du canal varie beaucoup plus lentement que le débit des symboles. Cette situation n'est autre que le scénario statique, qui est largement adopté dans la littérature, où le canal h est supposé aléatoire mais constant pendant la durée de la transmission. Dans ce cas, si h est en plus connu au niveau du récepteur, les effets de l'évanouissement peuvent être facilement éliminés. Le seul caractère aléatoire restant dans le canal est donc le BBAG. La capacité de Shannon d'un canal BBAG est donnée par

$$C = \log_2(1 + \rho), \tag{1.5}$$

où $\rho = P_s/\sigma^2$ est le rapport signal-à-bruit (RSB). De son côté, le TES correspondant à un canal BBAG est généralement exprimé comme suit

$$T = a\mathrm{Q}\left(\sqrt{b\rho}\right), \tag{1.6}$$

où a et b sont des paramètres relatifs à la modulation et $Q(\cdot)$ est la Fonction-Q.

1.1.3 Évanouissement rapide

On parle d'évanouissement rapide lorsque la durée d'un symbole transmis est équivalente à un nombre N_c d'intervalles de cohérence. Quand N_c est grand, l'évanouissement devient érgodique. Par conséquent, la moyenne sur l'ensemble de réalisations de l'évanouissement est équivalente à la moyenne temporelle du canal. Cette caractéristique s'avère être d'une grande utilité puisqu'elle permet le calcul de la capacité moyenne, aussi connue sous le nom de capacité érgodique.

L'utilisation de cette dernière à la place de la capacité instantanée rend, en fait, plus perspicace l'étude des performances des systèmes de communications sans fil subissant un évanouissement rapide. Ceci est à cause de la rapidité de la variation au cours du temps des canaux faisant l'objet d'un tel évanouissement. La capacité érgodique de ces canaux peut être exprimée comme suit :

$$\bar{C} = \mathrm{E}_{|h|} \left\{ \log_2 \left(1 + \frac{P_s}{\sigma^2} |h|^2 \right) \right\}. \tag{1.7}$$

Notons que l'expression ci-dessus n'est valable que lorsque les entrées du canal sont Gaussiennes. Concernant le TES de ces canaux, il est aussi remplacé par sa valeur moyenne pour les raisons évoqués ci-dessus. Généralement, le TES moyen est donné sous la forme suivante :

$$\bar{T} = \mathrm{E}_{|h|} \left\{ a\mathrm{Q} \left(\sqrt{\frac{bP_s}{\sigma^2} |h|^2} \right) \right\}. \tag{1.8}$$

Notons que le calcul de $\bar{C}$ et de $\bar{T}$ requiert la connaissance de la fonction de densité de probabilité (fdp) du canal qui diffère d'un modèle d'évanouissement à un autre, tel que discuté plutôt dans cette section.

Après avoir présenté les systèmes de communication opérant sur des canaux sans fil et discuté les caractéristiques de ces derniers, on va montrer, dans les sections suivantes, comment on peut améliorer les performances de tels systèmes par l'intégration de nouvelles technologies telles que le relayage et la communication multi-antennes.

1.2   Systèmes de communication avec relayage

Comme illustré dans la Figure 1.2, les systèmes de communication avec relayage se composent d'au moins trois terminaux : une source, une destination et un relai dont le rôle est la retransmission vers la destination des messages reçus par la source. Un relai est généralement incapable de transmettre et émettre simultanément (c-à-d, durant le même intervalle de temps (IT) ou sur la même fréquence) à cause des interferences croisées (" *cross-interference*") entre les signaux transmis et reçus. Mieux connue sous le nom de contrainte demi-duplex, ce problème peut facilement être surmonté en adoptant un schéma de communication à deux ITs ou deux fréquences. Par exemple, durant le premier IT, la source diffuse son message qui est reçu à la fois par la destination et le relais. Ensuite, ce dernier transmet le message à la destination durant le
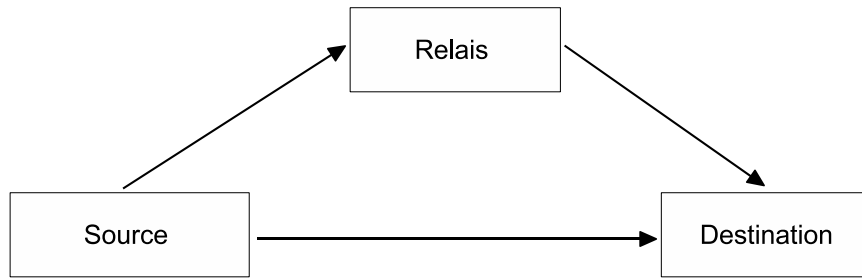
FIGURE 1.2 – Systèmes de communication avec relayage.

deuxième IT. À la fin des deux ITs, la destination aurait reçue deux copies du même message :
une directement de la source et l'autre via le relais et pourrait ainsi réaliser un gain de diversité.

Grâce à ses innombrables mérites, les systèmes de communication avec relayage ont sus-
cité récemment un grand intérêt chez la communauté scientifique [1]-[2]. En effet, ces systèmes
permettent d'améliorer :

– La fiabilité de la communication : ceci est surtout grâce à la diversité spatiale réalisée à la
destination. En effet, cette dernière reçoit deux copies du même message ayant parcouru
deux chemins statistiquement indépendants. Ainsi, la probabilité pour qu'on tombe sur un
évanouissement sévère (”*deep fading*”) est divisée sur deux améliorant, par conséquent, la
fiabilité.

– ”*Throughput*” : la communication via le relai peut être une meilleure alternative lorsque
le lien direct entre la source et la destination est mauvais ou inexistant, ce qui permet
d'augmenter le ”*throughput*” à la reception.

– Couverture : Un relais permet d'établir une communication entre une source et une desti-
nation plus éloignée sans pour autant diminuer la qualité de la communication.

– L'efficacité énergétique à la source : la présence d'un relais entre la source et la destination
permet de réduire la puissance à l'émission puisque le message parcourt moins de distance
lors du premier IT.

Depuis l'émergence des systèmes de communication avec relayage, plusieurs avancées ont été
accomplies, notamment en matière d'optimisation de leur performances [3]-[4]. En effet, plusieurs
études ont été réalisées au cours de la dernière décennie visant à trouver le nombre et surtout
l'emplacement idéaux des relais [5]. Une variété de topologies ont alors vu le jour telle que celle à
branches et à sauts multiples. La topologie à branches multiples est illustrée dans Figure 1.3(a).
En utilisant cette topologie, le destination reçoit plusieurs copies du même message à travers
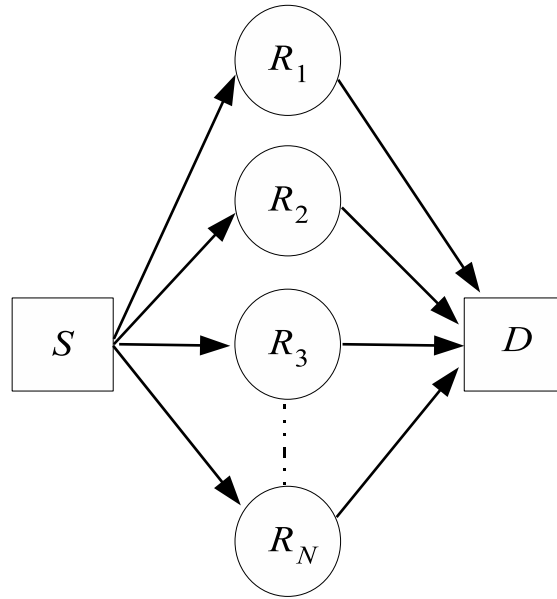
(a) Topologie à branches multiples.
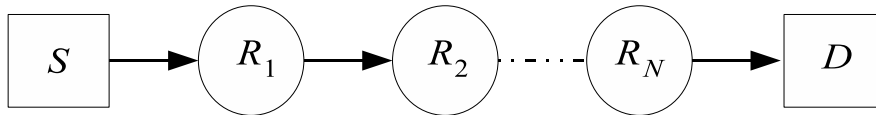
(b) Topologie à sauts multiples

FIGURE 1.3 – Les topologies à branches et sauts multiples.

différents chemins ce qui se traduit par un gain de diversité, puisque la probabilité d'avoir un évanouissement sévère diminue avec le nombre de relai. Cependant, la topologie à branches multiples ne permet pas d'élargir la couverture puisque la distance entre la source et le récepteur ne dépasse pas les deux sauts, comme on peut l'observer de la Figure 1.3(a). La topologie à sauts multiples, illustrée dans Figure 1.3(b), permet au contraire d'élargir significativement la couverture puisque la distance en sauts entre la source et le récepteur augmente avec le nombre de relais. Cependant, plus ce nombre est important moins le récepteur sera capable de retrouver le message original émis par la source. Un compromis entre les deux topologies est toutefois nécessaire pour assurer des performances optimales d'un système de communication avec relayage.

1.2.1   Protocole de relayage

Afin d'améliorer les performances des systèmes de communication sans fil, des traitements particuliers du message reçu pourraient être envisagés au niveau des relais. Chaque ensemble

de traitements définit un protocole de relayage dont la conception vise à atteindre des objectifs fixés au préalable selon le coût et la complexité désirés. Le sommaire des différents protocoles de relayage existants dans la littérature a été exposé dans [6]. Grâce à leurs efficacité et simplicité, seulement deux protocoles parmi eux ont été largement adoptés par la communauté scientifique : amplification-puis-transmission (''*amplify-and-forward*'') et décodage-puis-transmission (''*decode-and-forward*'').

Amplification-puis-transmission (AT)

Comme son nom l'indique, le protocole AT consiste en l'amplification du signal reçu au niveau du relai. Le signal résultant est ensuite transmis vers la destination. Aucune modification n'est ainsi apportée à l'information transmise par la source. L'implémentation d'un tel protocole est simple et ne requiert que le choix du gain d'amplification (GA) approprié ; une tâche critique car ce dernier affecte souvent les performances globales du système de communications [1]. Selon le GA choisi, on peut distinguer deux types de protocoles AT : à GA variable ou GA fixe.

Dans le protocole AT à GA variable, ce dernier est adapté pour fournir toujours la même puissance à la sortie du relai peut importe l'état du canal lors du premier saut. Dans ce cas, le GA dépend donc de la puissance de transmission de la source, du canal entre elle et le relais ainsi que tout bruit ou interference subite au niveau de ce dernier. En considérant l'exemple illustré dans la Figure 1.2, le GA variable est exprimé comme suit :

$$G^2 = \frac{P_r}{P_s|h_{sr}|^2 + \sigma^2}, \tag{1.9}$$

où P_r et P_s sont, respectivement, les puissances de transmissions de la source et du relais et h_{sr} est le canal entre ces deux terminaux.

Contrairement aux protocoles AT à GA variable, ceux à GA fixe ne nécessitent pas la connaissance instantanée de l'état du canal. Le GA fixe est généralement donné par

$$G^2 = \frac{1}{Ct\sigma^2}, \tag{1.10}$$

où Ct est une constante positive. Bien que les protocoles AT à GA variable surpassent en termes de performances ceux à GA fixe, ces derniers restent toutefois une solution plus attrayante grâce à leur simplicité.

Em résum, l'avantage principal des protocoles AT est qu'ils permettent d'éviter toute forme de traitement supplémentaire du message transmis par la source, rendant ainsi leurs implementation

plus simple. Cependant, ils présentent un inconvénient majeur qui consiste en l'amplification, en plus du signal utile, de tout bruit subit lors du premier saut. Ceci risque, en fait, d'augmenter significativement la distortion du signal à la destination.

Décodage-puis-transmission (DT)

En utilisant les protocoles DT, le relai décode le signal reçu afin de reconstituer le message original puis, ré-encode ce dernier avant de le transmettre à la destination [3]. Ces opérations de décodage et encodage rendent, malheureusement, les protocoles DT beaucoup plus complexes que les protocoles AT. Néanmoins, ils ont un sérieux avantages par rapport à ces derniers. En effet, avec les protocoles DT, le bruit du premier saut n'est pas retransmis avec le signal désiré, puisque le message original a été récupéré durant l'étape du décodage où tout effet du bruit a été éliminé. Dans cette thèse, on a cependant opté pour les protocoles AT puisqu'ils sont plus simples et faciles à implémenter. On va étudier, dans les prochains chapitres, les performances des systèmes de communication sont fils intégrant ce genre de protocoles.

Dans la section suivante, on va présenter la nouvelle technologie de transmission multi-antennes et expliquer les bénéfices de son intégration dans les systèmes de communication sans fil.

1.3 Communication multi-antennes

Durant la dernière décennie, la communication multi-antennes est devenue une technologie incontournable pour les communications sans fil. Elle a été incorporée dans tous les standards des réseaux avancés à hauts débits tels que les standards 3G (LTE) et 4G (LTE-A). De plus, cette technologie sera vraisemblablement le coeur même des futurs réseaux 5G [7]. Lorsqu'il existe plusieurs antennes à la fois à l'émission et la réception, on parle de communication MIMO ("*multiple-input multiple-output*"). Il a été prouvé que ce genre de communication permet de réaliser des gains non seulement de diversité mais aussi de multiplexage [8]-[9]. En effet, si les antennes sont convenablement espacées au niveau des terminaux, les liens entre chaque paire d'antennes émettrice et réceptrice subissent des évanouissements statistiquement indépendants. Dans ce cas, en diffusant le même message à travers toutes les antennes à l'émission, la proba-bilité pour que ce message ne puisse atteindre la réception à cause d'un évanouissement sévère

est diminuée, réalisant ainsi un gain de diversité. Plus ce gain augmente, plus fiable sera la communication. D'un autre côté, la configuration MIMO fournit plusieurs canaux ou chemins entre l'émetteur et le récepteur. Ces canaux pourraient acheminer en parallèle des blocs d'informations différents, réalisant ainsi un gain de multiplexage. Ce gain se traduit par un bénéfice substantiel en termes de débit de communication. Il est claire qu'un équilibre débit/fiabilité doit être atteint à travers un compromis inévitable entre les gains de diversité et de multiplexage. Afin d'assurer ces gains de diversités, les systèmes MIMO requièrent une connaissance de l'état de canal de propagation pour effectuer le précodage.

Considérons une communication MIMO entre un émetteur et un récepteur équipés de M et N antennes, respectivement. Notons par $\mathbf{y} \in \mathcal{C}^{N \times 1}$ le vecteur des signaux reçu à la destination donné par

$$\mathbf{y} = \mathbf{H}\mathbf{x} + \mathbf{n}, \tag{1.11}$$

où $\mathbf{H} \in \mathcal{C}^{N \times M}$ est la matrice des canaux dont le (i,j)-ème coefficient représente le canal entre la i-ème antenne émettrice et la j-ème antenne réceptrice, $\mathbf{x} \in \mathcal{C}^{M \times 1}$ est le vecteur des signaux transmis de puissance $P_{\mathbf{x}}$, et $\mathbf{n} \in \mathcal{C}^{N \times 1}$ est le vecteur des bruits de variance $\sigma^2 \mathbf{I}$. Mieux connue sous le nom de canal MIMO, $\mathbf{H}$ varie d'un environnement de propagation à un autre et ses caractéristiques et propriétés sont étroitement liées aux distributions statistiques de ses coefficients. Par exemple, les coefficients de $\mathbf{H}$ peuvent obéir aux lois de Rayleigh, Rice ou encore Nakagami-m selon le model de l'évanouissement considéré. En général, la capacité érgodique d'un canal MIMO avec des entrées de puissance unitaires Gaussiennes est donnée par [8]

$$C = \mathrm{E}_{\mathbf{H}}\{\log_2 \det \left(I_N + \rho \mathbf{H}\mathbf{H}^{\dagger}\right)\}. \tag{1.12}$$

1.4 Radio cognitive

Dans les sections précédentes, on a vu que l'intégration des technologies de relayage et/ou multi-antennes dans les systèmes de communication sans fil permet d'améliorer les performances de ces derniers en termes de débit, de fiabilité et de couverture. Dans un contexte de communication cellulaire, on ne pourra malheureusement pas profiter pleinement de ces avantages sans une utilisation optimale ou du moins efficace du spectre disponible. Le problème majeur avec cette resource est que toute la bande de fréquence est exclusivement allouée à des services spécifiques
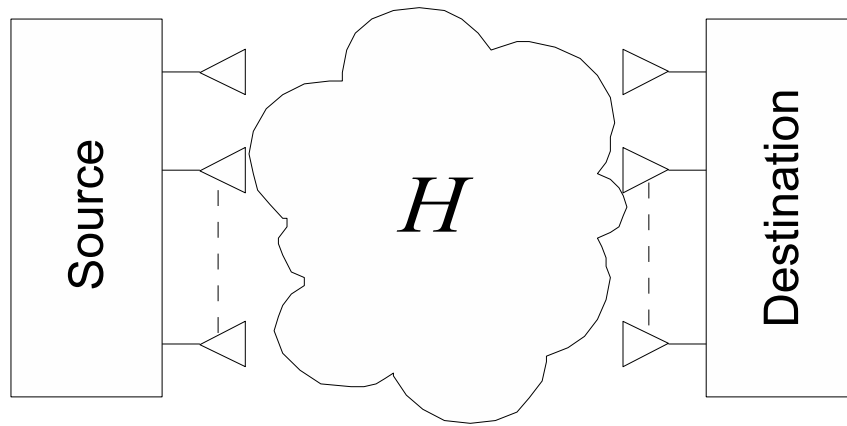
FIGURE 1.4 – Communication multi-antennes.

destinés à des usagers particuliers, appelés usagers primaires (UP)s. Visant à améliorer la gestion du spectre disponible afin d'assurer son utilisation optimale, la radio cognitive (RC) permet aux USs de partager la même bande de fréquence exploitée par les UPs sans pour autant diminuer la qualité de service perçue par ces derniers [10]. Plusieurs approches de RC existent dans la littérature mais seulement deux d'entre elles sont souvent adoptés : les approches "overlay" et "underlay".

1.4.1 Approche overlay

Cette approche repose sur la technologie de détection du spectre qui est utilisée au niveau de chaque US pour détecter la présence d'un éventuel UP sur sa bande de fréquence. Un US peut ainsi utiliser n'importe quel bande libre jusqu'à la réapparition d'un UP sur cette bande. Dans ce cas, l'US stoppe sa communication pour éviter d'interférer sur celle de l'UP. Cet US pourrait, ensuite, rétablir sa communication sur une autre bande libre ou attendre jusqu'à ce que sa bande initiale se libère.

L'inconvénient majeur de cette approche est que la détection de la présence des UPs est très complexe, spécialement lorsque ces derniers emploient des techniques de modulation, des débits de transmission et des puissances différents ; et subissent une variété d'évanouissement ainsi que des interférences d'ampleurs différentes.
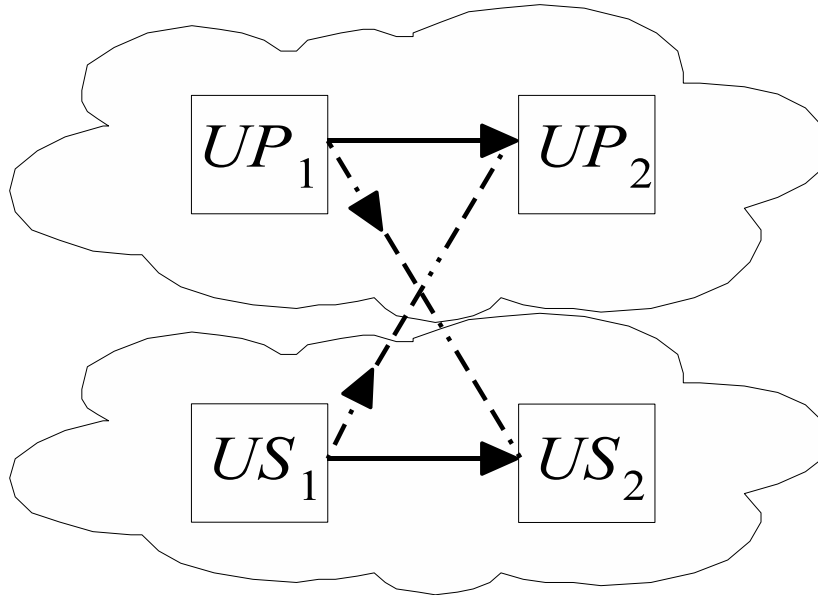
FIGURE 1.5 – Radio cognitive.

1.4.2 Approche underlay

Contrairement à la première approche, l'approche underlay donne la possibilité à un US de partager, sous certaines conditions, la même bande de fréquence simultanément avec un UP. Avec cette approche, un US peut maintenir sa communication si l'interférence qui en résulte ne dépasse pas certain niveau tolérable chez l'UP présent sur la même bande de fréquence. Ce seuil est le niveau d'interférence maximal tolérable au dessous duquel l'UP en question est capable de maintenir une communication fiable.

Dans cette thèse, on a choisi d'adopter cette approche lors des études de performances des systèmes de communication sans fil, dû surtout à sa simplicité.

Bibliographie

[1] J. N. Laneman, D. N. C. Tse, and G. W. Wornell, "Cooperative diversity in wireless networks : Efficient protocols and outage behavior,", *IEEE Transactions on Information Theory*, vol. 50, no. 12, pp. 3062-3080, 2004.

[2] M. Hasna and M.-S. Alouini, "End-to-end performance of transmission systems with relays over rayleigh-fading channels," *IEEE Trans. Wireless Comm.*, vol. 2, no. 6, pp. 1126-1131, Nov. 2003.

[3] A. A. El Gamal and T. M. Cover, "Capacity theorems for the relay channel," *IEEE Transactions on Information Theory,* vol. 25, no. 5, pp. 572-584, 1979.

[4] G. Kramer, I. Maric, and R. D. Yates, "Cooperative communications," *Foundations and Trends in Networking*, vol. 1, no. 3-4, pp. 271-425, 2006.

[5] J. Yackoski, L. Zhang, C.-C. Shen, L. Cimini, and B. Gui, "Networking with cooperative communications : Holistic design and realistic evaluation," *IEEE Communications Magazine,* vol. 47, no. 8, pp. 113-119, Aug. 2009.

[6] B. Zhao and M. C. Valenti, "Some new adaptive protocols for the wireless relay channel," *Monticello*, IL, USA, pp. 299-324, Oct. 2003.

[7] J. G. Andrews et al., "What will 5G be ?," *IEEE J. Sel. Areas Commun.,* vol. 32, pp. 1065-1082, June 2014.

[8] Foschini, G. J. and M. J. Gans, "On limits of wireless communication in a fading environment when using multiple antennas," *Wireless Per. Commun.,* Vol. 6, pp. 311-335, Mar. 1998.

[9] Vu, M. and A. Paulraj, "Optimal linear precoders for MIMO wireless correlated channels with nonzero mean in space-time coded systems," *IEEE Trans. Signal Processing,* vo. 54, no. 6, pp. 2318-2336, Jun. 2006.

[10] J. Mitola III and G. Maguire Jr., "Cognitive radio : Making software radios more personal," *IEEE Personal Communications*, vol. 6, no. 4, pp. 13-18, 1999.

Chapitre 2

Closed-Form Error Analysis of Variable-Gain Multihop Systems in Nakagami-m Fading Channels

Imène Trigui, Sofiène Affes, and Alex Stéphenne

Résumé : Ce chapitre considère des systèmes de communication à sauts multiples. Grâce à leurs innombrables avantages, tel que l'extension de la couverture et l'économie d'énergie, ces systèmes ont suscité un grand intérêt chez la communauté scientifique. Dans ce chapitre, On a développé pour la première fois des nouvelles expressions novatrices d'une forme intégrale infinie impliquant le produit de fonctions de Bessel. Ces expressions ont été d'une grande utilité pour le calcul et l'évaluation de la probabilité d'erreur des systèmes de communication à sauts multiples avec un nombre arbitraire de relais à gains variables subissant un évanouissement Nakagami-m. Les formules obtenues ont permis d'établir une connexion, jusqu'ici inconnue, entre la probabilité d'erreur relative à différentes modulations et la fonction Lauricella. Dans le cas spéciale où m est un multiple impaire de un-et-demi, des expressions plus simples de la probabilité d'erreur impliquant les fonctions hypergéométriques de Gauss ont été obtenues. Il a été prouvé que ces nouveaux formules généralisent des anciens résulats relatifs aux systèmes AT subissant des évanouissements non-identiques avec des paramètres entiers.

Abstract

In this paper, infinite integrals involving the product of Bessel functions of different arguments are solved in closed-form. The obtained solutions form a framework for the error probability analysis of wireless amplify and forward (AF) systems with an arbitrary number of variable-gain relays operating over independent but not necessarily identical Nakagami-m fading channels. Here we show that the error probability can be described by generalized hypergeometric functions, namely, Gauss's and Lauricella's multivariate hypergeometric functions. This work represents a significant improvement over previous contributions and extends previous formulas pertaining to dual-hop transmissions over identical Nakagami-m fading channels. Numerical examples show an excellent match between simulation and theoretical results.

2.1   Introduction

The performance analysis of digital communication systems over fading environments has attracted a lot of research endeavor over the recent past. The derivation of closed-form expressions for key performance measures, namely the average error probability, is central to such research. Such closed-form results alleviate the need for Monte-Carlo simulations thereby enabling easy optimization of the overall system performance. In particular, numerous studies have been devoted to the performance analysis of multi-hop wireless systems over fading channels. Recently, the multi-hop concept has gained momentum in the context of cooperative wireless systems where relaying is used as a form of spatial diversity to overcome highly shadowed or deeply faded links [1]. The main idea is that communication is achieved by relaying the signal from the source to the destination via many intermittent terminals in between called relays. With relays that merely amplify and forward the incoming signal prior to relaying, AF transmission is the simplest and the cheapest to implement. Performance of such a system can be analyzed through the theoretical evaluation of certain performance metrics, namely, the average error probability. So far, despite many valuable contributions [2]- [12], the error analysis of the dual-hop case is still incomplete and there are no closed-form expressions for AF multihop systems with an arbitrary number of relays. In [2], [3], Hasna and Alouini presented an error probability analysis for dual-hop relaying system over identical Nakagami-m fading. Only recently have the authors in [4]- [6] considered the non-identical case for dual-hop transmission, but merely for integer va-

lues of the Nakagami-m fading parameter. Nevertheless, in practical scenarios, the m parameters often adopt non-integer values [13], which exclude the generality of [4, 5] and [6]. Other error analysis approaches bind the output SNR of the multi-hop relay link. For instance, it was upper bounded by the minimum value and the geometric mean of the SNRs at the hops, in [6] and [8], respectively. So far, there is no closed-form error probability analysis reported in the literature for multihop relaying systems with an arbitrary number of variable-gain relays over Nakagami-m fading. The most valuable contributions in this context can be found in [9], [10] and [12]. In reference [9], [10], the error probabilities of multihop multibranch wireless communication systems are expressed as a double infinite integrals of the moment generating function (MGF) of the reciprocal of the instantaneous received SNR per branch. Therefore, in principle, exact evaluation of the error probability using the method in [9], [10] requires numerical computation of double integrals, which has been achieved by relying on the Gauss Quadrature Rule in [11]. In the theoretical approach presented in [12], the error probability performance of an AF multihop system is evaluated using single-integral expressions obtained in terms of the MGF of the reciprocal of the instantaneous received SNR. The obtained single integral formula is unfortunately not applicable to the multi-branch scenario, but it offers a more tractable solution than [9], [10] for the evaluation of the error probability of multihop transmissions. Motivated by the above considerations, in the present contribution, we derive for the first time this error probability in closed form. The obtained framework applies to the multihop scenario and can also be used to compute the exact formulas of the MGF of the end-to-end SNR in the multibranch multihop context. Our approach is inspired by [12] and generalizes both [2] and [4]. It turns out that the average error probability belongs to a special class of generalized hypergeometric series. These are the Lauricella's multivariate hypergeometric functions [12] of N variables $F_C^{(N)}$ for which some quite substantial mathematical apparatus is already known, like convergence properties and some analytical continuation formulas. Although the results are not expressible in common simple functions, they are at least expressible in this known type of functions, a significant improvement over previous results. In particular, new simple expressions for the error probability are derived in the dual-hop case, which is to date the most investigated one in the literature for its practical applications. The obtained formulas involve Appell's hypergeometric [12], Gauss' hypergeometric and Meijer's-G [21] functions.

The remainder of this paper is organized as follows. First, in section II, we derive closed-form

solutions to the infinite integral containing the product of Bessel functions. Based on the obtained solutions, the error-rate performance for a variety of modulation schemes of AF multihop relaying systems with variable-gain relays is evaluated in section III. Section IV, derives new error probability results for the dual-hop case and shows how these results specialize for some less general fading scenarios of interest. Some numerical results are provided in section V. Finally, we conclude the paper while summarizing the main results in section VI.

2.2   Solution to the infinite integral

This paper first addressees the calculation of the integrals

$$I(\nu, \mu, a, \Lambda, \beta) = \int_0^\infty s^\nu J_\mu\left(a\sqrt{s}\right) \prod_{i=1}^N K_{\lambda_i}\left(b_i\sqrt{s}\right) ds, \tag{2.1}$$

where $\Lambda = \{\lambda_1, ..., \lambda_N\}, \beta = \{b_1, ..., b_N\}, \Re(a), \mu > 0, N > 1$. In (2.1), $J_\mu(\cdot)$ is the bessel function of the first kind and order μ [21, Eq. (8.440)], and $K_\lambda(\cdot)$ is the modified bessel function of the second kind and order λ [21, Eq. (8.485)]. The integral in (2.1) occurs in a number of wireless applications including the evaluation of the error probabilities and the ergodic capacity of wireless multihop systems. Yet, to the best of the author's knowledge, a closed-form solution for this integral is not known. Furthermore, a closed-form solution to the special case of (2.1) obtained when $N = 2$, that is

$$I_s\left(\nu, \mu, a, \lambda_1, \lambda_2, b_1, b_2\right) = \int_0^\infty s^\nu J_\mu\left(a\sqrt{s}\right) K_{\lambda_1}\left(b_1\sqrt{s}\right) K_{\lambda_2}\left(b_2\sqrt{s}\right) ds, \tag{2.2}$$

is not widely known and seems to have been found only when $b_1 = b_2$ and $\lambda_1 = \lambda_2$ (see [23]). None of references [23] or [21] gives a closed-form solution for either I or I_s. Nor does Mathematica give a closed-form solution for I or I_s. In this paper, we derive an explicit and general solution to (2.1) for any number $N > 1$. Our analysis is only valid for real-valued non-integer λ_i. Nevertheless, practically, very similar results can be obtained at λ_i and $\lambda_i + \epsilon$ for sufficiently small ϵ values. By expressing the Bessel functions in terms of hypergeometric functions, namely, using

$$K_\lambda(z) = 2^{-\lambda-1}\Gamma(-\lambda)z^\lambda {}_0F_1(; 1+\lambda, \frac{z^2}{4}) + 2^{\lambda-1}\Gamma(\lambda)z^{-\lambda} {}_0F_1(; 1-\lambda, \frac{z^2}{4}), \tag{2.3}$$

and

$$J_\mu(z) = \frac{1}{\Gamma(\mu+1)} \left(\frac{z}{2}\right)^\mu {}_0F_1\left(; 1+\mu, -\frac{z^2}{4}\right), \tag{2.4}$$

27

where $_0F_1(a,b,z)$ denotes the confluent hypergeometric function [21], an alternative expression for I is shown to be given by

$$I(\nu,\mu,a,\Lambda,\beta) = \frac{a^\mu}{2^\mu \Gamma(\mu+1)} \int_0^\infty s^{\nu+\frac{\mu}{2}} K_{\lambda_N}(b_N\sqrt{s})_0F_1\left(;1+\mu,-\frac{a^2s}{4}\right)\prod_{i=1}^{N-1}[V_i+W_i]\,ds, \qquad (2.5)$$

where

$$V_i = 2^{\lambda_i-1}\Gamma(\lambda_i)\left(b_i\sqrt{s}\right)^{-\lambda_i}{}_0F_1\left(;1-\lambda_i,\frac{b_i^2s}{4}\right), \qquad (2.6)$$

and

$$W_i = 2^{-\lambda_i-1}\Gamma(-\lambda_i)\left(b_i\sqrt{s}\right)^{\lambda_i}{}_0F_1\left(;1+\lambda_i,\frac{b_i^2s}{4}\right). \qquad (2.7)$$

In subsequent derivations, a more convenient expression for the product involved in (2.5) will be given using the following lemma. Let $V_1,...,V_N$ and $W_1,...,W_N$ denote two sets of N variables. Then, the following equality holds

Lemma 1 :

$$\prod_{i=1}^{N-1}(V_i+W_i) = \sum_{i=0}^{N-1}\sum_{\tau(i,N-1)}\prod_{k=1}^{N-1}V_k^{i_k}W_k^{1-i_k}, \qquad (2.8)$$

where $\tau(i,N-1)$ is the set of $N-1$-tuples such that $\tau(i,N-1) = \{(i_1,...,i_{N-1}) : i_k \in \{0,1\}, \sum_{k=1}^{N-1}i_k = i\}$. Indeed, by expanding the left side of (2.8), we can clearly notice that the i-th term can be viewed as $\binom{N-1}{i}$ combinations of the product of i_k variables V_k and $1-i_k$ variables W_k. Note that, when V_k and W_k are equal, (2.8) reduces to the Newton's binomial. Using the above equality, (2.5) will be given by

$$I(\nu,\mu,a,\Lambda,\beta) = \frac{a^\mu}{2^{N-1+\mu}\Gamma(\mu+1)}\prod_{k=1}^{N-1}\left(\frac{b_k}{2}\right)^{\lambda_k}\sum_{i=0}^{N-1}\sum_{\tau(i,N-1)}\left\{\prod_{k=1}^{N-1}\left(\frac{2}{b_k}\right)^{2\lambda_k i_k}\Gamma(\lambda_k)^{i_k}\Gamma(-\lambda_k)^{1-i_k}\right\}M_{ij}, \quad (2.9)$$

where

$$M_{ij} = \int_0^\infty s^\delta K_{\lambda_N}(b_N\sqrt{s})\,{}_0F_1\left(;1+\mu,-\frac{a^2s}{4}\right)\prod_{k=1}^{N-1}\left[{}_0F_1\left(;1-\lambda_k,\frac{b_k^2s}{4}\right)\right]^{i_k}\left[{}_0F_1\left(;1+\lambda_k,\frac{b_k^2s}{4}\right)\right]^{1-i_k}ds, \tag{2.10}$$

whereby j stands for the j-th tuple of the set $\tau(i,N-1)$, and $\delta = \nu+\mu/2+\left(\sum_{k=1}^{N-1}\lambda_k\right)/2 - \sum_{k=1}^{N-1}\lambda_k i_k$. The integral M_{ij} can be solved by expressing the Bessel K integrand in terms of Meijer's G-functions [21, Eq. (9.301)], namely, using $K_{\lambda_N}(b_N\sqrt{s}) = G_{0,2}^{2,0}\left(b_N^2s/4\left|\begin{matrix}-\\\lambda_N/2,-\lambda_N/2\end{matrix}\right.\right)/2$.

Then, considering the change of variable $z = b_N^2 s/4$ yields

$$M_{ij} = \left(\frac{4}{b_N^2}\right)^{\delta+1} \int_0^\infty \frac{1}{2z} G_{0,2}^{2,0}\left(z \left|\begin{matrix} - \\ \xi, \xi - \lambda_N \end{matrix}\right.\right) {}_0F_1\left(;1+\mu, -\frac{a^2 z}{b_N^2}\right)$$

$$\prod_{k=1}^{N-1} \left[{}_0F_1\left(;1-\lambda_k, \frac{b_k^2 z}{b_N^2}\right)\right]^{i_k} \left[{}_0F_1\left(;1+\lambda_k, \frac{b_k^2 z}{b_N^2}\right)\right]^{1-i_k} dz, \qquad (2.11)$$

where $\xi = \delta + \lambda_N/2 + 1$. By further noticing that a single integral representation for the multivariate Lauricella hypergeometric function $F_C^{(n)}(a, b; c_1, ..., c_n; x_1, ..., x_n)$ is given by [12]

$$F_C^{(n)}(a, b; c_1, ..., c_n; x_1, ..., x_n) = \frac{1}{\Gamma(a)\Gamma(b)} \int_0^\infty G_{0,2}^{2,0}(t \,|a, b) \left(\prod_{k=1}^n {}_0F_1\left(; c_k, x_k t\right)\right) \frac{dt}{t}, \qquad (2.12)$$

one can easily recognize that $I(\nu, \mu, a, \Lambda, \beta)$ can be expressed in terms of (2.12) as

$$I(\nu, \mu, a, \Lambda, \beta) = \frac{\left(\frac{a}{b_N}\right)^\mu \prod_{k=1}^{N-1} \left(\frac{b_k}{b_N}\right)^{\lambda_k}}{2^N \Gamma(\mu+1)} \left(\frac{4}{b_N^2}\right)^{\nu+1} \sum_{i=0}^{N-1} \sum_{\tau(i,N-1)} \Gamma(\xi)\Gamma(\xi-\lambda_N) \left\{\prod_{k=1}^{N-1} \left(\frac{b_N}{b_k}\right)^{2\lambda_k i_k} \Gamma(\lambda_k)^{i_k} \Gamma(-\lambda_k)^{1-i_k}\right\}$$

$$F_C^{(N)}\left(\xi, \xi-\lambda_N, 1+\mu, \underbrace{1-\lambda_1}_{i_1}, \underbrace{1+\lambda_1}_{1-i_1}, ..., \underbrace{1-\lambda_{N-1}}_{i_{N-1}}, \underbrace{1+\lambda_{N-1}}_{1-i_{N-1}}; -\frac{a^2}{b_N^2}, \frac{b_1^2}{b_N^2}, ..., \frac{b_{N-1}^2}{b_N^2}\right). \qquad (2.13)$$

Using the multiples series representation of the Lauricella's hypergeometric function [12, Eq. (A.1.4)]

$$F_C^{(n)(a,b;c_1,...,c_n;x_1,...,x_n)} = \sum_{m_1=0}^\infty \cdots \sum_{m_n=0}^\infty \frac{(a)_{m_1+...m_n} (b_1)_{m_1+...m_n}}{(c_1)_{m_1}...(c_n)_{m_n}} \frac{x_1^{m_1}...x_n^{m_n}}{m_1!...m_n!}; \qquad (2.14)$$

$$\sqrt{|x_1|} + ... + \sqrt{|x_n|} < 1, \qquad (2.15)$$

where $(a)_k = \Gamma(a+k)/\Gamma(k)$ denotes the Pochhammer symbol, it can be noted that the convergence of the total sum involved in (2.13) is governed by the threshold condition

$$|a^2| < \left(\sqrt{|b_1^2|} + \sqrt{|b_2^2|} + ... + \sqrt{|b_N^2|}\right)^2. \qquad (2.16)$$

Hopefully, (2.13) can be extended to the complementary region of (2.16) by applying the analytical continuation formula of the Lauricella's hypergeometric function F_C [12]. Indeed, a Lauricella function in the argument z_i can be analytically continued to a sum of two Lauricella functions in the argument $z_i = x_i/x_n$ for $i = 1, ..., n-1$ and $z_n = 1/x_n$ according to the following expression :

$$F_C^{(n)}(a, b; c_1, ..., c_n; x_1, ..., x_n) = \frac{\Gamma(c_n)\Gamma(b-a)}{\Gamma(b)\Gamma(c_n-a)}(-x_n)^{-a} F_C^{(n)}(a, 1+a-c_n; c_1, ..., c_{n-1}, 1-b+a; z_1, ..., z_n)$$

$$+ \frac{\Gamma(c_n)\Gamma(a-b)}{\Gamma(a)\Gamma(c_n-b)}(-x_n)^{-b} F_C^{(n)}(b, 1+b-c_n; c_1, ..., c_{n-1}, 1-a+b; z_1, ..., z_n). \qquad (2.17)$$

Although the derived analytic continuation of (2.13) is not shown here for lack of space, the former ensures that for all $a > 0$ and all admissible values of $\{b_i\}_{i=1}^N$, the absolute convergence of the series (2.13) is always guaranteed.

We now simplify (2.13) in an important case corresponding to $N = 2$. In such a setting, I in (2.13) reduces to

$$
I_s\left(\nu, \mu, a, \lambda_1, \lambda_2, b_1, b_2\right) = \frac{\left(\frac{a}{b_2}\right)^\mu \left(\frac{b_1}{b_2}\right)^{\lambda_1} \left(\frac{4}{b_2^2}\right)^{\nu+1}}{4\Gamma(\mu+1)} \left\{ F_4\left(\xi_0, \xi_0 - \lambda_2, 1+\mu, 1+\lambda_1, -\frac{a^2}{b_2^2}, \frac{b_1^2}{b_2^2}\right) \Gamma(\xi_0) \right.
$$

$$
\left. \Gamma(\xi_0 - \lambda_2)\Gamma(-\lambda_1) + \left(\frac{b_2}{b_1}\right)^{2\lambda_1} \Gamma(\lambda_1)\Gamma(\xi_1)\Gamma(\xi_1 - \lambda_2) F_4\left(\xi_1, \xi_1 - \lambda_2, 1+\mu, 1-\lambda_1, -\frac{a^2}{b_2^2}, \frac{b_1^2}{b_2^2}\right) \right\}, \quad (2.18)
$$

where $\xi_0 = \nu + \mu/2 + \lambda_1 + \lambda_2/2 + 1$, $\xi_1 = \nu + \mu/2 + \lambda_2 - \lambda_1/2 + 1$ and $F_4 = F_C^{(2)}$ is the fourth Appel hypergeometric function which is defined as

$$
F_4[\alpha, \beta; \gamma, \gamma', x, y] = \sum_{j=0}^\infty \sum_{k=0}^\infty \frac{(\alpha)_{j+k}(\beta)_{j+k}}{(\gamma)_j(\gamma')_k} \frac{x^j}{j!} \frac{y^k}{k!}, \quad (2.19)
$$

$$
|x|^{1/2} + |y|^{1/2} < 1.
$$

The Appell functions [12] are well known, and numerical routines for their exact computation are available in packages such as Mathematica.

2.2.1 A simplified special case of I

In the following, a simplified version of I is obtained when $\lambda_i, i = 1, ..., N$ are constrained to take integers plus one-half values, i.e., $\lambda_i = n_i + 1/2$, where n_i is an integer. In such a setting, we have

$$
K_{\lambda_i}\left(b_i\sqrt{s}\right) = \sqrt{\frac{\pi}{2b_i}} e^{-b_i\sqrt{s}} \sum_{p=0}^{n_i} \frac{\Gamma(n_i+1+p)}{\Gamma(n_i+1-p)\Gamma(p+1)} (2b_i)^{-p}(\sqrt{s})^{-p-\frac{1}{2}}. \quad (2.20)
$$

By inserting (2.20) into (2.1), I can be written as

$$
I(\nu, \mu, a, \Lambda, \beta) = \frac{\frac{\pi}{2}^{N/2}}{\prod_{i=1}^N b_i} \int_0^\infty s^{\nu - \frac{N}{4}} J_\mu(a\sqrt{s}) e^{-\sum_{i=1}^N b_i\sqrt{s}} \prod_{i=1}^N \sum_{p=0}^{n_i} \Upsilon_{i,p}(\sqrt{s})^{-p} ds, \quad (2.21)
$$

where

$$
\Upsilon_{i,p} = \frac{\Gamma(n_i+1+p)(2b_i)^{-p}}{\Gamma(n_i+1-p)\Gamma(p+1)}. \quad (2.22)
$$

The expression above encompasses the product of a set of polynomials of $x = \sqrt{s}$. It is well known that the product of a set of polynomials is another polynomial whose degree is the sum

of the degrees of the polynomials in the set and the coefficient of x^p in the resulting polynomial is the sum of terms of the form $\prod_{k=1}^{N} b_{k,p_k}$ such that $\sum_{k=1}^{N} p_k = p$. Consequently, we obtain

Lemma 2 :

$$\prod_{i=1}^{N} \left(\sum_{p=0}^{n_i} \Upsilon_{i,p} \xi^{-p} \right) = \sum_{p=0}^{n_\Sigma} \left(\sum_{w(p,N)} \prod_{i=1}^{N} \Upsilon_{i,p_i} \right) \xi^{-p}, \tag{2.23}$$

where $n_\Sigma = \sum_{i=1}^{N} n_i$ and $w(p,N)$ is the set of N-tuples such that $w(p,N) = \big\{ (p_1,...,p_N) : p_k \in \{0,1,...,n_k\}, \sum_{k=1}^{N} p_k = p \big\}$. Using (2.23) and performing some algebraic manipulations, it follows that (2.21) reduces to

$$I(\nu,\mu,a,\Lambda,\beta) = \frac{\frac{\pi}{2}^{N/2}}{\prod_{i=1}^{N} b_i} \sum_{p=0}^{n_\Sigma} \left(\sum_{w(p,N)} \prod_{i=1}^{N} \Upsilon_{i,p_i} \right) \int_{0}^{\infty} s^{\nu-\frac{N}{4}-\frac{p}{2}} e^{-\sum_{i=1}^{N} b_i \sqrt{s}} J_\mu(a\sqrt{s}) ds. \tag{2.24}$$

Then, with the help of [21, Eq. (6.621)], the integral in (2.24) can be derived in closed form as

$$I(\nu,\mu,a,\Lambda,\beta) = \frac{\frac{\pi}{2}^{N/2}}{\prod_{i=1}^{N} b_i} \sum_{p=0}^{n_\Sigma} \left(\sum_{w(p,N)} \prod_{i=1}^{N} \Upsilon_{i,p_i} \right) \frac{\left(\frac{a}{2\sum_{i=1}^{N} b_i} \right)^{\mu} \Gamma\left(\mu + 2\nu - \frac{N}{2} - p + 2 \right)}{\left(\sum_{i=1}^{N} b_i \right)^{2\nu-\frac{N}{2}-p+2} \Gamma(\mu+1)}$$
$$F\left(\nu + \frac{\mu - \frac{N}{2} - p}{2} + 1, \nu + \frac{\mu - \frac{N}{2} - p + 3}{2}, \mu + 1, -\frac{a^2}{(\sum_{i=1}^{N} b_i)^2} \right), \tag{2.25}$$

where $F(a,b;c;x)$ is the Gauss hypergeometric function [21, Eq. (9.10)].

2.2.2 A simplified special case of I_s

A special case of I_s corresponds to $b_1 = b_2 = b$ and $\lambda_1 \neq \lambda_2$. In this case, making use of [21, Eq. (7.821.1)] along with the identity

$$K_{\lambda_1}(b\sqrt{s}) K_{\lambda_2}(b\sqrt{s}) = \frac{\sqrt{\pi}}{2} G_{2,4}^{4,0}\left(b^2 s \Big| 0, \frac{\lambda_1+\lambda_2}{4}, \frac{\lambda_1-\lambda_2}{2}, \frac{\lambda_2-\lambda_1}{2}, -\frac{\lambda_1+\lambda_2}{2} \right), \tag{2.26}$$

a closed form of I_s is shown to be given by

$$I_s(\nu,\mu,a,\lambda_1,\lambda_2,b,b) = \frac{\sqrt{\pi}}{2} \left(\frac{4}{a^2} \right)^{\nu+1} G_{4,4}^{4,1}\left(\frac{4b^2}{a^2} \Big| -\nu - \frac{\mu}{2}, 0, \frac{1}{2}, -\nu + \frac{\mu}{2} \frac{\lambda_1+\lambda_2}{2}, \frac{\lambda_1-\lambda_2}{2}, \frac{\lambda_2-\lambda_1}{2}, -\frac{\lambda_1+\lambda_2}{2} \right). \tag{2.27}$$

2.3 Application : error probabilities for amplify-and-forward multi-hop relaying systems

Let us consider an N-hop wireless communication system where a source S communicates with a destination D trough $N-1$ intermediate terminals called relays. In the k-th time slot,

the k-th relay R_k receives the signal from the immediately preceding relay and processes it by amplifying and forwarding it to the next hop R_{k+1}. Denoting by y_k the signal received by R_k, we have

$$y_k = v_k x_{k-1} + n_k, \quad k = 1, ..., N, \tag{2.28}$$

where v_k is the fading gain of the channel between terminals R_{k-1} and R_k, n_k denotes the additive white Gaussian noise received at the k-th terminal with power N_{0_k}, and x_k denotes the transmitted signal from the $(k-1)$-th relay given by

$$x_k = A_k y_k, \quad k = 1, ..., N - 1, \tag{2.29}$$

where A_k is the amplification gain of the k-th terminal. The end-to-end instantaneous received SNR is given by [8] as

$$\gamma = \frac{\prod_{k=1}^{N} A_k^2 \gamma_k}{\sum_{k=1}^{N} \prod_{j=k+1}^{N} A_j^2 \gamma_j}, \tag{2.30}$$

where $\gamma_k = P_k |v_k|^2 / N_{0_k}$ denotes the instantaneous received SNR over the channel between terminals R_{k-1} and R_k in which P_k is the transmitter power from terminal $R_{k-1}, k = 1, ..., N$. As seen in (2.30), the instantaneous received SNR in an AF multihop transmission system depends on the relay amplification gains and the fading channel gains. AF relays can be classified into two categories, namely, variable-gain relays and fixed-gain relays. In the first case, the relay uses the channel information of the preceding hop to control the relay gain. In contrast, systems with blind relays use amplifiers with fixed gains resulting in a signal with variable power at the relay output. In this paper, we consider the first type of amplification gain which is generally chosen as

$$A_k = \sqrt{\frac{P_k}{P_{k-1} |v_k|^2}}, \quad k = 1, ..., N - 1. \tag{2.31}$$

For this amplification gain, the relay amplifies its received signal, regardless of the received noise power [1]. Plugging this gain expression into (2.30), the end-to-end SNR is then given by

$$\gamma = \left[\sum_{l=1}^{N} \frac{1}{\gamma_l} \right]^{-1}. \tag{2.32}$$

Since the reciprocal of the end-to-end instantaneous received SNR γ is the sum of the inverse of the individual per-hop SNRs [8], then, the MGF of $\gamma^V = \frac{1}{\gamma}$ is the product of the individual

---

1. Since the amplification gain in systems with variable-gain relays is a function of the channel state information (CSI), variable-gain relays are also referred to as CSI-assisted relays [8], [9]

MGFs pertaining to the different hops, thus implying

$$M_{\gamma^V}(s) = \prod_{l=1}^{N} M_{\frac{1}{\gamma_l}}(s), \tag{2.33}$$

where $M_{\frac{1}{\gamma_l}}(s)$ is the MGF of the SNR on the l-th hop. In Nakagami-m fading, $M_{\gamma^V}(s)$ is given by [2]

$$M_{\gamma^V}(s) = 2^N \left(\prod_{l=1}^{N} \frac{\left(\frac{m_l}{\bar{\gamma}_l}\right)^{m_l/2}}{\Gamma(m_l)} \right) s^{\frac{m_\Sigma}{2}} \prod_{l=1}^{N} K_{m_l}\left(2\sqrt{\frac{sm_l}{\bar{\gamma}_l}}\right), \tag{2.34}$$

whereby $\bar{\gamma}_i = \mathrm{E}(\gamma_i)$, with $\mathrm{E}(\cdot)$ denoting expectation, $m_i \geq 1/2$ is the Nakagami-m factor of the i-th hop and $m_\Sigma = \sum_{l=1}^{N} m_l$ is defined for the sake of notational convenience.

In the sequel, considering AF multihop variable-gain relaying systems with operation over Nakagami-m fading channels, simple closed-form expressions for the error probabilities of AF multi-hop systems with variable gain relays are derived. Different modulation schemes are therefore considered, including binary and arbitrary rectangular M-QAM modulations.

2.3.1 Binary modulations

For different binary modulation schemes, the bit error probability was recently derived in [12, Eq. (4b)] as a single integral form given by

$$P_e = \frac{1}{2} - \frac{\tau^{\eta/2}}{2\Gamma(\eta)} \int_0^\infty s^{\frac{\eta}{2}-1} J_\eta(2\sqrt{\tau s}) M_{\gamma^V}(s) ds, \tag{2.35}$$

where the parameters τ and η depend on the type of modulation detection scheme given in [17, Tab. 8.1] and $\Gamma(\cdot,\cdot)$ is the incomplete gamma function [21, Eq. (8.350.2)]. By substituting appropriately (2.34) in (2.35) and using (2.1), P_e can be obtained as follows

$$P_e = \frac{1}{2} - \frac{2^{N-1}\tau^{\eta/2}}{\Gamma(\eta)} \left(\prod_{l=1}^{N} \frac{(\frac{m_l}{\bar{\gamma}_l})^{m_l/2}}{\Gamma(m_l)} \right) I\left(\frac{m_\Sigma + \eta}{2} - 1, \eta, 2\sqrt{\tau}, \Lambda, \beta \right), \tag{2.36}$$

where $\Lambda = \{m_1, m_2, ..., m_N\}$ and $\beta = \left\{ 2\sqrt{\frac{m_1}{\bar{\gamma}_1}}, ..., 2\sqrt{\frac{m_N}{\bar{\gamma}_N}} \right\}$. By properly substituting $I(\cdot,\cdot,\cdot,\cdot,\cdot)$ by its expression in (2.13), then after further manipulations, a closed-form expression of the error probability is obtained as

$$P_e = \frac{1}{2} - \frac{\tau^\eta \left(\prod_{l=1}^{N} \frac{(\frac{m_l \bar{\gamma}_N}{m_N \bar{\gamma}_l})^{m_l}}{\Gamma(m_l)} \right)}{2\Gamma(\eta)\Gamma(\eta+1)} \sum_{i=0}^{N-1} \sum_{\tau(i,N-1)} \Gamma(\xi_\eta)\Gamma(\xi_\eta - m_N) \left\{ \prod_{k=1}^{N-1} \left(\frac{m_N \bar{\gamma}_k}{m_k \bar{\gamma}_N} \right)^{m_k i_k} \Gamma(m_k)^{i_k} \Gamma(-m_k)^{1-i_k} \right\}$$

$$F_C^{(N)} \left(\xi_\eta, \xi_\eta - m_N, 1+\eta, \underbrace{1-m_1}_{i_1}, \underbrace{1+m_1}_{1-i_1}, ..., \underbrace{1-m_{N-1}}_{i_{N-1}}, \underbrace{1+m_{N-1}}_{1-i_{N-1}}; -\frac{\tau\bar{\gamma}_N}{m_N}, \frac{m_1\bar{\gamma}_N}{m_N\bar{\gamma}_1}, ..., \frac{m_{N-1}\bar{\gamma}_N}{m_N\gamma_{N-1}} \right). \tag{2.37}$$

33

where $\xi_\eta = m_\Sigma + \eta - \sum_{k=1}^{N-1} m_k i_k$. Note that equation (2.37) is a new closed-form expression for the bit error probability of binary modulations in AF relaying systems with variable gain relays under non-identical Nakagami-m fading. The values of the parameters η and τ are, for example, $(\eta, \tau) = (0.5, 1)$ for BPSK and $(\eta, \tau) = (0.5, 0.5)$ for BFSK modulation. Moreover, using the alternative expression of I when $m_i, i = 1, .., N$ are multiples of an integer plus one half, a simpler expression of P_e is obtained from (2.25) as

$$P_e = \frac{1}{2} - \frac{\tau^\eta \pi^{N/2}}{2^{m_\Sigma + 2\eta + 1} \Gamma(\eta) \Gamma(\eta+1)} \left(\prod_{i=1}^{N} \frac{\left(\frac{m_i}{\bar\gamma_i}\right)^{\frac{m_i-1}{2}}}{\Gamma(m_i)} \right) \sum_{p=0}^{n_\Sigma} \left(\sum_{w(p,N)} \prod_{i=1}^{N} \Upsilon'_{i,p_i} \right) \frac{\Gamma(2\eta + n_\Sigma - p)}{\left(\sum_{i=1}^{N} \sqrt{\frac{m_i}{\bar\gamma_i}}\right)^{2\eta + n_\Sigma - p}}$$

$$F\left(\eta + \frac{n_\Sigma - p}{2}, \eta + \frac{n_\Sigma - p + 1}{2}, \eta + 1, -\frac{\tau}{\left(\sum_{i=1}^{N} \sqrt{\frac{m_i}{\bar\gamma_i}}\right)^2} \right), \tag{2.38}$$

where $\Upsilon'_{i,p_i} = \left(\Gamma(n_i + 1 + p_i)/\Gamma(n_i + 1 - p_i)\Gamma(p+1)\right) \left(2\sqrt{\frac{m_i}{\bar\gamma_i}}\right)^{-p_i}$.

Notice that (2.38) is expressed in terms of the Gauss hypergeometric function $F(a; b, c; z)$, which is widely available.

2.3.2 M-Ary modulations

An arbitrary rectangular $M_I \times M_J$ QAM signal constellation is assumed to be formed by drawing the in-phase and quadrature components from two independent M-ary pulse amplitude modulation (PAM) schemes, M_I-ary PAM and M_J-ary PAM, respectively. The symbol error probability of the ensuing M-ary rectangular QAM ($M = M_I M_J$) is [17]

$$\begin{aligned} P_e &= 2\left(1 - \frac{1}{M_I}\right) \mathrm{E}\left(Q\left(A\sqrt{\gamma}\right)\right) + 2\left(1 - \frac{1}{M_J}\right) \mathrm{E}\left(Q\left(B\sqrt{\gamma}\right)\right) \\ &\quad - 4\left(1 - \frac{1}{M_I}\right)\left(1 - \frac{1}{M_J}\right) \mathrm{E}\left(Q\left(A\sqrt{\gamma}\right) Q\left(B\sqrt{\gamma}\right)\right), \end{aligned} \tag{2.39}$$

where $A = \sqrt{6/\left((M_I^2 - 1) + (M_J^2 - 1)\zeta\right)}$ and $B = \sqrt{\zeta}A$ where ζ denotes the squared quadrature to in-phase distance ratio. It is seen that the evaluation of (2.39) involves the evaluations of two expectation forms, namely, the expectation of the Gaussian-Q function and the expectation of the product of two Gaussian-Q functions with different arguments. On the basis of the prominent results presented in [12, Eq. (6c)] [2] the expectation of the Gaussian-Q function is obtained

---

2. It should be stressed that [12, Eq. (6c)] has a typo. It should read as in (2.40).

according to

$$\mathrm{E}\left(Q\left(A\sqrt{\gamma}\right)\right)=\frac{1}{2}-\frac{1}{2\pi}\int_0^\infty\frac{\sin\left(A\sqrt{2s}\right)}{s}M_{\gamma^V}(s)ds. \tag{2.40}$$

After substituting $M_{\gamma^V}(s)$ by its expression in (2.34) and making use of the identity

$$\sin\left(A\sqrt{2s}\right)=\sqrt{\frac{\pi A\sqrt{s}}{\sqrt{2}}}J_{\frac{1}{2}}\left(A\sqrt{2s}\right), \tag{2.41}$$

the expectation in (2.40) can be evaluated in closed form using (2.1) according to

$$\mathrm{E}\left(Q\left(A\sqrt{\gamma}\right)\right)=\frac{1}{2}-\frac{2^{N-1}\sqrt{A}}{\sqrt{\pi\sqrt{2}}}\left(\prod_{l=1}^N\frac{\left(\frac{m_l}{\bar{\gamma}_l}\right)^{m_l/2}}{\Gamma\left(m_l\right)}\right)I\left(\frac{m_\Sigma}{2}-\frac{3}{4},\frac{1}{2},A\sqrt{2},\Lambda,\beta\right), \tag{2.42}$$

where $I\left(\cdot,\cdot,\cdot,\cdot,\cdot\right)$ is obtained from (2.13). By properly substituting I by its expression, we obtain

$$\mathrm{E}(Q(A\sqrt{\gamma}))=\frac{1}{2}-\frac{A\left(\prod_{k=1}^N\frac{\left(\frac{m_k\bar{\gamma}_N}{m_N\bar{\gamma}_k}\right)^{m_k}}{\Gamma(m_k)}\right)}{\pi\sqrt{2}}\sum_{i=0}^{N-1}\sum_{\tau(i,N-1)}\Gamma(\xi_q)\Gamma(\xi_q-m_N)\left\{\prod_{k=1}^{N-1}(\frac{m_N\bar{\gamma}_k}{m_k\bar{\gamma}_N})^{m_ki_k}\Gamma(m_k)^{i_k}\Gamma(-m_k)^{1-i_k}\right\}$$

$$F_C^{(N)}\left(\xi_q,\xi_q-m_N,\frac{3}{2},\underbrace{1-m_1,1+m_1}_{i_1},...,\underbrace{1-m_{N-1},1+m_{N-1}}_{i_{N-1}};-\frac{A^2\bar{\gamma}_N}{2m_N},\frac{m_1\bar{\gamma}_N}{m_N\bar{\gamma}_1},...,\frac{m_{N-1}\bar{\gamma}_N}{m_N\gamma_{N-1}}\right), \tag{2.43}$$

where $\xi_q=m_\Sigma+\frac{1}{2}-\sum_{k=1}^{N-1}m_ki_k$.

By substituting A with B in (2.43), we obtain the closed-from solution for the second expectation with argument B in (2.39). Nevertheless, there are some challenges in the evaluation of the expectation of the product of two Gaussian Q-functions with different arguments, a process which involves the integration of the product of two Gaussian Q-functions with different arguments. In [18], the authors sidestepped this hurdle by introducing a simple and accurate exponential approximation of the product of two Gaussian Q-functions with different arguments given by

$$Q(A\sqrt{y})Q(B\sqrt{y})\simeq\sum_{i,j=1}^2c_ic_je^{-\left(A^2b_i+B^2b_j\right)y}, \tag{2.44}$$

where $\{c_i\}=\{\frac{1}{12},\frac{1}{4}\}$ and $\{b_i\}=\{\frac{1}{2},\frac{2}{3}\}$. The accuracy of the above tight upper bound was also discussed in [18]. Based on the above approximation and proceeding by using the McLauren series of $e^{(\cdot)}$ given in [21, Eq. (1.211.1)], it can be easily shown, using [21, Eq. (8.402)], that the expectation of the product of two Gaussian Q-functions with different arguments can be expressed as

$$\mathrm{E}\left(Q(A\sqrt{y})Q(B\sqrt{y})\right)=-\sum_{i,j=1}^2c_ic_j\sqrt{d_{ij}}\int_0^\infty M_{\gamma^V}(s)\frac{J_1\left(2\sqrt{d_{ij}s}\right)}{\sqrt{s}}ds, \tag{2.45}$$

where $d_{ij} = A^2 b_i + B^2 b_j$. Hence, a closed-form expression of (2.45) is obtained, using (2.1), as

$$
\mathrm{E}\left(Q(A\sqrt{y})Q(B\sqrt{y})\right) \simeq -2^N \left(\prod_{l=1}^{N} \frac{\left(\frac{m_l}{\bar{\gamma}_l}\right)^{m_l/2}}{\Gamma(m_l)}\right) \sum_{i,j=1}^{2} c_i c_j \sqrt{d_{ij}} I\left(\frac{m_\Sigma - 1}{2}, 1, 2\sqrt{d_{ij}}, \Lambda, \beta\right). \quad (2.46)
$$

By properly substituting I by its expression in (2.13), (2.46) can be evaluated as

$$
\mathrm{E}\left(Q(A\sqrt{y})Q(B\sqrt{y})\right) \simeq -\left(\prod_{k=1}^{N} \frac{\left(\frac{m_k \bar{\gamma}_N}{m_N \bar{\gamma}_k}\right)^{m_k}}{\Gamma(m_k)}\right) \sum_{i=0}^{N-1} \sum_{\tau(i,N-1)} \Gamma\left(\xi_q + \frac{1}{2}\right) \Gamma\left(\xi_q - m_N + \frac{1}{2}\right) \left\{\prod_{k=1}^{N-1} \left(\frac{m_N \bar{\gamma}_k}{m_k \bar{\gamma}_N}\right)^{m_k i_k}\right.
$$

$$
\left. \Gamma(m_k)^{i_k} \Gamma(-m_k)^{1-i_k}\right\} \sum_{i,j=1}^{2} c_i c_j d_{ij} F_C^{(N)}\left(\xi_q + \frac{1}{2}, \xi_q - m_N + \frac{1}{2}, 2, \underbrace{1-m_1}_{i_1}, \underbrace{1+m_1}_{1-i_1}, ..., \underbrace{1-m_{N-1}}_{i_{N-1}},\right.
$$

$$
\left. \underbrace{1+m_{N-1}}_{1-i_{N-1}}; -\frac{d_{ij}\bar{\gamma}_N}{m_N}, \frac{m_1\bar{\gamma}_N}{m_N\bar{\gamma}_1}, ..., \frac{m_{N-1}\bar{\gamma}_N}{m_N\gamma_{\bar{N-1}}}\right). \quad (2.47)
$$

It is observed that employing (2.44) allows to evaluate (2.45) in closed form. Moreover, owing to the structure of (2.44), the obtained formulas, i.e., (2.43) and (2.47), have similar structures. This fact facilitates further numerical calculations. In the special fading condition corresponding to the case when the fading parameters of the different hops $m_i, i = 1, ..., N$ are odd multiples of one half, alternative simpler expressions of (2.43) and (2.47) could be obtained. In such a setting, applying (2.25) to (2.40) and (2.45), respectively, yields

$$
\mathrm{E}(Q(A\sqrt{\gamma})) = \frac{1}{2} - \frac{A\pi^{\frac{N}{2}-1}}{2^{m_\Sigma + \frac{1}{2}}} \left(\prod_{i=1}^{N} \frac{\left(\frac{m_i}{\bar{\gamma}_i}\right)^{\frac{m_i-1}{2}}}{\Gamma(m_i)}\right) \sum_{p=0}^{n_\Sigma} \left(\sum_{w(p,N)} \prod_{i=1}^{N} \Upsilon'_{i,p_i}\right) \frac{\Gamma(n_\Sigma - p + \frac{3}{2})}{\left(\sum_{i=1}^{N} \sqrt{\frac{m_i}{\bar{\gamma}_i}}\right)^{n_\Sigma - p + \frac{3}{2}}}
$$

$$
F\left(\frac{n_\Sigma - p + \frac{3}{2}}{2}, \frac{n_\Sigma - p + \frac{5}{2}}{2}, \frac{3}{2}, -\frac{A^2}{\left(\sum_{i=1}^{N} \sqrt{\frac{m_i}{\bar{\gamma}_i}}\right)^2}\right), \quad (2.48)
$$

and

$$
\mathrm{E}\left(Q(A\sqrt{y})Q(B\sqrt{y})\right) \simeq -\frac{\pi^{\frac{N}{2}}}{2^{m_\Sigma + 2}} \left(\prod_{i=1}^{N} \frac{\left(\frac{m_i}{\bar{\gamma}_i}\right)^{\frac{m_i-1}{2}}}{\Gamma(m_i)}\right) \sum_{i,j=1}^{2} c_i c_j d_{ij} \sum_{p=0}^{n_\Sigma} \left(\sum_{w(p,N)} \prod_{i=1}^{N} \Upsilon'_{i,p_i}\right)
$$

$$
\frac{\Gamma(n_\Sigma - p + 2)}{\left(\sum_{i=1}^{N} \sqrt{\frac{m_i}{\bar{\gamma}_i}}\right)^{n_\Sigma - p + 2}} F\left(\frac{n_\Sigma - p}{2} + 1, \frac{n_\Sigma - p + 1}{2} + 1, 2, -\frac{d_{ij}}{(\sum_{i=1}^{N} \sqrt{\frac{m_i}{\bar{\gamma}_i}})^2}\right). \quad (2.49)
$$

Then, properly substituting (2.48) and (2.49) into (2.39) yields the error probability expression for multi-hop AF transmissions using an arbitrary M-QAM modulation over Nakagami-m fading

with an odd multiple of one half fading parameter as

$$P_e = \left(1 - \frac{1}{M_I}\right) + \left(1 - \frac{1}{M_J}\right) - \frac{\pi^{\frac{N}{2}-1}}{2^{m_\Sigma + \frac{1}{2}}}\left(\prod_{i=1}^{N} \frac{\left(\frac{m_i}{\bar{\gamma}_i}\right)^{\frac{m_i-1}{2}}}{\Gamma(m_i)}\right) \sum_{p=0}^{n_\Sigma}\left(\sum_{w(p,N)}\prod_{i=1}^{N}\Upsilon'_{i,p_i}\right)\left\{\left(1 - \frac{1}{M_I}\right) \times \right.$$

$$\frac{A\Gamma\left(n_\Sigma - p + \frac{3}{2}\right)}{\left(\sum_{i=1}^{N}\sqrt{\frac{m_i}{\bar{\gamma}_i}}\right)^{n_\Sigma - p + \frac{3}{2}}} F\left(\frac{n_\Sigma - p + \frac{3}{2}}{2}, \frac{n_\Sigma - p + \frac{5}{2}}{2}, \frac{3}{2}, -\frac{A^2}{\left(\sum_{i=1}^{N}\sqrt{\frac{m_i}{\bar{\gamma}_i}}\right)^2}\right) + \left(1 - \frac{1}{M_J}\right) \times$$

$$\frac{B\Gamma\left(n_\Sigma - p + \frac{3}{2}\right)}{\left(\sum_{i=1}^{N}\sqrt{\frac{m_i}{\bar{\gamma}_i}}\right)^{n_\Sigma - p + \frac{3}{2}}} F\left(\frac{n_\Sigma - p + \frac{3}{2}}{2}, \frac{n_\Sigma - p + \frac{5}{2}}{2}, \frac{3}{2}, -\frac{B^2}{\left(\sum_{i=1}^{N}\sqrt{\frac{m_i}{\bar{\gamma}_i}}\right)^2}\right) - \sqrt{2}\pi\left(1 - \frac{1}{M_I}\right)\left(1 - \frac{1}{M_J}\right) \times$$

$$\frac{\Gamma\left(n_\Sigma - p + 2\right)}{\left(\sum_{i=1}^{N}\sqrt{\frac{m_i}{\bar{\gamma}_i}}\right)^{n_\Sigma - p + 2}} \sum_{i,j=1}^{2} c_i c_j d_{ij} F\left(\frac{n_\Sigma - p}{2} + 1, \frac{n_\Sigma - p + 1}{2} + 1, 2, -\frac{d_{ij}}{\left(\sum_{i=1}^{N}\sqrt{\frac{m_i}{\bar{\gamma}_i}}\right)^2}\right)\right\}. \quad (2.50)$$

For an arbitrary $M_I \times M_J$ rectangular QAM constellation with Gray encoding, the error probability evaluation only involves taking the expectation of the Gaussian-Q function [19, Eq. (22)] according to

$$P_e = \frac{2}{\log_2(M_I \cdot M_J)}\left(\frac{1}{M_I}\sum_{k=1}^{\log_2(M_I)(1-2^{-k})M_I - 1}\sum_{i=0}^{} P(i,k)\mathrm{E}\left(Q\left(\sqrt{2w_i\gamma}\right)\right) + \right.$$

$$\left.\frac{1}{M_J}\sum_{p=1}^{\log_2(M_J)}\sum_{j=0}^{(1-2^{-p})M_J - 1} P(j,p)\mathrm{E}\left(Q\left(\sqrt{2w_j\gamma}\right)\right)\right), \quad (2.51)$$

where $w_k = (2k+1)^2\left(3\log_2(M_I \cdot M_J)/\left(M_I^2 + M_J^2 - 2\right)\right)$ and $P(i,j)$ are expressions of M_I and M_J given in [19]. In this case, using (2.42), we immediately obtain a closed-form expression for the error probability as

$$P_e = 1 - \frac{2^N}{\sqrt{\pi}\log_2(M_I M_J)}\left(\prod_{l=1}^{N}\frac{\left(\frac{m_l}{\bar{\gamma}_l}\right)^{\frac{m_l}{2}}}{\Gamma(m_l)}\right)\left(\frac{1}{M_I}\sum_{k=1}^{\log_2(I)(1-2^{-k})I - 1}\sum_{i=0}^{} P(i,k)\sqrt{w_i}I\left(\frac{m_\Sigma - 3/2}{2}, \frac{1}{2}, 2\sqrt{w_i}, \Lambda, \beta\right) + \right.$$

$$\left.\frac{1}{M_J}\sum_{p=1}^{\log_2(M_J)}\sum_{j=0}^{(1-2^{-p})M_J - 1} P(j,p)\sqrt{w_j}I\left(\frac{m_\Sigma - 3/2}{2}, \frac{1}{2}, 2\sqrt{w_j}, \Lambda, \beta\right)\right). \quad (2.52)$$

An alternative simpler expression of (2.52) is also obtained using (2.48).

2.4 Dual-hop AF transmission over non-identical Nakagami-m fading

In some practical applications, a dual-hop transmission, i.e., $N = 2$, may be sufficient [2]. In this context, many authors have considered the error probability evaluation over non-identical Nakagami-m fading. So far, closed-form expressions are only available for integer values of the fading parameter, i.e. $m_i, i = 1, 2 \in N$ [4], [5]. Nevertheless, in practical scenarios, the m parameters often take non-integer values [13]. In this work, we derive the error probability expressions in the m-complementary region of [4], i.e. $R \backslash N$. This allows applications of our analytical results over a larger range of the fading parameter values, thereby highlighting again the significance of this work. Using (2.18), the bit error probability for binary modulation of an AF dual-hop transmission is obtained as

$$P_e = \frac{1}{2} - \frac{\left(\frac{\tau\bar{\gamma}_2}{m_2}\right)^\eta \left(\frac{m_1\gamma_2}{m_2\bar{\gamma}_1}\right)^{m_1}}{\eta B(m_2, \eta)} \left\{ \frac{B(m_1+\eta, -m_1)}{B(m_2+\eta, m_1)} F_4\left(m_1+m_2+\eta, m_1+\eta, 1+\eta, 1+m_1, -\frac{\tau\bar{\gamma}_2}{m_2}, \frac{m_1\gamma_2}{m_2\bar{\gamma}_1}\right) + \right.$$

$$\left. \left(\frac{m_2\bar{\gamma}_1}{m_1\bar{\gamma}_2}\right)^{2m_1} F_4\left(m_2+\eta, \eta, 1+\eta, 1-m_1, -\frac{\tau\bar{\gamma}_2}{m_2}, \frac{m_1\bar{\gamma}2}{m_2\bar{\gamma}_1}\right) \right\}. \tag{2.53}$$

where $B(a, b) = \Gamma(a)\Gamma(b)/\Gamma(a + b)$ is the beta function [21, Eq. (8.384.1)]. The above new expression of the bit error probability is valid for any non-integer value of $m_i, i = 1, 2$. Another case, also not handled before, corresponds to identical ratios $\{m_l/\bar{\gamma}_l\}_{l=1}^2$ across the different hops, a scenario which includes as well the identically distributed fading [2], [3] as a special case. Defining $m/\bar{\gamma} = \{m_l/\bar{\gamma}_l\}_{l=1}^2$ and applying (2.27) yield

$$P_e = \frac{1}{2} - \frac{\left(\frac{m}{\tau\bar{\gamma}}\right)^{\frac{m_1+m_2}{2}} \sqrt{\pi}}{\Gamma(\eta)\Gamma(m_1)\Gamma(m_2)} G_{4,4}^{4,1}\left(\frac{4m}{\tau\bar{\gamma}} \left| \begin{matrix} 1-\eta-\frac{m_1+m_2}{2}, 0, \frac{1}{2}, 1-\frac{m_1+m_2}{2} \\ \frac{m_1+m_2}{2}, \frac{m_1-m_2}{2}, \frac{m_2-m_1}{2}, -\frac{m_1+m_2}{2} \end{matrix} \right. \right). \tag{2.54}$$

By setting $m = m_1 = m_2$ and $\eta = \tau = 1$, we obtain an equivalent alternative representation for Hasna and Alouini's main result [2, Eq. (12)]. To prove the concordance of the two formulas, we use the Meijer's-G function property in [21, Eq. (9.31.1)] along with the identity

$$G_{3,3}^{3,1}\left(z \left| \begin{matrix} a, c, a+1 \\ b, d, a \end{matrix} \right. \right) = \frac{\Gamma(b-1)\Gamma(d-1)}{\Gamma(c-a)} z^a \left(1 - {}_2F_1\left(b-a, d-a, c-a, -\frac{1}{z}\right)\right). \tag{2.55}$$

For completeness, it is worthwhile to mention that [2, Eq. (12)] can also be deduced from (2.53) by applying the analytical continuation formula of the Lauricella function followed by some

algebraic manipulations using the Burchnall formulas [20, Eq. (37)],

$$F_4(\alpha, \beta; \gamma, \gamma'; x, x) = {_4}F_3\left(\alpha, \beta, \frac{1}{2}(\gamma + \gamma'), \frac{1}{2}(\gamma + \gamma' - 1); \gamma, \gamma, \gamma + \gamma' - 1; 4x\right),\tag{2.56}$$

where $_pF_q(\cdot)$ is the generalized hypergeometric function [21, Eq. (9.14.1)]. In turn, the generalized hypergeometric function $_4F_3$ reduces to a simpler one when its parameters are constrained properly as

$$_4F_3\left(a_1, a_2, a_3, a_4; b_1, a_3, a_4, z\right) = {_2}F_1\left(a_1, a_2, b_1, z\right),\tag{2.57}$$

where $F(a, b, c, z)$ is the Gauss hypergeometric function [21, Eq. (9.14.2)]. Hence, applying (2.17), (2.56) and (2.57) to (2.53), when $m = m_1 = m_2, \bar{\gamma} = \bar{\gamma}_1 = \bar{\gamma}_2$ and $\eta = \tau = 1$, yields [2, Eq. (12)].

For M-ary modulations and still using I_s in (2.18), the expectation of the Gaussian-Q function in (2.42), reduces when $N = 2$ to

$$\mathrm{E}(Q(A\sqrt{\gamma})) = \frac{1}{2} - \frac{\sqrt{A\bar{\gamma}_1}}{\sqrt{m_1}B(\frac{1}{2}, m_2)}\left[\left(\frac{m_2\bar{\gamma}_1}{m_1\bar{\gamma}_2}\right)^{m_2}\frac{B(m_2 + \frac{1}{2}, -m_2)}{B(m_2 + \frac{1}{2}, m_1)}F_4\left(m_1 + m_2 + \frac{1}{2}, m_2 + \frac{1}{2}, \frac{3}{2}, 1 + m_2,\right.\right.$$

$$\left.\left. -A\frac{\bar{\gamma}_1}{m_1}, \frac{m_2\bar{\gamma}_1}{m_1\bar{\gamma}_2}\right) + F_4\left(m_1 + \frac{1}{2}, \frac{1}{2}, \frac{3}{2}, 1 - m_2, -A\frac{\bar{\gamma}_1}{m_1}, \frac{m_2\bar{\gamma}_1}{m_1\bar{\gamma}_2}\right)\right].\tag{2.58}$$

Moreover, when identical ratios $m/\bar{\gamma} = \{m_l/\bar{\gamma}_l\}_{l=1}^2$ are observed across the two hops, the expectation of the Gaussian-Q functions can be rewritten according to (2.27) as

$$\mathrm{E}(Q(A\sqrt{\gamma})) = \frac{1}{2} - \frac{1}{\Gamma(m_1)\Gamma(m_2)}\left(\frac{2m}{A^2\bar{\gamma}}\right)^{\frac{m_1+m_2}{2}}G_{4,4}^{4,1}\left(\frac{8m}{A^2\bar{\gamma}}\,\middle|\,\begin{matrix}\frac{1}{2} - \frac{m_1+m_2}{2}, 0, \frac{1}{2}, 1 - \frac{m_1+m_2}{2}\\ \frac{m_1+m_2}{2}, \frac{m_1-m_2}{2}, \frac{m_2-m_1}{2}, -\frac{m_1+m_2}{2}\end{matrix}\right).\tag{2.59}$$

Moreover, the expectation of the product of two Gaussian-Q functions with different arguments can be derived as

$$\mathrm{E}(Q(A\sqrt{\gamma})Q(B\sqrt{\gamma})) \approx -2\sqrt{\pi}\sum_{i,j=1}^2 c_ic_j\frac{\left(\frac{m}{d_{ij}\bar{\gamma}}\right)^{\frac{m_1+m_2}{2}}}{\Gamma(m_1)\Gamma(m_2)} \times$$

$$G_{4,4}^{4,1}\left(\frac{4m}{d_{ij}\bar{\gamma}}\,\middle|\,\begin{matrix}-\frac{m_1+m_2}{2}, 0, \frac{1}{2}, 1 - \frac{m_1+m_2}{2}\\ \frac{m_1+m_2}{2}, \frac{m_1-m_2}{2}, \frac{m_2-m_1}{2}, -\frac{m_1+m_2}{2}\end{matrix}\right).\tag{2.60}$$

The derivation of the error probability expression of M-QAM modulations is then straightforward using (2.39).

2.5   Computational methods and numerical examples

The aim of this section is to analyze the utility, accuracy, and numerical stability of the frameworks developed in the previous sections. All the results shown here have been analytically obtained by the direct evaluation of the expressions developed in this paper : either (2.37), (2.43), (2.47), (2.53), (2.59) and (2.60) for non-integer values of m, or (2.38), (2.48), (2.49) for integer plus one half values. The evaluation of these formulas involves the computation of some special hypergeometric functions, namely, the hypergeometric Lauricella functions.

2.5.1   Computational methods

The third Lauricella function $F_C^{(n)}$ is typically computed with a finite summation approximating the infinite summation given in (2.15) as

$$F_C^{(n)}(a, b; c_1, ..., c_n; x_1, ..., x_n) = \sum_{q=0}^{q_{max}} (a)_q (b)_q \sum_{\Omega(q,n)} \prod_{k=1}^{n} \frac{x_k^{q_k}}{(c_k)_{q_k} q_k!}, \tag{2.61}$$

where $\Omega(q, n)$ is the set of n-tuples such that $\Omega(q, n) = \{(q_1, ..., q_n) : q_k \in \{0, 1, ..., q\}, \sum_{k=1}^{n} q_k = q\}$. If a large q_{max} is required to obtain the desired accuracy, then (2.61) may have a high computational complexity. However, by reformulating the integral form of the Lauricella function in (2.12) such that it encompasses a term of $\exp(-t)$ [17, Ch. 2], the integral in (2.12) can be evaluated using the numerical integration method given in [18, Eq. (25.4.45)] for a variety of fading channel models. Then, one obtains

$$F_C^{(n)}(a, b; c_1, ..., c_n; x_1, ..., x_n) \approx \frac{\cos(\pi(a-b))}{2^{a+b-2}\Gamma(a)\Gamma(b)} \sum_{k=1}^{N_p} w_k t_k^{a+b-1} G_{1,2}^{2,1} \left(2t_k \left| \begin{matrix} \frac{1}{2} \\ b-a, a-b \end{matrix} \right. \right)$$
$$\left(\prod_{k=1}^{n} {}_0F_1\left(; c_k, x_k \frac{t_k^2}{4} \right) \right), \tag{2.62}$$

where t_k and w_k are, respectively, the k-th zero and weight of the Laguerre polynomial of order N_p [18, Eq. (25.4.45)]. Numerical results show that for $N_p = 30$, this approximation provides a relative error for the average error rate below 0.3%.

Notice that the other hypergeometric functions involved in this paper, namely, the Meijer's-G, Gauss hypergeometric and Appel functions are implemented in most popular computing softwares such as Matlab and Mathematica.

2.5.2 Numerical results

In Fig. 1 we have reported the bit error probability induced by 16-QAM and QPSK modulations in a multihop variable gain relaying system with $N = 2, 4$. The identical and non-identical distributed fading cases are analyzed with an overall system fading severity $m_\Sigma = \sum_{i=1}^{N} m_i$ fixed to N. For the identical Nakagami case, all the hops undergo Rayleigh fading with $m_i = 1, i = 1, ..., N$. For the non-identical case, the different hops may be subject to worse or better fading conditions than the identical case, such as $m_i \in \{0.5, 1.5\}_{i=1,...,N}$. Since our analysis is only valid for non-integer fading parameters, then all the Rayleigh-case results were obtained using [22, Eq. (14)]. The error performance of the non-identical case are computed using (2.48) and (2.52) as well as the comparison with simulations. We can see a very good match over the range of SNRs of interest. As expected, we can observe that the error probability increases with the number of hops. It turns out that, although the overall system fading severity is the same, better performances are achieved when the different hops undergo identical fading. This is due to the fact that the AF multihop channel is a cascaded one and can be modeled as the product of N statistically independent Nakagami-m fading amplitudes. Therefore, the effect of a bad fading condition in one hop deteriorates the overall system performance even in the presence of a better fading condition in the following or preceding hops. Hence, the relay link is dominated by the more severely faded hop. This comment further corroborates the generality and usefulness of the analytical frameworks introduced in this paper, since real multihop channels are most likely non-identically distributed.

For multihop systems with variable gain relays under identical Nakagami fading with non-integer m, the error probability results are plotted in Fig. 2 for BFSK modulation. The BEP computations were performed using (2.37) and the computational methods in (2.62). As expected, the error performance improves as the fading severity decreases. In Fig. 3 we investigate the effect of power imbalance between the hops in a dual-hop BPSK transmission over non-identical Nakagami-m fading. The error probability is plotted against the first hop average SNR for $m_1 = m_2 = 1.5$ and $m_1 = 0.7$ and $m_2 = 1.5$. The higher average SNR resulting from one of the relays may be due to a Line Of Sight (LOS) signal component between the source terminal and the relay, or equivalently between the relay and the destination. Such a situation may occur in a cell-site scheme. Here, good accuracy is retained by the analytical models (2.53), which turn out to be not only very accurate but also numerically stable. Moreover, we can easily figure out that,

such imbalance may be either beneficial or harmful for the overall system performance. Indeed, for $\bar{\gamma}_2 > \bar{\gamma}_1$, it is advantageous compared to the balanced case, otherwise, it is detrimental.

Fig. 4 compares the exact bit error probabilities of BPSK multihop systems with variable-gain relays with the lower bound given in [8, Eq.(25)]. It can be seen that the proposed bounds lose their tightness with increasing SNR and, therefore, are definitely inappropriate for the estimation of the error performance of multi-hop systems operating over non-identical Nakagami fading. This was also stipulated by the authors of [8].

Overall, the aforementioned numerical results unambiguously confirm the high accuracy and huge utility of the proposed framework for error probability analysis of AF multi-hop systems over not necessarily identical Nakagami-m fading conditions.
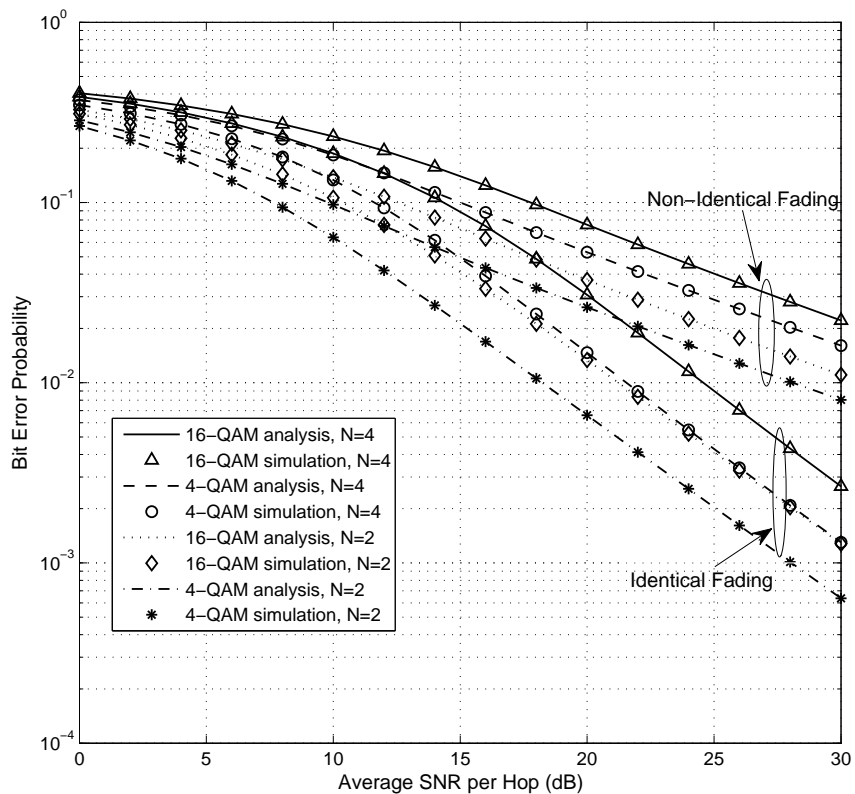
FIGURE 2.1 – Bit error probabilities for different QPSK and 16-QAM AF multihop transmission systems with variable-gain relays in identical and non identical Nakagami-m fading.
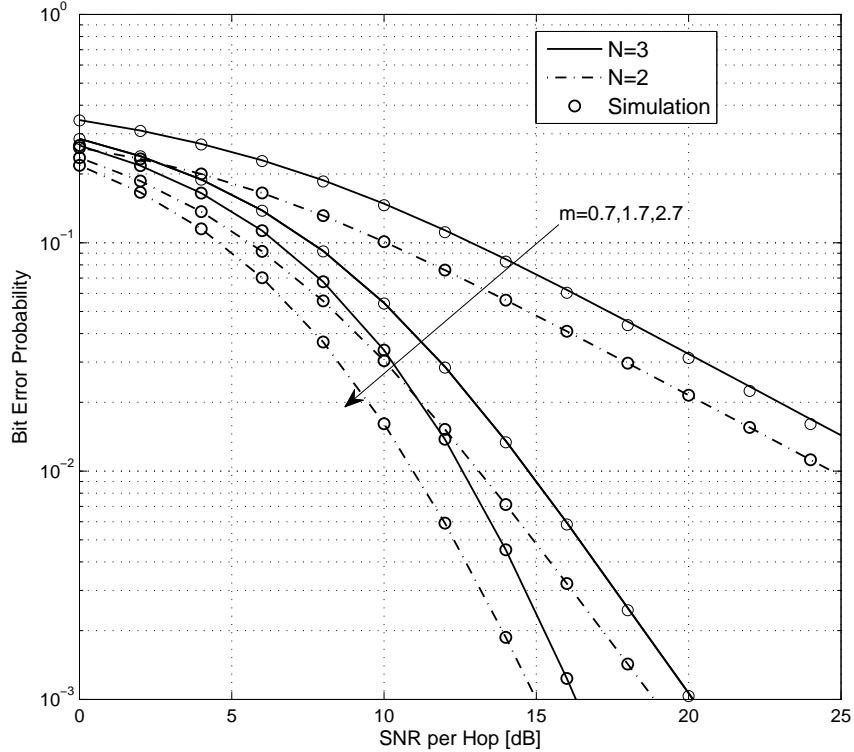
FIGURE 2.2 – Bit error probabilities vs. average SNR per hop for BFSK and different values of the fading parameter and number of hops $N = 2, 3$.

2.6 Conclusion

In this paper, we have developed an analytical framework for the analysis of error probabilities of AF multihop variable gain relaying systems over Nakagami-m fading channels. The numerical examples show the accuracy and usefulness of the proposed new error probability expressions along three main contributions :

1. We have proposed new solutions for infinite integral forms involving the product of Bessel functions. Theses solutions have been shown useful to the evaluation of the error probabilities of multihop systems with arbitrary number of variable-gain relays operating over Nakagami-m fading. The obtained formulas establish a connection, hitherto unknown, between the error probabilities and the Lauricella's functions.

2. In the special case of an odd multiple of one half fading parameters, simpler expressions for the error probabilities, involving the Gauss hypergeometric function, have been obtained.
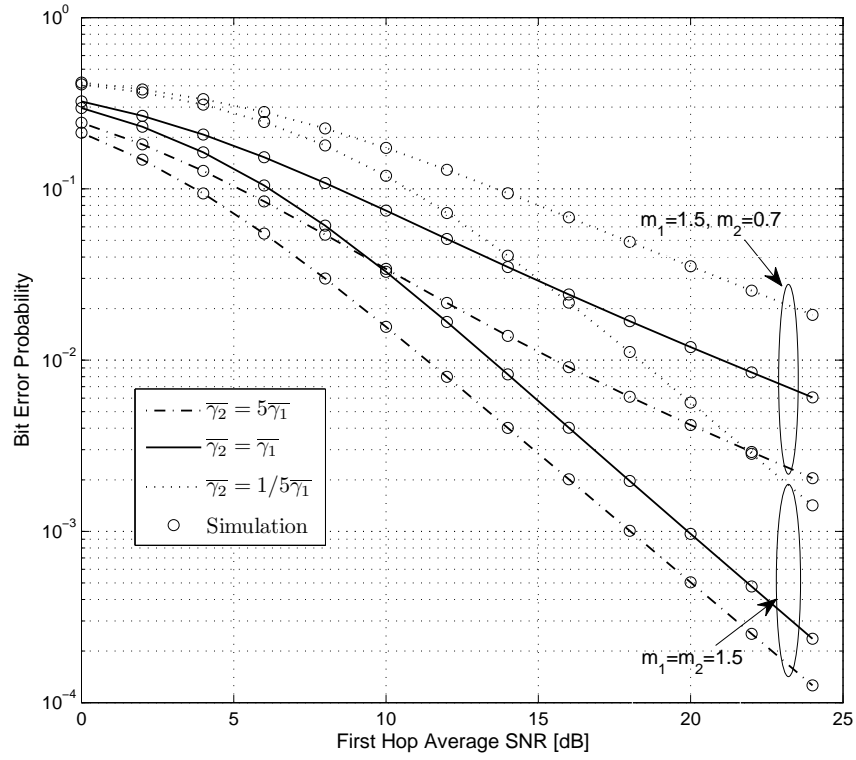
FIGURE 2.3 – Bit error probabilities for different BPSK AF multihop transmission systems with variable-gain relays over non identical Nakagami fading with unbalanced SNR.

3. As far as the dual-hop case is concerned, it is shown in this special case of interest that the new error probability formulas reduce to previously known results in the literature. Moreover, these new formulas generalize previously known results pertaining to AF transmissions over non-identical fading with integer parameter.
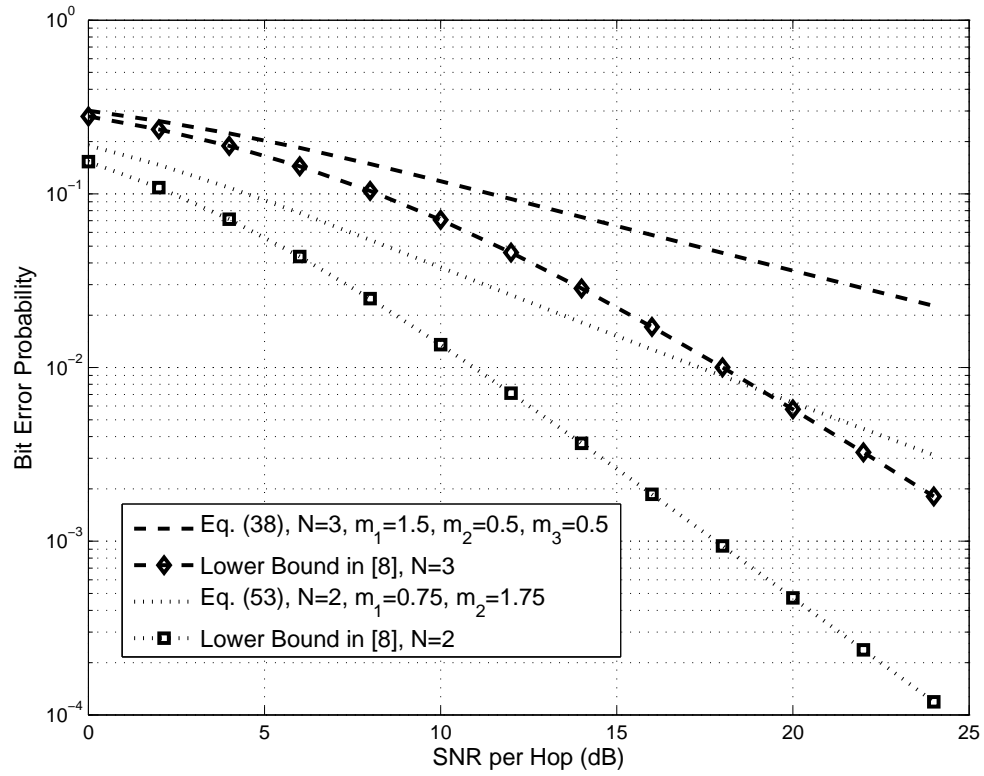
FIGURE 2.4 – Comparison between the exact bit error probability and the lower bound given in [8] for different BPSK AF multihop relaying systems with variable gain relays.

Bibliographie

[1] J.N. Laneman, D.N.C. Tse, and G.W. Wornell, " Cooperative diversity in wireless networks : efficient protocols and outage behaviour," *IEEE Trans. Inform. Theory,* vol. 50, pp. 3062-3080, Dec. 2004.

[2] M.O. Hasna and M.-S. Alouini, "Harmonic mean and end-to-end performance of transmission systems with relays," *IEEE Trans. Commun.,*vol. 52, pp. 130-135, Jan. 2004.

[3] M. O. Hasna and M. S. Alouini, "Outage Probability of Multihop Transmission over Nakagami Fading Channels," *IEEE Commun. Lett.,* vol. 7, no. 5, pp. 1963-1968, May 2003.

[4] D. Senaratne and C. Tellambura, "Unified exact performance analysis of two hop amplify and forward relaying in Nakagami fading," *IEEE Trans. Veh. Technol.*, Vol. 59, No. 3, pp. 1529-1534, March 2010.

[5] H. A. Suraweera and G. K. Karagiannidis, "Closed-form error analysis of the non-identical Nakagami-m relay fading channel," *IEEE Commun. Lett., vol.* 12, no. 4, pp. 259-261, Apr. 2008.

[6] B. Maham and A. Hjorungnes, "Asymptotic performance analysis of amplify-and-forward cooperative networks in a Nakagami-m fading environment," *IEEE Commun. Lett. ,* vol. 13, no 5, pp. 300-302, May 2009.

[7] S. S. Ikki and M. H. Ahmed, "Performance analysis of cooperative diversity wireless networks over Nakagami-m fading channel", *IEEE Commun. Lett.,* vol. 11, no. 4, pp. 334-336, Apr. 2007.

[8] G.K. Karagiannidis, T.A. Tsiftsis, and R.K. Mallik, "Bounds of multihop relayed communications in Nakagami-m fading," *IEEE Trans. Commun.,* vol. 54, pp. 18-22, Jan. 2006

[9] M. Di Renzo, F. Graziosi, and F. Santucci, "A unified framework for performance analysis of CSI-assisted cooperative communications over fading channels", *IEEE Trans. Commun.*, Vol. 57, No. 9, pp. 2552-2557, September 2009.

[10] M. Di Renzo, F. Graziosi, F. Santucci, "A comprehensive framework for performance analysis of dual-hop cooperative wireless systems with fixed-gain relays over generalized fading channels", *IEEE Trans. Wireless Commun.*, Vol. 8, No. 10, pp. 5060-5074, October 2009.

[11] M. Di Renzo, F. Graziosi, and F. Santucci, "A comprehensive framework for performance analysis of cooperative multi-Hop wireless systems over log-normal fading channels", *IEEE Trans. Commun.*, Vol. 58, No. 2, pp. 531-544, February 2010.

[12] G. Farhadi and N. C. Beaulieu, "A general framework for symbol error probability analysis of wireless systems and its application in Amplify-and-Forward Multihop Relaying", *IEEE Trans. Veh. Technol.*, vol. 59, no. 3, pp. 1505-1511, March 2010.

[13] R. Lorenzo, R. Juan, and C. Narcis, "Evaluation of Nakagami fading behaviour based on measurements in urban scenarios," *AEU INT. J. Electron. and Commun.*, vol. 61, no. 2, pp. 135-138, Feb. 2007.

[14] H. Exton, *Multiple Hypergeometric Functions and Applications*; New York : Jhon wiley, 1976.

[15] I.S. Gradshteyn and I.M. Ryzhik, *Table of Integrals, Series and Products,* 5th Ed., San Diego, CA : Academic, 1994.

[16] A. P. Prudnikov, Y. A. Brychkov, and O. I. Marichev, *Integrals and Series : More Special Functions*, Gordon and Breach Science, 1990, vol. 3, translated from the Russian by G. G. Gould.

[17] M.K. Simon, M.-S. Alouini, *Digital Communication over Fading Channels,* Second Ed., Wiley, New York, 2004.

[18] H.A. Suraweera and J. Armstrong, " A simple and accurate approximation to the SEP of rectangular QAM in arbitrary Nakagami-m fading channels", *IEEE Commun. Lett.,* vol. 11, no. 5, pp. 426-428, May 2007.

[19] K. Cho and D. Yoon, "On the general BER expression of one and two dimensional amplitude modulations," *IEEE Trans. Commun.,* vol. 50, pp. 1074-1080, July 2002.

[20] J.L. Burchnall, Quart. J. Math., Oxford Ser. vol.13, 1942.

[21] M. Abramowitz and I. A. Stegun, *Handbook of Mathematical Functions with Formulas, Graphs, and Mathematical Tables,* 10th ed. New York : Dover, 1972.

[22] R. H. Y. Louie, Y. Li, and B. Vucetic, "Performance analysis of beamforming in two hop amplify and forward relay networks with antenna correlation," *IEEE Trans. Wireless Commun.*, Vol. 8, No. 6, pp. 3132-3141, June 2009.

Chapitre 3

Ergodic Capacity Analysis for Interference-Limited AF Multi-Hop Relaying Channels in Nakagami-m Fading

Imène Trigui, Sofiène Affes, and Alex Stéphenne

Résumé : Ce chapitre examine les effets des interférences co-canal sur des systèmes de communication à sauts multiples subissant un évanouissement Rayleigh. Les expressions de la capacité érgodique exacte et de sa forme réduite à haut RSB sont présentées sous des formes élégantes et aisément interpretables. Il a été prouvé que les résultats obtenus sont valides pour des configurations arbitraires du système. Tous ces résultats sont verifiés par des simulations numériques.

Abstract

An analytical characterization of the ergodic capacity of interference-limited multihop wireless networks with amplify-and forward (AF) relaying is presented. In our analysis, we consider that transmissions are performed over Nakagami-m fading where channel state information is only known at the receiving terminals. We derive an exact expression for the ergodic capacity by exploiting the moment generating function (MGF) of the inverse signal-to-interference ratio (SIR). The result is applicable for arbitrary numbers of interfering signals at the receiving terminals and can be efficiently evaluated. Furthermore, considering the special case of dual-hop transmission, we propose a more refined characterization where the high-SIR capacity is expanded as an affine function. The zero-order term or the power offset for which we find insightful closed-form expressions, is shown to play a chief role in understanding the impact of interference and power on the system's capacity. Finally, some simulation results sustaining our analysis are provided.

3.1 Introduction

Multihop communications have been an outstanding topic of research in the last years due to their ability to provide broader coverage and higher reliability for many wireless communication systems (see e.g., [1] and [2] and references therein). The key advantage of relaying is to enable high capacity where traditional architectures are unsatisfactory due to location constraints (e.g., cell-edge, shadowing, indoor), leading to a more homogenous user experience. Depending on the nature and complexity of the relaying technique, relay nodes can be broadly categorized as either amplify and forward (AF) or decode and forward (DF) [1]. While AF relays act as repeaters, DF relays decode and recode the received signal prior to forwarding it to the receiver, thereby implying a larger delay than with a simple repeater.

In the open literature, several works investigating multihop communications exist (cf. [1]- [5] and references therein). Despite their importance, many of the existing results have been based on the assumption that the system is thermal-noise limited. However, relaying-access capacity is also affected by strong co-channel interference (CCI) due to the aggressive frequency reuse in cellular networks. Cochannel interference, which is an essential feature of wireless networks, can cause more severe performance degradation than thermal noise in many wireless networks.

Apart from the very recent works of [9] and [7], most of the performance analysis of multihop systems in the presence of interference has been restricted to dual-hop relay systems. In this case, contributions range from the analysis of interference-limited relay [3] or destination [4], [5] scenarios, to multiple interferers at both sides [5]. In this context, multiple closed-form expressions for the outage and error probabilities were derived. As far as the multihop case is considered, [9] analyzed the effect of co-channel interference assuming Rayleigh fading interfering signals affecting the relays. Specifically, the outage and error probabilities were investigated. An extension of [9] to the Nakagami-m fading scenario has been carried out in [7]. From the aforementioned up-to-date technical literature, it is fairly evident that this large number of contributions provide either outage or bit error rate analysis and that the ergodic capacity is almost unexplored from the analytical point of view.

This paper goes toward filling this gap by deriving a new exact analytical expression and insightful closed-form high-SIR approximations for the ergodic capacity of channel-assisted AF multihop relay systems in interference-limited Nakagami-m fading. It turns out that the ergodic capacity belongs to a special class of generalized hypergeometric series. These are the first Lauricella's multivariate hypergeometric functions of $N+1$ variables $\mathrm{F}_{\mathrm{A}}^{(\mathrm{N}+1)}$ [12], where N is the number of multihop links. This result is subsequently employed to derive simplified closed-form expressions for the ergodic capacity in the high-SIR regime.

Based on our analytical expressions, we investigate the impact of the prominent interference-relay channel features on the ergodic capacity. In the high-SIR regime, we present simple closed-form expressions for the key capacity parameters; the high-SIR slope and the high-SIR power offset. Whilst the former is fixed, the latter is a more intricate function capturing all the interference-relay channel features, namely the interferers number, the power gain and the fading severity.

The remainder of this paper is organized as follows : In Section II, the basic definitions and background related to multihop AF relaying suffering interference are provided. In section III, a closed-form expression for the the ergodic capacity of interference-limited multihop systems subject to Nakagami-m fading is derived. In Section VI, this general closed-form expression is reduced in the dual-hop case to an elegant and simple expression that is suitable for the high-SIR regime. Section V assesses the performance analysis by numerical examples. Finally, some concluding remarks are presented in Section VI.

3.2 Interference-limited relaying : system model

Let us consider a communication system where several AF relays $\{R_n, n = 1, N - 1\}$ are employed to assist a generic transmitter send an encoded message to a remote destination. We assume that the relays and the destination are affected by $\{L_n, n = 1, N\}$ co-channel interferers (CCI). At the n-th time slot, the n-th relay node R_n receives a faded signal from the immediately preceding transmitting terminal R_{n-1} and L_n faded co-channel interfering signals written as

$$y_n = \sqrt{E_{n-1}} h_n x_{n-1} + \sqrt{E_{I_n}} \sum_{l=1}^{L_n} c_{l,n} g_{l,n}, \tag{3.1}$$

where h_n denotes the fading gain of the channel between terminals R_{n-1} and R_n, following a flat Nakagami-m fading distribution; x_{n-1} denotes the unit-energy signal transmitted from the $(n-1)$th node; and E_{n-1} indicates the transmit energy from the said node. In the second term of the right-hand-side (RHS) of (3.1), $c_{l,n}$ is the l-th cochannel interferer's signal affecting the nth relay with energy equal to E_{I_n}, and $g_{l,n}$ is the flat Nakagami-m fading coefficient of the l-th interference channel affecting the nth relay. In an interference-limited wireless communication system, the effect of additive white Gaussian noise can usually be neglected. Interference-limited scenarios, in fact, are very relevant to modern cellular systems, which tend to operate precisely in such conditions.

The amplification process at the nth relay consists of generating the signal $x_n = (\frac{1}{\sqrt{E_{n-1}|h_n|^2}}) y_n$ and transmitting it to the next node. In this case, a relay just amplifies the incoming signal with the inverse of the channel of the previous hop, regardless of the interference level of that hop.

By following the same procedure as in [9], the end-to-end signal-to-interference ratio (SIR) at the destination can be obtained as [7], [4]

$$\gamma = \left[\sum_{n=1}^{N} \frac{\sum_{l=1}^{L_n} Z_{l,n}}{Y_n} \right]^{-1} = \left[\sum_{n=1}^{N} \frac{1}{\gamma_n} \right]^{-1}, \tag{3.2}$$

with $Y_n = E_{n-1}|h_n|^2$ being the fading amplitude of the desired signal at the n-th node and $Z_{l,n} = E_{I_n}|g_{l,n}|^2; l = 1, \ldots, L_n, n = 1, \ldots, N$ being the instantaneous power of the l-th interferer to the n-th node. Accordingly, γ_n represents the instantaneous SIR at the n-th hop. Hereafter, we consider that the cooperative links undergo independent and non-identically distributed (i.n.i.d.) Nakagami-m fading with arbitrary fading parameters and arbitrary average powers. Nonetheless, for the sake of simplicity, we assume that the interference links are subject

to identically-distributed Nakagami-m fading. Thus, Y_n and $\tilde{Z}_n = \sum_{l=1}^{L_n} Z_{l,n}$, follow a Gamma distribution with probability density functions given by

$$
\begin{aligned}
p_{Y_n}(y) &= \frac{m_{r,n}^{m_{r,n}}}{\Gamma(m_{r,n})\Omega_{r,n}^{m_{r,n}}} y^{m_{r,n}-1} \exp\left(-\frac{m_{r,n}y}{\Omega_{r,n}}\right) \\
p_{\tilde{Z}_n}(z) &= \frac{m_{I,n}^{L_n m_{I,n}} z^{L_n m_{I,n}-1}}{\Gamma(L_n m_{I,n})\Omega_{I_n}^{L_n m_{I,n}}} \exp\left(-\frac{m_{I,n}z}{\Omega_{I,n}}\right),
\end{aligned}
\tag{3.3}
$$

where $\Gamma(\cdot)$ is the Gamma function [21, Eq.(8.310.1)]. Furthermore in (3.3), $m_{r,n}$ and $\Omega_{r,n}$ are, respectively, the Nakagami fading parameter and the average power of the desired signal at the n-th relay. Similarly, $m_{I,n}$ and $\Omega_{I,n}$ are the Nakagami fading parameter and the average power of each interfering signal at the n-th relay, respectively. The total interference at each hop $\tilde{Z}_n$ is the sum of L_n independent Gamma distributed random variables with parameters $L_n m_{I,n}$ and $L_n \Omega_{I,n}$. The average SIR of each interferer at the n-th relay is defined as $\Lambda_n \triangleq \Omega_{r,n}/\Omega_{I,n}$.

3.3 Multihop performance

Capacity analysis is of extreme importance in the design of wireless systems since it determines the maximum achievable rates in the network. A reliable capacity performance study has to take into account important issues such as co-channel interference. In this context, we propose hereafter new closed-form expressions for the ergodic capacity of multihop AF systems suffering interference in Nakagami-m fading.

3.3.1 Ergodic capacity

In a N-hop cooperative relaying system, the end-to-end ergodic capacity can be expressed as

$$
C_E = \frac{1}{N}\mathrm{E}\left[\log_2\left(1+\gamma\right)\right],
\tag{3.4}
$$

in which the factor $1/N$ accounts for the total number of time slots required for the transmission and $\mathrm{E}[\cdot]$ denotes mathematical expectation.

Theorem 1 : Let Z be an arbitrary non-negative random variable. Then

$$
\mathrm{E}\left[\ln\left(1+Z\right)\right] = \int_0^\infty \frac{1-e^{-s}}{s} M_{\frac{1}{Z}}(s)ds,
\tag{3.5}
$$

53

where $M_z(\cdot)$ stands for the MGF of z. *Proof :* In order to give a formal proof of (3.5), consider the following Taylor series expansion of $\ln(1 + z)$ valid for all $z \geq 0$, [21, Eq. (4.1.25)]

$$\ln(1 + Z) = \sum_{n=1}^{\infty} \frac{1}{n} \left(\frac{Z}{Z + 1} \right)^n, \qquad \forall Z \geq 0. \tag{3.6}$$

Then, by taking the expectation at both sides of (3.6), we obtain (3.5) when we substitute

$$\mathrm{E}\left\{ \left(\frac{1}{1 + Z^{-1}} \right)^n \right\} = \frac{1}{(n - 1)!} \int_0^{\infty} s^{n-1} e^{-s} M_{Z^{-1}}(s) ds. \tag{3.7}$$

The interchange of summation and integration is valid since the series $\sum_{n=1}^{\infty} s^{n-1}/n!$ is uniformly convergent for $s \geq 0$.

Corollary 1 : The ergodic capacity of an interference-limited multi-hop AF relaying system in arbitrary Nakagami-m fading is given by

$$C_E = \frac{1}{N \ln(2)} \sum_{\eta \in P_N} \Gamma \left(\Omega(\eta) + 1 \right) \prod_{n=1}^{N} \left(\frac{\Gamma(-m_{r,n}) \left(\frac{m_{r,n}}{m_{I,n}\Lambda_n} \right)^{m_{r,n}}}{\mathrm{B}(m_{r,n}, L_n m_{I,n})} \right)^{1-\eta_n} \times \mathrm{F}_A^{(N+1)} \left(\Omega(\eta) + 1; \right.$$

$$1, L_1 m_{I,1} + (1-\eta_1) m_{r,1}, \ldots, L_N m_{I,N} + (1-\eta_N) m_{r,N}; 2, 1 - \delta_{\eta_1} m_{r,1}, \ldots, 1 - \delta_{\eta_N} m_{r,N}; 1, \frac{m_{r,1}}{m_{I,1}\Lambda_1}, \ldots, \frac{m_{r,N}}{m_{I,N}\Lambda_N} \right), \tag{3.8}$$

where $\delta_{\eta_k} = \mathrm{sign}(\eta_k - 1/2), k = 1, ..., N$ and $\mathrm{F}_A^{(r)}$ is the first Lauricella hypergeometric function of r variables [12]. *Proof :* Recalling (3.4) and applying *Theorem 1* yields

$$C_E = \frac{1}{N \ln(2)} \int_0^{\infty} \frac{1 - e^{-s}}{s} M_{\gamma^{-1}}(s) ds. \tag{3.9}$$

Since the cooperative links are statistically independent, the MGF of γ^{-1} can be expressed by the product of the corresponding marginal MGFs pertaining to the N hops as follows

$$M_{\gamma^{-1}}(s) = \prod_{n=1}^{N} M_{\gamma_n^{-1}}(s) ds, \tag{3.10}$$

where $M_{\gamma_n^{-1}}$ can be expressed, using (3.3) and exploiting [21, Eqs. (3.351.3) and (9.211.4)], as

$$M_{\gamma_n^{-1}}(s) = \frac{\Gamma(m_{r,n} + L_n m_{I,n})}{\Gamma(m_{r,n})} \Psi \left(L_n m_{I,n}; 1 - m_{r,n}; \frac{m_{r,n}}{m_{I,n}\Lambda_n} s \right), \tag{3.11}$$

with $\Psi(a; b; z)$ being the Triconomi confluent hypergeometric function [21, Eq. (9.211.1)]. Next, a closed-form expression for (3.9) will be derived. Making use of [21, Eq. (9.210.2)], we start by representing the Triconomi function in terms of the confluent Hypergeometric function

$_1F_1(a; b; z)$ [21, Eq. (9.210.1)] [1], as

$$\Psi\left(L_n m_{I,n}; 1 - m_{r,n}; \frac{m_{r,n}}{m_{I,n}\Lambda_n}s\right) = \frac{\Gamma(m_{r,n})}{\Gamma(m_{r,n} + L_n m_{I,n})}{}_1F_1\left(L_n m_{I,n}; 1 - m_{r,n}; \frac{m_{r,n}}{m_{I,n}\Lambda_n}s\right) +$$
$$\frac{\Gamma(-m_{r,n})}{\Gamma(L_n m_{I,n})}\left(\frac{m_{r,n}}{m_{I,n}\Lambda_n}s\right)^{m_{r,n}}{}_1F_1\left(m_{r,n} + L_n m_{I,n}; 1 + m_{r,n}; \frac{m_{r,n}}{m_{I,n}\Lambda_n}s\right). \quad (3.12)$$

Likewise, the function $(1 - e^{-s})/s$ can be expressed in terms of $_1F_1(a; b; z)$ as $(1 - e^{-s})/s = e^{-s}{}_1F_1(1; 2; s)$. Thus, performing the necessary substitutions and simplifying leads to

$$C_E = \frac{1}{N\ln(2)}\int_0^\infty e^{-s}{}_1F_1(1; 2; s)\prod_{n=1}^N\left[{}_1F_1\left(L_n m_{I,n}; 1 - m_{r,n}; \frac{m_{r,n}s}{m_{I,n}\Lambda_n}\right) + \frac{\Gamma(-m_{r,n})\left(\frac{m_{r,n}s}{m_{I,n}\Lambda_n}\right)^{m_{r,n}}}{B(L_n m_{I,n}, m_{r,n})}\right.$$
$$\left.{}_1F_1\left(m_{r,n} + L_n m_{I,n}; 1 + m_{r,n}; \frac{m_{r,n}s}{m_{I,n}\Lambda_n}\right)\right]ds. \quad (3.13)$$

Using the following alternate expression for the product involved in (3.13) which is of the form

$$\prod_{n=1}^N(X_n + Y_n) = \sum_{\eta \in \mathcal{P}_N}\prod_{n=1}^N X_n^{\eta_n}Y_n^{1-\eta_n}, \quad (3.14)$$

where $\mathcal{P}_N \triangleq \{\eta = (\eta_1, \eta_2, ..., \eta_N) : \eta \in \{0, 1\}\}$, (3.13) can be rewritten, after some algebraic manipulations, as

$$C_E = \frac{1}{N\ln(2)}\sum_{\eta \in \mathcal{P}_N}\prod_{n=1}^N\left(\frac{\Gamma(-m_{r,n})\left(\frac{m_{r,n}}{m_{I,n}\Lambda_n}\right)^{m_{r,n}}}{B(m_{r,n}, L_n m_{I,n})}\right)^{1-\eta_n}\int_0^\infty s^{\Omega(\eta)}e^{-s}{}_1F_1(1; 2; s)$$
$$\prod_{n=1}^N\left[{}_1F_1\left(L_n m_{I,n}; 1 - m_{r,n}; \frac{m_{r,n}s}{m_{I,n}\Lambda_n}\right)\right]^{\eta_n}\left[{}_1F_1\left(L_n m_{I,n} + m_{r,n}; 1 + m_{r,n}; \frac{m_{r,n}s}{m_{I,n}\Lambda_n}\right)\right]^{1-\eta_n}ds, \quad (3.15)$$

where $\Omega(\eta) = \sum_{n=1}^N m_{r,n} - \sum_{n=1}^N m_{r,n}\eta_n$ and $B(a, b) = \Gamma(a)\Gamma(b)/\Gamma(a + b)$ is the Beta function [21, Eq. (8.380.1)]. A careful inspection of (3.15) reveals that the modified version of the first Lauricella hypergeometric function, which is given by [12, Eq. (2.4.2)]

$$F_A^{(r)}\left(a; b_1, \ldots, b_r; c_1, \ldots, c_r; \frac{x_1}{\nu}, \ldots, \frac{x_r}{\nu}\right) = \frac{\nu^a}{\Gamma(a)}\int_0^\infty e^{-\nu t}t^{a-1}\left(\prod_{k=1}^r {}_1F_1(b_k; c_k, x_k t)\right)dt; \, (\Re\mathfrak{e}(a) > 0), \quad (3.16)$$

can be applied to solve the integrals involved in (3.15). Therefore, with the help of (3.16) and after some manipulations, a closed-form expression for the ergodic capacity is obtained as in

---

1. Note that (3.12) is valid only for real-valued non-integer values of $m_{r,n}$. However, practically, very similar results are obtained for integer values of $m_{r,n}$ and $m_{r,n} + \epsilon$ for sufficiently small ϵ values.

(3.8). To the best of the authors' knowledge, this result is new. In addition, it is worthwhile to mention that, even in the Rayleigh case, such closed-form expression was not proposed in the technical literature before.

Reminiscent that the outage probability of this system has recently been expressed in terms of the second Lauricella function of r variables $F_B^{(r)}(\cdot)$ in [7]. In an interference-free environment, the authors of [2] have shown that the error probability of the multihop AF system can be described by the Lauricella function of the third type $F_C^{(r)}(\cdot)$.

3.3.2 One-term continuation relation for $F_A^{(r)}$

The multivariable Lauricella function $F_A^{(r)}$ is usually defined via its series representation given by [12, Eq. (2.1.1)], and its convergence is assured whenever $\sum_{i=1}^{r} |x_i| < 1$. Under its Laplace-type integral representation (3.16), the $F_A^{(r)}$ is convergent whenever $\Re\left(\sum_{i=1}^{r} x_i\right) < 1$ [17, Eq.(2)]. Nevertheless, the convergence of $F_A^{(r)}$ may often be improved by the use of analytic continuations formulas. In this section, a one-term continuation relation is obtained for the Lauricella $F_A^{(r)}$ by making use of its Barnes integral representation. In what follows, let us assume that only one argument of the Lauricella function is greater that one (say x_r) and the remaining are less than one with $\Re\left(\sum_{i=1}^{r-1} x_i\right) < 1$. We shall obtain one-term continuation relation for the F_A function by using the Barnes integral representation given by [12, Eq. (2.5.3)]

$$\frac{\Gamma(a)\Gamma(b_r)}{\Gamma(c_r)}F_A^{(r)}(a;b_1,\ldots,b_r;c_1,\ldots,c_r;x_1,\ldots,x_r) = \frac{1}{2\pi i}\int_{-i\infty}^{i\infty}\frac{\Gamma(a+t)\Gamma(b_r+t)}{\Gamma(c_r+t)}\Gamma(-t)(-x_r)^t \times$$
$$F_A^{(r-1)}(a+t;b_1,\ldots,b_{r-1};c_1,\ldots,c_{r-1};x_1,\ldots,x_{r-1})\,dt. \quad (3.17)$$

Apart from the numerical integration of (3.16), the integrand $F_A^{(r-1)}$ in (3.17), which converges uniformly, can readily be computed via Gauss-Laguerre quadrature (GLQ) [2], as suggested in [14, Eq. (44)], according to

$$F_A^{(r-1)}(a+t;b_1,\ldots,b_{r-1};c_1,\ldots,c_{r-1};x_1,\ldots,x_{r-1}) \approx \sum_{k=0}^{N_p} w_k \xi_k^{a+t-1} \prod_{i=1}^{r-1} {}_1F_1(b_i;c_i;x_i\xi_k), \quad (3.18)$$

---

2. Note that one could also use the semi-infinite GLQ method presented in [16] for higher accuracy.

where t_k and w_k are, respectively, the $k-$th zero and weight of the Laguerre polynomial of order N_p [18]. Then, after plugging (3.18) into (3.17) and using [12, Eq. (1.21.7)], we obtain

$$\mathrm{F}_A^{(r)}\left(a; b_1, \ldots, b_r; c_1, \ldots, c_r; x_1, \ldots, x_r\right) \approx \sum_{k=0}^{N_p} w_k \xi_k^{a-1} \left(\prod_{i=1}^{r-1} {}_1F_1(b_i; c_i; x_i\xi_k)\right) {}_2F_1(a, b_r; c_r, x_r\xi_k);$$

$$\left(x_r \geq 1, \mathfrak{Re}\left(\sum_{i=1}^{r-1} x_i\right) < 1\right), \tag{3.19}$$

which is the the continuation of $\mathrm{F}_A^{(r)}$ to a different region of its arguments x_r. Note that one can always modify the arguments x_i in (3.17) in order for the convergence of the integrand $\mathrm{F}_A^{(r-1)}$ to be satisfied, by making use of the following Euler integral transformation [12, Eq. (4.2.2)]

$$\mathrm{F}_A^{(r-1)}(a; b_1, \ldots, b_{r-1}, c_1, \ldots, c_{r-1}; x_1, \ldots, x_{r-1}) = (1-x_j)^{-a} \mathrm{F}_A^{(r-1)}\left(a; b_1, \ldots, c_j - b_j, b_{r-1}; c_1, \ldots, c_{r-1};\right.$$

$$\left.\frac{x_1}{1-x_j}, \ldots, \frac{x_j}{x_j-1}, \frac{x_{r-1}}{x_j-1}\right). \tag{3.20}$$

Note that an r-fold repetition of the preceding operations can leads to the continuation of the Lauricella function outside its region of convergence. Nevertheless, the result is not necessarily convenient in form. Finally, the new continuation formula obtained in (3.19) can be used for calculating the Lauricella $\mathrm{F}_A^{(r)}$ function occurring in the analysis of the ergodic capacity of interference-limited multihop AF network, as shown in (3.8).

3.4 Dual-hop performance

Due to their practical merits, dual-hop AF relaying schemes have been adopted for cellular communications by next generation wireless standards, namely IEEE 802.16j and 3GPP-LTE [2]. In subsection IV.A, we analyze dual-hop performance in the general case of SIR values while in subsection IV.B, we restrict it to the high-SIR regime.

3.4.1 General case of SIR values

Assuming a dual-hop cooperative system ($N = 2$) and using (3.8) yields the ergodic capacity expression given by

$$
C_E = \frac{1}{2\ln(2)} \sum_{\eta \in P_2} \Gamma(\Omega(\eta)+1) \prod_{n=1}^{2} \left(\frac{\Gamma(-m_{r,n})\left(\frac{m_{r,n}}{m_{I,n}\Lambda_n}\right)^{m_{r,n}}}{\mathrm{B}(m_{r,n}, L_n m_{I,n})} \right)^{1-\eta_n} \mathrm{F}_A^{(3)} \Bigg(\Omega(\eta)+1; 1, L_1 m_{I,1}+(1-\eta_1)m_{r,1},
$$

$$
L_2 m_{I,2} + (1-\eta_2)m_{r,2}; 2, 1-\delta_{\eta_1} m_{r,1}, 1-\delta_{\eta_2} m_{r,2}; 1, X_1, X_2 \Bigg), \tag{3.21}
$$

where $X_1 = \frac{m_{r,1}}{m_{I,1}\Lambda_1}$ and $X_2 = \frac{m_{r,2}}{m_{I,2}\Lambda_2}$. By virtue of the decomposition formulas of the Lauricella function of three variables $F_A^{(3)}$ in [17], we obtain an alternative expression for the ergodic capacity in (3.21) given by

$$
C_E = \frac{1}{2\ln(2)} \sum_{\eta \in P_2} \frac{\Gamma(\Omega(\eta)+1)}{(1-X_2)^{\Omega(\eta)+1}} \prod_{n=1}^{2} \left(\frac{\Gamma(-m_{r,n})X_n^{m_{r,n}}}{\mathrm{B}(m_{r,n}, L_n m_{I,n})} \right)^{1-\eta_n} \sum_{i=0}^{\infty} A_{\eta,i} \left(\frac{X_2}{X_2-1} \right)^i
$$

$$
\mathrm{F}_2 \left(\Omega(\eta) + 1 + i; 1, L_1 m_{I,1} + (1-\eta_1)m_{r,1}, ; 2, 1 - \delta_{\eta_1} m_{r,1}; \frac{1}{1-X_2}, \frac{X_1}{1-X_2} \right), \tag{3.22}
$$

where $A_{\eta,i} = (\Omega(n) + 1)_i \, (1-\delta_{\eta_2} m_{r,2} - L_2 m_{I,2} - (1-\eta_2)m_{r,2})_i / \, (1 - \delta_{\eta_2} m_{r,2})_i \, i!$, with $(a)_n$ being the Pochhammer symbol. Moreover, in (3.22), F_2 is the Appell hypergeometric function of the second type [12]. In turn, the Appell's hypergeometric function F_2 in (3.22) verifies some reduction formulas involving series of simpler hypergeometric functions [19, Theorem 1]. Nevertheless, applying these reduction formulas requires separate treatment in the cases $\eta = \{1,1\}$ and $\eta \in P_2 \backslash \{1,1\}$. Therefore, in order to proceed, it is adequate to rewrite (3.22) as

$$
C_E = \frac{1}{2\ln(2)} \sum_{\eta \in P_2} \Psi_\eta = \frac{1}{2\ln(2)} \left\{ \Psi_{\eta=\{1,1\}} + \sum_{\eta \in P_2\backslash\{1,1\}} \Psi_\eta \right\}, \tag{3.23}
$$

where Ψ_η can be easily identified from (3.22). Now, by the help of [19, Theorem 1], and after several manipulations, we show that $\Psi_{\eta=\{1,1\}}$ and $\Psi_{\eta \in P_2\backslash\{1,1\}}$ can be, respectively, expressed as

$$
\Psi_{\eta=\{1,1\}} = -\ln(\frac{X_2}{X_2-1}) - \frac{L_1 m_{I_1}}{1-m_{r,1}} \left\{ \frac{X_1}{X_2} {}_3F_2 \left(L_1 m_{I,1}, 1, 1; 2 - m_{r,1}, 2; -\frac{X_1}{X_2} \right) + \frac{X_1}{1-X_2} \right.
$$

$$
{}_3F_2 \left(L_1 m_{I,1}, 1, 1; 2 - m_{r,1}, 2; \frac{X_1}{1-X_2} \right) \bigg\} + \sum_{i=1}^{\infty} \frac{A_{\eta=\{1,1\},i}}{i} \left\{ {}_2F_1 \left(i, L_1 m_{I,1}; 1 - m_{r,1}; -\frac{X_1}{X_2} \right) \right.
$$

$$
\left. - \left(\frac{X_2}{X_2-1} \right)^i {}_2F_1 \left(i, L_1 m_{I,1}; 1 - m_{r,1}; \frac{X_1}{1-X_2} \right) \right\}, \tag{3.24}
$$

and

$$\Psi_{\eta \in \mathcal{P}_2 \setminus \{1,1\}} = \Gamma(\Omega(\eta) + 1)(-1)^{\Omega(\eta)} \left(\frac{X_1}{X_2}\right)^{m_{r,1}(1-\eta_1)} \prod_{n=1}^{2} \left(\frac{\Gamma(-m_{r,n})}{\mathrm{B}(m_{r,n}, L_n m_{I,n})}\right)^{1-\eta_n} \sum_{i=0}^{\infty} \frac{A_{\eta,i}}{(\Omega(\eta) + i)}$$

$$\left\{ {}_2F_1\left(\Omega(\eta) + i, L_1 m_{I,1} + (1-\eta_1)m_{r,1}; 1 - \delta_{\eta_1} m_{r,1}; -\frac{X_1}{X_2}\right) - \left(\frac{X_2}{X_2 - 1}\right)^{\Omega(\eta)+i} {}_2F_1\left(\Omega(\eta) + i, \right. \right.$$

$$\left. \left. L_1 m_{I,1} + (1-\eta_1)m_{r,1}; 1 - \delta_{\eta_1} m_{r,1}; \frac{X_1}{1 - X_2}\right) \right\}, \tag{3.25}$$

where ${}_2F_1(a,b;c;z)$ and ${}_3F_2(a,b,c;d;z)$ denote the Gauss hypergeometric function and the generalized hypergeometric function, respectively. Plugging (3.24) and (3.25) into (3.23) yields an alternative expression for the ergodic capacity of interference-limited dual-hop relay channels. The latter involves common simple functions and thus has the advantage of being directly computable using mathematical software packages. Most importantly, in contrast to (3.8) and (3.21), the result in (3.23) allows for high-SIR performance analysis and hence gives more insights into the effect of the system parameters on the ergodic capacity.

3.4.2 High-SIR regime

In the high-SIR regime, we consider two important scenarios; namely, one where the relay and destination SIRs grow large but in the same proportion, and one where the relay SIR grows large but the destination SIR is kept fixed.

Large per hop SIR

Here, we have $\Lambda_1 \to \infty$, $\Lambda_2 \to \infty$ with $\beta = \Lambda_2/\Lambda_1$ for some fixed β. In this case, the ergodic capacity can be expressed according to the affine expansion [20]

$$C_E^{\infty} = \mathcal{S}_{\infty}\left(\frac{\Lambda_1|\mathrm{dB}}{3\ \mathrm{dB}} - \mathcal{L}_{\infty}\right) + o(1), \tag{3.26}$$

with $\mathcal{S}_{\infty}$ denoting the high-SIR slope in bits/s/Hz/ (3 dB) given by

$$\mathcal{S}_{\infty} = \lim_{\Lambda_1 \to \infty} \frac{C_E|_{\Lambda_2 \to \infty, \Lambda_2/\Lambda_1 = \beta}}{\log_2(\Lambda_1)}, \tag{3.27}$$

and $\mathcal{L}_{\infty}$ representing the high-SIR power offset in 3 dB units given by

$$\mathcal{L}_{\infty} = \lim_{\Lambda_1 \to \infty} \left(\log_2(\Lambda_1) - \frac{C_E|_{\Lambda_2 \to \infty, \Lambda_2/\Lambda_1 = \beta}}{\mathcal{S}_{\infty}}\right). \tag{3.28}$$

From (3.24) and (3.25), we can evaluate $\mathcal{S}_\infty$ and $\mathcal{L}_\infty$ in closed-form as follows.

Theorem 2 : When $\Lambda_1 \to \infty$ and $\Lambda_2 \to \infty$ with $\beta = \Lambda_2/\Lambda_1$, the high-SIR slope $\mathcal{S}_\infty$ and the high-SIR power offset $\mathcal{L}_\infty$ of interference-limited AF dual-hop systems are given by

$$\mathcal{S}_\infty = \frac{1}{2} \quad \text{b/s/Hz (3 dB)}, \tag{3.29}$$

and

$$\mathcal{L}_\infty(L_1, L_2) = \log_2\left(\frac{m_{r,2}}{m_{I,2}\beta}\right) + \frac{1}{\ln(2)}\Upsilon, \tag{3.30}$$

where Υ is given by

$$\Upsilon = \frac{L_1 m_{I_1}}{1 - m_{r,1}} \frac{\beta}{\Delta} {}_3F_2\left(L_1 m_{I,1}, 1, 1; 2 - m_{r,1}, 2; -\frac{\beta}{\Delta}\right) - \sum_{i=1}^{\infty} \frac{A_{\eta=\{1,1\},i}}{i} {}_2F_1\left(i, L_1 m_{I,1}; 1 - m_{r,1}; -\frac{\beta}{\Delta}\right) -$$

$$\sum_{\eta \in \mathcal{P}_2 \backslash \{1,1\}} \Gamma(\Omega(\eta) + 1) \frac{(-1)^{\Omega(\eta)} \prod_{n=1}^{2} \Gamma(-m_{r,n})^{1-\eta_n}}{\prod_{n=1}^{2} \mathrm{B}(m_{r,n}, L_n m_{I,n})^{1-\eta_n}} \left(\frac{\beta}{\Delta}\right)^{m_{r,1}(1-\eta_1)} \sum_{i=0}^{\infty} \frac{A_{\eta,i}}{(\Omega(\eta) + i)} \times$$

$${}_2F_1\left(\Omega(\eta) + i, L_1 m_{I,1} + (1-\eta_1)m_{r,1}; 1 - \delta_{\eta_1} m_{r,1}; -\frac{\beta}{\Delta}\right). \tag{3.31}$$

with $\Delta = m_{r,2} m_{I,1}/m_{r,1} m_{I,2}$.

Proof : We start by applying the following identity to (3.24)

$$\ln\left(\frac{X_2}{X_2 - 1}\right) = \ln\left(\frac{m_{r,2}}{m_{I,2}\beta}\right) - \ln\left(\frac{m_{r,2}}{m_{I,2}\beta} - \Lambda_1\right)$$

$$\underset{\Lambda_1 \to \infty}{\simeq} \ln\left(\frac{m_{r,2}}{m_{I,2}\beta}\right) - \ln(\Lambda_1). \tag{3.32}$$

By performing the limit operations on the right hand side (R.H.S) of (3.24) and (3.25) and exploiting the result in (3.32), we obtain the ergodic capacity, in the high-SIR regime, as

$$\lim_{\Lambda_1, \Lambda_2 \to \infty, \beta = \Lambda_2/\Lambda_1} C_E = \frac{1}{2}\left\{\log_2(\Lambda_1) - \log_2\left(\frac{m_{r,2}}{m_{I,2}\beta}\right) - \frac{1}{\ln(2)}\Upsilon\right\}. \tag{3.33}$$

Finally, by invoking (3.27) and (3.28), the claimed expressions of the high-SIR slope and the high-SIR power offset are found.

It is important to note that (3.29) and (3.30) allow an exact characterization of the key high-SIR ergodic capacity for arbitrary numbers of interferers at the relay and the destination and for an arbitrary Nakagami-m distribution of the interference-relay channel. In particular, (3.29) reveals the intuitive result that the multiplexing gain of dual-hop AF networks is unsensitive to the presence of interference. Indeed, the authors of [5] proved that the multiplexing gain of an

interference-free dual-hop relaying system is also equal to 1/2. On the other hand, the power offset in (3.30) is a more intricate function capturing all the interference and relay channels parameters.

For a fixed β, adding K interferers at the first hop and P interferers at the second hop, while not altering $\mathcal{S}_\infty$, would induce a high-SIR power offset shift given by

$$\delta\mathcal{L}_\infty(P, K) \triangleq \mathcal{L}_\infty(L_1 + K, L_2 + P) - \mathcal{L}_\infty(L_1, L_2). \tag{3.34}$$

Since the the computation of a closed-form expression of the high-SIR power offset shift in (3.34) is quite complicated, the effect of adding more interferers at each hop will be illustrated numerically in the next section.

Also of interest is the effect of the power gain β on the ergodic capacity. While the high-SIR slope is invariant to β, the power offset captures the sensitivity of the high-SIR capacity to the power gain. Indeed, asymptotically, the optimal power gain is the one that minimizes the power offset.

Large first-hop SIR and fixed second-Hop SIR

In this case, we have $\Lambda_1 \to \infty$ and Λ_2 is fixed. Considering the alternative expression for the ergodic capacity obtained in (3.23), then as $\Lambda_1 \to \infty$, we obtain

$$\lim_{\Lambda_1 \to \infty} C_E \;=\; \frac{1}{2\ln(2)} \left\{ \lim_{X_1 \to 0} \Psi_{\eta=\{1,1\}} + \sum_{\eta \in P_2 \setminus \{1,1\}} \lim_{X_1 \to 0} \Psi_\eta \right\}. \tag{3.35}$$

Recalling the fact that $_2F_1(a, b; c; 0) = 1$ and $_3F_1(a, b, c; e, f; 0) = 1$ yields

$$\lim_{X_1 \to 0} \Psi_{\eta=\{1,1\}} \;=\; -\log_2\left(\frac{X_2}{X_2 - 1}\right) + \sum_{i=1}^{\infty} \frac{A_{\eta=\{1,1\},i}}{i}\left(1 - \left(\frac{X_2}{X_2 - 1}\right)^i\right), \tag{3.36}$$

and

$$\lim_{X_1 \to 0} \Psi_{\eta \in \mathcal{P}_2 \setminus \{1,1\}} = \frac{(-1)^{m_{r,2}}\Gamma(m_{r,2} + 1)\Gamma(-m_{r,2})}{\mathrm{B}(L_2 m_{I,2}, m_{r,2})} \sum_{i=0}^{\infty} \frac{A_{\eta=\{1,0\},i}}{(m_{r,2} + i)}\left(1 - \left(\frac{X_2}{X_2 - 1}\right)^{m_{r,2}+i}\right). \tag{3.37}$$

Substituting (3.36) and (3.37) into (3.35), and performing some algebraic manipulations leads to the closed-form expression in (3.38) for the ergodic capacity of interference-limited AF dual-hop

systems as the first hop SIR grows large for fixed relay and destination interference powers.

$$\lim_{\Lambda_1 \to \infty} C_E = -\frac{1}{2} \log_2 \left(\frac{X_2}{X_2 - 1} \right) + \frac{1}{2 \log(2)} \left\{ \psi(1 - m_{r,2}) - \psi(L_2 m_{I,2}) - \frac{X_2}{X_2 - 1} \left(1 - \frac{L_2 m_{I,2}}{1 - m_{r,2}} \right) \right.$$

$$\left. {}_3F_2 \left(1, 1, 2 - L_2 m_{I,2} - m_{r,2}; 2, 2 - m_{r,2}; \frac{X_2}{X_2 - 1} \right) + (-1)^{m_{r,2}+1} \Gamma(m_{r,2} + 1) \Gamma(-m_{r,2}) \right.$$

$$\left. \left(1 - \frac{\left(\frac{X_2}{X_2 - 1} \right)^{m_{r,2}}}{m_{r,2} B(m_{r,2}, L_2 m_{I,2})} {}_2F_1 \left(m_{r,2}, 1 - L_2 m_{I,2}; 1 + m_{r,2}; \frac{X_2}{X_2 - 1} \right) \right) \right\}, \tag{3.38}$$

where $\psi(\cdot)$ stands for the Digamma function [21, Eq. (8.361)]. The obtained result in (3.38) shows that if we fix Λ_2 and take large Λ_1, then the ergodic capacity of interference-limited AF dual-hop systems remains bounded (as a function of Λ_2). This confirms the intuitive notion that the capacity is restricted by the weakest link in the relay network; namely the relay-destination link in this case.
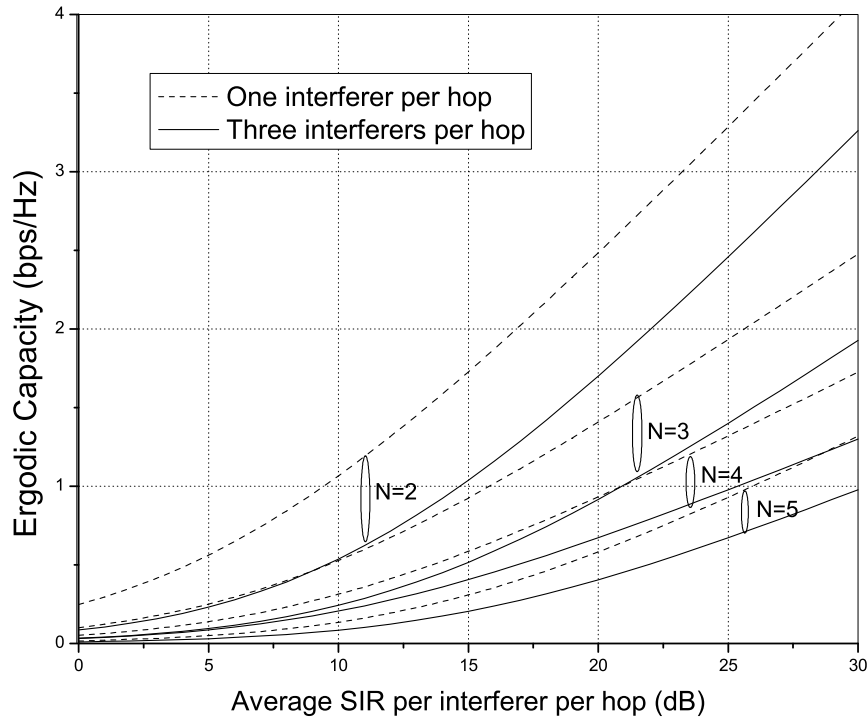
FIGURE 3.1 – Ergodic capacity of multihop AF relaying in the presence of cochannel interference for different numbers of hops N.
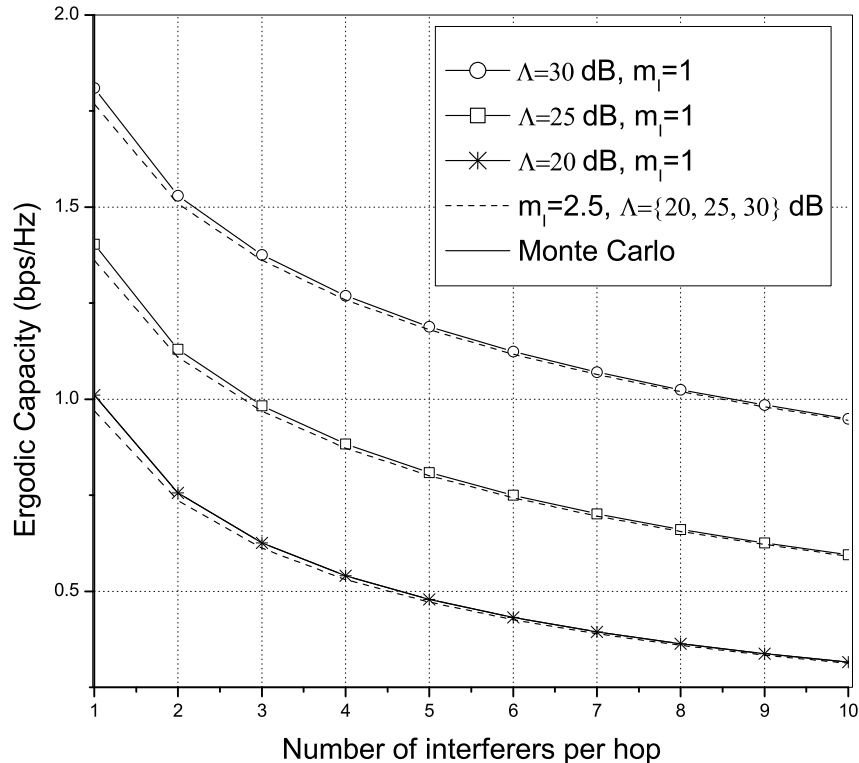
FIGURE 3.2 – Ergodic capacity of an interference-limited four-hop AF relay system against the number of interferers in each hop. Results are shown for i.i.d Nakagami-m faded links with $m_{r,n} = 1.5, n = 1, \ldots, 4$.

3.5 Illustrative numerical results

The aim of this section is to illustrate the expressions derived in Sections 3.3 and 3.4 using numerical examples and examine the effect of interference on the system's capacity. All the results shown here have been analytically obtained by the direct evaluation of the expressions developed in this paper : either (3.8) for an arbitrary number of hops N or (3.23), (3.26) and (3.38) for exact and asymptotic capacity of the dual-hop case. For the evaluation of (3.8) and (3.21), we exploit the algorithm proposed in Section 3.3.2 for the implementation of the Lauricella hypergeometric function F_A. Moreover, the accuracy of the proposed formulas have been verified by Monte Carlo simulations.

Fig. 1 shows the ergodic capacity of $N = \{2, 3, 4, 5\}$-hop AF relaying system in an interference-impaired Nakagami-m fading channel with $L_n = \{1, 3\}, n = 1, .., N$. The results are obtained in
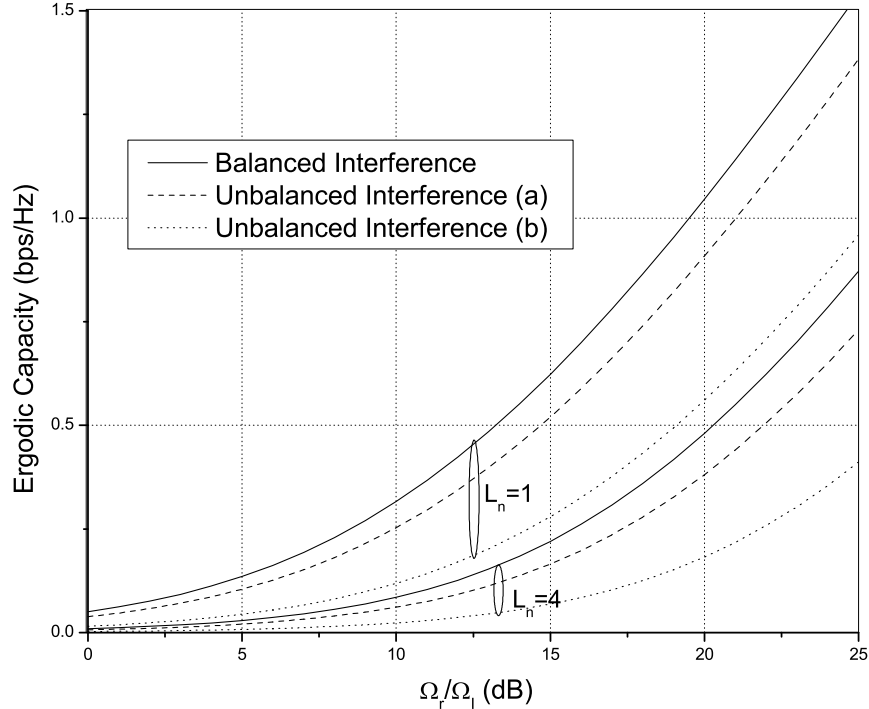
FIGURE 3.3 – Ergodic capacity of three-hop AF relaying in the presence of balanced and unbalanced cochannel interference for $L_n = \{1, 4\}, n = \{1, 2, 3\}$. Unbalanced (a) : $\Omega_{I,n} = (0.45, 0.45, 0.1)\Omega_I$. Unbalanced (b) : $\Omega_{I,n} = (0.9, 0.05, 0.05)\Omega_I$.

the case of i.i.d. channel gains and interfering signals between the relay links with $m_{r,n} = 1.5$ and $m_{I,n} = 2.5$. As observed, increasing N does not improve the channel capacity, due to the fact that the number of orthogonal channels needed increases as the number of hops increases, thus decreasing the channel capacity by a factor of N. Nevertheless, increasing N reduces the effect of interference. Indeed, the capacity loss is halved when considering the five-hop scenario instead of the dual-hop scenario.

Fig. 2 shows the ergodic capacity of four-hop AF relaying systems versus the number of interferers for i.i.d. Nakagami-m fading channels with $m_{r,n} = 1.5, n = 1, ..4, m_{I,n} = m_I = \{1, 2.5\}$ and $\Lambda_{I,n} = \Lambda = \{20, 25, 30\}$ dB. As can be seen, the analytical and simulation results are in excellent agreement. Moreover, we can quantify the performance degradation that occurs as the number of interferers increases. On the other hand, for a given interference power limit, it is seen that the ergodic capacity varies very slightly with the fading parameters of the interference channels.
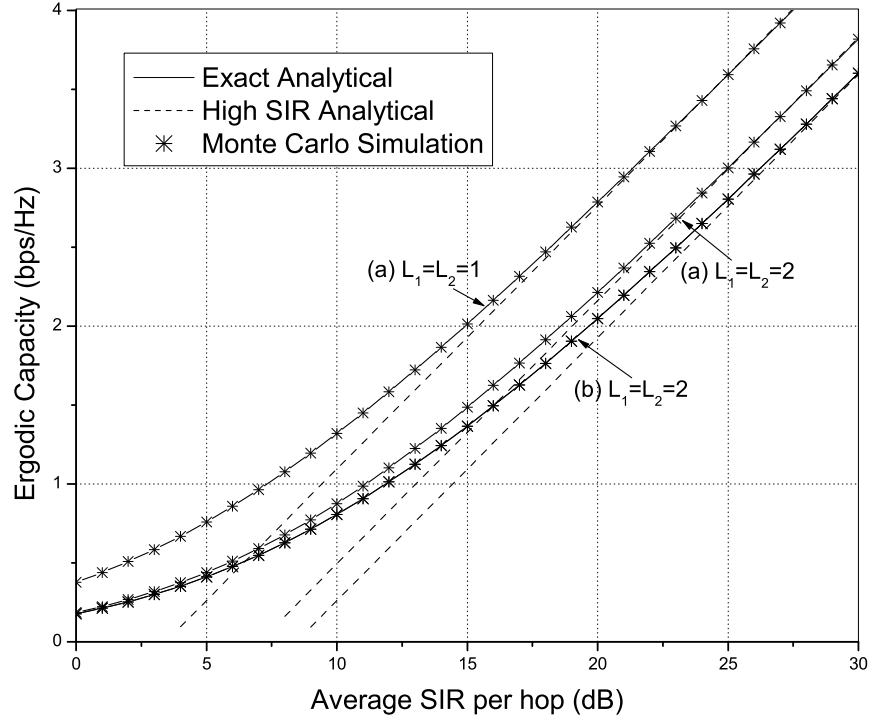
FIGURE 3.4 – Comparison of exact analytical, high-SIR analytical, and Monte Carlo simulation results for the ergodic capacity of interference-limited AF dual-hop systems with different interference and fading configurations. Results are shown for Rayleigh-faded interferers, $\Lambda_2/\Lambda_1 = 2$, (a) : $m_1 = m_2 = 1.75$ and (b) : $m_1 = m_2 = 0.75$.

Fig. 3 investigates the impact of interference power unbalance on the ergodic capacity of a three-hop AF relaying system. Different per hop interference power configurations have been considered while maintaining the overall interference power constant. The results are shown for $L_n = \{1, 4\}$, $m_{r,n} = 1.5$, and $m_{I,n} = 1$, $n = 1, 2, 3$. As can be seen, the ergodic capacity decreases as the links become highly unbalanced in terms of their perceived interference power, thereby highlighting the significance of the joint optimization of power allocation and relay location for AF network to enhance the system performance. It can also be seen that unbalanced interferers have less impact on the system's ergodic capacity as the interferers number increases.

Fig. 4 depicts the analytical high-SIR capacity approximations for interference-limited AF dual-hop systems, based on (3.29) and (3.30). The results are shown as a function of the first-hop SIR Λ_1 with $\beta = \Lambda_2/\Lambda_1 = 2$. These approximations are seen to converge to their respective exact capacity curves for quite moderate SIR levels (e.g., $\Lambda_1 \approx 15$ dB). We also see that when the

number of interferers at the relay and/or the destination increases, the high-SIR power offset is increased, thereby yielding an overall deterioration of the ergodic capacity. Again, the analytical results match the simulation results perfectly. Fig. 4 also investigates the effect of the fading severity on every relay link which, in contrast to the fading severity of the interfering link, turns out to be considerable.
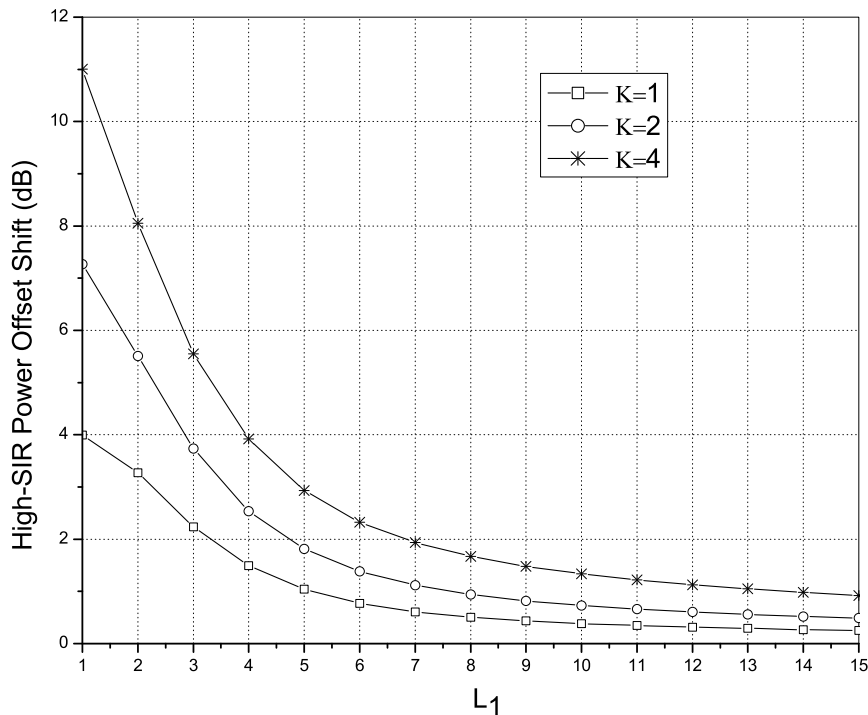
FIGURE 3.5 – High-SIR power offset shift, in decibels, obtaining by adding either (a) one interferer at the first hop ($K = 1$), (b) two interferers at the first hop ($K = 2$), or (c) four interferers at the first hop ($K = 4$). Results are shown for Rayleigh faded interferers with $L_2 = 1$, $m_{r,1} = m_{r,2} = 1.5$ and $\beta = 2$.

Fig. 5 illustrates the relationship in (3.34) where the high-SIR power offset shift is plotted against L_1, for $K = \{1, 2, 4\}$. It is clear that the excess power offset induced by interference is positive, thereby confirming the intuitive notion that the presence of more interferers has the effect of deteriorating the ergodic capacity. Moreover, for a fixed value of K, the high-SIR power offset shift is a decreasing function of L_1. We see that when L_1 (resp. L_2) is small, then a small increase in L_1 (resp. L_2) yields an important decrease in terms of the high-SIR power offset. However, in agreement with Fig. 5, as L_1 goes large, the impact of interference on the overall
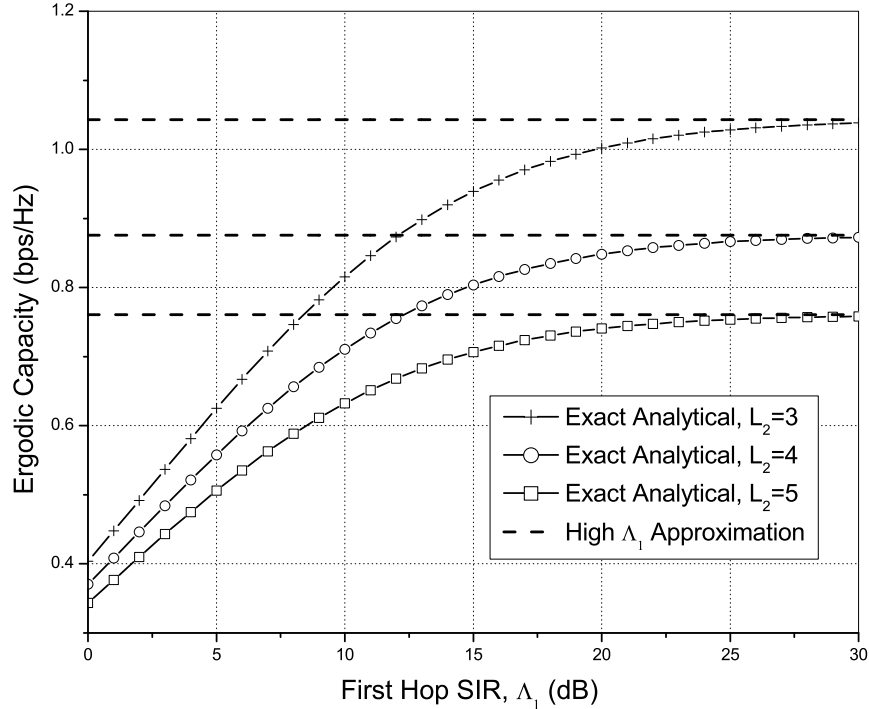
FIGURE 3.6 – Comparison of the high-SIR Λ_1 approximation and the exact analytical results for different numbers of interferers at the second hop. Results are shown for $L_1 = 1$, $\Lambda_2 = 10$ dB, $m_{r,1} = m_{r,2} = 1.5$, $m_{I,1} = 2$, and $m_{I,2} = 1.5$.

system's capacity approaches a limit.

Fig. 6 plots the closed-form high-SIR regime ergodic capacity based on (3.35) and the exact analytical ergodic capacity based on (3.21), for an AF dual-hop system suffering interference for different values of L_2. The results are presented as a function of the first-hop SIR Λ_1. It can be seen that the asymptotic approximations converge to their respective exact capacity curves for moderate values of λ_1 (e.g., within $\lambda_1 \approx 20$ dB).

3.6   Conclusion

In this paper we presented an analytical characterization of the ergodic capacity of multihop AF relay channels with interference in Nakagami-m fading. The derived expression for the ergodic capacity provides a good match with the simulation results. Furthermore, exploiting recent advances in the hypergeometric functions theory, we derive simple and informative closed-form expressions for the high-SIR regime where the capacity is expanded as an affine function of the

per hop SIR$|_{\text{dB}}$. The zero-order term or power offset for which we find insightful closed-form expressions, is shown to play a chief role in understanding the impact of interference and power on the system's capacity. Finally, it is worth remarking that the expressions presented in this paper have direct operational significance in ergodic interference-limited multihop channels.

Bibliographie

[1] M. O. Hasna and M.-S. Alouini, "Outage probability of multihop transmission over Naka-gami fading channels," *IEEE Commun. Lett.,* vol. 7, no. 5, pp. 216-218, May 2003.

[2] I. Trigui, S. Affes, and A. Stéphenne, "Closed-form error analysis of variable-gain multihop systems in Nakagami-m fading channels" , *IEEE Trans. Commun.,* vol. 59, no. 8, pp. 2285-2295, Aug. 2011.

[3] J. N. Laneman, D. N. C. Tse, and G. W. Wornell,"Cooperative diversity in wireless net-works : efficient protocols and outage behaviour," *IEEE Trans. Inform. Theory,* vol. 50, pp. 3062-3080, Dec. 2004.

[4] I. Trigui, S. Affes, and A. Stéphenne, "Exact error analysis of dual-hop fixed-gain AF relaying over arbitrary Nakagami-*m* f;ading", *Vehicular Technolqgy Conf.*, pp. 1-5, Sept. 2012.

[5] S. Jin, M. R. McKay, C. Zhong, and K-Kit Wong, "Ergodic capacity cnalysis of amplify-and-forward MIMO dual-hop systems," *IEEE Trans. Inf. Theory,* vol. 56, no. 5, May 2010.

[6] S. Ikki and S. Aissa, "Multihop wireless relaying systems in the presence of co-channel interferences : performance analysis and design optimization", *IEEE Trans. Veh. Technol.*, vol 61, no. 2, Feb. 2012.

[7] T. Soithong, V. A. Aalo, G. P. Efthymoglou, and C. Chayawan, "Outage analysis of multi-hop relay systems in interference-limited Nakagami-m fading channels", *IEEE Trans. Veh. Technol.*, vol. 61, no. 3, Mar. 2012.

[8] H. A. Suraweera, H. K. Garg, and A. Nallanathan, "Performance analysis of two hop amplify-and-forward systems with interference at the relay," *IEEE Commun. Lett.,* vol. 14, no. 8, pp. 692-694, Aug. 2010.

[9] D. Lee and J. H. Lee, "Outage probability for dual-hop relaying systems with multiple interferers over Rayleigh fading channels," *IEEE Trans. Veh. Technol.,* vol. 60, no. 1, pp. 333-338, Jan. 2011.

[10] C. Zhong, S. Jin, and K. K.Wong, "Dual-hop systems with noisy relay and interference-limited destination," *IEEE Trans. Commun.,* vol. 58, no. 3, pp. 764-768, Mar. 2010.

[11] F. S. Al-Qahtani, T. Q. Duong, C. Zhong, K. A. Qaraqe, and H. Alnuweiri, "Performance analysis of dual-hop AF systems with interference in Nakagami-m fading channels," *IEEE Signal Process. Lett.,* vol. 18, no. 8, pp. 454-457, Aug. 2011.

[12] H. Exton, *Multiple Hypergeometric Functions and Applications*; New York : Jhon wiley, 1976.

[13] Q. Shi and Y. Karasawa, " Some applications of Lauricella hypergeometric function F_A in performance analysis of wireless communications", *IEEE Commun. Let.,* vol. 16, no. 5, May 2012.

[14] J. M. Romero-Jerez and A. J. Goldsmith, "Performance of multichannel reception with transmit antenna selection in arbitrarily distributed Nagakami fading channels," *IEEE Trans. Wireless Commun.,* vol. 8, no. 4, pp. 2006-2013, Apr. 2009.

[15] W. Chen, J. Montojo, A. Golitschek, C. Koutsimanis, and S. Xiaodong, "Relaying operation in 3GPP LTE : challenges and solutions," *IEEE Commun. Mag.,* vol. 50, no. 2, pp. 156-162, Feb. 2012.

[16] I. S. Gradshteyn and I. M. Ryzhik, *Table of Integrals, Series and Products,* 5th Ed., San Diego, CA : Academic, 1994.

[17] A. Hasanov and H. M. Srivastava, "Some decomposition formulas associated with the Lauricella function F_A^r and other multiple hypergeometric functions", *App. Math. Lett.,* vol. 19, pp. 113-121, 2006.

[18] M. Abramowitz and I. A. Stegun, *Handbook of Mathematical Functions with Formulas, Graphs, and Mathematical Tables,* 10th ed. New York : Dover, 1972.

[19] S. B. Opps, S. Nasser, and H. M. Srivastava , "Some reduction and transformation formulas for the Appell hypergeometric function F_2", *Math. Anal. Appl.,* vol. 302, pp. 180-195, 2005.

[20] A. Lozano, A. M. Tulino, and S. Verdu, "High-SNR power offset in multiantenna communication," *IEEE Trans. Inf. Theory,* vol. 51, pp. 4134-4151, Dec. 2005.

Chapitre 4

On the Ergodic Capacity of Amplify-and-Forward Relay Channels with Interference in Nakagami-m Fading

Imène Trigui, Sofiène Affes, and Alex Stéphenne

Résumé : Dans ce chapitre, on présente pour la première fois une analyse complète et unifiée de la capacité érgodique des systèmes avec relayage à double sauts utilisant un gain fixe et opérant en présence du bruit et d'interférences. Les résultats analytiques montrent que la capacité érgodique est dominée par les interférences du premier saut et qu'elle s'améliore très lentement lorsque le RSB augmente. Ils montrent également que la capacité érgodique se détériore légèrement lorsque l'évanouissement subit par les interférences est atténué. En plus, les résultats obtenus ont permis d'examiner les effets de l'emplacement du relai sur les performances du système.

Abstract

Integrating relaying techniques into cellular communications sheds new light on higher capacity and broader coverage. However, applying relaying techniques in practice has to take into account important issues such as co-channel interference (CCI). In this work, a generalized framework for the ergodic capacity analysis of dual-hop fixed-gain amplify and forward (AF) relaying systems in the presence of interference is presented. New expressions for the ergodic capacity are derived considering transmissions over independent but not necessarily identically distributed Nakagami-m fading channels in the presence of a finite number of co-channel interferers. Our results establish that the ergodic capacity is dominated by the source-relay interference power and that it improves slowly with the average signal-to-noise ratio (SNR) increasing. It slightly deteriorates, however, with a larger Nakagami-m fading parameter for interference channels. Furthermore, our results offer an analytical insight into the key impact of relay placement on performance. Our new ergodic capacity expressions could therefore provide a very practical/low-cost performance optimization tool for relayed-communication system designers.

4.1 Introduction

Recent proposals for new wireless standards such as IEEE 802.16j and 3GPP-LTE have adopted two-hop relay transmission for cellular communications [2]. The key advantage of relaying is to enable high capacity where traditional architectures are unsatisfactory due to location constraints (cell-edge, shadowing, indoor), leading to a more homogenous user experience. Depending on the nature and complexity of the relaying technique, relay nodes can be broadly categorized as either amplify and forward (AF) or decode and forward (DF) [1]. While AF relays act as repeaters, DF relays decode and recode the received signal prior to forwarding it to the receiver, thereby implying a larger delay than with a simple repeater.

In the open literature, several works investigating relaying communications exist (cf. [1]-[12] and references therein). Despite their importance, many of the existing results have been based on the assumption that the system is thermal-noise limited. However, relaying-access capacity is also affected by strong co-channel interference due to the aggressive frequency reuse in cellular networks. Cochannel interference, which is an essential feature of wireless networks, can cause more severe performance degradation than thermal noise in many wireless networks.

In a variable-gain relay scenario, existing contributions range from the analysis of interference-limited relay [3], [5] or destination [4], to multiple interferers at both sides [6]. Apart from the very recent work of [5] and [6], existing works that have studied the effects of interference on the performance of variable-gain AF relaying have mainly considered Rayleigh fading channels. By deriving expressions for the outage probability and the average bit error rate (BER), the performance of variable-gain AF relaying over Nakagami-m channels with interference has been investigated in [5].

Other works have considered fixed-gain relaying [5]- [10]. In [5], the outage probability of a fixed-gain AF relay system with interference-limited destination has been derived assuming Rayleigh fading channels. The analysis has been later extended in [8] and [9] to the case of multiple interferers at both relay and destination. Recently, the outage probability of fixed-gain AF relaying systems with a single interferer were analyzed by Surawera et al. [10], where both the desired signal have an integer Nakagami-m distribution. Although being a long-standing open problem, the capacity of multihop relaying systems has gained less attention over the last years. Only few contributions have been, so far, proposed, notably [12] and [13]. In [12], Y. Chen et al. provided an upper bound on the transmission capacity defined as the number of successful transmissions that can occur per unit area. Previously, the authors of [13] proposed some throughput scaling laws of multihop systems over generalized fading.

From the aforementioned up-to-date technical literature, there appear to be no analytical ergodic capacity results which apply for fixed-gain dual-hop systems with arbitrary channel configurations.

This paper goes toward filling this gap by deriving new exact analytical expressions for the ergodic capacity of fixed-gain AF single-relay systems in interference-impaired channels. In contrast to previous results, our expressions apply for any finite number of interferers at the relay and the destination and for arbitrary Nakagami-m fading on the desired and interfering links.

Based on our analytical expressions, we investigate the effect of different system and channel parameters on the ergodic capacity. For example, we show that the ergodic capacity is dominated by the source-relay interference constraint and that it improves slowly with the average SNR increasing. Furthermore, a larger Nakagami-m fading parameter for interference channels slightly deteriorates the system's performance. Moreover, in a distance relay-dependent link layout, our

results show that the new ergodic capacity expressions provide a very practical tool for the optimization of relay location to significantly improve the system's capacity.

The remainder of this paper is organized as follows : In Section II, the basic definitions and background related to the dual-hop fixed-gain relaying suffering interference are provided. Section III presents our new integral relations of the ergodic capacity evaluation. These integrals are subsequently used to derive more compact forms for the ergodic capacity under integer Nakagami-m fading in Sections IV. Section V assesses the performance analysis by numerical examples, and Section IV concludes the paper. All of the main mathematical proofs have been placed in the Appendices.

4.2   Interference-limited relaying : system model
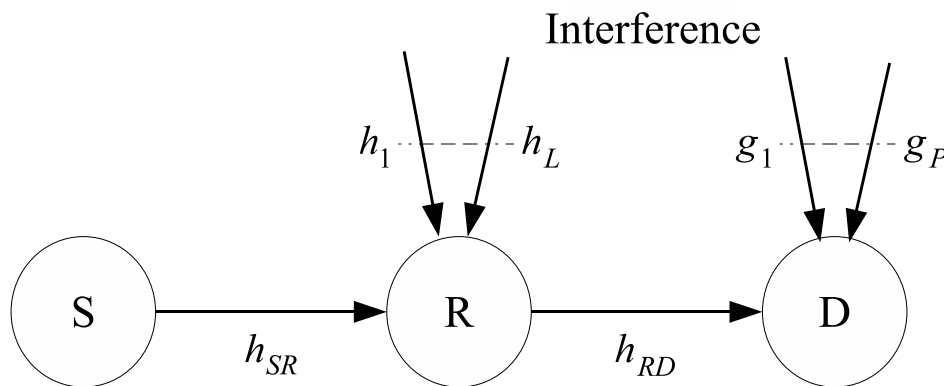
FIGURE 4.1 – Single-relay transmission system with cochannel interference.

Fig. 1 illustrates a single-relay system. The fading gains from the source-to-relay and relay-to-destination are denoted by h_{SR} and h_{RD}, respectively. These channel gains are assumed to be independently and identically distributed (i.i.d.) Nakagami-m fading. In the first time slot, the relay node receives a faded noisy signal from the source and a finite number of faded cochannel interfering signals from L external interferers. Thus, the signal received at the relay node is given by

$$y_{SR} = \sqrt{P_s}h_{SR}s_0 + \sum_{l=1}^{L}\sqrt{\alpha_l}h_l s_l + n_r, \tag{4.1}$$

where s_0 denotes the unit-energy signal transmitted from the source ; and P_s indicates the transmit energy from the said node. In the second term of the right-hand-side (RHS) of (4.1),

74

s_l is the l-th cochannel interferer's signal affecting the relay with energy equal to α_l, L is the total number of interferers that affect the relay, and h_l is the flat Nakagami-m fading coefficient of the l-th interference channel. Finally, the third term of the RHS of (4.1), i.e., n_r, represents the additive white Gaussian noise (AWGN) term at the relay, with zero mean and variance σ_R^2. In the second time slot, the relay forwards a scaled version of the received signal y_{SR} to the destination

$$y_{RD} = b_F h_{RD} y_{SR} + \sum_{p=1}^{P} \sqrt{\beta_p} g_p c_p + n_d, \tag{4.2}$$

where b_F is the amplification coefficient aiming to guarantee that the average transmitted power does not exceed the power budget available at the relay node. As such, let P_r be the transmission power available at the relay, then the amplification coefficient is chosen as

$$b_F = \sqrt{\mathrm{E}\left[Pr/(Ps|h_{SR}|^2 + \sum_{l=1}^{L} \alpha_l|h_l|^2 + \sigma_R^2)\right]}. \tag{4.3}$$

In the R.H.S of (4.2), c_p is the p-th cochannel interferer's signal affecting the destination with energy equal to β_p, P is the total number of interferers that affect the destination, and g_p is the flat Nakagami-m fading coefficient of the p-th interference channel. Finally, n_d represents the AWGN term at the destination, with zero mean and variance σ_D^2. By assuming mutual independency between the different links, the end-to-end signal-to-interference-plus-noise ratio (SINR) at the destination can be obtained as

$$\gamma = \frac{b_F^2 P_s |h_{SR}|^2 |h_{RD}|^2}{b_F^2 |h_{RD}|^2 \sigma_R^2 + b_F^2 |h_{RD}|^2 \sum_{l=1}^{L} \alpha_l |h_l|^2 + \sum_{p=1}^{P} \beta_p |g_p|^2 + \sigma_D^2}. \tag{4.4}$$

After some manipulations, (4.4) can be further simplified to

$$\begin{aligned}
\gamma &= \frac{\gamma_1 \gamma_2}{\gamma_2 \left(1 + \sum_{l=1}^{L} Y_l\right) + \frac{P_s}{\sigma_R^2 b_F^2} \left(1 + \sum_{p=1}^{P} Z_p\right)} \\
&= \frac{\gamma_1 \gamma_2}{\gamma_2 (1 + \lambda) + G_F (1 + \chi)},
\end{aligned} \tag{4.5}$$

where $\gamma_1 = P_s|h_{SR}|^2/\sigma_R^2$ and $\gamma_2 = P_r|h_{RD}|^2/\sigma_D^2$ indicate the instantaneous SNR of the source-to-relay and the relay-to-destination links, respectively. Likewise, $\lambda = \sum_{l=1}^{L} Y_l$ and $\chi = \sum_{p=1}^{P} Z_p$ denote the total interference-to-noise ratios (INRs) at the relay and the destination, respectively, whereby $Y_l = \alpha_l|h_l|^2/\sigma_R^2$ and $Z_p = \beta_p|g_p|^2/\sigma_D^2$. Finally, $G_F = P_r/\sigma_R^2 b_F^2$.

4.3 Ergodic capacity analysis : integral Form

Capacity analysis is of extreme importance in the design of wireless systems since it determines the maximum achievable rates in the network. A reliable capacity performance study has to take into account important issues such as co-channel interference. This motivates us to introduce the following theorem :

Theorem 1 : The ergodic capacity [1] (bit/s/Hz) of dual-hop fixed gain relaying systems suffering interference is given by

$$C_E = \frac{1}{2\ln(2)} \left\{ \int_0^\infty E_0(\xi)\, M_\lambda(\xi) M_{\frac{1+\chi}{\gamma_2}}\left(G_F \xi\right) d\xi - \int_0^\infty E_0\left(\xi\right) M_{\gamma_1}(\xi) M_\lambda(\xi) M_{\frac{1+\chi}{\gamma_2}}\left(G_F \xi\right) d\xi \right\}, (4.6)$$

where $M_z(\cdot)$ stands for the moment generating function (MGF) of z and $E_\nu(\cdot)$ denotes the exponential integral function of order ν [21, Eq. (8.485)]. *Proof :* See Appendix A.

The result in (4.6) offers a flexible and simple MGF-based approach for the computation of the ergodic capacity of fixed-gain relaying systems suffering interference. (4.6) relies on the knowledge of the MGFs of the first-hop SNR and INR γ_1 and λ, as well as the second-hop inverse SINR $(1+\chi)/\gamma_2$. To the best of our knowledge, closed-form and exact expressions for these MGFs exist for most fading models.

Most importantly, with respect to the MGF-based approach for the ergodic capacity computation in [11], the final result in (4.6) is much more easier to compute given that : i) [11, Eq. (7)] employs the end-to-end MGF expression which turns out to be untractable for fixed-gain relaying systems suffering interference, and ii) [11, Eq. (7)] requires the first and the second derivatives of the MGF, a fact that can highly increase the computational burden of the ergodic capacity calculation, notably when the MGF is expressed as a product of more than two functions. Therefore, though considered as a prominent contribution to the ergodic capacity analysis, the unified approach proposed in [11] cannot be applied here.

Hereafter, we will restrict the scope of (4.6) to the yet challenging scenario of non-identically distributed Nakagami-m fading channels. In this context, new expressions for the ergodic capacity are presented where AWGN is neglected at the destination and, hence, the second-hop SIR is given by $U = \chi/\gamma_2$. It is noteworthy that this case is often encountered in real-world applications especially when the destination is located at the cell-edge where the received interference is

---

1. In this paper, the ergodic capacity is a measure that corresponds to the long-term average achievable rate over all states of the time-varying fading channel [17].

dominant.

Corollary 1 : The ergodic capacity of an interference-limited multi-hop AF relaying system in arbitrary Nakagami-m fading is given by

$$C_E = \sum_{p=1}^{P} \sum_{k=1}^{m_{Z_p}} \frac{G_F^{m_2} A_{p,n}}{2\ln(2)} \int_0^{\infty} \xi^{m_2} E_0(\xi) \prod_{l=1}^{L} \left(1 + \frac{\bar{Y}_l}{m_{Y_l}}\xi\right)^{-m_{Y_l}} \left(1 - \left(1 + \frac{\bar{\gamma}_1}{m_1}\xi\right)^{-m_1}\right)$$
$$\Psi\left(m_2 + k; m_2 + 1; \frac{G_F m_2 \bar{Z}_p}{m_{Z_p} \bar{\gamma}_2}\xi\right) d\xi, \tag{4.7}$$

where $\Psi(a; b; z)$ is the Triconomi confluent hypergeometric function [21, Eq. (9.211.4)].

Proof : Under Nakagami-m fading, the MGFs of the SNR γ_1 (or γ_2) and individual INR Y_l (or Z_p) are given by

$$M_{\gamma_1}(s) = \left(1 + \frac{\bar{\gamma}_1}{m_1}s\right)^{-m_1},$$
$$M_{Y_l}(s) = \left(1 + \frac{\bar{Y}_l}{m_{Y_l}}s\right)^{-m_{Y_l}}, \tag{4.8}$$

where m_1 (or m_2) and $\bar{\gamma}_1$ (or $\bar{\gamma}_2$) are, respectively, the Nakagami fading parameter and the average power of the desired signal. Similarly, m_{Y_l} (or m_{Z_p}) and $\bar{Y}_l$ (or $\bar{Z}_p$) are the Nakagami fading parameter and the average power of the l-th interfering signal to the relay (or the p-th interfering signal to the destination), respectively. On the other hand, the MGF of the combined INR λ (or χ), which is the sum of independent Gamma-distributed random variables Y_l (or Z_p), is equal to the product of the individual MGFs, yielding

$$M_\lambda(s) = \prod_{l=1}^{L} M_{Y_l}(s) = \prod_{l=1}^{L} \left(1 + \frac{\bar{Y}_l}{m_{Y_l}}s\right)^{-m_{Y_l}}. \tag{4.9}$$

When the Nakagami shape factor is assumed to be an integer value, the product of the MGFs of P Gamma-distributed random variables can be further derived using [18] as

$$\prod_{p=1}^{P} (1 + \alpha_p z)^{-m_{Z_p}} = \sum_{p=1}^{P} \sum_{k=1}^{m_{Z_p}} \frac{\beta_{p,k}}{(\alpha_p z + 1)^k}, \tag{4.10}$$

where

$$\beta_{p,k} = \alpha_p^{k-m_{Z_p}} \sum_{\tau(p,k)} \sum_{i=1, i \neq p}^{P} \binom{m_{Z_i} + q_i - 1}{q_i} \frac{(-\alpha_i)^{q_i}}{\left(1 - \frac{\alpha_i}{\alpha_l}\right)^{m_{Z_i} + q_i}}, \tag{4.11}$$

with $\alpha_i = \bar{Z}_i / m_{Z_i}$ and $\tau(p, k)$ denotes a set of P-tuples such that $\tau(i, j) = \{(q_1, ..., q_P) : q_i = 0, \sum_{k=1}^{P} q_k = (m_{Z_i} - j)\}$ where q_is are non-negative integers.

To solve (4.6), the MGF of the ratio $\frac{\chi}{\gamma_2}$ is required. For convenience, let $U = \frac{\chi}{\gamma_2}$, then the MGF of U is shown to be given by

$$M_U(s) = \sum_{p=1}^{P} \sum_{k=1}^{m_{Z_p}} A_{p,k} s^{m_2} \Psi\left(m_2 + k; m_2 + 1; \frac{m_2 \bar{Z}_p}{m_{Z_p} \bar{\gamma}_2}s\right), \tag{4.12}$$

77

where

$$A_{p,k} = \frac{\left(\frac{m_2 \bar{Z}_p}{m_{Z_p} \bar{\gamma}_2}\right)^{m_2} \beta_{p,k} \Gamma(m_2 + k)}{\left(\frac{m_{Z_p}}{\bar{Z}_p}\right)^k \Gamma(m_2)\Gamma(k)}, \tag{4.13}$$

Proof : See appendix B.

Hence, substituting (4.8) and (4.12) into (4.6) yields the end-to-end ergodic capacity expression under Nakagami-m fading as given in (4.7). The latter holds for arbitrary Nakagami-m factors m_1, m_2 and $m_{Y_l}, l = 1, ..., L$. Nevertheless, $m_{Z_p}, p = 1, ..., P$, are constrained to have non-negative integer values. To overcome this shortcoming, we consider the special case of Nakagami-m fading channel with P independent identically distributed (i.i.d.) interfering signals at the destination.

Corollary 2 : The ergodic capacity of an interference-limited AF relaying system with i.i.d interferers at the destination in Nakagami-m fading is given by

$$C_E = \frac{\Gamma(m_2 + Pm_I)}{2\ln(2)\Gamma(m_2)} \int_0^\infty E_0(\xi) \prod_{l=1}^L \left(1 + \frac{\bar{Y}_l}{m_{Y_l}}\xi\right)^{-m_{Y_l}} \left(1 - \left(1 + \frac{\bar{\gamma}_1}{m_1}\xi\right)^{-m_1}\right) \Psi\left(Pm_I; 1 - m_2; \frac{G_F m_2 \bar{Z}_I}{m_I \bar{\gamma}_2}\xi\right) d\xi, \tag{4.14}$$

Proof : By following the same rationale to obtain (4.12), the MGF of $U = \chi/\gamma_2$ can be readily derived as

$$M_U(s) = \frac{\Gamma(m_2 + Pm_I)\left(\frac{m_2 \bar{Z}_I s}{m_I \bar{\gamma}_2}\right)^{m_2}}{\Gamma(m_2)} \Psi\left(m_2 + Pm_I; m_2 + 1; \frac{m_2 \bar{Z}_I}{m_I \bar{\gamma}_2}s\right), \tag{4.15}$$

where $m_{Z_1} = ... = m_{Z_P} = m_I$ and $\bar{Z}_1 = ... = \bar{Z}_P = \bar{Z}_I$. Substituting (4.15) leads to the desired result in (4.14).

Here, we would like to emphasize the fact that the scenario pertaining to $L = P = 1$ in (4.14) has been recently addressed in [3], where the authors have provided a closed-form expression for the probability density function (pdf) of the output SINR. The latter can therefore be exploited to derive the ergodic capacity which is expected to have an infinite integral form similar to (4.14). Unfortunately, this pdf-based approach owes its tractability to the assumption of integer Nakagami-m fading on the first hop [3]. Unlike [3], the result in (4.14) avoids this limitation and is therefore more general.

Also of interest is the case of dual-hop relaying in interference-free fading. Such a useful result stands as a benchmark that can highlight the effect of interference on the system's performance. Therefore, substituting $\lambda = \chi = 0$ in (4.6) yields the ergodic capacity in the absence

of interference given by

$$C_E = \frac{1}{2\ln(2)} \left\{ \int_0^\infty E_0(\xi) M_{\gamma_2^{-1}}(G_F\xi)\, d\xi - \int_0^\infty E_0(\xi) M_{\gamma_1}(\xi) M_{\gamma_2^{-1}}(G_F\xi)\, d\xi \right\}. \qquad (4.16)$$

Interference-free relaying has been extensively studied in the literature, particulary under Nakagami-m fading (c.f., [12] and references therein). However, to the best of our knowledge, there appears to be no analytical ergodic capacity expression which applies for arbitrary Nakagami-m fading. While the MGF of the first-hop SNR γ_1 is given in (4.8), the MGF of the second-hop inverse SNR γ_2^{-1} is given by [12] as

$$M_{\gamma_2^{-1}}(s) = 2 \frac{\left(\frac{m_2}{\bar{\gamma_2}}\right)^{\frac{m_2}{2}}}{\Gamma(m_2)} s^{\frac{m_2}{2}} K_{m_2}\left(2\sqrt{\frac{sm_2}{\bar{\gamma_2}}}\right), \qquad (4.17)$$

where $K_\lambda(\cdot)$ is the modified Bessel function of the second kind and order λ [21, Eq. (8.432.1)]. Accordingly, the ergodic capacity of a single-relay system in Nakagami-m is given by

$$C_E = \frac{\left(\frac{G_F m_2}{\bar{\gamma_2}}\right)^{\frac{m_2}{2}}}{\ln(2)\Gamma(m_2)} \int_0^\infty \xi^{\frac{m_2}{2}} E_0(\xi) \left(1 - \left(1 + \frac{\bar{\gamma_1}}{m_1}\xi\right)^{-m_1}\right) K_{m_2}\left(2\sqrt{\frac{G_F\xi m_2}{\bar{\gamma_2}}}\right) d\xi. \quad (4.18)$$

Note that, although closed-form expressions for (4.7), (4.14) and (4.18) cannot be obtained in general, they can be easily evaluated numerically since their integrands involve only elementary functions and hypergeometric and exponential integral built-in functions available in most popular mathematical software. As far as the numerical evaluation of (4.7) and (4.14) is concerned, it can be seen that their integrands are continuous and possess all derivatives for $\xi > 0$. Moreover, it can be easily shown that the integrands are bounded and non negative (and therefore have no singular points) in the range of integration. Nevertheless, to compute (4.7), (4.14) and (4.18), an analytical expression of G_F is required. The latter is shown to be given by

$$G_F^{-1} = \frac{m_1}{\bar{\gamma_1}} \Phi_2\left(1; m_{Y_1}, ..., m_{Y_L}; m_1; \frac{\bar{Y_1}m_1}{m_{Y_1}\bar{\gamma_1}}, ..., \frac{\bar{Y_L}m_1}{m_{Y_L}\bar{\gamma_1}}, \frac{m_1}{\bar{\gamma_1}}\right), \qquad (4.19)$$

where $\Phi_2(a; b_1, ..., b_K; z; x_1, ..., x_K, y)$ is the second-kind confluent hypergeometric function of multiple variables given by [11]

$$\Phi_2(a; b_1, ..., b_K; z; x_1, ..., x_K, y) = \frac{1}{\Gamma(a)} \int_0^\infty \exp(-yt) t^{a-1}(1+t)^{a-z-1} \prod_{k=1}^K (1+x_i t)^{-b_i} dt. \quad (4.20)$$

Proof : Recalling the definition of G_F in section II, this constant can be calculated in view

of [12] as

$$G_F^{-1} = \mathrm{E}\left\{\frac{1}{\gamma_1 + \lambda + 1}\right\} = \int_0^\infty \exp(-\xi) M_{\gamma_1}(\xi) M_\lambda(\xi) d\xi,$$

$$= \int_0^\infty \exp(-\xi)\left(1+\frac{\bar{\gamma}_1}{m_1}\xi\right)^{-m_1} \prod_{l=1}^L \left(1+\frac{\bar{Y}_l}{m_{Y_l}}\xi\right)^{-m_{Y_l}} d\xi. \tag{4.21}$$

By performing the change of variable $z = \frac{\bar{\gamma}_1}{m_1}\xi$ in (4.21), one can recognize that the latter can be expressed in terms of $\Phi_2\left(a; b_1, ..., b_K; z; x_1, ..., x_K, y\right)$ as shown in (4.19). Note that in the absence of interference, G_F reduces to the already known expression in the literature [12], given by

$$G_F = \left[\frac{m_1}{\bar{\gamma}_1}\Psi\left(1; 2 - m_1; \frac{m_1}{\bar{\gamma}_1}\right)\right]^{-1}. \tag{4.22}$$

4.4   Ergodic capacity analysis : compact form

Due to the high degree of difficulty in resolving the problem it raises with respect to the current state of the art and given the complicated structure of the integral-based ergodic capacity expressions obtained in the previous section, the authors are unaware of any closed-form solution to these integrals. However, under some special circumstances, compact forms for the ergodic capacity in terms of a special function, namely the Meijer's G-function of two variables, is possible. The Meijer's G-function of two variables is a non-elementary or a built-in function about which a significant literature has developed because of its importance in either mathematical theory or in practice [20], [22]. Recently, an excellent algorithm for the computation of the bivariate Meijer's G-function has been developed in [24]. In what follows let

$$G_{A,[C,E],B,[D,F]}^{p,q,k,r,l}\left(z_1, z_2 \left| \begin{array}{c} \alpha_1, ..., \alpha_A; \gamma_1, ..., \gamma_C; \epsilon_1, ..., \epsilon_E \\ \beta_1, ..., \beta_B; \delta_1, ..., \delta_D; \phi_1, ..., \phi_F \end{array}\right.\right), \tag{4.23}$$

denote the Meijer's G-function of two variables z_1 and z_2 defined in [22, Eq. (2.3)].

Corollary 3 : The ergodic capacity of fixed-gain relaying in an interference-limited destination scenario with an integer Nakagami-m fading parameter of the useful/interfering information-bearing first link is expressed as

$$C_E = \frac{1}{2\ln(2)\Gamma(m_2)\Gamma(Pm_I)} \sum_{k=1}^{m_1}\binom{m_1}{k}\left(\frac{\bar{\gamma}_1}{m_1}\right)^k \sum_{l=1}^{L+1}\sum_{p=1}^{M_l}\Upsilon_{l,p}$$

$$G_{2,[1:1],1,[1:2]}^{2,1,1,1,2}\left(\frac{G_F m_2 \bar{Z}_I}{m_{Z_I}\bar{\gamma}_2}, \Delta_l \left| \begin{array}{c} 1-k, -k; p, Pm_I \\ k+1; 0; 0, m_2 \end{array}\right.\right). \tag{4.24}$$

80

Note that in an interference-limited destination scenario, the relay experiences interference and AWGN, while the destination is AWGN-free and subject to interference only. This case amounts to a downlink communication, in which the destination is close to the cell boundary.

Proof : Under the assumption that the Nakagami-m factors m_1 and $m_{Y_l}, l = 1, ..., L$ are integer values, we have

$$\prod_{l=1}^{L}\left(1+\frac{\bar{Y}_l}{m_{Y_l}}\xi\right)^{-m_{Y_l}}\left(1-\left(1+\frac{\bar{\gamma}_1}{m_1}\xi\right)^{-m_1}\right) = \sum_{k=1}^{m_1}\binom{m_1}{k}\left(\frac{\bar{\gamma}_1}{m_1}\right)^k\sum_{l=1}^{L+1}\sum_{p=1}^{M_l}\frac{\Upsilon_{l,p}\xi^k}{(\Delta_l\xi+1)^p}, \quad (4.25)$$

whereby $M = \{m_1, m_{Y_1}, m_{Y_2}, ..., m_{Y_L}\}$, $\Delta = \{\bar{\gamma}_1/m_1, \bar{Y}_1/m_{Y_1}, ..., \bar{Y}_L/m_{Y_L}\}$, and

$$\Upsilon_{l,k} = \Delta_l^{k-M_l}\sum_{\tau(l,k)}\sum_{i=1,i\neq l}^{L+1}\binom{M_i + q_i - 1}{q_i}\frac{(-\Delta_i)^{q_i}}{\left(1 - \frac{\Delta_i}{\Delta_l}\right)^{M_i+q_i}}, \quad (4.26)$$

where, to obtain (4.25), we exploited (4.10) and the binomial expansion theorem in [21, Eq. (1.111)]. Hence, upon substitution of (4.25) into (4.7), it follows that the ergodic capacity can be expressed as

$$C_E=\frac{\Gamma(m_2+Pm_I)}{2\ln(2)\Gamma(m_2)}\sum_{k=1}^{m_1}\binom{m_1}{k}\left(\frac{\bar{\gamma}_1}{m_1}\right)^k\sum_{l=1}^{L+1}\sum_{p=1}^{M_l}\Upsilon_{l,p}\underbrace{\int_0^\infty\frac{\xi^k E_0(\xi)}{(\Delta_l\xi+1)^p}\Psi\left(Pm_I;1-m_2;\frac{G_Fm_2\bar{Z}_I}{m_{Z_I}\bar{\gamma}_2}\xi\right)d\xi}_{\Phi}.$$

$$(4.27)$$

We now have to solve the integral Φ in order to derive the ergodic capacity for the relaying system under consideration. For the purpose of further analytical evaluation of Φ, we represent the functions constituting the integrands as Meijer's G-functions. Therefore, using [23, Eqs. (8.4.3.1) and (8.5.2.5)], we have

$$E_0(x) = G_{1,2}^{2,0}\left(z\,\middle|\,\begin{matrix}0\\-1,0\end{matrix}\right) \quad \text{and} \quad (1+z)^{-\nu} = \frac{1}{\Gamma(\nu)}G_{1,1}^{1,1}\left(z\,\middle|\,\begin{matrix}1-\nu\\0\end{matrix}\right), \nu \geq 0, \quad (4.28)$$

and, using [23, Eq. (8.4.46.1)], we get

$$\Psi(a, b; z) = \frac{1}{\Gamma(a)\Gamma(a-b+1)}G_{1,2}^{2,1}\left(z\,\middle|\,\begin{matrix}1-a\\0,1-b\end{matrix}\right). \quad (4.29)$$

Upon substitution of (4.28) and (4.29) into Φ, we obtain

$$\Phi = A\int_0^\infty\xi^k G_{1,2}^{2,0}\left(\xi\,\middle|\,\begin{matrix}0\\-1,0\end{matrix}\right)G_{1,1}^{1,1}\left(\Delta_l\xi\,\middle|\,\begin{matrix}1-p\\0\end{matrix}\right)G_{1,2}^{2,1}\left(\frac{G_Fm_2\bar{Z}_I}{m_{Z_I}\bar{\gamma}_2}\xi\,\middle|\,\begin{matrix}1-Pm_I\\0,m_2\end{matrix}\right)d\xi, \quad (4.30)$$

81

where $A = 1/\Gamma(Pm_I)\Gamma(Pm_I + m_2)$. The second and third Meijer's G-functions in the R.H.S of (4.30) are transformed into a Meijer's G-function of two variables according to the functional relation

$$
\mathrm{G}_{C,D}^{r,q}\left(z_1 \,\middle|\, \begin{matrix} \gamma_1, ..., \gamma_c \\ \delta_1, ..., \delta_D \end{matrix} \right) \mathrm{G}_{E,F}^{l,k}\left(z_2 \,\middle|\, \begin{matrix} \epsilon_1, ..., \epsilon_E \\ \phi_1, ..., \phi_F \end{matrix} \right) =
$$

$$
\mathrm{G}_{0,[C,E],0,[D,F]}^{0,q,k,r,l}\left(z_1, z_2 \,\middle|\, \begin{matrix} ...; 1 - \gamma_1, ..., 1 - \gamma_C; 1 - \epsilon_1, ..., 1 - \epsilon_E \\ ....; \delta_1, ..., \delta_D; \phi_1, ..., \phi_F \end{matrix} \right). \quad (4.31)
$$

Then, by exploiting [22, Eq. (3.2)], we obtain

$$
\Phi = A\mathrm{G}_{2,[1:1],1,[1:2]}^{2,1,1,1,2}\left(\frac{G_F m_2 \bar{Z}_I}{m_{Z_I}\bar{\gamma}_2}, \Delta_l \,\middle|\, \begin{matrix} 1 - k, -k; p, Pm_I \\ k + 1; 0; 0, m_2 \end{matrix} \right). \quad (4.32)
$$

Finally, substituting (4.32) into (4.27) yields the desired result.

Corollary 4 : Under an interference-free destination scenario, the relay experiences interference and AWGN while the destination is interference-free and subject to AWGN only. This case amounts to an uplink communication in which the destination communicates with the source using a relay, which is located in the proximity of the cell edge. Thus the ergodic capacity becomes

$$
C_E = \frac{(G_F \frac{m_2}{\bar{\gamma}_2})^{\frac{m_2}{2}}}{\ln(2)\Gamma(m_2)} \sum_{k=1}^{m_1} \binom{m_1}{k} \left(\frac{\bar{\gamma}_1}{m_1} \right)^k \sum_{l=1}^{L+1} \sum_{p=1}^{M_l} \Upsilon_{l,p} \mathrm{G}_{2,[1:0],1,[1:2]}^{2,1,0,1,2}\left(\frac{G_F m_2}{\bar{\gamma}_2}, \Delta_l \,\middle|\, \begin{matrix} 1 - k - \frac{m_2}{2}, -\frac{m_2}{2} - k; p; ... \\ \frac{m_2}{2} + k + 1; 0; \frac{m_2}{2}, -\frac{m_2}{2} \end{matrix} \right).
$$
$$(4.33)$$

Proof : When $\chi = 0$, the ergodic capacity can be expressed by inserting (4.8), (4.9) and (4.17) into (4.6). Then, (4.33) is obtained by following the same rationale to obtain (4.24) upon representing the Bessel K function using the Meijer's G-function[2] as [23, Eq. (8.4.23.1)]

$$
K_\lambda\left(\sqrt{\beta}x \right) = \frac{1}{4}\mathrm{G}_{2,0}^{0,2}\left(\frac{\beta x^2}{4} \,\middle|\, \begin{matrix} - \\ \frac{\lambda}{2}, \frac{-\lambda}{2} \end{matrix} \right). \quad (4.34)
$$

---

2. Notice that the Meijer's G-function of two variables in (4.23) converges if the following conditions are satisfied [20] : $A + D + B + C < 2(r + q + p)$ and $A + F + B + E < 2(l + k + p)$. It is straightforward to show that the parameters of the Meijer's G-function in (4.24) and (4.33) satisfy these sufficient conditions, and therefore the Meijer's G-functions converge.

4.5 Numerical examples and discussions

The aim of this section is to illustrate the expressions derived in Sections III and IV using numerical examples and examine the effect of interference on the system's capacity.

In Figs. 2-4, to exclude the effect of the relay's placement, we assume a symmetric network such that the relay sits half-way between the source and the destination, so that $\bar{\gamma}_1 = \bar{\gamma}_2 = \bar{\gamma}$. The interference is assumed to be i.i.d on each link with mean power $\bar{Y}_I$ and $\bar{Z}_I$. To exclude the effect of the interference positions, we also assume that $\bar{Y}_I = \bar{Z}_I = \bar{\gamma}_I$. The effect of varying the relative placement of the relay and interference will be treated later in Figs. 5 and 6.
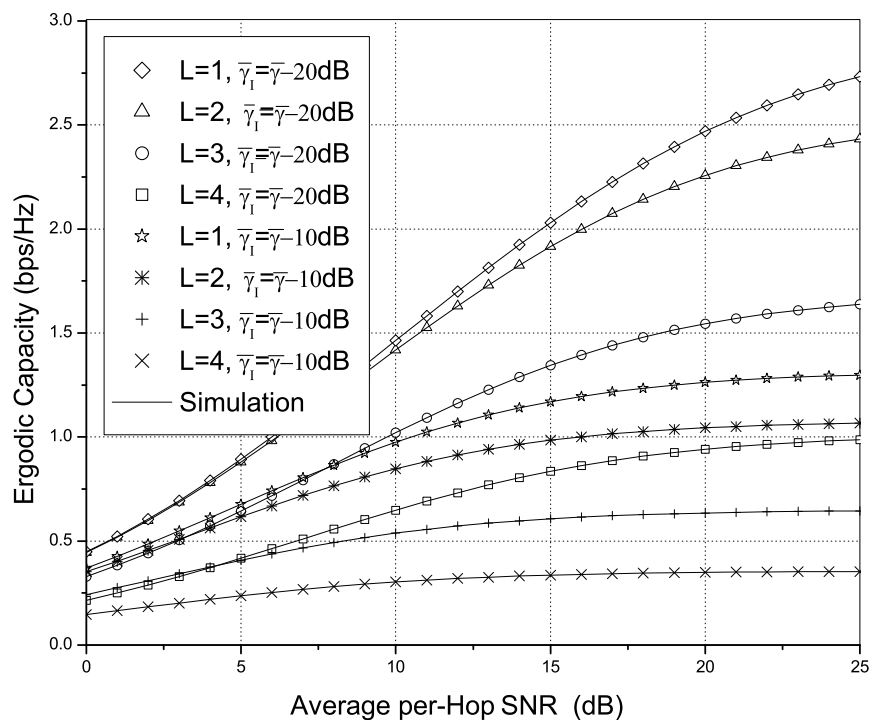
FIGURE 4.2 – Ergodic capacity for different numbers of interferers at the relay and the destination when $P = L$, $m_1 = m_2 = 1.5$, $m_I = 1$, and $\bar{\gamma}_I = \bar{\gamma} - \{10, 20\}$ dB.

Fig. 2 shows the ergodic capacity performance when the number of interferers increases from 1 to 4, and the average strength of the interfering links varies between 10 and 20 dB lower than that of the useful link so that $\bar{\gamma}_I = \bar{\gamma} - 10$ dB and $\bar{\gamma}_I = \bar{\gamma} - 20$ dB. We can see that as the number of interferers increases, the ergodic capacity relatively improves very slowly with increasing SNR. Moreover, the ergodic capacity attains a saturation level which is

more noticeable when the difference between the received powers of the useful and interfering signals decreases. Hence, interference imposes severe constraints on the system's capacity, thereby highlighting the significance of using interference cancelation techniques in interference-impaired relay systems in order to attain the beneficial effects of relaying.

Fig. 3 deals with fixed-gain relaying under interference-free and interference-limited destination scenarios and illustrates the ergodic capacity performance obtained from *Corollaries* 3 and 4. The average strength of the interference link was set in both cases to $3, 10$ and 20 dB lower than that of the useful link. Here, we observe cross-over points in the ergodic capacity curves, in the low-to-moderate SNR region, where the interference-limited destination scenario performs better than the interference-free destination scenario, especially in the presence of weak interference. This observation can be explained by the fact that in the low-to-moderate SNR region, the noise-dominant configuration shows the worst ergodic capacity performance for all channel conditions. Therefore, a low interference power, $\bar{\gamma}_I = \bar{\gamma} - 20$ dB at the destination can lead to a higher ergodic capacity in the case of interference-limited reception, as compared to high AWGN power at the destination in case of an interference-free destination scenario. As the SNR increases, the performance gaps among the considered interference scenarios become larger and the interference-dominant configuration has the worst performance in the high-SNR region. Furthermore, since in the interference-limited destination scenario both the relay and the destination experience cochannel interference, the saturation level on the ergodic capacity performance is reached at lower SNR values (i.e., 5 dB), compared to the interference-free destination scenario (i.e., 15 dB). Hence, it is shown that the downlink is more vulnerable to the presence of interference than the uplink.

When mapped into a link-level study, the observations made above can lead to useful decisions about relay placement/selection options to improve performance on both downlink and uplink in different regions of the cell experiencing different interference levels.

From this figure, a good accuracy is retained by the analytical expressions, which turn out to be not only very accurate but also numerically stable.

Fig. 4 plots the ergodic capacity of a dual-hop fixed-gain relaying system under interference-free Nakagami-m fading, as computed with (4.18), and compares it with Monte Carlo simulations. As can be seen from this figure, a very good match is retained over the SNR range of interest. To highlight the importance of the proposed framework, we also report in Fig. 4 the ergodic
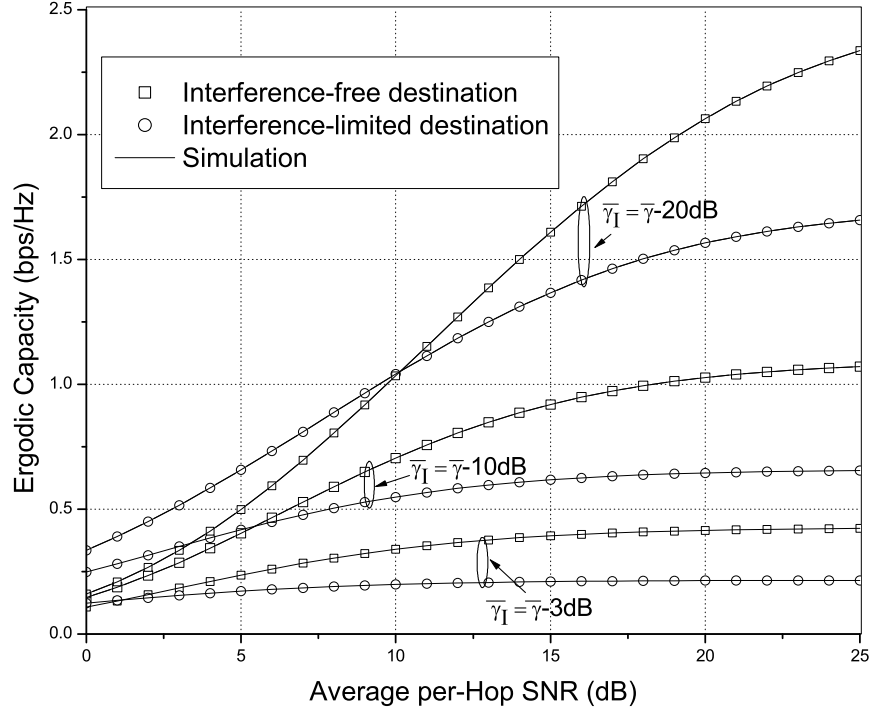
FIGURE 4.3 – Ergodic capacity of both interference-free ($L = 3$, $P = 0$) and interference-limited ($L = 3$, $P = 3$) destination scenarios when $m_1 = 1$, $m_2 = 1.5$, and $m_I = 1$.

capacity bounds obtained in [14, Eq. (8)]. As can be seen, in the SNR range of interest, these bounds are not sufficiently tight to be considered for predicting the ergodic capacity of dual-hop fixed gain relaying. Although the tightness of the proposed bounds improves with m, it is more likely to decrease for the new communication systems, such as LTE-Advanced [2], where the fading is more pronounced (i.e., lower values of m) due to the terminal's mobility and the high level of shadowing.

Fig. 5 investigates the impact of the relay location on the AF system's capacity with a single interferer at both the relay and the destination. In this figure, it is assumed that the relay is arbitrarily located between the source and the destination. To compare the effect of network geometry fairly and generally, the distance between nodes can be normalized by the length of the source-to-destination link. Therefore, the normalized local mean SNR of the source-to-relay and the relay-to-destination links can be, respectively, expressed by

$$\bar{\gamma}_1 = \left(\frac{d_{\mathbf{S-D}}}{d_{\mathbf{S-R}}}\right)^{\alpha} \Omega, \quad \bar{\gamma}_2 = \left(\frac{d_{\mathbf{S-D}}}{d_{\mathbf{R-D}}}\right)^{\alpha} \Omega, \tag{4.35}$$
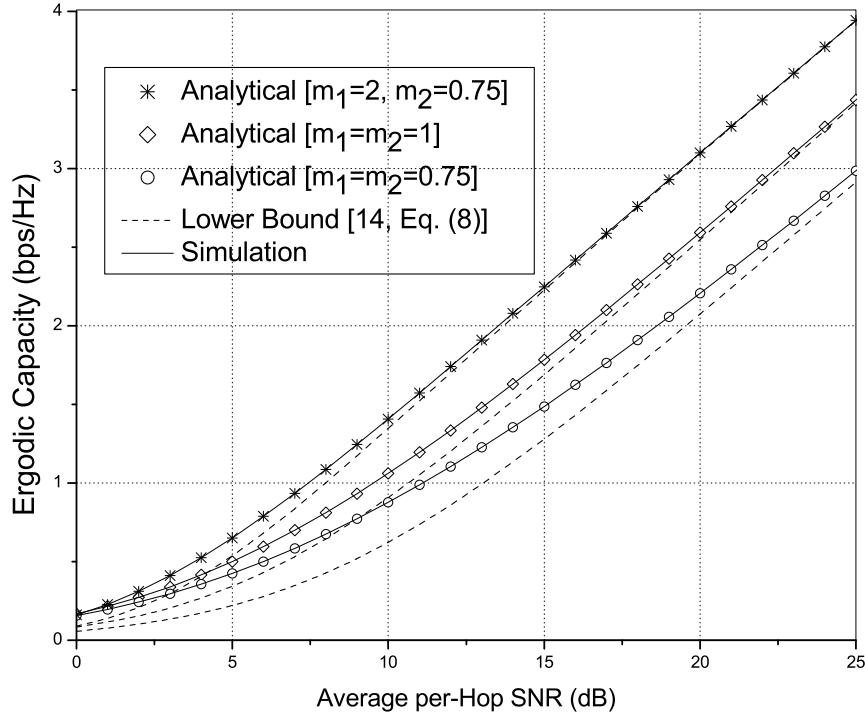
FIGURE 4.4 – Ergodic capacity of fixed-gain AF dual-hop systems in Nakagami-m fading channels : simulation and analytical/exact results and lower bound. $\bar{\gamma}_1 = \bar{\gamma}_2$.

where α is the pathloss exponent and Ω is the transmitter's SNR. An interferer is said to be far from the relay (or the destination) if $\bar{Y}_I$(or $\bar{Z}_I$) $= \Omega - 30$ dB and close to the relay (or the destination) if $\bar{Y}_I$(or $\bar{Z}_I$) $= \Omega - 5$ dB. The obtained curves illustrate the ergodic capacity against the normalized source-relay distance i.e., $d_{\mathbf{S-R}}/d_{\mathbf{S-D}}$ with $\alpha = 4$, as the relay moves on the **S-D** line (a serial configuration is assumed).

It can be seen from Fig. 5 that as the interference at the relay becomes stringent, the optimal position for the relay will be closer to the source, and vice-versa. This behavior can be expected since as the source-relay link gets worse, the relay needs to be closer to the source so as to compensate for its low quality. However, we observe that the relay has to approach the source more than the destination. The reason is that the relay requires higher SINR than the destination as the interference increases, since the relay is more vulnerable to interference than the destination. It can also be seen that under a strong interference regime and for identical interference channels, i.e., when $\bar{Y}_I = \bar{Z}_I = \Omega - 5$ dB, the midpoint relay position is almost the optimal solution with a

slight advantage for the source direction. Nevertheless, for identical weak interference channels, the optimal position for the relay will be closer to the source. From Fig. 5, it can be seen that the ergodic capacity decreases very quickly as the relay moves form his best position. Therefore, choosing the optimal relay location significantly improves the system's capacity. On the other hand, for a given interference power limit, it is seen that the ergodic capacity varies very slightly with the fading parameters of the interference channels. Moreover, when the interference power is important, the scenario where interference channels are subject to Rayleigh fading performs slightly better than the scenario where interference channels are subject to Nakagami-m fading.
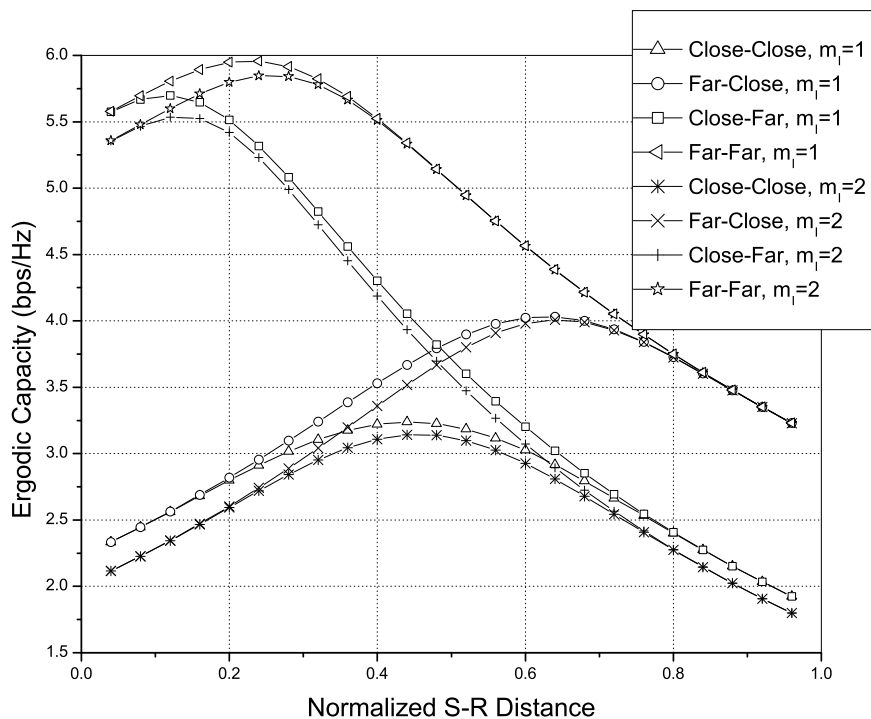
FIGURE 4.5 – Ergodic capacity versus the normalized source-to-relay distance for various interference configurations when $m_1 = m_2 = 2.5$. Far-Far : $\bar{Y}_I = \bar{Z}_I = \Omega - 30$ dB ; Close-Close : $\bar{Y}_I = \bar{Z}_I = \Omega - 5$ dB.

Fig. 6 shows the effect of imbalanced interference powers at the relay and the destination on the ergodic capacity of the AF relaying system. In this figure, it is assumed that a cluster of L interferers is located between the relay and the destination and the interference power is $\bar{\gamma}_I$. Thus, the local mean of the INRs of the interference-to-relay and the interference-to-destination
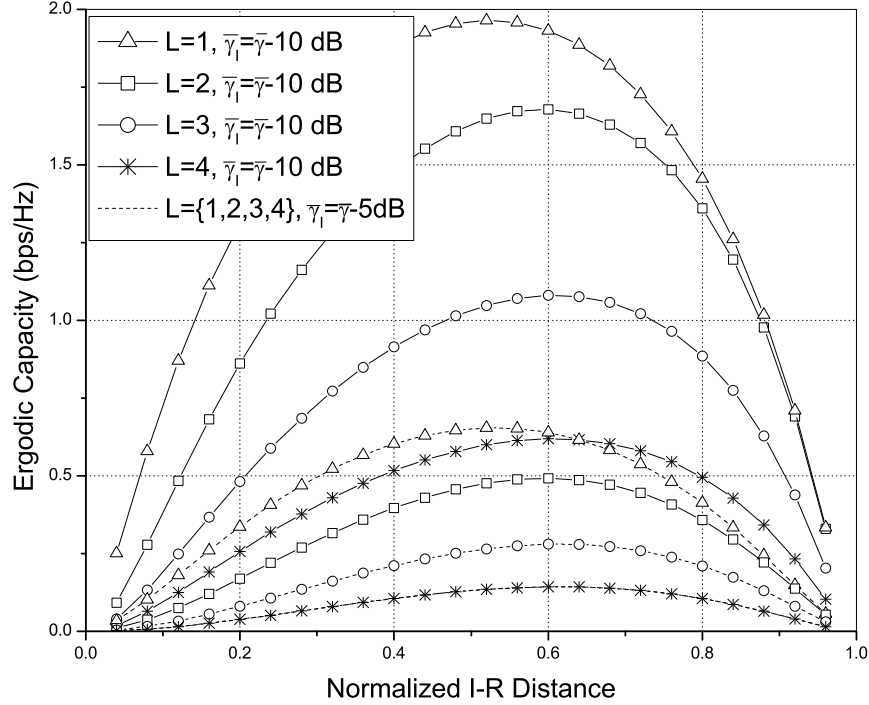
FIGURE 4.6 – Ergodic capacity versus normalized interference-to-relay distance for various numbers of interferers when $m_1 = m_2 = 2.5$, $m_I = 2$, $\bar{\gamma}_I = \bar{\gamma} - 10$ dB and $\bar{\gamma}_I = \bar{\gamma} - 5$ dB.

can be expressed as

$$\bar{Y}_I = \left(\frac{d_{\mathbf{S-D}}}{d_{\mathbf{I-R}}}\right)^\alpha \bar{\gamma}_I, \quad \bar{Z}_I = \left(\frac{d_{\mathbf{S-D}}}{d_{\mathbf{I-D}}}\right)^\alpha \bar{\gamma}_I, \tag{4.36}$$

respectively. The obtained curves illustrate the ergodic capacity against the normalized interference-relay distance, i.e., $d_{\mathbf{I-R}}/d_{\mathbf{S-D}}$ with $\alpha = 4$. As can be seen, the best position of the interference moves from the relay to the destination as L increases. We therefore observe the same behavior previously reported from Fig. 5 in that the relay is more susceptible to interference.

Combining all the observations from Figs. 2 to 6, we conclude that our new analytical expressions provide an invaluable analytical insight on : 1) how the ergodic capacity is dominated by the average interference power and how it improves slowly with the average SNR increasing, thereby inducing saturation levels ; 2) how a larger Nakagami-m fading parameter on interference channels slightly deteriorates the ergodic capacity ; 3) how instantly identifying the optimal relay location owing to our analytical/exact results (i.e., without heavy simulations) can quickly and simply help significantly increase the system's capacity.

4.6 Conclusion

In this paper we presented a comprehensive framework for the ergodic capacity evaluation of dual-hop fixed-gain relaying systems in interference-limited channels. The obtained results are useful to understand how fading and interference at the relay and/or the destination can degrade the ergodic capacity performance of the considered system. Our results show that the ergodic capacity is dominated by the average interference power, especially at the relay. Moreover, it slowly improves with the average SNR increasing while it slightly deteriorates with larger values of the Nakagami-m fading parameters pertaining to the interference channels. Furthermore, our results offer an analytical insight into the key impact of relay placement on performance. Our new ergodic capacity expressions could therefore provide a very practical/low-cost performance optimization tool for relayed-communication system designers.

Appendix A : proof of Theorem 1

The fixed-gain single relay ergodic capacity in interference-limited fading can be developed as

$$C_E = \frac{1}{2}\mathrm{E}\left\{\log_2\left(1 + \frac{\gamma_1\gamma_2}{\gamma_2\left(1+\lambda\right) + C\left(1+\chi\right)}\right)\right\},\tag{4.37}$$

which can be further expanded as

$$C_E = \frac{\mathrm{E}\left[\ln(1+\gamma_1+\lambda+\frac{C(1+\chi)}{\gamma_2})\right] - \mathrm{E}\left[\ln(1+\lambda+\frac{C(1+\chi)}{\gamma_2})\right]}{2\ln(2)}.\tag{4.38}$$

In order to give a formal proof of (4.6), consider the following Taylor series expansion of $\ln(1+z)$ valid for all $z \geq 0$, [21, Eq. (1.512.3)]

$$\ln(1+Z) = \sum_{n=1}^{\infty}\frac{1}{n}\left(\frac{Z}{Z+1}\right)^n, \qquad \forall Z \geq 0.\tag{4.39}$$

Accordingly, we can write

$$\mathrm{E}\left[\ln\left(1+Z\right)\right] = \mathrm{E}\left[\sum_{n=1}^{\infty}\frac{1}{n}\left(\frac{1}{1+\frac{1}{Z}}\right)^n\right]\tag{4.40}$$

$$= \int_0^{\infty}\sum_{n=1}^{\infty}\frac{s^{n-1}}{n!}e^{-s}M_{\frac{1}{Z}}(s)ds$$

$$= \int_0^{\infty}\frac{1-e^{-s}}{s}M_{\frac{1}{Z}}(s)ds.\tag{4.41}$$

Recalling the MGF-based relation between a random variable Z and its inverse $1/Z$ in [24, Theorme 1] and carrying out the change of variable $\xi^2 = \tan(z)$, we obtain

$$M_Z(s) = 1 - 2\sqrt{s} \int_0^\infty J_1(2\sqrt{s}\xi) M_{Z^{-1}}(\xi^2) d\xi, \tag{4.42}$$

where $J_1(\cdot)$ is the Bessel function of the first kind, it follows that

$$\mathrm{E}\left[\ln\left(1+Z\right)\right] = \int_0^\infty \frac{1-e^{-s}}{s} ds - 2 \int_0^\infty \underbrace{\int_0^\infty \frac{1-e^{-s}}{\sqrt{s}} J_1(2\sqrt{s}\xi)}_{\Sigma} M_Z(\xi^2) ds d\xi, \tag{4.43}$$

where, using [21, Eq. (7.811.1)], we get

$$\Sigma = \frac{1}{\xi} \mathrm{G}_{3,2}^{1,2}\left(\frac{1}{\xi^2} \left|\begin{array}{c} 0, 1, 1 \\ 1, 0 \end{array}\right.\right) = \xi E_0(\xi^2). \tag{4.44}$$

Finally, substituting (4.44) into (4.43) and exploiting the mutual independency between γ_1, γ_2, λ and χ, we obtain

$$\mathrm{E}\left[\ln\left(1+\gamma_1+\lambda+\frac{C(1+\chi)}{\gamma_2}\right)\right] = \int_0^\infty \frac{1-e^{-s}}{s} ds - 2 \int_0^\infty \xi E_0(\xi^2) M_{\gamma_1}(\xi^2) M_\lambda(\xi^2) M_{\frac{1+\chi}{\gamma_2}}(C\xi^2) d\xi. \tag{4.45}$$

In a similar fashion, the second expectation form in (4.38) can be expressed as

$$\mathrm{E}\left[\ln\left(1+\lambda+\frac{C(1+\chi)}{\gamma_2}\right)\right] = \int_0^\infty \frac{1-e^{-s}}{s} ds - 2 \int_0^\infty \xi E_0(\xi^2) M_\lambda(\xi^2) M_{\frac{1+\chi}{\gamma_2}}(C\xi^2) d\xi. \tag{4.46}$$

Finally, substituting (4.45) and (4.46) into (4.38) and performing the necessary mathematical manipulations, (4.6) is easily proven.

Appendix B

The MGF of $U = \frac{\chi}{\gamma_2}$ can be expressed as

$$M_U(s) = \int_0^\infty \int_0^\infty e^{-s\frac{x}{y}} p_{\gamma_2}(y) p_\chi(x) dx dy \tag{4.47}$$

where the pdfs of γ_2 and χ can be obtained by applying the inverse Laplace transform to (4.8) and (4.9), thereby yielding

$$p_{\gamma_2}(y) = \frac{m_2^{m_2}}{\Gamma(m_2)\bar{\gamma}_2^{m_2}} y^{m_2-1} \exp\left(-\frac{m_2 y}{\bar{\gamma}_2}\right), \tag{4.48}$$

$$p_\chi(x) = \sum_{p=1}^{P} \sum_{k=1}^{m_{Z_p}} \frac{\beta_{p,k}}{(k-1)!} x^{k-1} \exp\left(-\frac{m_{Z_p}}{\bar{Z}_p} x\right). \tag{4.49}$$

Then the MFG of U can be derived as follows

$$
\begin{aligned}
M_U(s) &= \int_0^\infty p_{\gamma_2}(y) \int_0^\infty e^{-s\frac{x}{y}} p_\chi(x) dx dy \\
&= \sum_{p=1}^{P} \sum_{k=1}^{m_{Z_p}} \frac{\beta_{p,k}}{(k-1)!} \int_0^\infty p_{\gamma_2}(y) \int_0^\infty x^{k-1} e^{-x\left(\frac{s}{y} + \frac{m_{Z_p}}{Z_p}\right)} dx dy \\
&= \frac{m_2^{m_2}}{\Gamma(m_2)\bar{\gamma}_2^{m_2}} \sum_{p=1}^{P} \sum_{k=1}^{m_{Z_p}} \beta_{p,k} \int_0^\infty \frac{y^{m_2-1} e^{-\frac{m_2 y}{\bar{\gamma}_2}}}{\left(\frac{s}{y} + \frac{m_{Z_p}}{Z_p}\right)^k} dy.
\end{aligned}
$$

Finally, by the help of [21, Eq. (9.211.4)], the MGF of U is obtained as shown in (4.12).

Bibliographie

[1] W. Chen, J. Montojo, A. Golitschek, C. Koutsimanis, and S. Xiaodong, "Relaying operation in 3GPP LTE : challenges and solutions," *IEEE Commun. Mag.,* vol. 50, no. 2, pp. 156-162, Feb. 2012.

[2] J. N. Laneman, D. N. C. Tse, and G. W. Wornell, "Cooperative diversity in wireless networks : efficient protocols and outage behaviour," *IEEE Trans. Inform. Theory,* vol. 50, pp. 3062-3080, Dec. 2004.

[3] H. A. Suraweera, H. K. Garg, and A. Nallanathan, "Performance analysis of two hop amplify-and-forward systems with interference at the relay," *IEEE Commun. Lett.,* vol. 14, no. 8, pp. 692-694, Aug. 2010.

[4] D. Lee and J. H. Lee, "Outage probability for dual-hop relaying systems with multiple interferers over Rayleigh fading channels," *IEEE Trans. Veh. Technol.,* vol. 60, no. 1, pp. 333-338, Jan. 2011.

[5] F. S. Al-Qahtani, T. Q. Duong, C. Zhong, K. A. Qaraqe, and H. Alnuweiri, "Performance analysis of dual-hop AF systems with interference in Nakagami-m fading channels," *IEEE Signal Process. Lett.,* vol. 18, no. 8, pp. 454-457, Aug. 2011.

[6] S. Ikki and S. Aissa, "Multihop wireless relaying systems in the presence of co-channel interferences : performance analysis and design optimization", *IEEE Trans. Veh. Technol.,* vol 61, no. 2, pp. 565-573, Feb. 2012.

[7] C. Zhong, S. Jin, and K. K.Wong, "Dual-hop systems with noisy relay and interference-limited destination," *IEEE Trans. Commun.,* vol. 58, no. 3, pp. 764-768, Mar. 2010.

[8] X. Wei, J. Zhang, and P. Zhang, "Outage probability of two-hop fixed-gain relay with interference at the relay and destination," *IEEE Commun. Lett.,* vol. 15, no. 6, pp. 608-610, June 2011.

[9] S. Ikki and S. Aissa, "Performance analysis of two-way amplify-and-forward relaying in the presence of co-channel interferences", *IEEE Trans. Commun.,* vol. 60, no. 4, pp. 933-939, Apr. 2012.

[10] H. A. Suraweera, D. S. Michalopoulos, and C. Yuen, "Performance analysis of fixed gain relay systems with a single interferer in Nakagami-m fading channels," *IEEE Trans. Veh. Technol.,* vol. 61, no. 3, Mar. 2012

[11] M. Di Renzo, F. Graziosi, and F. Santucci, "Channel capacity over generalized fading channels : a novel MGF-based approach for performance analysis and design of wireless communication systems", *IEEE Trans. Veh. Technol.,* vol. 59, no. 1, pp. 127-148, Mar. 2010.

[12] Y. Chen, J. G. Andrews, "An upper bound on multihop transmission capacity with dynamic routing selection," *IEEE Trans. on Info. Theory,* vol. 15, no. 9, pp. 3751-3765, Sept. 2012.

[13] M. Kountouris and J. G. Andrews, "Throughput scaling laws for wireless ad hoc networks with relay selection," *Vehicular Technolqgy Conf.,* pp. 1-5, Sept. 2009.

[14] C. Zhong, M. Matthaiou, G. K. Karagiannidis and T. Ratnarajah, "Generic ergodic capacity bounds for fixed-gain AF dual-hop relaying systems," *IEEE Trans. Veh. Technol.,* vol 60, no. 8, pp. 3814-3824, Oct. 2011

[15] I. Trigui, S. Affes, and A. Stéphenne, "Exact error analysis of dual-hop fixed-gain AF relaying over arbitrary Nakagami-m fading", *Vehicular Technolqgy Conf.,* pp. 1-5, Sept. 2012.

[16] I. S. Gradshteyn and I.M. Ryzhik, *Table of Integrals, Series and Products,* 5th Ed., San Diego, CA : Academic, 1994.

[17] E. Biglieri, J. Proakis, and S. Shamai, "Fading channels : informationtheoretic and communications aspects," *IEEE Trans. Inf. Theory,* vol. 44, no. 6, pp. 2619-2692, Oct. 1998.

[18] H. Yu, I. H. Lee, and G. L. Stuber, "Outage probability of decode-and-forward cooperative relaying systems with co-channel interference", *IEEE Trans. Wireless Commun.,* vol. 11, no. 1, pp. 266-274, Jan. 2012.

[19] H. Exton, *Multiple Hypergeometric Functions and Applications*; New York : Jhon wiley, 1976.

[20] R. P. Agrawal, "On certain transformation formulae and Meijer's G-function of two variables", *Indian J. Pure Appl. Math.,* vol.1, no. 4, pp. 537-551, 1970.

[21] R. U. Verma, "On some integrals involving Meijer's G-fucntion of two variables", *Proc. Nat. Inst. Sci. India*, vol. 39, Jan. 1966.

[22] I. S. Ansari, S. Al-Ahmadi, F. Yilmaz, M.-S. Alouini, and H. Yanikomeroglu, "A new formula for the BER of binary modulations with dual-branche selection over gereralized-m composite fading channels," *IEEE Trans. Commun.,* vol. 59, no. 10, pp. 2654-2658, Oct. 2011

[23] A. P. Prudnikov, Y. A. Brychkov, and O. I. Marichev, *Integrals and Series : More Special Functions*, Gordon and Breach Science, 1990.

[24] M. Renzo, F. Graziosi, and F. Santucci, "On the performance of CSI-assisted cooperative communications over generalized fading channels," *in Proc. IEEE International Commun. Conf., ICC'08,* China, pp. 1001-1007, May 2008.

Chapitre 5

Capacity and Error Rate Analysis of Cognitive MIMO AF Relaying Systems

Imène Trigui, Imen Mechmeche, Sofiène Affes, and Alex Stéphenne

IEEE Wireless Communications Letters, vol.3, no. 6, Dec. 2014.

Résumé : Dans ce chapitre, la performance et la qualité de service des systèmes RC sont évaluées au moyen du taux d'erreur symbole et de la capacité érgodique. On a supposé que les USs et UPs se partagent le spectre et sont sujets à une contrainte jointe de puissances reçues aux récepteurs des UPs. Dans ces systèmes, les sources secondaires ne peuvent pas communiquer directement à cause d'un évanouissement sévère. Il a été démontré que le gain de diversité est indépendant des UPs.

Abstract

This letter investigates spectrum-sharing cognitive amplify-and-forward (AF) relay networks employing the maximum ratio transmission/maximum ratio combining (MRT/MRC) scheme at the multiple-antenna source-destination pair. It derives closed-from expressions for the ergodic capacity as well as for the symbol error rate (SER) lower bound and its asymptotic value when considering Nakagami-m fading and interference constraints on N primary receivers.

5.1 Introduction

Due to its strong potential in increasing transmission coverage and link reliability, relaying has garnered a wide interest from the wireless communication community [1]- [2]. Knowing that multiple antennas provide enormous performance gains in wireless systems, the idea of multiple-input multiple-output (MIMO) relaying is being investigated for emergent wireless system standards [2]. Nevertheless, terminals in such standards, will, inevitably, face a complex co-channel interference environment due to the highly aggressive frequency reuse. In this respect, cognitive spectrum sharing has arisen as a promising technique to combat spectrum scarcity in wireless relay networks. A common approach to cognitive spectrum sharing is the underlay model where the transmit power at the secondary users must be managed under a peak interference temperature to guarantee reliable communication between the primary users [3].

Aiming at understanding the performance limit of cognitive relay networks, significant contributions investigating such systems in various practical scenarios have appeared. As far as the analysis of single-antenna systems is concerned, some insightful results can be found in [4]-[8], where outage probability (OP) and symbol error rate expressions where derived for decode-and-forward (DF) and amplify-and-forward (AF) relaying in Nakagami-m fading. Recently, [9] and [10] investigated the OP of cognitive spectrum sharing from the viewpoint of multiple-input multiple-output (MIMO) in the primary and/or the secondary networks. Although, due to the prominence of multiple antennas in future cognitive networks, the findings in [9] and [10] are instructional, closed-form expressions were obtained therein only for integer Nakagami-m fading, thereby reducing their scope.

Here, we examine cognitive spectrum-sharing relay networks with multiple antennas at the secondary source-destination pair and provide new results for the ergodic capacity and error rate

analysis in the presence of multiple primary users. It is noteworthy that such analysis has not thus far been addressed in Nakagami-m fading.

5.2   System and channel models

Consider a two-hop spectrum-sharing relay network consisting of one secondary user (SU) source S, one SU destination D, and N primary user (PU) receivers $PU_l(l = 1, \ldots, N)$. The SU source and destination are equipped with N_s and N_d antennas, respectively, communicate through a single-antenna SU relay R. Multiple-antenna source-destination pair and single-antenna relay systems are relevant for multipoint-to multipoint communications and cooperative virtual MIMO systems.

Let [1] the $N_v \times 1$ vectors $\mathbf{h}_i$, $(v, i) \in \{(s, 1), (d, 2)\}$ denote the channels for the source-relay and the relay-destination links, respectively, with entries following independent identically distributed (i.i.d) Nakagami-m random variables (RVs) with parameters (m_i, λ_i), $i = \{1, 2\}$. Let also x denote the source symbol satisfying $\mathrm{E}\{xx^*\} = P_s$, and $\mathbf{n}_u$, $u \in \{r, d\}$ denote the $N_v \times 1$ AWGN at the relay and destination nodes, respectively, with $\mathrm{E}\{\mathbf{n}_u\mathbf{n}_u^*\} = N_0\mathbf{I}$, where $\mathbf{I}$ is the identity matrix. Then the received signals at both the relay and the destination are given by $y_r = \mathbf{h}_1^\dagger\mathbf{w}_1 x + n_r$, and $y_d = \widetilde{\mathbf{w}}_2^\dagger[\mathbf{h}_2 y_r + \mathbf{n}_d]$, where, for MRT/MRC, $\mathbf{w}_1$ is set to match the first hop, i.e., $\mathbf{w}_1 = \mathbf{h}_1/\|\mathbf{h}_1\|$ and $\widetilde{\mathbf{w}}_2 = w\mathbf{w}_2$ where w is the power constraint factor and $\mathbf{w}_2$ is set to match the second hop, i.e., $\mathbf{w}_2 = \mathbf{h}_2/\|\mathbf{h}_2\|$. The relay mode is non-regenerative with a variable gain in which the amplification factor is determined by the instantaneous channel statistics of the source-relay link. Hence w^2 can be computed as $w^2 = P_r/(P_s\mathbf{h}_1^\dagger\mathbf{h}_1)$, where $P_r = \mathrm{E}\{\|\widetilde{\mathbf{w}}_2 y_r\|^2\}$. In CRNs, the interference from the SU should be strictly constrained below a maximum tolerable interference level I_p at the PU receiver. Let the $N_S \times 1$ vector $\mathbf{g}_{1j}$ denote the channel form the SU source to the jth PU with coefficients g_{1jl}, $l = 1, \ldots, N_s$, and g_{2j}, $j = 1, \ldots, N$ denote the channel coefficient form the relay to the jth PU, all following i.i.d Nakagami-m RVs with parameters (m_{I_i}, λ_{I_i}), $i = \{1, 2\}$. Then, by considering MRC at the PU receivers, the SUs should adaptively adjust their transmit powers [2] as $P_s \leq I_p/|\mathbf{g}_{1j*}|^2$ and $P_r \leq I_p/|g_{2j*}|^2$, where

---

1. Bold lower case letters denote vectors and lower case letters denote scalars. $\mathrm{E}\{x\}$ stands for the expectation of the random variable x, $*$ denotes the conjugate operator and, $\dagger$ denotes the conjugate transpose operator.

2. When S and R are not power-limited terminals, the transmit power constraint depends on interference only.

$|\mathbf{g}_{1j*}| = \max_{j=1,...,N}\{|\mathbf{g}_{1j}|\}$ and $|g_{2j*}| = \max_{j=1,...,N}|g_{2j}|$. Therefore, the end-to-end SNR of the SU $S \to R \to D$ link can be expressed as

$$\gamma = \frac{\gamma_r\gamma_d}{\gamma_r + \gamma_d}, \tag{5.1}$$

where $\gamma_r = \bar{\gamma}|\mathbf{h}_1|^2/|\mathbf{g}_{1j*}|^2$, $\gamma_d = \bar{\gamma}|\mathbf{h}_2|^2/|g_{2j*}|^2$, and $\bar{\gamma} = I_p/N_0$.

5.3 Ergodic capacity

The ergodic capacity is an important performance metric since it quantifies the maximum achievable transmission rate under which errors are recoverable.

Lemma 1 : Let F_A be the Lauricella hypergeometric function of the first kind [11], then the ergodic capacity of CRNs employing AF relaying over Nakagami-m fading is given by

$$C = \frac{N^2}{2\ln(2)}\sum_{n,p=0}^{N-1}(-1)^{n+p}\binom{N-1}{n}\binom{N-1}{p}\widetilde{\sum}n!p!\Gamma(\delta_n)\Gamma(\delta_p)\left(\prod_{t=0}^{N_sm_{I_1}-1}\left(\frac{1}{t!}\right)^{n_t+1}\right)\left(\prod_{l=0}^{m_{I_2}-1}\left(\frac{1}{l!}\right)^{n_l+1}\right)$$

$$\frac{\prod_{i=1}^{N_sm_{I_1}}n_i!\prod_{i=1}^{m_{I_2}}p_i!B(\delta_n,N_sm_{I_1})B(\delta_p,m_{I_2})(n+1)^{\delta_n+N_sm_{I_1}}(p+1)^{\delta_p+m_{I_2}}}{F_A(\Xi_1,\Pi)+\rho_n\Gamma(1+N_sm_1)F_A(\Xi_2,\Pi)+\rho_p\Gamma(1+N_dm_2)F_A(\Xi_3,\Pi!)+\rho_n\rho_p\Gamma(1+N_sm_1+N_dm_2)F_A(\Xi_4,\Pi)}, \tag{5.2}$$

where $\widetilde{\sum} = \sum_{\Omega(n,N_sm_{I_1}),\Omega(p,m_{I_2})}$, $\Omega(n,m_i) = \{(n_1,...,n_{m_i}) : n_k \geq 0; \sum_{k=1}^{m_i}n_k = n\}$, $\delta_n = \sum_{l=0}^{N_vm_{I_i}-1}ln_{l+1}$, $\Pi = \{1,\frac{m_1\lambda_{I_1}}{m_{I_1}\lambda_1(n+1)\bar{\gamma}},\frac{m_2\lambda_{I_2}}{m_{I_2}\lambda_2(p+1)\bar{\gamma}})\}$, $\Xi_1 = \{1,1,\delta_n+N_sm_{I_1},\delta_p+m_{I_2};2,1-N_sm_1,1-N_dm_2\}$, $\Xi_2 = \{1+N_sm_1;1,\delta_n+N_sm_{I_1}+N_sm_1,\delta_p+m_{I_2},2,1+N_sm_1,1-N_dm_2\}$, $\Xi_3 = \{1+N_dm_2;1,\delta_p+m_{I_2}+N_dm_2,\delta_n+N_sm_{I_1};2,1+N_dm_2,1-N_sm_1\}$, $\Xi_4 = \{1+N_sm_1+N_dm_2;1,\delta_n+N_sm_{I_1}+N_sm_1,\delta_p+m_{I_2}+N_dm_2;2,1+N_sm_1,1+N_dm_2\}$.

Proof : Resorting to the moment generating function (MGF)-based approach proposed in [12], the ergodic capacity can be computed as

$$C = \frac{1}{2}E[\log_2(1+\gamma)] = \frac{1}{2\ln(2)}\int_0^\infty\frac{1-e^{-s}}{s}M_{\gamma^{-1}}ds, \tag{5.3}$$

where $M_{\gamma^{-1}}(s) = M_{\gamma_r}^{-1}(s)M_{\gamma_d}^{-1}(s)$ is the MGF of the end-to-end SNR. In its turn, the per-hop SNR MGF $M_{\gamma_X^{-1}}(s), X \in \{r,d\}$ is derived as

$$M_{\gamma_X^{-1}}(s) = \int_0^\infty\int_0^\infty e^{-s\frac{\bar{\gamma}z}{y}}f_{|\mathbf{h}_i|^2}(y)f_{|\mathbf{g}_{ij*}|^2}(z)dydz, \tag{5.4}$$

where $f_{|\mathbf{h}_i|^2}$ and $f_{|\mathbf{g}_{ij*}|^2}$ denote the probability density functions (PDFs) of $|\mathbf{h}_i|^2$ and $|\mathbf{g}_{ij*}|^2$ and are, respectively, given by

$$f_{|\mathbf{h}_i|^2}(x) = \frac{\left(\frac{m_i}{\lambda_i}\right)^{N_u m_i}}{\Gamma(N_u m_i)} x^{N_u m_i - 1} e^{-\frac{m_i}{\lambda_i} x}, \tag{5.5}$$

with $(u,i) = \{(s,1),(d,2)\}$, and

$$f_{|\mathbf{g}_{ij^*}|}(x) = \frac{N \left(\frac{m_{I_i}}{\lambda_{I_i}}\right)^{N_v m_{I_i}} x^{N_v m_{I_i} - 1} e^{-\frac{m_{I_i}}{\lambda_{I_i}} x}}{\Gamma(N_v m_{I_i})} \left(1 - \frac{\Gamma(N_v m_{I_i}, \frac{m_{I_i}}{\lambda_{I_i}} x)}{\Gamma(N_v m_{I_i})}\right)^{N-1}, \tag{5.6}$$

with $(v,i) = \{(s,1),(r,2)\}$ and $N_r = 1$. By performing the necessary substitutions in (5.4) along with [21, Eqs. (3.351.3) and (9.211.4)], we obtain

$$M_{\gamma_X^{-1}}(s) = \frac{N \left(\frac{m_{I_i}}{\lambda_{I_i}}\right)^{N_v m_{I_i}}}{\Gamma(N_u m_i)\Gamma(N_v m_{I_i})} \sum_{n=0}^{N-1} \binom{N-1}{n} (-1)^n \sum_{\Omega(n,N_u m_i)} \tau_\Omega^n \Psi\left(\delta_n + N_v m_{I_i}, 1 - N_u m_i, \frac{m_i \lambda_{I_i}}{m_{I_i} \lambda_i (n+1)\bar{\gamma}} s\right), \tag{5.7}$$

where $X \in \{r,d\}$, $(i,u,v) = \{(1,s,s),(2,r,d)\}$ with $N_r = 1$, $\Psi(a;b;z)$ denotes the Triconomi confluent hypergeometric function [21, Eq. (9.211.1)] and τ_Ω^n is given by

$$\tau_\Omega^n = \frac{n!\Gamma(\delta_n + N_v m_{I_i})\Gamma(\delta_n + N_v m_{I_i} + N_u m_i)}{\left(\frac{m_{I_i}}{\lambda_{I_i}}(n+1)\right)^{\delta_n + N_v m_{I_i}} \prod_{k=1}^{N_v m_{I_i}} n_k! \prod_{p=0}^{N_v m_{I_i} - 1} \left(\frac{\left(\frac{m_{I_i}}{\lambda_{I_i}}\right)^p}{p!}\right)^{-n_{p+1}}}. \tag{5.8}$$

Subsequently, the ergodic capacity is derived by replacing (5.7) into (5.3) as

$$C = \frac{N^2 \left(\frac{m_{I_1}}{\lambda_{I_1}}\right)^{m_{I_1}} \left(\frac{m_{I_2}}{\lambda_{I_2}}\right)^{m_{I_2}}}{2\ln(2)\Gamma(N_s m_1)\Gamma(N_s m_{I_1})\Gamma(N_d m_2)\Gamma(m_{I_2})} \sum_{n,p=0}^{N-1} \binom{N-1}{n}\binom{N-1}{p}(-1)^{n+p} \widetilde{\sum} \tau_\Omega^n \tau_\Omega^p I_{n,p}, \tag{5.9}$$

where

$$I_{n,p} = \int_0^\infty \frac{1 - e^{-s}}{s} \Psi\left(\delta_n + N_s m_{I_1}, 1 - N_s m_1, \frac{m_1 \lambda_{I_1}}{m_{I_1} \lambda_1 (n+1)\bar{\gamma}} s\right) \Psi\left(\delta_p + m_{I_2}, 1 - N_d m_2, \frac{m_2 \lambda_{I_2}}{m_{I_2} \lambda_2 (p+1)\bar{\gamma}} s\right) ds. \tag{5.10}$$

To resolve (5.10), we invoke the expansion formulas of Ψ in terms of the confluent hypergeometric function $_1F_1$ in [21, Eq. (9.210.1)] and the fact that $(1 - e^{-s})/s = e^{-s}{}_1F_1(1;2;s)$. Subsequently, we can obtain the following expression of $I_{n,p}$

$$I_{n,p} = \frac{\Gamma(N_s m_1)\Gamma(N_d m_2)}{\Gamma(N_s m_1 + \delta_n + N_s m_{I_1})\Gamma(N_d m_2 + \delta_p + m_{I_2})} \int_0^\infty e^{-s}{}_1F_1(1;2;s)\left(_1F_1\left(\delta_n + N_s m_{I_1};1 - N_s m_1;\frac{m_1 \lambda_{I_1}}{m_{I_1}\lambda_1(n+1)\bar{\gamma}} s\right)\right.$$

$$+ \rho_{n1} {}_1F_1\left(N_s m_1 + \delta_n + N_s m_{I_1};1 + N_s m_1;\frac{m_1 \lambda_{I_1}}{m_{I_1}\lambda_1(n+1)\bar{\gamma}} s\right)\right)\left(_1F_1\left(\delta_p + m_{I_2};1 - N_d m_2;\frac{m_2 \lambda_{I_2}}{m_{I_2}\lambda_2(p+1)\bar{\gamma}} s\right)\right.$$

$$+ \rho_{p1} {}_1F_1\left(N_d m_2 + \delta_p, 1 + m_{I_2};1 + N_d m_2;\frac{m_2 \lambda_{I_2}}{m_{I_2}\lambda_2(p+1)\bar{\gamma}} s\right)\right) ds, \tag{5.11}$$

where $\rho_k = \frac{\Gamma(-m_i)\left(\frac{m_i\lambda_{I_i}}{m_{I_i}\lambda_i(k+1)\bar{\gamma}}\right)^{m_i}}{\mathrm{B}(\delta_k+N_v m_{I_i}, m_i)}$ with $(k,i,v) \in \{(n,1,s),(p,2,r)\}$. Now from (5.9) and (5.11),

the desired result can be obtained by appealing to [11]

$$F_A^{(r)}\left(a;b_1,\ldots,b_r;c_1,\ldots,c_r;\frac{x_1}{\nu},\ldots,\frac{x_r}{\nu}\right) = \frac{\nu^a}{\Gamma(a)}\int_0^\infty e^{-\nu t}t^{a-1}\left(\prod_{k=1}^r {}_1F_1(b_k;c_k,x_k t)\right)dt; \Re(a)>0.$$

$$(5.12)$$

5.4 Symbol error rate

The SER is expressed in terms of the cumulative density function (CDF) of γ denoted by F_γ

as [14]

$$P_e = \frac{a\sqrt{b}}{2\sqrt{\pi}}\int_0^\infty \frac{e^{-by}}{\sqrt{y}}F_\gamma(y)dy,$$

$$(5.13)$$

where $a,b > 0$ are modulation-specific constants. Unfortunately, for the MIMO CRN under

study, F_γ is untractable in closed-form hampering the obtainment of (5.13). To simplify the

analysis, an upper bound on γ is used as follows [6]

$$\gamma < \gamma_{up} = \min(\gamma_r, \gamma_d).$$

$$(5.14)$$

Lemma 2 : Let Φ_2 be the confluent hypergeometric function of the second kind [11], then the

average SER of CRNs employing AF relays over Nakagami-m is lower bounded by [3].

$$P_e^l = \frac{a\sqrt{b}N}{2\sqrt{2\pi}}\left[\sum_{n=0}^{N-1}\sum_{\Omega(n,N_s m_{I_1})}\sum_{l=0}^{N_s m_{I_1}-1}\frac{\Sigma(1,s,s)}{\sqrt{\frac{m_1\lambda_{I_1}}{m_{I_1}\lambda_1(n+1)\bar{\gamma}}}}\Gamma(l+\frac{1}{2}+N_s m_1)\Psi\left(N_s m_1+\frac{1}{2}+l,\frac{3}{2},\frac{bm_{I_1}\lambda_1(n+1)\bar{\gamma}}{2m_1\lambda_{I_1}}\right)+\right.$$

$$\sum_{n=0}^{N-1}\sum_{\Omega(n,m_{I_2})}\sum_{l=0}^{m_{I_2}-1}\frac{\Sigma(2,r,d)_{N_r=1}}{\sqrt{\frac{m_2\lambda_{I_2}}{m_{I_2}\lambda_2(n+1)\bar{\gamma}}}}\Gamma(l+\frac{1}{2}+N_d m_2)\Psi\left(N_d m_2+\frac{1}{2}+l,\frac{3}{2},\frac{bm_{I_2}\lambda_2(n+1)\bar{\gamma}}{2m_2\lambda_{I_2}}\right)-$$

$$N\sum_{n,p=0}^{N-1}\widetilde{\sum_{t=0}^{N_s m_{I_1}-1}}\sum_{l=0}^{m_{I_2}-1}\frac{\Sigma(1,s,s)}{\left(\frac{m_1\lambda_{I_1}}{m_{I_1}\lambda_1(n+1)\bar{\gamma}}\right)^{-t-N_s m_1}}\frac{\Sigma(2,r,d)_{N_r=1}}{\left(\frac{m_2\lambda_{I_2}}{m_{I_2}\lambda_2(p+1)\bar{\gamma}}\right)^{-l-N_d m_2}}\Gamma(l+t+\frac{1}{2}+N_s m_1+N_d m_2)$$

$$\Phi_2\left(N_s m_1+N_d m_2+l+t+\frac{1}{2};N_s m_1+l,N_d m_2+t;N_s m_1+N_d m_2+l+t-\frac{1}{2};\frac{m_1\lambda_{I_1}}{m_{I_1}\lambda_1(n+1)\bar{\gamma}},\right.$$

$$\left.\left.\frac{m_2\lambda_{I_2}}{m_{I_2}\lambda_2(p+1)\bar{\gamma}},\frac{b}{2}\right)\right],$$

$$(5.15)$$

3. Note that the obtainment of (5.15) inflicts the quantities $N_s m_{I_1}$ and m_{I_2} to be integer valued. However, this does not limit the scope of the paper since we already show in [12] that only interference power and number affect the system performance.

where

$$\Sigma(i,u,v)_{n,l} = \frac{\binom{N-1}{n}(-1)^n \tau_\Omega^n \left(\frac{m_{I_i}}{\lambda_{I_i}}\right)^{N_v m_{I_i}} (1 - N_v m_{I_i})_l (N_u m_i)_l}{N_u m_i \Gamma(N_v m_{I_i}) B(N_u m_i, N_v m_{I_i}) \Gamma(\delta_n + N_v m_{I_i} + N_u m_i)(1 + N_u m_i)_l}. \tag{5.16}$$

Proof : The CDF of γ^{up} can be written as

$$F_{\gamma_{up}}(x) = F_{\gamma_r}(x) + F_{\gamma_d}(x) - F_{\gamma_r}(x)F_{\gamma_d}(x), \tag{5.17}$$

where from (5.5) and (5.6) and appealing to [21, Eq. (3.194.1)], we obtain F_{γ_X}, $X \in \{r,d\}$ as

$$F_{\gamma_X}(x) = \sum_{n=0}^{N-1} \sum_{\Omega(n,N_v m_{I_i})} \Theta_n \frac{\left(\frac{m_i \lambda_{I_i}}{m_{I_i} \lambda_i (n+1)\bar\gamma} x\right)^{N_u m_i}}{N_u m_i} {}_2F_1\left(N_u m_i, N_u m_i + N_v m_{I_i}, N_u m_i + 1, \frac{-m_i \lambda_{I_i} x}{m_{I_i} \lambda_i (n+1)\bar\gamma}\right), \tag{5.18}$$

where $\Theta_n = \frac{N\binom{N-1}{n}(-1)^n \tau_\Omega^n \left(\frac{m_{I_i}}{\lambda_{I_i}}\right)^{N_v m_{I_i}}}{B(N_u m_i, N_v m_{I_i})\Gamma(\delta_n + N_v m_{I_i} + N_u m_i)}$, and ${}_2F_1$ is the Gauss hypergeometric function [21, Eq. (9.100)].

Substituting (5.17) and (5.18) into (5.13) and resorting to the key transformation

$$_2F_1(a, b, b-n, z) = (1-z)^{-a-n} \sum_{k=0}^{n} \frac{(-n)_k (b-a-n)_k}{(b-n)_k} \left(\frac{z}{1+z}\right)^k, \tag{5.19}$$

the desired result is obtained after applying [21, Eq. (9.211.1)] and recognizing the fact that

$$\Phi_2(a; b_1, ..., b_K; z; x_1, ..., x_K, y) = \frac{1}{\Gamma(a)} \int_0^\infty \exp(-yt) t^{a-1}(1+t)^{a-z-1} \prod_{k=1}^{K}(1+x_k t)^{-b_k} dt. \tag{5.20}$$

5.4.1 Asymptotic SER

Corollary 1 : The asymptotic SER of multiple antenna CRNs with AF relaying in (5.15), derived as $\bar\gamma \to \infty$, is

$$P_e^{l\infty} = \frac{aN}{2\sqrt\pi}\left[\sum_{n=0}^{N-1}\sum_{\Omega(n,N_s m_{I_1})} \frac{\widetilde\Sigma(1,s,s)\Gamma(\frac{1}{2}+N_s m_1)}{\left(\frac{b m_{I_1}\lambda_1(n+1)}{2m_1\lambda_{I_1}}\right)^{N_s m_1}}\bar\gamma^{-N_s m_1} + \sum_{n=0}^{N-1}\sum_{\Omega(n,m_{I_2})} \frac{\widetilde\Sigma(2,r,d)_{N_r=1}\Gamma(\frac{1}{2}+N_d m_2)}{\left(\frac{b m_{I_2}\lambda_2(n+1)}{2m_2\lambda_{I_2}}\right)^{N_d m_2}}\bar\gamma^{-N_d m_2}\right.$$
$$\left. -N\sum_{n,p=0}^{N-1}\widetilde{\widetilde\Sigma}\frac{\widetilde\Sigma(1,s,s)\widetilde\Sigma(2,r,d)_{N_r=1}}{\left(\frac{b m_{I_1}\lambda_1(n+1)}{m_1\lambda_{I_1}}\right)^{N_s m_1}\left(\frac{b m_{I_2}\lambda_2(p+1)}{m_2\lambda_{I_2}}\right)^{N_d m_2}}\Gamma(\frac{1}{2}+N_s m_1 + N_d m_2)\bar\gamma^{-N_s m_1 - N_d m_2}\right], \tag{5.21}$$

where
$$\widetilde\Sigma(i,u,v) = \frac{\binom{N-1}{n}(-1)^n \tau_\Omega^n \alpha_{I_i}^{N_v m_{I_i}} B(N_u m_i, N_v m_{I_i})^{-1}}{N_u m_i \Gamma(N_v m_{I_i})\Gamma(\delta_n + N_v m_{I_i} + N_u m_i)}. \tag{5.22}$$

Proof : The result follows by using $\Psi(a,b;z) \underset{z\to\infty}{\approx} z^{-a}$ and $\Phi_2(c, b_1, b_2, c-1; x, y, z) \underset{x,y\to 0}{\approx} z^{-c}$ along with some series manipulations.

Corollary 2 : The diversity and coding gains of multiple-antenna CRNs with AF relaying are, respectively, given by

$$G_d = \min(N_s m_1, N_d m_2), \qquad (5.23)$$

$$G_a = \begin{cases} \Delta(1,s,s)^{-\frac{1}{G_d}} & N_s m_1 < N_d m_2 \, ; \\ (\Delta(1,s,s)+\Delta(2,r,d))^{-\frac{1}{G_d}} & , N_s m_1 = N_d m_2 \, ; \\ \Delta(2,r,d)^{-\frac{1}{G_d}}, & N_s m_1 > N_d m_2 \, ; \end{cases} \qquad (5.24)$$

where

$$\Delta(i,u,v) = \frac{aN}{2\sqrt{\pi}} \sum_{n=0}^{N-1} \sum_{\Omega(n,N_v m_{I_i})} \frac{\widetilde{\Sigma}(i,u,v)\Gamma(\frac{1}{2}+N_u m_i)}{\left(\frac{b m_{I_i} \lambda_i (n+1)}{2 m_i \lambda_{I_i}}\right)^{N_u m_i}}. \qquad (5.25)$$

Proof : Since the asymptomatic SER in (5.21) is dominated by the first and second summations, then re-expressing the SER in (5.21) as $P_e^{l\infty} = (G_a \bar{\gamma})^{-G_d}$, where G_d is the diversity order, and G_a is the array gain [15], yields the desired result.

5.5 Illustrative numerical results

Fig. 1 confirms that the theoretical results match perfectly their empirical counterparts, hence confirming their correctness. It also suggests significant capacity improvement when increasing the number of antennas, more so at the destination (i.e., Nd) than at the source (Ns). Moreover, it clearly appears that the capacity gap due to the increase of the number of PUs diminishes as the number of antennas increases. This implies that a MIMO CRN is able to maintain its performance in dynamic environments where PUs vary in number when the antenna arrays are relatively large.

Fig. 2 plots the SER lower bound and its true value via computer simulations. We can readily note that the lower bound remains sufficiently tight across the entire SNR range of interest, meaning that it is able to serve as an effective approximation for the exact SER. As expected, the SER increases with N while the diversity gain remains unchanged. This increase can be easily evaluated using (5.24). We also observe at high SNR that AF MIMO CRNs exhibit similar error rates with more antennas at the source or the destination.

5.6 Conclusion

In this letter, new closed-from expressions for the ergodic capacity as well as the average error rate lower bound and its asymptotic value were derived for spectrum-sharing cognitive
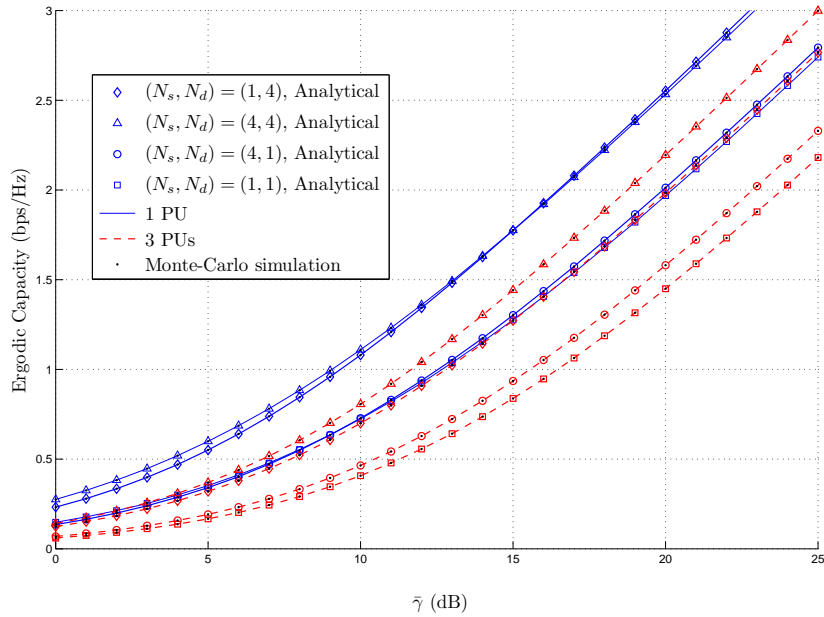
FIGURE 5.1 – The impact of the S-R MIMO link size (N_s, N_d) and PUs number N on the ergodic capacity of two-hop AF MIMO CRNs, with $m_1 = m_2 = 0.7$, $m_{I_1} = m_{I_1} = 1$, $\lambda_1 = \lambda_2 = 2$ dB, $\lambda_{I_1} = \lambda_{I_2} = 1$ dB.

amplify-and-forward (AF) relay networks employing maximum ratio transmission/maximum ratio combining (MRT/MRC) schemes at the multiple-antenna source-destination pair. The findings of the paper are instructional on how the parameters of the secondary and/or primary networks affect the performance of the system.
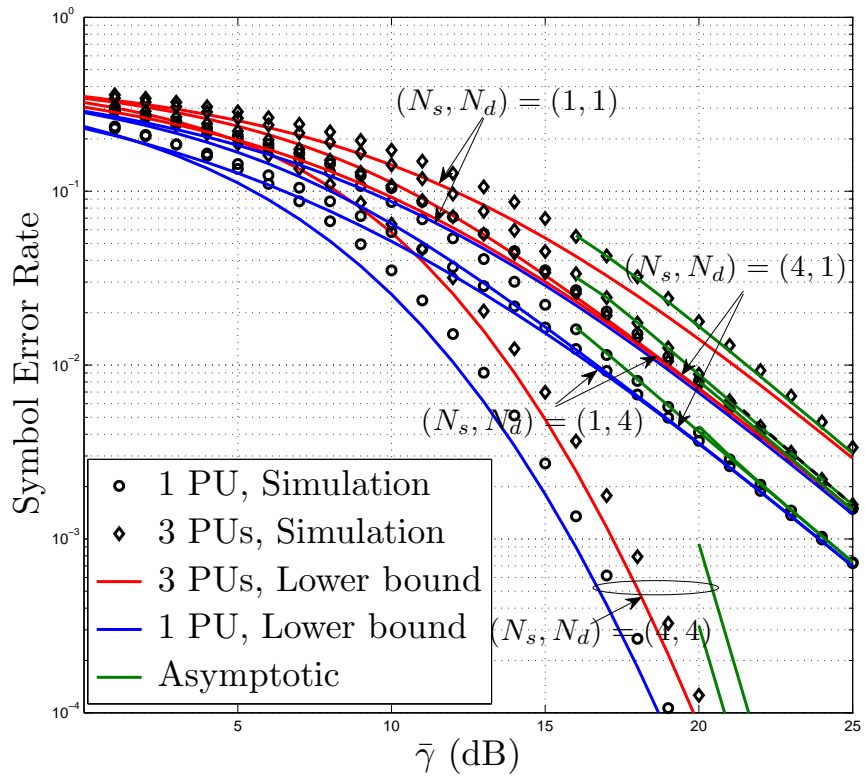
FIGURE 5.2 – The impact of the S-R MIMO link size (N_s, N_d) and PUs number N on the SER of two-hop AF MIMO CRNs, with $m_1 = m_2 = 1.5$, $m_{I_1} = m_{I_1} = 1$, $\lambda_1 = \lambda_2 = 2$ dB, $\lambda_{I_1} = \lambda_{I_2} = 1$ dB, $a = 0.5$, $b = 1$.

Bibliographie

[1] J. N. Laneman, D. N. C. Tse, and G. W. Wornell,"Cooperative diversity in wireless networks : efficient protocols and outage behaviour," *IEEE Trans. Inform. Theory,* vol. 50, pp. 3062-3080, Dec. 2004.

[2] W. Chen, J. Montojo, A. Golitschek, C. Koutsimanis, and S. Xiaodong, "Relaying operation in 3GPP LTE : challenges and solutions," *IEEE Commun. Mag.,* vol. 50, no. 2, pp. 156-162, Feb. 2012.

[3] A. Ghasemi and E. S. Sousa, "Fundamental limits of spectrum-sharing environments," *IEEE Trans. Wireless Commun.,* vol. 6, no. 2, pp. 649-658, Feb. 2007.

[4] T. Q. Duong, D. B. da Costa, T. A. Tsiftsis, C. Zhong, and A. Nallanathan, "Outage and diversity of cognitive relaying systems under spectrum sharing environments in nakagami-m fading," *IEEE Commun. Lett.,* vol. 16, no. 12, Dec. 2012.

[5] C. Zhong, T. Ratnarajah, and K.-K. Wong, "Outage analysis of decode-and-forward cognitive dual-hop systems with the interference constraint in Nakagami-m fading channels," *IEEE Trans. Veh. Tech.,* vol. 60, no. 6, pp. 2875-2879, July 2011.

[6] T. Q. Doung, D. B. da Costa, M. Elkashlan, and V. N. Q. Bao, "Cognitive amplify-and-forward relay networks over Nakagami-m fading," *IEEE Trans. Veh. Tech.,* vol. 61, no. 5, pp. 2368-2374, June 2012.

[7] H. Yu, W. Tang, and S. Li, "Outage probability and SER of amplify-and-forward cognitive relay networks," *IEEE Wireless Commun. Lett.,* vol. 2, no. 2, Apr. 2014

[8] A. M. Salhab, S. A. Zummo, "Cognitive amplify-and-forward relay networks with switch-and-examine relaying in Rayleigh fading Channels",*IEEE Commun. Lett.,* vol. 18, no. 5, May 2014.

[9] P. L. Yeoh, M. Elkashlan, T. Q. Duong, N. Yang, and D. B. da Costa, "Transmit antenna selection for interference management in cognitive relay networks", *IEEE Trans. Veh. Tech.*, accepetd for publication.

[10] S. Hua, H. Liu, M. Wu, and S. S. Panwar, "Exploiting MIMO antennas in cooperative cognitive radio networks", in *IEEE INFOCOM*, Shanghai, China, 2011.

[11] H. Exton, *Multiple Hypergeometric Functions and Applications*; New York : Jhon Wiley, 1976.

[12] I. Trigui, S. Affes, and A. Stéphenne, "On the ergodic capacity of amplify-and-forward relay channels with interference in Nakagami-m fading," *IEEE Trans. Commun.*, vol. 61, no. 8, pp. 3136-3145, Aug. 2013.

[13] I. S. Gradshteyn and I. M. Ryzhik, *Table of Integrals, Series and Products,* 5th Ed., San Diego, CA : Academic, 1994.

[14] M. R. Mckay, A. J. Grant, and I. B. Collings, "Performance analysis of MIMO-MRC in double-correlated Rayleigh environments," *IEEE Trans. Commun.* , vol. 55, no. 3, pp. 497-507, Mar. 2007.

[15] Z. Wang and G. B. Giannakis, "A simple and general parameterization quantifying performance in fading channels," *IEEE Trans. Commun.,* vol. 51, no. 8, pp. 1389-1398, Aug. 2003.

[16] Q. Shi and Y. Karasawa, " Some Applications of Lauricella Hypergeometric Function F_A in Performance Analysis of Wireless Communications", *IEEE Commun. Let.*, vol. 16, no. 5, May 2012.

Chapitre 6

Ergodic Capacity of Two-Hop Multiple Antenna AF Systems with Co-Channel Interference

Imène Trigui, Sofiène Affes, and Alex Stéphenne

Résumé : Dans ce chapitre, des systèmes à double sauts avec transmission MIMO sont considérés. Un relai MIMO subissant des interférences co-canal est utilisé afin d'assister la communication entre une source et une destination dotée de plusieurs antennes. Ce chapitre développe une transformation novatrice et la propose comme moyen universel pour le calcul de la capacité érgodique.

Abstract

In this paper, we analyze the ergodic capacity of a two-hop multiple-antenna amplify and forward (AF) system, where the relay is subject to co-channel interference (CCI) while the destination is corrupted by additive white Gaussian noise (AWGN) only. A novel integral transform, called the complementary moment generating function transform (CMGF), is proposed as a unified tool to compute the ergodic capacity. When both the relay and destination perform maximum ratio combining (MRC), we derive a new analytical exact expression for the ergodic capacity. It is shown that the ergodic capacity is better improved by increasing the number of antennas at the relay N_r than that at destination N_d. Unfortunately, the system shows an incapability of canceling interference even if N_r and/or N_d grows large.

6.1 Introduction

The deployment of wireless relays has rekindled a wide interest from the wireless communication community as a means of achieving high throughput where traditional architectures are unsatisfactory, such as in cell-edge, indoor, etc.. Several relaying protocols have been introduced in the literature [1]. Of particular interest is the amplify-and-forward (AF) scheme due to its low complexity. In such a scheme, in fact, each relay mimics a simple repeater by forwarding a scaled version of the received signal to the destination node.

Nevertheless, deployed relays in future wireless systems generations will, inevitably, face a complex co-channel interference environment due to the highly aggressive frequency reuse. The latter actually causes a more severe performance degradation than thermal noise [2].

Aiming to understand the performance limitations of relaying systems in the presence of interference, significant contributions investigating the ergodic capacity in various practical scenarios have appeared. As far as the analysis of single antenna systems is concerned, some insightful results can be found in [11]-[12]. These studies have shed new insights into how the ergodic capacity is dominated by the interference power, especially at the relay. Recently, most research activity has been devoted to the analysis of multiple antenna (MIMO) systems, which have been shown to provide significant improvements to the achievable data rates. Some relevant contributions on the analysis of channel capacity for these systems are [5]-[10], where analytical bounds for the channel capacity over Rayleigh fading channels with various diversity-combining techniques are

obtained.

This paper is a nontrivial and useful add-on of the framework proposed by [10], with the main objective and motivation of taking advantage of an MGF-based approach to obtain new closed-form expressions for the ergodic capacity of two-hop MIMO AF systems, an objective deemed impossible to acheive by the authors of [10].

6.2 System model

Let us consider the two-hop MIMO network in Fig. 1, where both the relay R and destination D are equipped with N_r and N_d antennas, respectively, while the source S is equipped with a single antenna. We assume that the relay is subjected to M independently but not necessarily identically distributed co-channel interferers that dominate the noise effect, while the destination is corrupted by AWGN only. Interference-limited relay and noisy destination stems from cell-edge or frequency-division relaying [12], [7].
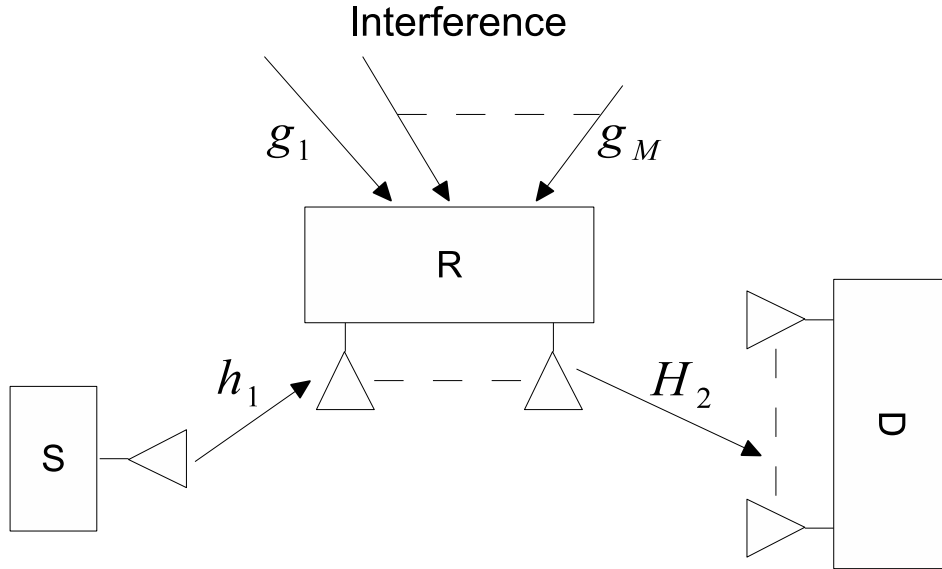
FIGURE 6.1 – System model.

Let [1] the $N_r \times 1$ vectors $\{\mathbf{h}_1, \mathbf{g}_i\}$, $i = 1, \ldots, M$ denote the channels for the source-relay and i-th interference-relay links, respectively, with entries following identically independently distributed (i.i.d) complex circular Gaussian random variables $\mathcal{CN}(0, 1)$. Let also x and s_{I_i} denote the source

---

1. Bold lower case letters denote vectors and lower case letters denote scalars. E$\{x\}$ stands for the expectation of the random variable x, $*$ denotes the conjugate operator and, $\dagger$ denotes the conjugate transpose operator.

and the i-th interferer symbol satisfying $\mathrm{E}\{xx^*\} = P_s$ and $\mathrm{E}\{s_{I_i}s_{I_i}^*\} = P_{I_i}$, $i = 1, \ldots, M$. Then the received signal at the interference-limited relay is given by

$$y_r = \mathbf{w}^\dagger \left[\mathbf{h}_1 x + \sum_{i=1}^{M} \mathbf{g}_i s_{I_i} \right], \tag{6.1}$$

where $\mathbf{w}$ is set to match the first hop, i.e., $\mathbf{w} = \mathbf{h}_1/\|\mathbf{h}_1\|$, also known as the MRC combiner. The relay node transmits a transformed version of the received signal to the destination such that

$$y_d = \mathbf{u}^\dagger \left[G\mathbf{H}_2\mathbf{v}y_r + \mathbf{n} \right], \tag{6.2}$$

where $\mathbf{H}_2 = [h_{2_{i,j}}]_{i,j=1}^{N_r,N_d}$ is a $N_r \times N_d$ matrix and denotes the channel for the relay-destination link with entries following i.i.d $\mathcal{CN}(0,1)$, $\mathbf{n}$ is the $N_d \times 1$ AWGN vector at the destination node with $\mathrm{E}\{\mathbf{nn}^*\} = N_0\mathbf{I}$, where $\mathbf{I}$ is the identity matrix, $\mathbf{u}$ and $\mathbf{v}$ are the transmit precoding and receive filtering vectors at R and D, selected by using the channel matrix $\mathbf{H}_2$ as the first columns of $\mathbf{U}$ and $\mathbf{V}$, respectively, corresponding to the largest singular value of $\mathbf{H}_2$ [2]. Combining (6.1) and (6.2), the end-to-end signal-to-interference-plus-noise ratio (SINR) of the system can be expressed as

$$\gamma = \frac{P_s \Lambda G^2 |\mathbf{w}^\dagger \mathbf{h}_1|^2}{G^2 \Lambda \sum_{i=1}^{M} |\mathbf{w}^\dagger \mathbf{g}_i|^2 P_{I_i} + N_0}, \tag{6.3}$$

where Λ is the largest eigenvalue of the Wishart matrix $\mathbf{H}_2^\dagger\mathbf{H}_2$ and G is the power constraint factor given by

$$G^2 = \frac{P_r}{P_s\mathbf{h}_1^\dagger\mathbf{h}_1 + \sum_{i=1}^{M} |\mathbf{w}^\dagger \mathbf{g}_i|^2 P_{I_i}}. \tag{6.4}$$

By substituting (6.4) into (6.3), we obtain

$$\gamma = \frac{\Lambda|\mathbf{h}_1|^2 P_s}{\Lambda\frac{\sum_{i=1}^{M} |\mathbf{h_1}^\dagger\mathbf{g}_i|^2 P_{I_i}}{\|\mathbf{h_1}\|^2} + \frac{N_0}{P_r}\left(|\mathbf{h}_1|^2 P_s + \frac{\sum_{i=1}^{M} |\mathbf{h_1}^\dagger\mathbf{g}_i|^2 P_{I_i}}{\|\mathbf{h_1}\|^2}\right)}. \tag{6.5}$$

Finally, after noting $\rho_1 = P_s/N_0$, $\rho_2 = P_r/N_0$, and $\rho_{I_i} = P_{I_i}/N_0, i = 1, \ldots, M$, a more compact form of (6.5) is obtained, after some manipulations, as

$$\gamma = \frac{\gamma_1\gamma_2}{\gamma_2 + \gamma_1 + 1}, \tag{6.6}$$

where $\gamma_1 = |\mathbf{h}_1|^2\rho_1/\chi$, $\chi = \sum_{i=1}^{M} |\mathbf{h_1}^\dagger\mathbf{g}_i|^2\rho_{I_i}/\|\mathbf{h_1}\|^2$, and $\gamma_2 = \Lambda\rho_2$.

---

2. The singular value decomposition of $\mathbf{H}_2$ is given by $\mathbf{H}_2 = \mathbf{U}\mathbf{\Sigma}\mathbf{V}^\dagger$, where $\mathbf{\Sigma}$ is the $N_d \times N_r$ matrix having the largest singular value $\sqrt{\Lambda}$ as the first element on the main diagonal. Further, $\mathbf{U}$ and $\mathbf{V}$, are unitary $N_d \times N_d$ and $N_r \times N_r$ matrices, respectively.

6.3 Ergodic capacity analysis

The ergodic capacity is defined as the expected values of the instantaneous mutual information and is mathematically expressed as

$$C = \frac{1}{2}\mathrm{E}\left[\log_2\left(1+\gamma\right)\right], \tag{6.7}$$

in which γ stands for the end-to-end SINR and the factor $1/2$ accounts for the total number of time slots required for the transmission.

6.3.1 Novel MGF-based approach for two-hop channel capacity computation

In this section, we propose a new integral transform for channel capacity computation by relying on the knowledge of the first hop complementary CDF (CCDF) and the second hop MGF.

Theorem 1 : The ergodic capacity of two-hop AF relaying system can be computed as

$$C = \frac{1}{2\ln(2)}\left(\int_0^\infty e^{-s}\widehat{M}_{\gamma_1}(s)ds - \int_0^\infty e^{-s}\widehat{M}_{\gamma_1}(s)M_{\gamma_2}(s)ds\right) = \widehat{C}_1 - \widehat{C}_{12}, \tag{6.8}$$

where $M_X(\cdot)$ stands for the MGF of X and $\widehat{M}_X(\cdot)$ denotes the complementary MGF (CMGF) defined as

$$\widehat{M}_X(s) \triangleq \int_0^\infty e^{-sx}\widehat{F}_X(x)dx, \tag{6.9}$$

with $\widehat{F}_X(x)$ denoting the CCDF of X. In this paper, the integral in (6.8) is called CMGF transform, as it relies on a CMGF kernel function.

Proof : Combining (6.6) and (6.7), the ergodic capacity of the system can be computed by

$$C = \frac{1}{2}\mathrm{E}\left[\log_2\left(\frac{(1+\gamma_1)(1+\gamma_2)}{1+\gamma_1+\gamma_2}\right)\right] = C_{\gamma_1} + C_{\gamma_2} - C_{\gamma_T}, \tag{6.10}$$

where $C_{\gamma_i} = \frac{1}{2\ln(2)}\mathrm{E}\left[\ln\left(1+\gamma_i\right)\right]_{i=1,2}$ and $C_{\gamma_T} = \frac{1}{2\ln(2)}\mathrm{E}\left[\ln\left(1+\gamma_1+\gamma_2\right)\right]$. Noticing that the quantities $C_{\gamma_X}, X \in \{1,2,T\}$ can be expressed by means of the MGF-based approach in [8] as

$$C_{\gamma_X} = \frac{1}{2\ln(2)}\int_0^\infty \frac{e^{-s}}{s}\left(1 - M_{\gamma_X}(s)\right)ds, \tag{6.11}$$

and resorting to the key transformation

$$M_{\gamma_X}(s) = 1 - s\int_0^\infty e^{-sx}\widehat{F}_{\gamma_X}(x)dx, \tag{6.12}$$

then, pulling all together in (6.10), the ergodic capacity can be expressed as

$$C = \frac{1}{2\ln(2)} \left(\int_0^\infty e^{-s} \frac{1 - \left(1 - s\widehat{M}_{\gamma_1}(s)\right)}{s} ds + \int_0^\infty e^{-s} \frac{1 - M_{\gamma_2}(s)}{s} ds - \int_0^\infty e^{-s} \frac{1 - \left(1 - s\widehat{M}_{\gamma_1}(s)\right) M_{\gamma_2}(s)}{s} ds \right),$$

(6.13)

where $\widehat{M}$ is defined in (6.9). To this end, simplifying (6.13) yields the desired result.

We remark that the result in (6.8) offers a flexible and simple approach for the computation of the ergodic capacity that relies on the knowledge of the first-hop SIR CMGF and the second-hop SNR MGF. To the best of our knowledge, closed-form and exact expressions for these quantities do exist for most fading models. Moreover, in those scenarios where very complicated expressions of the CMGF/MGF of the per-hop SIR/SNR do not allow easy computation of the aforementioned integral in closed form, the result in (6.8) can efficiently and easily be obtained using standard computing environments, such as Mathematica. In fact, in contrast to [8], it is worth noting that the singularity of the $\frac{e^{-s}}{s}$ kernel function around zero is avoided by the integral simplification performed in (6.13) and that the evaluation of (6.8) does not face, in general, numerical problems.

6.3.2 Ergodic capacity of two-hop MIMO AF systems with interference in rayleigh fading

Hereafter, we will restrict the scope of (6.8) to the yet challenging scenario described in section II.

Corollary 1 : The ergodic capacity of two-hop MIMO AF systems with interference is obtained as

$$C = \frac{1}{2\ln(2)} \sum_{k=0}^{N_r-1} \sum_{i=1}^{\rho(\mathbf{D})} \sum_{j=1}^{\tau_i(\mathbf{D})} \zeta_{i,j}(\mathbf{D}) \left(\frac{\Psi_{k,j}}{k+j} - \frac{1}{\Gamma(j)\Gamma(k+1)} \sum_{a=1}^{P} \sum_{b=Q}^{(P+Q)a-2a^2} \frac{\beta(a,b)}{\Gamma(b+1)} \Sigma_{k,j} \right),$$

(6.14)

where

$$\Psi_{k,j} = \begin{cases} {}_2F_1\left(1, j, k+j+1; 1 - \frac{\rho_{I<i>}}{\rho_1}\right), \left|1 - \frac{\rho_{I<i>}}{\rho_1}\right| < 1; \\ {}_2F_1\left(k+1, 1, k+j+1; 1 - \frac{\rho_1}{\rho_{I<i>}}\right), \frac{\rho_{I<i>}}{\rho_1} > \frac{1}{2}, \end{cases}$$

(6.15)

and

$$\Sigma_{k,j} = G_{1,[1,1],0,[1,2]}^{1,1,1,1,2} \left(\frac{\rho_2}{a}, \frac{\rho_1}{\rho_{I<i>}} \, \middle| \, \begin{array}{c} 0; 1+b; 1+k \\ \ldots; 0; 0, j-1 \end{array} \right),$$

(6.16)

wherein ${}_2F_1(\cdot)$ and $G_{A,[C,E],B,[D,F]}^{p,q,k,r,l}(\cdot, \cdot)$ denote the Gauss hypergeometric function [21, Eq(9.100)] and the generalized Meijer-G function [22], respectively. Moreover in (6.14), $\mathbf{D} = \mathrm{diag}(\rho_{I_1}, \rho_{I_2}, \ldots,$

ρ_{I_M}), $\rho(\mathbf{D})$ is the number of distinct diagonal elements of $\mathbf{D}$, $\rho_{I_{<1>}} > \rho_{I_{<2>}} > \ldots > \rho_{I_{<M>}}$ are the distinct diagonal elements in decreasing order, $\tau_{\mathbf{i}}(\mathbf{D})$ is the multiplicity of $\rho_{I_{<i>}}$ and $\zeta_{i,j}(\mathbf{D})$ is the (i,j)-th characteristic coefficient of $\mathbf{D}$ [23]. For instance, when non-equal-power interferers are considered, we have $\tau_i(\mathbf{D}) = 1$ and $\zeta_{i,1}(\mathbf{D}) = \prod_{k=1,k\neq i}^{\rho(\mathbf{D})} 1/\left(1 - \frac{\rho_{I_{<k>}}}{\rho_{I_{<i>}}}\right)$. In (6.14), we also note that the coefficients $\beta(a,b)$ are given by [3]

$$\beta(a,b) = \frac{c_{a,b}b!}{a^{b+1}\prod_{l=1}^{P}(P-l)!(Q-l)!}, \tag{6.17}$$

where $P = \min(N_r, N_d)$ and $Q = \max(N_r, N_d)$.

Proof : According to the CMGF transform and the SINR expression in (6.6), the ergodic capacity of two-hop AF systems with multiple antennas at the relay-destination pair, interference at the relay and noise at the destination is obtained by the calculation of the two items $\widehat{C}_1$ and $\widehat{C}_{12}$.

Calculation of $\widehat{C}_1$

In order to proceed, we need to find out the statistics of $\gamma_1 = \frac{|\mathbf{h}_1|^2 \rho_1}{\chi}$ where $\chi = \frac{\sum_{i=1}^{M}|\mathbf{h}_1^\dagger \mathbf{g}_i|^2 \rho_{I_i}}{\|\mathbf{h}_1\|^2}$. It is easy to observe that $|\mathbf{h}_1|^2$ is an exponential random variable with pdf

$$f_{|\mathbf{h}_1|^2}(x) = \frac{x^{N_r-1}}{(N_r-1)!}e^{-x}. \tag{6.18}$$

Also, according to [23], χ follows an hyper-exponential distribution with pdf

$$f_\chi(x) = \sum_{i=1}^{\rho(\mathbf{D})}\sum_{j=1}^{\tau_i(\mathbf{D})} \zeta_{i,j}(\mathbf{D})\frac{\rho_{I_{<i>}}^{-j} x^{j-1}}{(j-1)!}e^{-x}. \tag{6.19}$$

Then invoking [21, Eq. (3.381.8)] and [21, Eq. (3.381.4)], the CCDF of γ_1 is obtained after some manipulations as

$$\widehat{F}_{\gamma_1}(x) = \sum_{k=0}^{N_r-1}\sum_{i=1}^{\rho(\mathbf{D})}\sum_{j=1}^{\tau_i(\mathbf{D})} \zeta_{i,j}(\mathbf{D})\frac{\Gamma(k+j)}{\Gamma(j)k!}\left(\frac{x\rho_{I_{<i>}}}{\rho_1}\right)^k\left(\frac{\rho_1}{\rho_{I_{<i>}}x+\rho_1}\right)^{k+j}. \tag{6.20}$$

The next step is to calculate $\widehat{M}_{\gamma_1}$. From (6.9), and using (6.20), along with some basic algebraic manipulations, we arrive at

$$\widehat{M}_{\gamma_1}(s) = \sum_{k=0}^{N_r-1}\sum_{i=1}^{\rho(\mathbf{D})}\sum_{j=1}^{\tau_i(\mathbf{D})} \zeta_{i,j}(\mathbf{D})\frac{\Gamma(k+j)}{\Gamma(j)}\frac{\rho_1}{\rho_{I_{<i>}}}\Psi\left(k+1, 2-j; \frac{\rho_1}{\rho_{I_{<i>}}}s\right), \tag{6.21}$$

---

3. $c_{a,b}$ is the coefficient of $e^{-ax}x^b$ in the expansion of $\frac{d}{dx}\det[S(x)]$, where $S(x)$ is an $P \times P$ Hankel matrix with elements $S_{i,j} = \gamma(Q-P+i+j-1,x)$, with $\gamma(\cdot)$ denoting the incomplete Gamma function [21, Eq (6.5.3)]. The coefficients $c_{a,b}$ can be readily determined using mathematical softwares such as Maple or Mathematica.

where $\Psi(a;b;z)$ denotes the Triconomi confluent hypergeometric function [21, Eq. (9.211.1)]. Then, substituting (6.21) into $\widehat{C}_1$, the latter can be evaluated as

$$\widehat{C}_1 = \frac{1}{2\ln(2)} \sum_{k=0}^{N_r-1} \sum_{i=1}^{\rho(\mathbf{D})} \sum_{j=1}^{\tau_i(\mathbf{D})} \zeta_{i,j}(\mathbf{D}) \frac{\Gamma(k+j)}{\Gamma(j)} \underbrace{\int_0^\infty e^{-\frac{\rho_{I_{<i>}}}{\rho_1}s} \Psi(k+1, 2-j, s)\, ds}_{I}. \tag{6.22}$$

Utilizing, [21, Eq. (7.621.6)], we obtain

$$I = \frac{\Gamma(j)}{\Gamma(k+j+1)} \Psi_{k,j}, \tag{6.23}$$

wherein $\Psi_{k,j}$ is given in (6.15). Finally, substituting (6.23) into (6.22) yields the desired result.

Calculation of $\widehat{C}_{12}$

Since $\widehat{M}_{\gamma_1}(s)$ is derived in (6.21), the remaining task is to figure out $M_{\gamma_2}(s)$. In order to derive the latter, one needs the closed-form statistics of Λ_2, the largest eigenvalues of the central Wishart matrix $\mathbf{H}_2^\dagger \mathbf{H}_2$. According to [12], f_{γ_2} can be expressed as

$$f_{\gamma_2}(x) = \sum_{a=1}^{P} \sum_{b=Q}^{(P+Q)a-2a^2} \beta(a,b) \frac{a^{b+1}x^b}{\rho_2^{b+1}b!} e^{-\frac{ax}{\rho_2}}, \tag{6.24}$$

where $\beta(a,b)$ is defined in (6.17). Then, the MGF of γ_2 is obtained as

$$M_{\gamma_2}(s) = \sum_{a=1}^{P} \sum_{b=Q}^{(P+Q)a-2a^2} \frac{\beta(a,b)}{\left(\frac{\rho_2}{a}s+1\right)^{b+1}}. \tag{6.25}$$

To this end, substituting (6.21) and (6.25) into $\widehat{C}_{12}$, the latter can be evaluated as

$$\widehat{C}_{12} = \frac{1}{2\ln(2)} \sum_{k=0}^{N_r-1} \sum_{i=1}^{\rho(\mathbf{D})} \sum_{j=1}^{\tau_i(\mathbf{D})} \zeta_{i,j}(\mathbf{D}) \frac{\Gamma(k+j)}{\Gamma(j)} \sum_{a=1}^{P} \sum_{b=Q}^{(P+Q)a-2a^2} \beta(a,b) \frac{\rho_1}{\rho_{I_{<i>}}} \underbrace{\int_0^\infty e^{-s} \frac{\Psi\left(k+1, 2-j, \frac{\rho_1}{\rho_{I_{<i>}}}s\right)}{\left(\frac{\rho_2}{a}s+1\right)^{b+1}}\, ds}_{\Phi}. \tag{6.26}$$

We now have to solve the integral Φ in order to derive $\widehat{C}_{12}$. To this end, noticing that $(1+\beta x)^{-\alpha} = \frac{1}{\Gamma(\alpha)} G_{1,1}^{1,1}\left(\beta x \,\middle|\, \begin{matrix} 1-\alpha \\ 0 \end{matrix}\right)$ [21, Eq. (9.34.3)] and, $\Psi(a,b;z) = \frac{1}{\Gamma(a)\Gamma(a-b+1)} G_{1,2}^{2,1}\left(z \,\middle|\, \begin{matrix} 1-a \\ 0, 1-b \end{matrix}\right)$ [21, Eq. (9.34.3)], the integral Φ is now given by

$$\Phi = A \int_0^\infty e^{-s} G_{1,1}^{1,1}\left(\frac{\rho_2}{a}s \,\middle|\, \begin{matrix} -b \\ 0 \end{matrix}\right) G_{1,2}^{2,1}\left(\frac{\rho_1}{\rho_{I_{<i>}}}s \,\middle|\, \begin{matrix} -k \\ 0, j-1 \end{matrix}\right)\, ds, \tag{6.27}$$

where $A = 1/\Gamma(b+1)\Gamma(k+1)\Gamma(k+j)$. Integrals of this type can be evaluated by means of a G-function of two variables [22, Eq. (1.2)], as can be seen from a more general integral formula due to [22, Eq. (3.2)]. Accordingly and under consideration of the functional relation

$$
\mathrm{G}_{C,D}^{r,q}\left(z_1 \left|\begin{array}{c}\gamma_1, ..., \gamma_c \\ \delta_1, ..., \delta_D\end{array}\right.\right) \mathrm{G}_{E,F}^{l,k}\left(z_2 \left|\begin{array}{c}\epsilon_1, ..., \epsilon_E \\ \phi_1, ..., \phi_F\end{array}\right.\right) = \mathrm{G}_{0[CE],0,[DF]}^{0qkrl}\left(z_1, z_2 \left|\begin{array}{c}...; 1-\gamma_1, ..., 1-\gamma_C; 1-\epsilon_1, ..., 1-\epsilon_E \\ ....; \delta_1, ..., \delta_D; \phi_1, ..., \phi_F\end{array}\right.\right),
$$

(6.28)

we obtain

$$
\Phi = \frac{1}{\Gamma(b+1)\Gamma(k+1)\Gamma(k+j)}\mathrm{G}_{1,[1,1],0,[1,2]}^{1,1,1,1,2}\left(\frac{\rho_2}{a}, \frac{\rho_1}{\rho_{I_{<i>}}}\left|\begin{array}{c}0; 1+b; 1+k \\ ...; 0; 0, j-1\end{array}\right.\right).
$$

(6.29)

Finally, substituting (6.29) into (6.26), $\widehat{C}_{12}$ can be expressed in a compact-form as

$$
\widehat{C}_{12} = \frac{1}{2\ln(2)}\sum_{k=0}^{N_r-1}\sum_{i=1}^{\rho(\mathbf{D})}\sum_{j=1}^{\tau_i(\mathbf{D})}\frac{\zeta_{i,j}(\mathbf{D})}{\Gamma(j)\Gamma(k+1)}\sum_{a=1}^{P}\sum_{b=Q}^{(P+Q)a-2a^2}\frac{\beta(a,b)}{\Gamma(b+1)}\mathrm{G}_{1,[1,1],0,[1,2]}^{1,1,1,1,2}\left(\frac{\rho_2}{a}, \frac{\rho_1}{\rho_{I_{<i>}}}\left|\begin{array}{c}0; 1+b; 1+k \\ ...; 0; 0, j-1\end{array}\right.\right).
$$

(6.30)

Finally, pulling everything together yields the desired result[4].

6.4   Numerical results

Fig. 2 plots the ergodic capacity of two-hop multiple-antenna AF systems with different values of N_r and N_d under different interference power levels, i.e., weak interference $\rho_I = 0$ dB and strong interference $\rho_I = 25$ dB. As shown in the figure, the theoretical results match perfectly their empirical counterparts, confirming thereby the correctness of the analytical expressions. It is observed that the ergodic capacity is better improved by increasing the number of antennas at the relay N_r than that at the destination N_d. However, as the interference power grows large, the capacity gap between the different antenna configurations narrows down at low SNR. On the other hand, stronger interference has a detrimental effect on the capacity performance of the MRC scheme as shown by the considerable gap between the two interference power scenarios.

Fig. 3 investigates the interference reduction capability of two-hop MIMO AF systems. By letting N_r grow, we observe that the ergodic capacity increases at a rate that gradually becomes smaller without attaining the performance of an interference-free system. On the other hand increasing N_d is useless, more so when M is larger.

---

4. An accurate routine for the evaluation of the bivariate Meijer's G function can be found in [24].

6.5   Conclusion

Named as CMGF, a novel integral transform was proposed as a unified tool to compute the ergodic of a two-hop multiple-antenna AF system, where the relay is subject to CCI, while the destination is only corrupted by AWGN. When both the relay and destination perform maximum ratio combining, we have been able to derive a new analytical exact expression for the ergodic capacity. The paper's findings have shed new lights on how the antenna number, the CCI numbers, and the interference power affect the performance of the system.
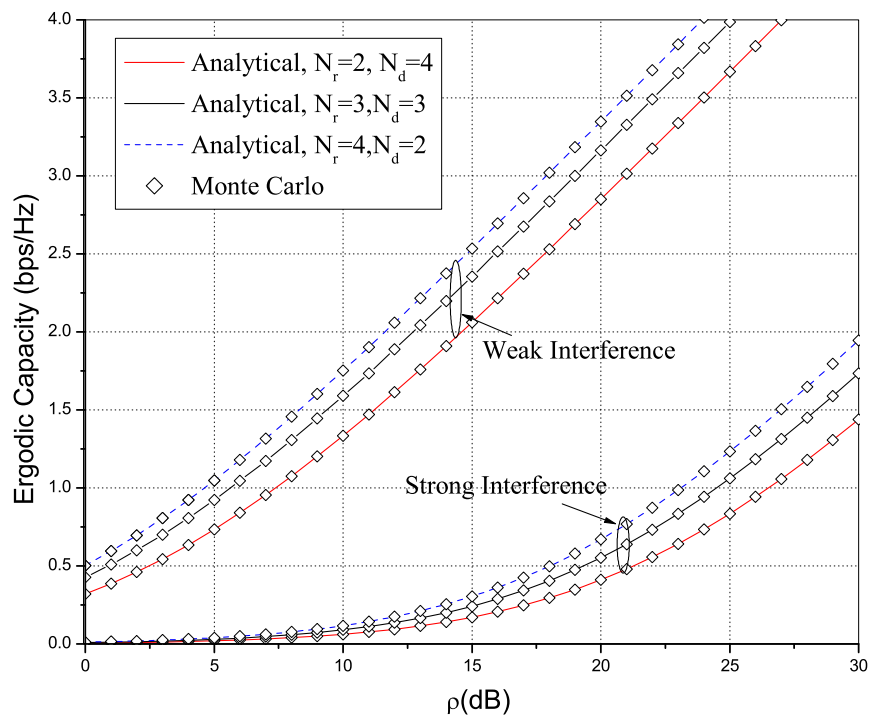

FIGURE 6.2 – The impact of the R-D MIMO link size $(N_r,\ N_d)$ and the interference power ρ_I on the ergodic capacity of two-hop MIMO AF systems with $\rho_1 = \rho_2 = \rho$, and $M = 3$.
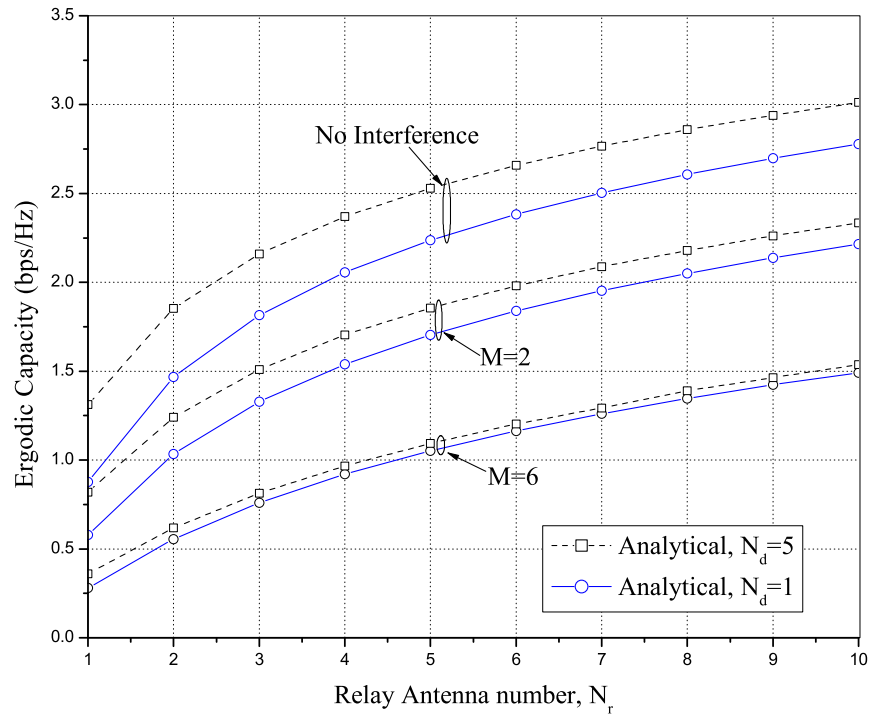
FIGURE 6.3 – Ergodic capacity versus the relay antenna number N_r with $\rho_1 = \rho_2 = 10$ dB, $\rho_I = [1, 5]$ dB for $M = 2$ and $\rho_I = [1, 2, 3, 4, 5, 6]$ dB for $M = 6$.

Bibliographie

[1] J. N. Laneman, D. N. C. Tse, and G. W. Wornell," Cooperative diversity in wireless networks : efficient protocols and outage behaviour," *IEEE Trans. Inform. Theory,* vol. 50, pp. 3062-3080, Dec. 2004.

[2] J. H. Winters, "Optimum combining in digital mobile radio with cochannel interference," *IEEE J. Select. Areas Commun.*, vol. 2, no. 4, pp. 529-539, July 1984.

[3] I. Trigui, S. Affes, and A. Stéphenne, "Ergodic capacity analysis for interference-limited AF multi-hop relaying channels in Nakagami-m fading," *IEEE Trans. Commun.,* vol. 61, no. 7, pp. 2726-2734, July 2013.

[4] I. Trigui, S. Affes, and A. Stéphenne, "On the ergodic capacity of amplify-and-forward relay channels with interference in Nakagami-m fading," *IEEE Trans. Commun.*, vol. 61, no. 8, pp. 3136-3145, Aug. 2013.

[5] Y. Huang, C. Li, C. Zhong, J. Wang, Y. Cheng and Q. Wu, "On the capacity of dual-hop multiple antenna AF relaying systems with feedback delay and CCI," *IEEE Commun. Lett.*, vol. 17, no. 6, pp. 1200-1203, June 2013.

[6] G. Zhu, C. Zhong, H. A. Suraweera, Z. Zhang and C. Yuen, "Ergodic capacity comparison of different relay precoding schemes in dual-hop AF systems with co-channel interference," *IEEE Trans. Commun. ,* vol. 62, no. 7, pp. 2314-2328, July 2014.

[7] R. Pabst, B. H. Walke, D. C. Schultz, P. Herhold, H. Yanikomeroglu, S.Mukerjee, H. Viswanathan, M. Lott, W. Zirwas, M. Dohler, H. Aghvami, D. D. Falconer, and G. P. Fettweis, "Relay-based deployment concepts for wireless and mobile broadband radio," *IEEE Commun. Mag.*, vol. 42, pp. 80-89, Sept. 2004.

[8] K. A. Hamdi, "Capacity of MRC on correlated Rician fading channels," *IEEE Trans. Commun.*, vol. 56, no. 5, pp. 708-711, May. 2008

[9] I. S. Gradshteyn and I. M. Ryzhik, *Table of Integrals, Series and Products,* 5th Ed., San Diego, CA : Academic, 1994.

[10] R. U. Verma, "On some integrals involving Meijer's G-fucntion of two variables", *Proc. Nat. Inst. Sci. India,* vol. 39, Jan. 1966.

[11] H. Shin and M. Z. Win, "MIMO diversity in the presence of double scattering," *IEEE Trans. Inform. Theory,* vol. 54, no. 7, pp. 2976-2996, July 2008.

[12] Y. Chen and C. Tellambura, "Performance analysis of maximum ratio transmission with imperfect channel estimation," *IEEE Commun. Lett.,* vol. 9, no. 4, pp. 322-324, Apr. 2005.

[13] I. S. Ansari, S. Al-Ahmadi, F. Yilmaz, M.-S. Alouini, and H. Yanikomeroglu, "A new formula for the BER of binary modulations with dual-branch selection over gereralized-m composite fading channels," *IEEE Trans. Commun.,* vol. 59, no. 10, pp. 2654-2658, Oct. 2011

Chapitre 7

Design and Capacity of Interference-Limited Multiuser MIMO AF Relay Systems

Imène Trigui, Imen Mechmeche, Sofiène Affes, and Alex Stéphenne

Résumé : Les systèmes considérés jusqu'ici sont à un seul et unique usager. Plusieurs études ont, cependant, démontré que les systèmes à plusieurs usagers peuvent eux aussi bénéficier du relayage. Dans ce chapitre, on étudie alors la capacité érgodique des systèmes multi-antennes à plusieurs usagers avec relayage en présence d'interférences co-canal. En recourant à la théorie de la valeur extrême, des expressions simplifiées de la capacité sont obtenues lorsque le nombre d'usagers et/ou le nombre d'antennes sont suffisamment grands. Ces expressions quantifient pour la première fois la perte de capacité dû à la présence d'interférences dans le système. En exploitant ces résulats, on montre que la capacité du système considérée est la moitié de celle d'un système MIMO à saut unique. On montre aussi que le gain multi-usagers grâce à la sélection basée sur le RSI est supérieur à celle basée sur l'état du canal.

Abstract

In this paper, multiuser multiple-antenna (MU-MIMO) relay networks employing opportunistic scheduling and operating in the presence of rayleigh fading and co-channel interference are analyzed. Notwithstanding the system complexity, due to the newly found complementary moment generating function (CMGF) transform, an exact expression for the capacity under general conditions is obtained. Moreover, driven by the fact that communication devices have grown much faster than the infrastructure relay support, a specific wireless setup, which consists of a large number of source antennas or/and users K and a relatively small relay antenna number is investigated. The large scale analysis embodies popular observations, so far intuitively or empirically disclosed, through analytically insightful new formulas. An interesting aspect of this analysis comes from an altered view of multiuser diversity in the context of cellular systems. Previously, multiuser diversity capacity gain has been known to grow as $O(\ln\ln(K))$, from selecting the maximum of K exponentially-distributed powers. Because interference aware scheduling is considered, we find instead that the gain is $O(\ln(K^{1/Q}))$ where Q is the number of interferers. Simulation results indicate a rather fast convergence to the asymptotic limits with the system's size, thereby demonstrating the practical importance of the scaling results.

7.1 Introduction

Driven by the surge of shared data volume and connected devices, multiuser multiple-antenna (MU-MIMO) relaying networks have drawn recently a significant attention, as a promising solution to cope with the necessities of more efficient and larger networks. Aiming to enhance multiuser capacity, multiple antenna communications have been actually identified as a key enabling technique to secure the unprecedented data deluge these large networks are deemed to convey [1]-[2]. As such, there has been prominent activity in the past decade toward understanding the fundamental system capacity limits of such architectures, notably when interference-limited, the ultimate nature of future cellular networks [3]-[4].

Many contributions spearheaded this line of research by considering the combination of cooperative and multiuser diversities in the context of single-antenna communications [5]-[7]. It has been shown in multiuser dual-hop amplify-and-forward (AF) relaying networks, that the end-to-end signal-to-noise ratio (SNR) is an inadequate criterion for reduced-feedback approaches

with threshold-based SNR. Alternatively, the second-hop SNR which requires less attendant in complexity at the relay, turns out to be more promising in terms of achieved capacity.

Aiming to further increase the system capacity and reliability, another line of work dedicated to multiuser relay-assisted networks with multi-antenna communications is longing for understanding such systems [8]-[9]. In [9], capacity in the rage of of bits per second per hertz (b/s/Hz) is achieved by allowing the communication, through an AF relay, of multiple antenna devices and a source, using receive antenna diversity. A full knowledge of local channels (backward channels from all source antennas and forward channels to all destinations) was assumed at the relay, making thereby distributed beamforming possible. It has been shown, only through empirical trials, that spatial diversity at the destinations deteriorates the system capacity and, further, burdens the feedback cost.

Although these works have made great strides toward understanding MU-MIMO relay-assisted communications, they all rely on the absence of the harmful effect of co-channel interference (CCI). The recognition of the interference-limited nature of emerging communication systems, such as heterogeneous cellular networks, has motivated several works to investigate the impact of CCI on the performance of relay networks for different fading models and communication setups [10]-[13]. In [11], a novel analytical capacity expression for two-hop multiple antenna AF relaying systems have been proposed. The more general case of multihop interference-limited communications has also been treated in [12]. However the works in [10] and [13] only consider a single-user scenario. So far, CCI assessment in the context of multiuser relaying networks has only recently been considered in [14] by harnessing on opportunistic scheduling. This work, however, provides only bounds on the system capacity without characterizing its scaling laws.

The ultimate goal of this paper is to quantify more accurately the capacity of MU-MIMO relay-assisted networks if straightforward opportunistic scheduling is employed among users and transmit selection is employed among sources's antennas in a cellular environment. More importantly, it shows that understanding how CCI affects multiuser and spatial diversity gains become feasible by exploiting some newly derived scaling laws. The main contributions of this work are summarized as follows.

- A novel single-integral relation to compute the channel capacity is provided in terms of the CMGFs of the per-hop SIRs. This relation is resolved in closed-form, providing thereby a useful add-on of the framework proposed by [10] which claims some capacity bounds.

122

- Through asymptotic analysis and simulations, this paper shows that the the capacity scaling laws are governed by the ratio $\frac{\ln M^{1/L}}{K^{1/Q}-1}$ when SIR-based selection among K users and transmit selection among M antennas is considered in an AF relay network in the presence of L and Q interferers at each hop.

- When $\frac{\ln M^{1/L}}{K^{1/Q}-1}$ goes to zero, we prove that the system capacity scales as $\ln(\ln(M)) - H_{L-1}$ bits/s/Hz, whereby H_n stands for the harmonic number of order n.

- When $\frac{\ln M^{1/L}}{K^{1/Q}-1}$ goes to infinity, we show that the system capacity scales as $\ln\left(K^{1/Q}\right)$ whereas it has previously been known to grow only as $\ln\ln(K)$ from selecting the maximum of K exponentially-distributed powers.

The rest of the paper is organized as follows. Section II introduces the system model and the proposed two-phase relay protocol. Section III presents the analytical exact expression for the capacity that applies to general system configurations. Sections IV and V characterize the system capacity and its scaling laws in the regime of large user or/and source antenna number/s, and a fixed relay antenna number. Section VI presents numerical performance results while Section VII briefly discusses the impact of interference and system's size on capacity. Finally, Section VIII concludes the paper. Technical details and proofs are placed in appendices.

Notation : † is the transpose complex conjugate operator. $\stackrel{d}{=}$ denotes an equality in distribution. $\mathcal{CN}(\mu, \sigma^2)$ is a complex Gaussian Random Variable (RV) with mean μ and variance σ^2. $E\{\cdot\}$ is the expectation operator. $M_X(s) = E\{e^{-sX}\}$ is the MGF of RV X. $F_X(z) = Pr(X \leq z)$ is the Cumulative Distribution Function (CDF) of X and $F_X^{(c)}(z) = 1 - F_X(z)$ is its Complementary Cumulative Distribution Function (CCDF). $M_X^{(c)}(s) = 1 - sM_X(s)$ is the complementary MGF of X while $f_X(x)$ is its Probability Density Function (PDF). $\Gamma(z, x)$, $\Psi(a, b, z)$, and $_2\mathrm{F}_1(a, b, c, x)$ denote the upper incomplete gamma function [21, Eq.(8.350.2)], the Triconomi confluent hypergeometric function [21, Eq. (9.211.1)], the Gauss hypergeometric function [21, Eq.(9.100)], respectively. In turn, the second-type Bessel function of order ν and the exponential integral function are, respectively, denoted by $\mathrm{K}_\nu(x)$ and $\mathrm{E_i}(x)$ [21, Eq.(8.222.1)]. $\mathrm{W}(a, b, z)$ is the Whittaker hypergeometric function [21, Eq.(9.222.1)] and $\mathrm{G}_{A,[C,E],B,[D,F]}^{p,q,k,r,l}(\cdot, \cdot)$ is the generalized Meijer-G-function of two variables [22]. "$\chi(2p)$" denotes a chi-square random variable with $2p$ degrees of freedom. For two functions $f(n)$ and $g(n)$, $f(n) = O(g(n))$ means $\lim_{n\to\infty} |f(n)/g(n)| < \infty$.

7.2   System model

Consider a half-duplex multiple-antenna AF relay network with a source and a relay equipped with M and N antennas, respectively, and K single-antenna receivers (or users). The system setup operates in an interference-limited environment over frequency-flat Rayleigh fading. Let $\mathbf{Y}_i$ be the $1 \times N$ received signal vector at the relay from the i-th source's antenna element given by

$$\mathbf{Y}_i = \sqrt{P_S}\mathbf{h}_i^S x + \underbrace{\sum_{l=1}^{L}\sqrt{\mu_l}\mathbf{v}_l b_l}_{\mathbf{i}_{T_1}}, \qquad i = 1, \ldots, M \qquad (7.1)$$

where $\mathbf{h}_i^S$ is a $1 \times N$ complex channel vector from the i-th source's antenna element to the relay and $\mathbf{v}_l, l = 1, \ldots, L$ is the l-th interference vector. The entries of $\mathbf{h}_i^S$ and $\mathbf{v}_l$ are assumed, in what follows, to be independent and identically distributed (i.i.d.) zero mean complex Gaussian random variables. Let us denote by ρ the received power from the i-th transmit antenna and, hence, from (7.1), $\rho = P_s E\left\{\left|\mathbf{h}_i^S x\right|^2\right\}$. We also denote by $\mathbf{i}_{T_1}$ the aggregate interference vector due to L interferers at the relay. Upon reception of the source's signal, the relay employs the receive-MRC reconstitution to obtain $y_i = \mathbf{w}_i^\dagger \mathbf{Y}_i$ where $\mathbf{w}_i = \mathbf{h}_i^S/\|\mathbf{h}_i^S\|$. Afterward, y_i is amplified with a gain $G = \sqrt{\left(P_S|\mathbf{h}_i^S|^2 + \sum_{l=1}^{L}\mu_l|\mathbf{v}_l|^2\right)^{-1}}$ before transmission to the j-th user which is surrounded by Q_j interferences. The received signal at the j-th user is then given by

$$z_j = \mathbf{F}_j^\dagger \sqrt{P_r}G\mathbf{h}_j^R y_i + \underbrace{\sum_{q=1}^{Q_j}\sqrt{\nu_{j,q}}u_{j,q}c_{j,q}}_{\mathbf{i}_{T_{2j}}}, \qquad j = 1, \ldots, K \qquad (7.2)$$

where $\mathbf{h}_j^R$ is a $1 \times N$ complex channel vector from the relay to the j-th user and $u_{j,l}$ is the channel between the latter and the q-th interference. It follows from (7.2) that the received power at the j-th user is $\lambda_j = P_r E\left\{\left|\mathbf{h}_j^R\right|^2\right\}, j = 1, \ldots, K$. In (7.2), $\mathbf{i}_{T_{2j}}$ the aggregate interference due to Q_j interferers at the j-th user. In the sequel, we assume that the entries of $\mathbf{h}_i^R$ and $u_{j,l}\ j = 1, \ldots, K; l = 1\ldots, Q_j$ are i.i.d. zero mean complex Gaussian random variables. In order to recover the original signal at the j-th user, the relay recurs to the transmit beamforming vector $\mathbf{F}_j = \mathbf{h}_j^R/\|\mathbf{h}_j^R\|$. The channel gains $|\mathbf{h}_i^S|^2, i = 1\ldots, M$ and $|\mathbf{h}_j^R|^2, j = 1, \ldots, K$ are assumed here to be quasi-static, i.e., they remain unchanged during a complete two-hop transmission session but vary independently in different sessions. We also assume that the relay and the j-th user are aware of their backward channels $\mathbf{h}_i^S$ and $\mathbf{h}_j^R$, respectively, i.e., the CSI at the receiver (CSIR)

assumption is adopted. It is noteworthy that the assumption on the channel knowledge entails acceptable signaling overhead deemed reasonable even for decentralized implementation. In this paper, $\{x, b_i, c_{j,l}\}, i = 1 \ldots L, j = 1, \ldots, K, l = 1 \ldots, Q_j$ are letters from codewords of a Gaussian capacity-achieving codebook.

Now, let us describe the scheduling scheme employed at each hop. As far as the first hop (i.e., source to relay communication) is concerned, the relay is aware of $\mathbf{h}_i^S, i = 1, \ldots, M$ and, hence, able to schedule the transmission of the strongest source antenna, say $i_M = \underset{i=1\ldots M}{\operatorname{argmax}}|\mathbf{h}_i^S|^2$, by feeding back the index i_M at the beginning of the data bloc. The overhead incurred at this phase of the protocol does not exceed a single integer. Commonly known as transmit antenna selection (TAS) [15], this technique requires an instantaneous and error-free feedback from the relay. Using TAS, the relay receives a superposition of the i_M-th transmitted signal and CCI. Its received signal-to-interference ratio (SIR) is then given by

$$SIR^{H_1} = \frac{P_s|\mathbf{h}_{i_M}^S|^2}{\sum_{l=1}^L \mu_l|\mathbf{v}_l|^2}. \tag{7.3}$$

where the superscript H_1 refers to the first hop. At the second hop, due the CSIR assumption, the relay is oblivious to the interference pertaining to the K users. The latter are, therefore, responsible for making scheduling decisions. According to (7.2), the SIR at receiver j is given by

$$SIR_j^{H_2} = \frac{P_r|\mathbf{h}_j^R|^2}{\sum_{l=1}^{Q_j} \nu_l|u_{jl}|^2}, \quad j = 1, \ldots, K, \tag{7.4}$$

where the superscript H_2 refers the second hop. At this hop, please note that each user feeds back its SIR value to the relay which selects the scheduled user (i.e., with the highest SIR value).

The achieved capacity of the two-hop AF relaying system with TAS/MRC on the first hop and interference-aware user scheduling on the second hop is given by

$$C = \frac{1}{2}\mathbb{E}\left\{ \ln_2\left(1 + \frac{\frac{P_sX_M}{\sum_{l=1}^L \mu_l|\mathbf{v}_l|^2}Z_K}{1 + \frac{P_sX_M}{\sum_{l=1}^L \mu_l|\mathbf{v}_l|^2} + Z_K}\right)\right\}, \tag{7.5}$$

where $X_M = \underset{i=1\ldots,M}{\max}|\mathbf{h}_i^S|^2$ and $Z_K = \underset{k=1,\ldots,K}{\max} SIR_j^{H_2}$. Drawing a comparison, in this paper, between interference-aware (i.e., SIR based) and interference-oblivious (i.e., CSI based) user scheduling will be certainly useful for quantifying the potential gain that originates from interference-awareness and, further, understanding whether this gain justifies the required high-complexity signal processing (demodulation and parameters estimation).

In this paper, without loss of generality, a homogeneous network in which all users are clustered together, whereby $\lambda_j = \lambda, j = 1 \ldots K$ are considered. This policy guarantees a uniform user experience, saves valuable energy at terminals, and avoids near-far blockage where the receiver's limited dynamic range makes weak signals drown in stronger ones. Moreover, we assume that all users have the same statistical behavior with equal interference number $Q_j = Q, j = 1 \ldots K$ and similar interference distribution.

7.3 Exact analysis of the capacity

The objective herein is to compute the end-to-end capacity and to study the asymptotic regime of the dual-hop multiuser network described in Section II. Unfortunately, it turns out that it is impossible to express this capacity in closed form, due to the complexity of such a system. In order to circumvent this issue, we recur to a two-step methodology in which the end-to-end capacity C may be formulated as a linear combination of integrals and, hence, given by

$$
\begin{aligned}
C &\stackrel{(a)}{=} \frac{1}{2\ln(2)} \int_0^\infty se^{-s} \left(1 - s\mathbb{E}_{\mathbf{h},i_T}\{e^{-sSIR^{H_1}}\}\right) \left(1 - s\mathbb{E}_{\mathbf{h},i_T}\{e^{-sSIR^{H_2}}\}\right) ds \\
&\stackrel{(b)}{=} \frac{1}{2\ln(2)} \int_0^\infty se^{-s} M_{SIR^{H_1}}^{(c)}(s) M_{SIR^{H_2}}^{(c)}(s),
\end{aligned}
\tag{7.6}
$$

where $\mathbf{h}$, i_T are short-hands collecting the RVs $(\mathbf{h}^S, \mathbf{h}^R)$ and $(\mathbf{i}_{T_1}, i_{T_2})$. Please note that the two-step methodology applied in (7.6) is a powerful tool allowing to gain insights into the overall system performance while separately treating its components (hops and RVs pertaining to them). The equalities in (7.6.a) and (7.6.b) correspond to the first and second step of this methodology, respectively. As far as (7.6.a) is concerned, its computation may be avoided by resorting to the CMGF

$$
M_X^{(c)}(s) \triangleq \int_0^\infty e^{-sx} F_X^{(c)}(x) dx,
\tag{7.7}
$$

Proof : Interested readers are referred to the proof in [13, Theorem 1] omitted here for conciseness. Note that equation (7.6.b) is directly obtained from [13, Theorem 1, Eq.] by applying $M_X^{(c)}(s) = 1 - sM_X(s)$ on the second hop and simplifying.

It is noteworthy that (7.7) is very convenient since the SIR's CCDF of single-hop communication systems over fading channels has been widely studied in the literature ([12] and references

therein)[1]. Exploiting the methodology in (7.6), the rest of this section is devoted then to the calculation of the capacity achieved by the system model in Section II. The obtained result is stated in the following lemma.

Lemma 1 : Let the system model in section II, then for any propagation setup in terms of pathloss, antenna number, and CCI, the achievable capacity is given by

$$
C = \frac{1}{2\ln(2)} \sum_{n=0}^{M-1} \sum_{\Omega(n,N)} \sum_{i=1}^{\rho(\mathbf{D})} \sum_{j=1}^{\tau_i(\mathbf{D})} \sum_{k=0}^{N+\delta_n-1} \frac{\Theta_n \zeta_i^j(\mathbf{D})\Gamma(k+j)\rho}{(j-1)!\mu_{<1i>}} \frac{\lambda M(N+\delta_n-1)!}{\nu(n+1)^{N+\delta_n+1}\Gamma(N)}
$$

$$
\left(\sum_{m=0}^{K(Q+N-1)-1} \binom{K(Q+N-1)}{m} \Gamma(m+1)\Xi_m + \sum_{n=1}^{K} \sum_{\Omega(n,Q-1)} \binom{K}{n} \alpha_n \Gamma(\delta_n+K(L+N-1)+n(1-L)+1)\Pi_n \right),
$$

(7.8)

where

$$
\Xi_m = \int_0^\infty se^{-s} \Psi\left(m+1, m+2-K(Q+N-1), \frac{\lambda s}{\nu} \right) \Psi\left(k+1, 2-j, \frac{\rho s}{\mu_{<i>}(n+1)} \right) ds, \quad (7.9)
$$

and

$$
\Pi_n = \int_0^\infty se^{-s} \Psi\left(\delta_n+K(Q+N-1)+n(1-Q)+1, \delta_n+2-n(Q-1), \frac{\lambda s}{\nu} \right) \Psi\left(k+1, 2-j, \frac{\rho s}{\mu_{<i>}(n+1)} \right) ds. \quad (7.10)
$$

In (7.8), $\Theta_n = \frac{(-1)^n n! \prod_{p=0}^{N-1} \left(\frac{1}{p!}\right)^{n_{p+1}}}{\prod_{k=1}^{N} n_k!}$, $\Omega(n,N) = \{(n_1,...,n_N) : n_k \geq 0; \sum_{k=1}^{N} n_k = n\}$, and $\delta_n = \sum_{l=0}^{N_r-1} l\ n_{l+1}$. Moreover, $\mathbf{D} = \text{diag}(\mu_1, \mu_2, \ldots, \mu_L)$, $\rho(\mathbf{D})$ is the number of distinct diagonal elements of $\mathbf{D}$, $\mu_{<1>} > \mu_{<2>} > \ldots > \mu_{<L>}$ are the distinct diagonal elements in decreasing order, $\tau_\mathbf{i}(\mathbf{D})$ is the multiplicity of $\mu_{<i>}$ and $\zeta_{i,j}(\mathbf{D})$ is the (i,j)-th characteristic coefficient of $\mathbf{D}$ [23]. For instance, when non-equal-power interferers are considered, we have $\tau_i(\mathbf{D}) = 1$ and $\zeta_{i,1}(\mathbf{D}) = \prod_{k=1,k\neq i}^{\rho(\mathbf{D})} 1/\left(1 - \frac{\mu_{<k>}}{\mu_{<i>}}\right)$.

Proof : The direct application of the proposed two-step method in (7.6) using the results in Appendix A pertaining to the per-hop SIR CMGF calculation completes the proof.

It is worthwhile to mention that integrals like in (7.9)-(7.10) can be evaluated by means of the generalized Meijer's G-function of two variables, as can be seen from a more general integral formula due to [22, Eq. (3.2)]. We begin by expressing the Triconomi functions $\Psi(a,b,c)$ in the integrands of Ξ_m and Π_n in terms of the Meijers's G-function as

$$
\Psi\ (a,b,c,z) = \frac{1}{\Gamma(a)\Gamma(a-b+1)} G_{1,2}^{2,1}\left(z \ \middle| \ \begin{matrix} 1-a \\ 0, 1-b \end{matrix} \right). \quad (7.11)
$$

---

1. Although for brevity we limit our discussion to Rayleigh fading channels, many other channels, such as Nakagami-m channels, may be considered here.

Then performing the Laplace transform over the product of two Meijer's G-functions (see [22, Eq. (3.2)]), (7.8) can be expressed according to

$$
C = \frac{1}{2\ln(2)} \sum_{n=0}^{M-1} \sum_{\Omega(n,N)} \sum_{i=1}^{\rho(\mathbf{D})\tau_i(\mathbf{D})} \sum_{j=1}^{N+\delta_n-1} \sum_{k=0}^{N+\delta_n-1} \frac{\Theta_n \zeta_i^j(\mathbf{D})\Gamma(k+j)\rho}{(j-1)!\mu_{<i>}} \frac{\lambda M(N+\delta_n-1)}{\nu(n+1)^{N+\delta_n+1}\Gamma(N)} \sum_{m=0}^{K(Q+N-1)-1} \frac{\binom{K(Q+N-1)}{m}}{\Gamma(K(Q+N-1))}
$$

$$
G_{1,[1,1],0,[1,2]}^{1,1,1,1,2} \left(\frac{\frac{\rho}{\mu_{<i>}}}{n+1}, \frac{\lambda}{\nu} \middle| \begin{array}{c} \ldots; 1+k; 1+m \\ \ldots; 0, j-1; 0, K(Q+N-1)-m-1 \end{array} \right) + \sum_{n=1}^{K} \sum_{\Omega(n,Q-1)} \frac{\binom{K}{n}\alpha_n}{\Gamma(K(Q+N-1))}
$$

$$
G_{1,[1,1],0,[1,2]}^{1,1,1,1,2} \left(\frac{\frac{\rho}{\mu_{<i>}}}{n+1}, \frac{\lambda}{\nu} \middle| \ldots; 1+k; 1+\delta_n+K(Q+N-1)+n(1-Q); 0, j-1; 0, -\delta_n-1+n(1-Q) \right),
$$

$$(7.12)$$

where $G[\cdot,\cdot]$ denotes the generalized Meijer's G function of two variables defined in [22, Eq. (1.2)] [2].

The result accounts for almost all relevant propagation parameters including the antenna and user numbers, path loss and interference power. To gain more insight into these parameters, we propose in the next section more convenient capacity expressions obtained for large numbers of users K and antennas M. We underline the fact that this large scale case is of significant importance in future wireless systems, where the use of a large number of antennas to serve a tremendously increasing number of user terminals of various types is expected to drastically improve spectral efficiency. However due to complexity constraints and space limitations, relays are often equipped with a finite number of antennas. It is therefore useful to investigate the large scale case. In what follows, we will focus on the scaling laws of the capacity for large K.

7.4 Asymptotic analysis of the capacity : M, N are fixed

In this section, we study the asymptotic capacity for a large number of users K, but for a small and finite number of antennas at the source M and at the relay N. We will state a theorem that gives the closed-form expression for the achievable capacity for large K. After proving the theorem, we summarize in some key results the new insights gained thereof. To this end, the asymptotic behavior of the distribution of the maximum of K i.i.d. random variables is studied. In Appendix B, we review some useful properties that we needed to state the following result.

---

2. Please note that the generalized Meijer's G-function of two variables is a build-in function in Mathematica, hence can be directly computed. Alternatively, an efficient approach developed in [24] could be used to evaluate the expression.

Theorem 1 : When M, N and the ASIRs[3] are fixed, the capacity of AF MU-MIMO with interference-aware scheduling for large K is asymptotically given by

$$
C = \frac{1}{2\ln(2)} \sum_{n=0}^{M-1} \sum_{\Omega(n,N)} \sum_{i=1}^{\rho(D)} \sum_{j=1}^{\tau_i} \sum_{k=0}^{N+\delta_n-1} \frac{\Theta_n \zeta_i^j \rho}{(n+1)^{N+\delta_n+1} \mu_{<i>}} \frac{M(N+\delta_n-1)!}{\Gamma(N)(k+j)}
$$
$$
\left({}_2F_1\left(k+1, 1, k+j+1, 1-\frac{\rho}{\mu_{<i>}} \frac{}{(n+1)} \right) - \left(\frac{NK\lambda}{4\nu}+1 \right)^{-1} {}_2F_1\left(k+1, 1, k+j+1, 1-\frac{\rho}{\mu_{<i>}} \frac{}{\left(\frac{NK\lambda}{4\nu}+1\right)(n+1)} \right) \right),
$$
(7.13)

when $Q = 1, \forall\, N$, while it is given by

$$
C = \frac{1}{2\ln(2)} \sum_{n=0}^{M-1} \sum_{i=1}^{\rho(D)} \sum_{j=1}^{\tau_i} \frac{M\Theta_n \zeta_i^j \rho}{j(n+1)\mu_{<i>}} \left({}_2F_1\left(1, 1, 1+j, 1-\frac{\rho}{\mu_{<i>}} \frac{}{(n+1)} \right) - \left(\frac{\lambda}{\nu} \left(\frac{K^{\frac{1}{Q}}-1}{4^{\frac{1}{Q}}} \right)+1 \right)^{-1} \right.
$$
$$
\left. {}_2F_1\left(1, 1, 1+j, 1-\frac{\rho/\mu_{<i>}}{\left(\frac{\lambda}{\nu}\left((K^{1/Q}-1)/4^{1/Q}\right)+1\right)(n+1)} \right) \right),
$$
(7.14)

when $N = 1, \forall\, Q$.

Proof : In order to evaluate the capacity, we have to obtain the asymptotic distribution of the maximum of K i.i.d SIRs denoted by $Z_K = \frac{\lambda}{\nu} \max\limits_{j=1,\ldots,K} \frac{|\mathbf{h}_j^R|^2}{\sum_{l=1}^{Q}|u_l|^2}$. Before embarking on the proof, it is worth examining the SIRs $Z_j = \frac{|\mathbf{h}_j^R|^2}{\sum_{l=1}^{Q}|u_l|^2}$. We have $Z_j \stackrel{d}{=} \frac{\chi(2N)}{\chi(2Q)}, j = 1\ldots,K$ who are K i.i.d random variables with CDF

$$
F_Z(x) = \frac{x^N\, {}_2F_1\left(N+Q, N, 1+N, -x\right)}{N B(N,Q)}
$$
(7.15)

implying that $F_{Z_K}(x) = [F_Z(\frac{\nu}{\lambda}x)]^K$. Next, we use Corollary A in Appendix B to find the asymptotic distribution of Z_K. We show that

$$
\lim_{x\to\infty} \frac{1-F_Z(x)}{1-F_Z(tx)} = \lim_{x\to\infty} \frac{t^{-N}(1+tx)^{N+Q}}{(1+x)^{N+Q}}
$$
(7.16)
$$
= t^Q,
$$
(7.17)

where to get from (7.16) to (7.17) we use the Hospital rule after substituting the hypergeometric function by its equivalent ${}_2F_1(a,b;b+1;z) = bz^{-b}B_z(b,1-a)$ where $B_z(c,d)$ is the Beta function [21, Eq.(8.380.1)]. On the other hand and in view of Corollary A, it is easy to show that the upper endpoint of F_Z is equal zero, meaning that $\varepsilon(F) = 0$ and implying that the limit distribution of Z_K lies in the domain of maximal attraction of Frechet distribution [20, Theroem 10.5.2], i.e.

$$
[F_Z(a_K x)]^K = e^{-x^{-Q}}, x \geq 0,
$$
(7.18)

---

3. ASIR refers to the ratios $\frac{\rho}{\mu}$ and $\frac{\lambda}{\nu}$

where a_K is a normalizing parameter defined such that $F_Z(a_K) = 1 - \frac{1}{K}$. In order to find a_K while keeping the analytical complexity tractable, we concentrate the following analysis on cases i) $Q = 1, \forall\ N$, and ii) $N = 1, \forall\ Q$. The results can be extended to other values of N, Q, however the analysis is very challenging. The arbitrary N, Q case can be handled using bounding techniques but thwarting the paper goal of exact capacity analysis. In case $i)$, by exploiting the $_2\text{F}_1$ reduction formulas $_2\text{F}_1(b, a; a; z) = (1 - z)^{-b}$, we show that a_K satisfies

$$
\begin{aligned}
\frac{a_K^N}{(1 + a_K)^N} &= 1 - \frac{1}{K} \\
\implies a_K &= \frac{(1 - 1/K)^{1/N}}{1 - (1 - 1/K)^{1/N}} \\
&\underset{K \to \infty}{\approx} NK.
\end{aligned}
\tag{7.19}
$$

In case $ii)$, we have $N = 1$ thereby enabling the simplification of $F_Z(x)$ relying on the fact that $_2\text{F}_1(1, b; 2; z) = \frac{(1-z)^{-b}-1}{(b-1)z}$. The parameter a_k is therefore obtained as follows

$$
\begin{aligned}
(1 + a_K)^{-Q} &= \frac{1}{K} \\
\implies a_K &\underset{K \to \infty}{\approx} K^{1/Q} - 1.
\end{aligned}
\tag{7.20}
$$

Substituting a_K into (7.18), we obtain as $K \to \infty$

$$
F_{Z_K}(x) = \begin{cases} e^{-\frac{NK\lambda}{\nu x}}, & Q = 1, \forall\ N \\ e^{-\left(\frac{\left(K^{1/Q}-1\right)\lambda}{\nu x}\right)^Q}, & N = 1, \forall\ Q \end{cases}
\tag{7.21}
$$

Fig. 1 shows the exact and asymptotic CDFs of Z_K for different values of N and Q. We observe that the asymptotic distribution in (7.21) is a good approximation even for small values of N and Q and the approximation becomes more accurate by increasing the value of K.

As for the CMGF of Z_K, replacing (7.21) into (7.7) and performing some algebraic manipulations, we get

$$
M_{Z_K}^{(c)}(s) \overset{(a)}{\approx} \begin{cases} \frac{1}{s}\left(1 - e^{-\frac{NK\lambda}{4\mu}s}\right), & Q = 1, \forall\ N \\ \frac{1}{s}\left(1 - e^{-\frac{\lambda}{\mu}\left(\frac{K^{\frac{1}{Q}}-1}{4^{\frac{1}{Q}}}\right)s}\right), & N = 1, \forall\ Q \end{cases}
\tag{7.22}
$$

where (a) follows from the fact that $1 - e^{-x} \underset{x \geq 4}{\approx} 1$. At this step, recalling the first-hop CMGF derived in section III as shown in Appendix A, the end-to-end capacity of tow-hop AF relaying

with interference-aware scheduling as K goes large is obtained from applying (7.6). For instance, case i) yields

$$C = \frac{1}{2 \ln(2)} \sum_{n=0}^{M-1} \sum_{\Omega(n,N)} \sum_{i=1}^{\rho_1} \sum_{j=1}^{\tau_i} \sum_{k=0}^{N+\delta_n-1} \frac{\Theta_n \zeta_i^j \Gamma(k+j)\rho}{(j-1)!\mu_{<1i>}} \frac{M(N+\delta_n-1)!}{(n+1)^{N+\delta_n+1}\Gamma(N)} \int_0^\infty e^{-s} \left(1 - e^{-\frac{NK\lambda}{4\mu}s}\right)$$

$$\Psi\left(k+1, 2-j, s\frac{\rho}{\mu_{<i>}(n+1)}\right) ds, \tag{7.23}$$

where [21, Eq.(8.380.1)] was employed to reach the closed-form expression of C shown in Theorem 1. The capacity expression for large K in case ii) i.e., $N = 1$ and arbitrary Q can be derived similarly.

Remark 1 : For fixed M, N and ASIRS, the capacity for large K reaches its maximum value C_{max} given by

$$C_{max} = \frac{1}{2 \ln(2)} \sum_{n=0}^{M-1} \sum_{\Omega(n,N)} \sum_{i=1}^{\rho(D)} \sum_{j=1}^{\tau_i} \sum_{k=0}^{N+\delta_n-1} \frac{\Theta_n \zeta_i^j \rho M(N+\delta_n-1)!}{(n+1)^{N!+\delta_n+1}\mu_{<i>}\Gamma(N)(k+j)} {}_2\mathrm{F}_1\left(k+1, 1, k+!j+1, 1-\frac{\frac{\rho}{\mu_{<i>}}}{(n+1)}\right).$$
$$\tag{7.24}$$

Proof : (7.24) follows by resorting to the series expansion of the ${}_2\mathrm{F}_1$ function near 1 and performing the limit operation as K goes to infinity.

From (7.24), it is apparent that when $M \ll K$, the end-to-end capacity no longer depend on the number users, or in other words, the contribution of multiuser diversity becomes negligible. This is because the performance of a two-hop communication system is limited by the weakest link. In such scenarios, the first hop becomes the bottleneck and hence the CCI has the dominating effect on system capacity.

Remark 2 : As the number of users grows large (i.e., $K \to \infty$) the ergodic capacity of AF multiuser MIMO dual-hop systems becomes

$$\lim_{K \to \infty} C = \frac{1}{2} C^{SH-TAS/MRC}\left(M, N, L, \frac{\rho}{\mu}\right), \tag{7.25}$$

where $C^{SH-TAS/MRC}(M, N, L, \frac{\rho}{\mu})$ is the ergodic capacity of a single-hop TAS/MRC channel with M transmit antennas and N receive antennas in the presence of L interferers at the receiver with average SIR $\frac{\rho}{\mu}$. The result is trivially obtained by directly averaging $F^{(c)}_{\frac{X_M}{|i_{T_1}|^2}}(x)/(1+x)$ in (7.63) and using [21, Eq. 3.197.5].

7.5 Asymptotic analysis of the capacity : N is fixed

Here, we study the capacity scaling laws for the antenna selection and interference-aware user scheduling schemes in the regime of a large number of transmit antennas M and users K, but for a small and finite number of relay antennas N. This consideration is deemed in line with the current wireless communication landscape, which portray a tremendous increase in the number of wireless terminals of various types yet only a small increase in the number of wireless infrastructure (relay) support. Emphasis is placed on showing the affordable scaling speed of the number of antennas M and users K. Similar to the previous section, we need to analyze the asymptotic behavior of the first hop's maximum SIR when M goes to infinity. The system's capacity for the antenna selection and user scheduling scheme when both M and K grow to infinity constitutes the third main contribution of this paper. Obviously, the scaling laws will depend on the growth rate of K relative to M.

Theorem 2 : For sufficiently large M and K and fixed N and AISRs, the capacity of two-hop AF relaying under interference-aware user scheduling is given by

$$C = \frac{1}{2\ln(2)}\left(\ln\left(\alpha_K\right) - e^{\frac{\beta_M^2}{\alpha_K}}\Gamma\left(0,\frac{\beta_M^2}{\alpha_K}\right) - e^{\beta_M^2}\mathrm{E_i}\left(-\beta_M^2\right) - \right.$$

$$\left. \sum_{n=1}^{L-1}\frac{\beta_M^n}{n}\left(e^{\frac{\beta_M^2}{2}}W_{-\frac{n}{2},\frac{n-1}{2}}\left(\beta_M^2\right) - \frac{e^{\frac{\beta_M^2}{2\alpha_K}}}{\alpha_K^{n/2}}W_{-\frac{n}{2},\frac{n-1}{2}}\left(\frac{\beta_M^2}{\alpha_K}\right)\right)\right), \qquad (7.26)$$

where $\beta_M = \sqrt{\frac{b_M - \rho\ln(4)}{\mu}}$ and $\alpha_K = 1 + \frac{\widehat{a}_K\lambda}{\nu}$. with

$$\widehat{a}_K = \begin{cases} \frac{NK}{4}, & Q = 1, \forall\, N \\ \frac{K^{\frac{1}{Q}-1}}{4^{\frac{1}{Q}}}, & N = 1, \forall\, Q \end{cases} \qquad (7.27)$$

Proof : Since M is going to infinity, we use Corollary B.2 in Appendix B to find the asymptotic distribution of the maximum of M i.i.d. random variables $Y_i = \rho|\mathbf{h}_i^S|^2 \overset{d}{=} \rho\chi(2N)$ with PDF and CDF given, respectively by, $f_Y(x) = \frac{(\frac{x}{\rho})^{N-1}}{N!}e^{-\frac{x}{\rho}}$ and $F_Y(x) = 1 - \frac{\Gamma(N,\frac{x}{\rho})}{\Gamma(N)}$. Let $X_M = \max_{i=1,\dots,M} Y_i$. In what follows, we show that Y_i meets all the three conditions stated in Appendix B.2. We start by calculating the growth function $g(x)$ which can be expressed as

$$g(x) = \frac{1 - F_Y(x)}{f_Y(x)} = \frac{\Gamma(N,\frac{x}{\rho})}{(\frac{x}{\rho})^{N-1}e^{-\frac{x}{\rho}}} \xrightarrow[x\to\infty]{} \rho > 0. \qquad (7.28)$$

The second step is showing that $b_M = O(\ln(M))$. To find b_M, we apply the asymptotic expansion of the incomplete Gamma function given by [21, Eq.8.257] leading to

$$1 - F_Y(b_M) = \frac{b_M^{N-1}}{\rho} e^{-\frac{b_M}{\rho}} (1 + O(1/b_M)) = \frac{1}{M}$$

$$\implies \frac{b_M}{\rho} - (N-1) \ln \left(\frac{b_M}{\rho} \right) = \ln(M), \tag{7.29}$$

and implying that

$$b_M = \rho \ln(M) + \rho(N-1) \ln \ln(M) + O(\ln \ln \ln(M)). \tag{7.30}$$

Also from (7.28) and (7.30), it is easy to verify that b_M satisfies $g^{(m)}(b_M) = 0$. Therefore, from [20], we have

$$F_{X_M}(x + b_M) = e^{-e^{-\frac{x}{\rho}}}, \quad x \geq 0. \tag{7.31}$$

Substituting b_M in (7.30), we get

$$F_{X_M}(x) = e^{-e^{-\frac{x}{\rho} + \ln(M) + (N-1) \ln \ln(M)}}, \quad x \geq 0. \tag{7.32}$$

Since the relay is subject to L interferences assumed for sake of tractability and conciseness to be i.i.d with mean power μ, the CCDF of the first hop SIR $X = X_M/|i_{T_1}|^2$ is obtained as

$$F_X^{(c)}(x) = \int_0^\infty F_{X_M}^{(c)}(xy) f_{|i_{T_1}|^2}(y) dy, \tag{7.33}$$

where for L i.i.d interferences at the relay we have $f_{|i_{T_1}|^2}(y) = \frac{\mu^{-L}}{\Gamma(L)} y^{L-1} e^{-\frac{y}{\mu}}$. Accordingly, using (7.32) we get

$$F_X^{(c)}(x) = \frac{\mu^{-L}}{\Gamma(L)} \int_0^\infty y^{L-1} e^{-\frac{y}{\mu}} \left(1 - e^{-e^{-\frac{yx - b_M}{\rho}}} \right) dy. \tag{7.34}$$

By letting $t = e^{-\frac{yx}{\rho}}$, we have $y = -\frac{\rho}{x} \ln(t)$. Furthermore, for notational simplicity, we define $\zeta = e^{\frac{b_M}{\rho}}$, thus (7.34) can be rewritten as

$$F_X^{(c)}(x) = \frac{(-1)^{L-1} \left(\frac{\rho}{\mu x} \right)^L}{\Gamma(L)} \left(\int_0^{\frac{4}{\zeta}} \ln(t)^{L-1} t^{\frac{\rho}{\mu x} - 1} \left(1 - e^{-\zeta t} \right) dt + \int_{\frac{4}{\zeta}}^1 \ln(t)^{L-1} t^{\frac{\rho}{\mu x} - 1} dt \right). \tag{7.35}$$

Recalling (7.30), we can easily see that the limit of the first term on the R.H.S. of (7.35) becomes vanishingly small as $\lim_{M \to \infty} \frac{4}{\zeta} \approx \frac{4}{M} = 0$. Furthermore, the limit of the second term can be simplified using [21, Eq. (3.381.1)] as

$$F_X^{(c)}(x) \stackrel{(a)}{\simeq} 1 - \frac{\Gamma \left(L, \frac{\beta_M^2}{x} \right)}{\Gamma(L)}, \tag{7.36}$$

133

where β_M is defined in Theorem 2. In turn, a closed-form expression of the CMGF of the fist hop SIR $X = X_M/|i_{T_1}|^2$ when M geos to infinity follows form plugging (7.36) into (7.7) as

$$
\begin{aligned}
M_X^{(c)}(s) &= \int_0^\infty e^{-sx} \left(1 - \frac{\Gamma\left(L, \frac{\beta_M^2}{x}\right)}{\Gamma(L)} \right) dx \\
&= \frac{1}{s} - 2 \sum_{n=0}^{L-1} \frac{\beta_M^{n+1}}{n!} s^{\frac{n-1}{2}} K_{n-1}\left(2\beta_M\sqrt{s}\right),
\end{aligned}
\tag{7.37}
$$

after using [21, Eq.(8.352.2)] and [21, Eq.(3.471.9)]. Using the obtained first-hop SIR CMGF along with CMGF expression of the second-hop SIR previously obtained in section III as K goes large, we can now evaluate the capacity as

$$
C = \frac{1}{2\ln(2)} \left(\int_0^\infty \frac{e^{-s}}{s}\left(1 - e^{-\frac{\widehat{a}_K\lambda}{\mu}s}\right) ds - 2\beta_M \Phi_0\left(\frac{\widehat{a}_K\lambda}{\nu}, \beta_M\right) - 2\sum_{n=1}^{L-1} \frac{\beta_M^{n+1}}{n!} \Phi_n\left(\frac{\widehat{a}_K\lambda}{\nu}, \beta_M\right) \right), \tag{7.38}
$$

whereby

$$
\Phi_n(a,b) \underset{n\geq 0}{=} \int_0^\infty e^{-s} s^{\frac{n-1}{2}} \left(1 - e^{-as}\right) K_{n-1}\left(2b\sqrt{s}\right) ds. \tag{7.39}
$$

Using the results of Appendix C, a closed-form expression for Φ_0 is obtained as

$$
\Phi_0(a,b) = \frac{1}{2b}\left(e^{\frac{b^2}{1+a}}\Gamma\left(0, \frac{b^2}{1+a}\right) + e^{b^2}\mathrm{E_i}\left(-b^2\right)\right). \tag{7.40}
$$

Furthermore, applying [21, Eq.6.643], a closed-from expression for Φ_n is obtained after some manipulations as

$$
\Phi_n(a,b) \underset{n\geq 1}{=} \frac{\Gamma(n)}{2b}\left(e^{\frac{b^2}{2}}W_{-\frac{n}{2},\frac{n-1}{2}}\left(b^2\right) - \frac{e^{\frac{b^2}{2(1+a)}}}{(1+a)^{n/2}}W_{-\frac{n}{2},\frac{n-1}{2}}\left(\frac{b^2}{1+a}\right)\right). \tag{7.41}
$$

Finally, substituting (7.40) and (7.41) into (7.38) and resorting to [21, Eq. 3.421.5] completes the proof.

Corollary 1 (Large M and K with arbitrary L and fixed N) : Either we have $Q = 1$ or assuming that each user has only to estimate the CSI of its strongest interferer, when K grows faster than $\ln(M)$ (i.e., $\lim\limits_{M,K\longrightarrow\infty} K/\ln(M) = \infty$, which include the case $K=M$), it holds that

$$
C \approx \frac{1}{2\ln(2)}\left(\ln\left(\frac{\rho}{\mu}\left(\ln(M) + (N-1)\ln\ln(M)\right)\right) + \gamma - H_{L-1}\right), \tag{7.42}
$$

where γ is the Euler-Mascheroni constant [21, Eq.(8.367.1)] and H_n is the harmonic number of order n.

Proof : As $\frac{K}{\ln(M)} \longrightarrow \infty$, we have $\beta_M \underset{M \to \infty}{\longrightarrow} \infty$ and $\frac{\beta_M}{\alpha_K} \underset{M,K \to \infty}{\longrightarrow} 0$, then the following approximations hold : $\Gamma(0,z) \underset{z \to 0}{=} -\ln(z) - \gamma$, $e^z \underset{z \to 0}{=} 1 + o(z)$, and $e^z E_i(-z) \underset{z \to \infty}{=} 0$, $e^{z/2} W_{a,b}(z) \underset{z \to \infty}{\approx} z^a$, $z^{n/2} e^{z/2} W_{-n/2,b}(z) \underset{z \to 0}{=} 0$. Considering all these facts, C reduces after several manipulations to

$$C \approx \frac{1}{2\ln(2)} \left(\ln\left(\beta_M^2\right) + \gamma - \sum_{n=1}^{L-1} \frac{1}{n} \right), \qquad (7.43)$$

proving thereby (7.42).

Remark 3 : For m antenna-user pairs ($M = K = m$) that communicate through a relay with N antenna, corollary 1 reveals that in the Rayleigh-fading case multiuser diversity schedules the best user for transmission, and boosts the average SIR by a factor of $\ln(m) + (N-1)\ln\ln(m)$. It should be stressed that despite the low-rate CSI feedback working considered system, the latter exhibits the pre-ln ln factor of the scaling law of the capacity of more intensive schemes with full CSI. Indeed, the capacity scaling of the dirty paper coding (DPC) scheme is shown in [16] to be $\ln\ln(m)$, which is also the capacity scaling for MIMO-broadcast channels (MIMO-BC) [17]. Therefore, as far as the scaling law of the capacity is concerned, we are not losing anything in terms of the capacity provided that N is fixed and K grow as faster as M. Note that It is reasonable to expect that a higher capacity can be achieved if we allow rate adaptation and interference cancelation at the relay at the cost of more feedback overhead and higher computational complexity. However, what corollary 1 tells us is that the return is at most $\frac{1}{2\ln(2)}\left(\ln\left(\ln(m)+(N-1)\ln\ln(m)\right)+\gamma\right)$ obtained after canceling the term H_{L-1}. Simulation results in Section V indicate a rather fast convergence to the asymptotic limits with increasing m.

Lemma 2 (Capacity loss due to the interference at the relay) : It is straightforward to show from Theorem 3 for large scale MU-MIMO, that the capacity loss due to the increase of $P > 0$ i.i.d interferences at the relay is

$$\begin{aligned} \Delta_P &= \frac{1}{2\ln(2)} \left(H_{L-1} - H_{L+P-1} \right) \\ &= -\frac{1}{2\ln(2)} \sum_{k=0}^{P} \frac{1}{P+k}. \end{aligned} \qquad (7.44)$$

The result above is of interest since it allows the prediction of the exact amount of capacity loss due to any increase in the number of interferers, when M is large enough. Such information is highly desired in wireless communication networks to anticipate in a timely manner the

degradation of the quality of service (QoS).

Lemma 3 : The capacity of large-scale MU-MIMO (with $K \gg \ln(M)$) in the presence of a large number of interferers L behaves as

$$2^{2C} \approx \frac{\rho}{\mu} \frac{\ln(M) + (N-1) \ln \ln(M)}{L}. \tag{7.45}$$

Proof : Resorting to the approximation of the Harmonic number as L goes large given by

$$H_{L-1} = \gamma + \ln(L-1) + O(L^{-2}), \tag{7.46}$$

it follows from (7.42) that

$$C \approx \frac{1}{2 \ln(2)} \left(\ln \left(\rho \left(\ln(M) + (N-1) \ln \ln(M) \right) \right) - \ln(\mu L) \right), \tag{7.47}$$

yielding (7.45) after using some logarithmic identities. It can be inferred from Lemma 3 that the capacity loss due to an increased dimensionality of spatial interference is much more pronounced than any improvement resulting form adding more active transmit antennas at the source. This is due to the fact that C decreases with $\ln(L)$ while it increases with $\ln \ln(M)$, respectively. In view of this it is not surprising that recent research on spatial multiplexing in cellular systems has reached the common conclusion that adding more transmit antennas or data streams at each base station can actually decrease the capacity at low SIR due to the increased dimensionality of spatial interference [18], [4].

Corollary 2 (Large M and K with arbitrary Q, L, and N = 1 : large Q) Consider the setting of Theorem 2 where the relay and each of the K users is prone to L and Q interferences, respectively. If $Q \gg \left\lfloor \frac{\ln(K)}{\ln \ln(M)} \right\rfloor$, where $\lfloor x \rfloor$ denotes the integer part of x, then it holds that

$$C \approx \frac{1}{2 \ln(2)} \left(\ln \left(1 + \frac{\lambda}{\nu} \left(K^{\frac{1}{Q}} - 1 \right) \right) - L \frac{\frac{\lambda}{\nu} \left(K^{\frac{1}{Q}} - 1 \right)}{\frac{\rho}{\mu} \ln(M)} \right). \tag{7.48}$$

Proof : According to (7.26), the growth of $K^{1/Q} - 1$ with respect to $\ln(M)$ is crucial for the capacity scaling law. In fact it is easy to show for $\left\lfloor \frac{\ln(K)}{\ln \ln(M)} \right\rfloor \ll Q$ that we have

$$\frac{\beta_M^2}{\alpha_K} \underset{M,K \to \infty}{\approx} \frac{\ln(M)}{K^{1/Q} - 1} \longrightarrow \infty. \tag{7.49}$$

Then it follows immediately that all the terms but the first on in the first term on the RHS of (7.26) become vanishingly small as M and K grow large with $\frac{\ln(M)}{K^{1/Q}-1} \longrightarrow \infty$. In fact, considering

that $e^z \Gamma(0, z) \underset{z \to \infty}{=} \frac{1}{z}$, $e^z E_i(-z) \underset{z \to \infty}{=} -\frac{1}{z}$, and $z^{n/2} e^{z/2} W_{-n/2, \frac{n-1}{2}}(z) \underset{z \to \infty}{=} 1 - \frac{n}{z}$, it follows after some manipulations that

$$C \approx \frac{1}{2\ln(2)} \left(\ln\left(1 + \frac{\lambda}{\nu}\left(K^{\frac{1}{Q}} - 1\right)\right) - L\left(\frac{1 + \frac{\lambda}{\nu}(K^{\frac{1}{Q}} - 1)}{\frac{\rho}{\mu}\ln(M)} - \frac{1}{\frac{\rho}{\mu}\ln(M)}\right)\right), \tag{7.50}$$

thereby concluding the proof. More importantly, despite imposing (7.49), the latter appears to be insufficient to ensure the multiuser diversity gain in (7.48). In fact, C is a monotonically increasing function of K if and only if the following condition holds

$$\ln(M^{1/L}) \gg K^{1/Q} - 1, \tag{7.51}$$

where (7.59) verifies $\frac{dC}{dK} > 0$.

From (7.48), while $\frac{L(K^{\frac{1}{Q}} - 1)}{\ln(M)} \longrightarrow 0$ (ex : when $L = 1$), the capacity scales as

$$C \approx \frac{1}{2\ln(2)} \ln\left(1 + \frac{\lambda}{\nu}\left(K^{\frac{1}{Q}} - 1\right)\right). \tag{7.52}$$

When Q is small, (7.52) can be further simplified to

$$C \underset{K \to \infty}{\overset{(a)}{\approx}} \frac{1}{2\ln(2)} \left(\ln\left(\frac{\lambda}{\nu}\right) + \frac{\ln(K)}{Q}\right), \tag{7.53}$$

where (a) follows form the fact that $\ln(1 + x) \approx \ln(x)$ when x is large enough. Nevertheless, when Q is large, $\ln(1 + x) \approx \ln(x)$ does not hold true. Instead, we have

$$K^{1/Q} - 1 \underset{Q \gg 1}{\approx} \frac{\ln(K)}{Q}. \tag{7.54}$$

Substituting (7.54) into (7.52) yields the capacity scaling law as Q goes large as

$$C \approx \frac{1}{2\ln(2)} \ln\left(1 + \frac{\lambda}{\nu}\frac{\ln(K)}{Q}\right). \tag{7.55}$$

Accordingly, it follows that as $\frac{L(K^{\frac{1}{Q}} - 1)}{\ln(M)} \longrightarrow 0$, we have

$$\begin{cases} 2^{2C} \approx \frac{\lambda}{\nu}K^{1/Q}, & \text{for small } Q \\ 2^{2C} - 1 \approx \frac{\lambda}{\nu}\frac{\ln(K)}{Q}, & \text{for large } Q. \end{cases} \tag{7.56}$$

From (7.42), (7.45) and (7.48), if the CSI is estimated in the second hop instead of SIR, the capacity will scale as $\ln\ln(K)$ when Q is small. The SIR-based scheduling outperforms then its CSI-based counterpart, since $K > \ln(K)$ always holds when $K \gg 1$. This proves the advantage of having global CSI knowledge to mitigate the interference. The latter comes, however, at the

expense of prohibitive power and overhead consumptions at the user device. A cost/performnce tradeoff must be envisaged for system deployment. This result further proves the rule of thumb that having an order of magnitude more antennas at the source than the number of scheduled users improves the system capacity since in this case $K^{1/Q}/\ln(M)$ goes to zero even for small Q thereby entailing a scaling law of $\ln(K)$ instead of $\ln\ln(M)$. When Q is large, the SIR-based scheduling still outperforms its CSI-based counterpart especially at low SIR. However, it exhibits the pre-loglog behavior of the CSI-based scheme leading to slow increase of C as K goes to infinity. Obviously, when this slight gain is hindered by the overhead cost due to large Q, CSI-based scheduling proves to be a more attractive alternative.

Lemma 4 (Capacity loss due to Q interferences at each user) : Let C_1 and C_2 be the capacities of the two-hop AF relaying with interference-aware scheduling subject to L_1, Q_1 and L_2, Q_2 interferences at the relay and each destination, respectively. For tractability and without loss of generality, we assume that $M = K$ and $\frac{\rho}{\mu} = \frac{\lambda}{\nu}$. Then resorting to (7.48), it follows that the capacity loss due to $\{L_2, Q_2\} > \{L_1, Q_1\}$ is

$$\Delta_Q = \frac{1}{2\ln(2)} \left(\ln\left(\frac{Q_1}{Q_2}\right) - \frac{L_1}{Q_1} + \frac{L_2}{Q_2} \right). \tag{7.57}$$

Proof : (7.57) is obtained from (7.48) after invoking (7.54) along with some manipulations.

Corollary 2 (Large M and K with arbitrary Q, L, and N = 1 : small to moderate Q) When $\frac{\ln(M)}{K^{1/Q}-1} \longrightarrow 0$, valid for small to moderate values of Q, the scaling law for arbitrary L is given by

$$C \approx \frac{1}{2\ln(2)} \left(\ln\left(\frac{\rho}{\mu}\ln(M)\right) + \gamma - H_{L-1} - \frac{1}{L}\frac{\frac{\rho}{\mu}\ln(M)}{\frac{\lambda}{\nu}(K^{1/Q} - 1)} \right), \tag{7.58}$$

Proof : (7.58) is obtained in the same line of (7.42). The forth term in the R.H.S of (7.58) follows form resorting to the series expansion of the Whittaker function near zero. It is easy to prove that (7.58) is an increasing function of M as if

$$\ln(M^{1/L}) \ll K^{1/Q} - 1, \tag{7.59}$$

thereby avoiding impeding the diversity gain.

Equations (7.48) and (7.58) analytically unarguably confirm the common intuitive observation that AF relaying performance is ultimately the performance of one of its hops.. This dominance is usually the output of the system's parametric objective function that quantifies the link strength. So far, in the literature, several functions defining the link's strength were

proposed, namely, the antenna number, the fading shape, or the product of both[4]. Oblivious to the interference number, these rules turn out to be totally inaccurate in interference-limited environments. This work remedies, for the first time this shortcoming. Indeed, the obtained results not only exemplify the interference nature of the considered system, but also analytically quantify through, simple formulas, the capacity loss due to interference.

7.6   Numerical and simulation results

Here, we provide some numerical examples to illustrate : 1) the tightness of the proposed approximations for large scale MU-MIMO relay networks ; and 2) the impact of interference on spatial and multiuser diversity. The simulations set-up consists of an (M-N-K) MU-MIMO AF relaying system where the relay and each destination is subject to L and Q i.i.d. interferers, respectively. We also assume, without loss of generality, equal per-hop ASIR $\frac{\rho}{\mu} = \frac{\lambda}{\nu}$ shorthanded in the plots as SIR.

We show in Fig. 2 the average capacity for two-hop AF network where a source with $M = 3$ antennas is communicating with K users through a relay with $N = 1, 2, 4$ antennas under Rayleigh fading. The simulated curves were obtained by averaging over 10000 channel realizations. The "approximation" curves refer to the average capacity using (7.13) in case i) $Q = 1, \forall\, N$, and (7.14) in case ii) $N = 1, \forall\, Q$. These two curves match each other very well even for small K, which establishes the fact that considering the large-K assumption leads to tight capacity approximations thereby alleviating the need for evaluating the cumbersome Meijer's G-function in (7.12). In Fig. 2 (a), we highlight the system's behavior under equitable interference conditions on the two hops, i.e., $L = Q = 1$ and for different relay antenna numbers N. One can see that, as K goes large, the capacity of opportunistic scheduling continuously approaches the asymptotic value C_{max} in (7.24) which constitutes the bottleneck of the system capacity. In Fig. 2 (b), the system capacity is depicted for different values of Q with $L = 2$. It can be seen that, for fixed K, as Q increases the capacity gain from multiuser diversity cannot compensate for the harmful interference ; thus, the system capacity begins to decline monotonically. In fact, the capacity is governed by the order of multiuser diversity defined as the ratio of the desired

---

4. These rules are usually obtained via a diversity order analysis by assuming equal per-hop ASIRs (cf. [13] and references therein).
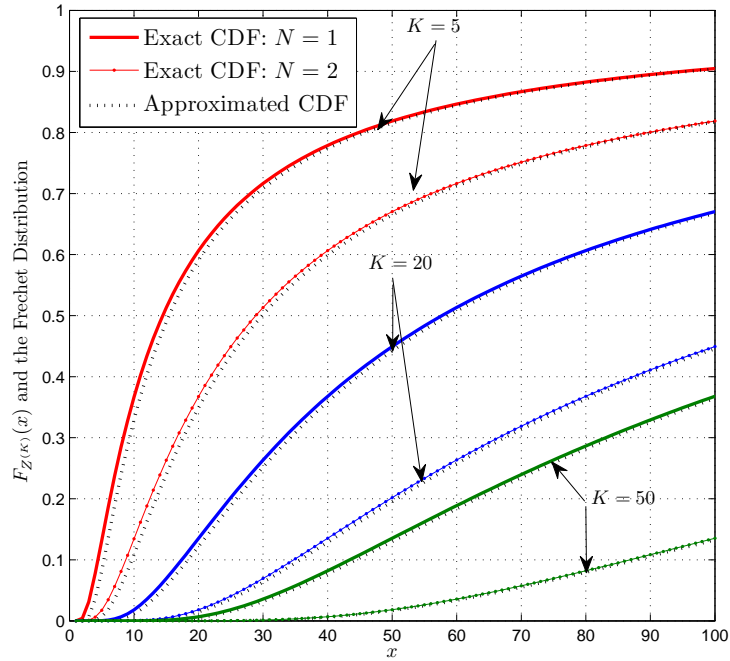
(a)
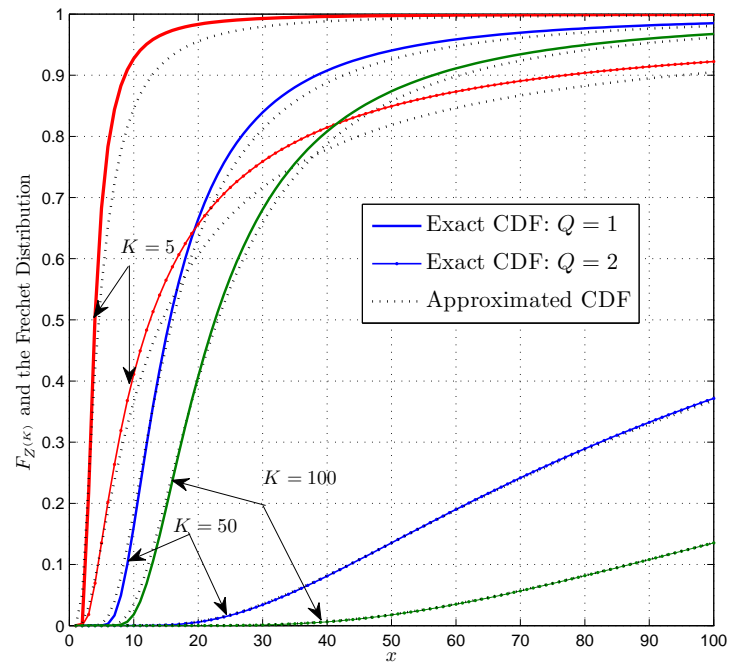
(b)

FIGURE 7.1 – The exact and asymptotic distribution of $F_{z^{(K)}}$ for different values of (a) N and (b) Q.

signal strength (i.e., the multiuser diversity gain), which we have shown in Section V to scale as $\ln(K)$ for Rayleigh fading, to the aggregate interference power which is proportional to the interference number Q.

In Figs. 3 and 4, we illustrate the capacity for large M and K but finite and small relay antenna number N. The "approximation" curves refer to the average capacity using (7.26). These curves are in very good match with their stimulated counterparts, showing the accuracy and effectiveness of the proposed new approximations. We observe form Fig. 4 that the capacity exhibits the trend, $\ln(\ln(M) + (N-1)\ln\ln(M)) + \gamma + H_{L-1}$, as predicted by Theorem 4. More importantly, the capacity loss due the increase of the number L of i.i.d interferences at the relay is consistent with the analysis. However, as the number of interference L exceeds a threshold, the capacity exhibits the trend in lemma 3.

In Figs, 5 and 6, the capacity of the two-hop opportunistic relaying scheme is shown as a function of increasing antenna number M and user number K for several numbers of interferences at the relay L and the users Q. The "approximation" curve refers to the average capacity using (7.26). These curves are in very good agreement with their stimulated counterparts. In Fig. 5 we observe that the capacity exhibits the trend predicted by Corollary 2 as long as $\ln(M^{1/L}) \gg K^{1/Q} - 1$. The latter condition is, however, not satisfied for $L = 3, Q = 4$ and $L = 4, Q = 5$ even though $Q > \left\lfloor \frac{\ln(K)}{\ln\ln(M)} \right\rfloor$ is always verified, impeding the inaccuracy of the scaling law in these cases. In Fig. 6 we observe that the capacity exhibits the trend predicted by (7.52) while we have neglected the second term of the R.H.S of (7.50) since $\frac{L(K^{\frac{1}{Q}}-1)}{\ln(M)} \longrightarrow 0$ when $L = 1$. However, neither K nor Q is sufficiently large so that the trends in (7.53) and (7.55) can be verified. But since Q implies a steady loss as K goes large, this loss is verified even for moderate value of K. The capacity loss due to the increase of Q corroborates the analytical loss obtained using (7.57). Notice that, the tightness of the scaling law is poor when Q is near $\frac{\ln(K)}{\ln\ln(M)}$ which is equal to 4 when $K = M = 700$. In fact, when Q is at the vicinity of $\frac{\ln(K)}{\ln\ln(M^{1/L})}$, the capacity scaling law is more accurately predicted using (7.26).

7.7 Conclusion

In this work, we have considered opportunistic scheduling design and analysis for two-hop MIMO AF relay networks in interference-limited environments. The scheme entails a two-hop
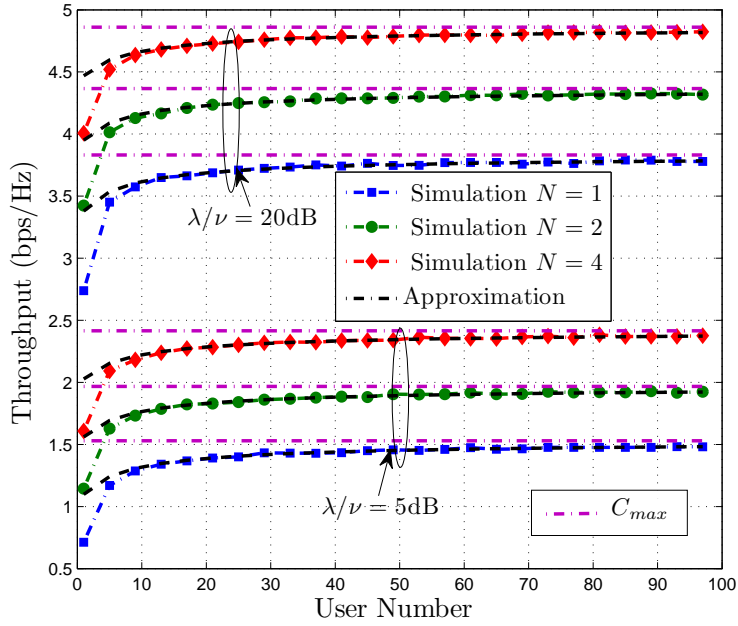
(a)
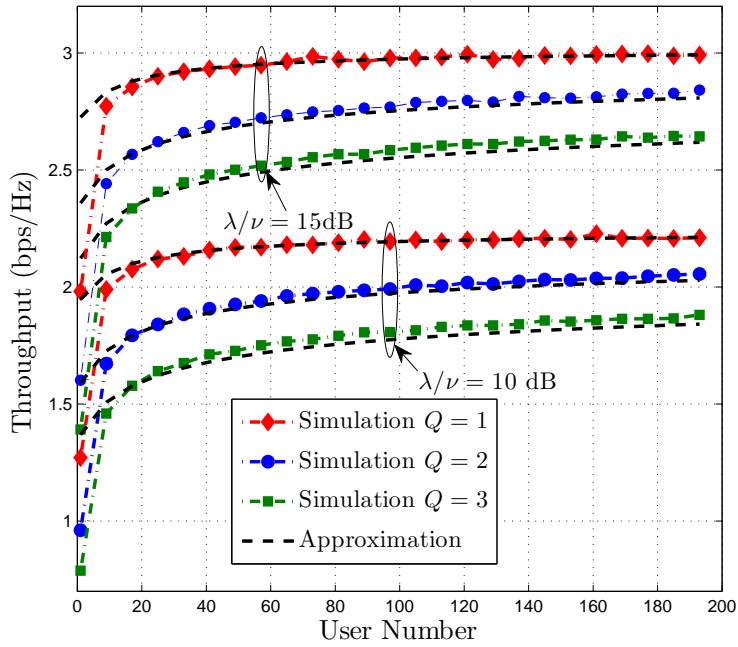
(b)

FIGURE 7.2 – System average capacity as a function of the number of users K. For different values of N :(a) and different values of Q :(b)
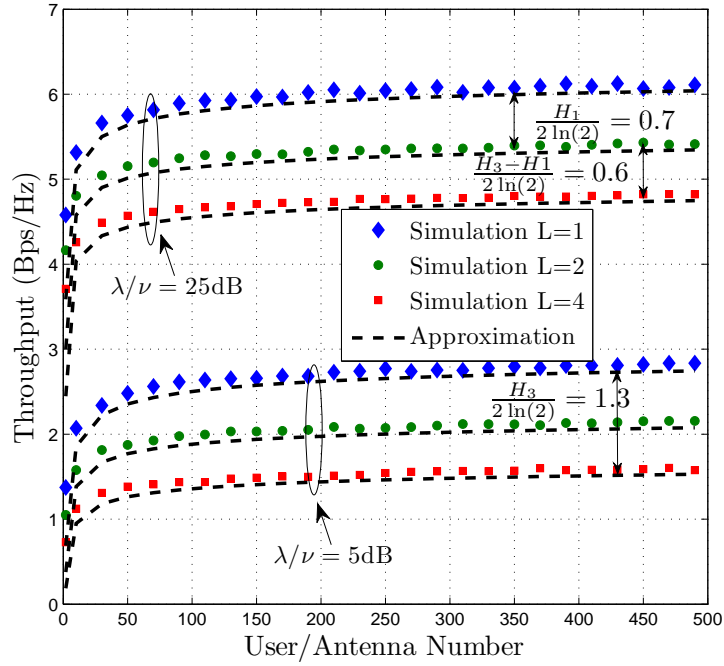
FIGURE 7.3 – System average capacity as a function of $M = K$ increasing when $Q = 1$ and $N = 2$ for different vales of L and P.
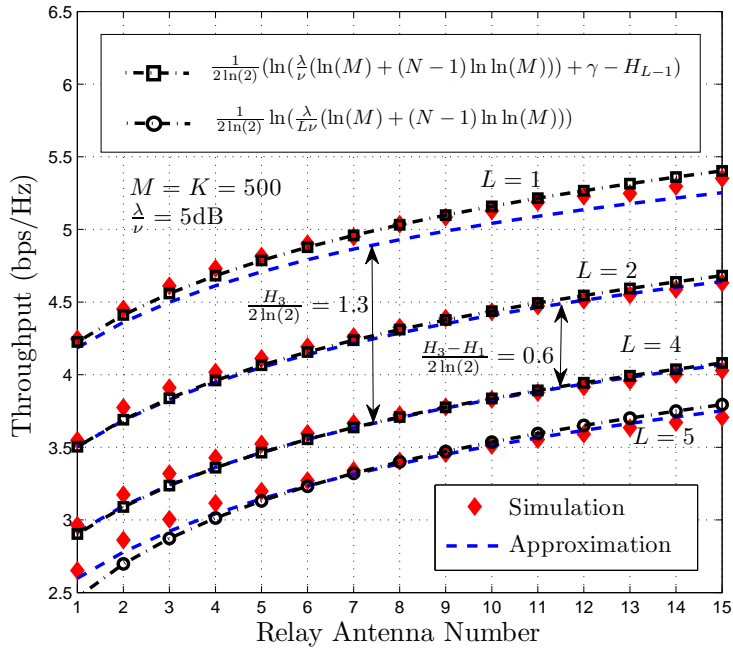

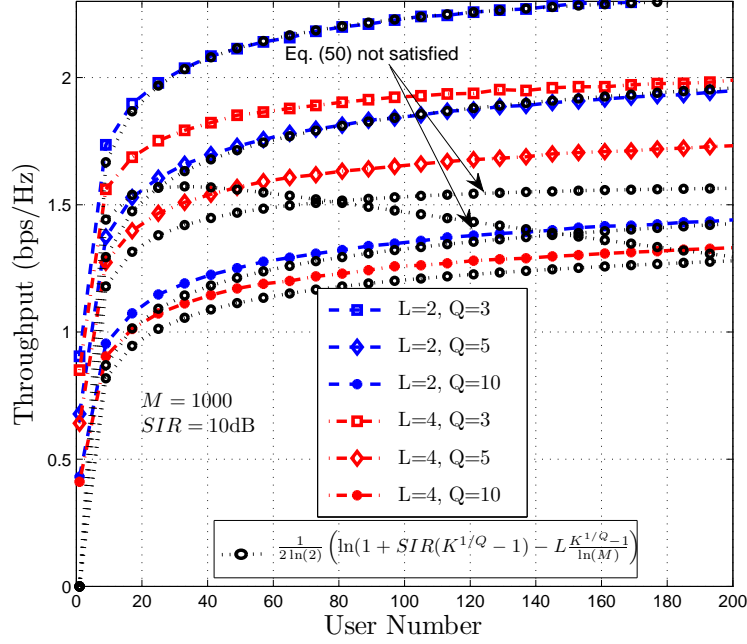FIGURE 7.4 – System average capacity versus the relay antenna number N.

FIGURE 7.5 – System average capacity as a function of $M = K$ increasing when $L = 1$ and $N = 1$ for different vales of Q.
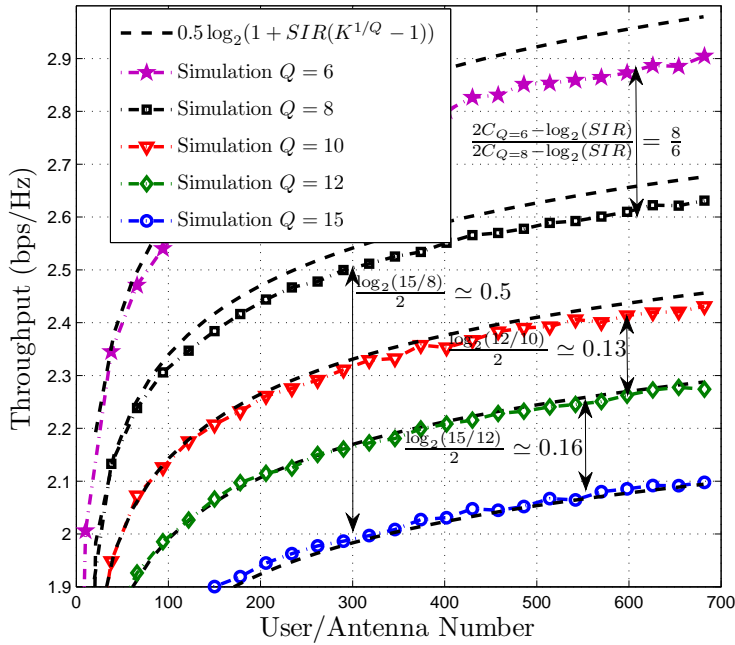

FIGURE 7.6 – System average capacity as a function of $M = K$ increasing versus L, Q.

144

communication protocol, in which an M-antenna source can communicate with K destinations only through a half-duplex multi-antenna relay. Through the asymptotic analysis for large M, K and simulations, it has been shown that interference-aware scheduling achieves an expanded multiuser diversity gain, however being conditioned. This analysis found that the multiuser diversity gain when $\ln(M^{1/L})$ grows faster than $K^{1/Q}$ is $\ln(K^{1/Q})$ whereas previous results have concluded that the maximum gain scales like $\ln\ln(K)$ when only an idealistic Rayleigh fading is considered. This result further proves the rule of thumb that having an order of magnitude more antennas at the source than the number of scheduled users improves the system's capacity. In this paper, the capacity losses due the increase of interferences numbers L and Q have been analytically quantified and verified via simulations.

Appendix A : per hop CMGF calculation

In this Appendix, the CMGF of $SIR^{H_1} = X_M/|i_{T_1}|^2$ and $SIR^{H_2} = Z_K$ are computed. To this end, in view of (7.7), we need expressions for the CCDFs $F^{(c)}_{X_M/|i_{T_1}|^2}$ and $F^{(c)}_{Z_K}$. As for X_M, its PDF is given by

$$
\begin{aligned}
f_{X_M}(x) &= \frac{M x^{N-1} e^{-\frac{x}{\rho}}}{\rho^N \Gamma(N)} \left(1 - \frac{\Gamma(N, \frac{x}{\rho})}{\Gamma(N)} \right)^{M-1} \\
&\stackrel{(a)}{=} \frac{M}{\rho^N \Gamma(N)} \sum_{n=0}^{M-1} \sum_{\Omega(n,N)} \frac{(-1)^n \binom{M-1}{n} n!}{\prod_{k=1}^{N} n_k!} \frac{\prod_{p=0}^{N-1} \left(\frac{1}{p!}\right)^{n_{p+1}} x^{N+\delta_n-1} e^{-\frac{x(n+1)}{\rho}}}{\rho^{\delta_n}},
\end{aligned}
\tag{7.60}
$$

where (a) follows form using the binomial expansion [21, Eq.(1.111.1)]. Note that in (7.60) we denote $\Omega(n, N_r) = \{(n_1, \ldots, n_N) : n_k \geq 0; \sum_{k=1}^{N} n_k = n\}$; and $\delta_n = \sum_{l=0}^{N_r-1} l n_{l+1}$. In its turn the CCDF expression of X_M is obtained after some manipulations using [21, Eq.(3.351.2)] as

$$
F^{(c)}_{X_M}(x) = \sum_{n=0}^{M-1} \sum_{\Omega(n,N)} \binom{M-1}{n} \frac{\Theta_n M \Gamma\left(N + \delta_n, \frac{x(n+1)}{\rho}\right)}{(n+1)^{N+\delta_n} \Gamma(N)}.
\tag{7.61}
$$

In addition according to [23], $|i_{T_1}|^2$ follows an hyper-exponential distribution with pdf

$$
f_{|i_{T_1}|^2}(x) = \sum_{i=1}^{\rho(\mathbf{D})} \sum_{j=1}^{\tau_i(\mathbf{D})} \zeta_{i,j}(\mathbf{D}) \frac{\mu_{<i>}^{-j} x^{j-1}}{(j-1)!} e^{-\frac{x}{\mu_{<i>}}}.
\tag{7.62}
$$

145

Therefore invoking [21, Eq. (3.381.8)] and [21, Eq. (3.381.4)], the CCDF of $\text{SIR}^{H_1} = X_M/|i_{T_1}|^2$ is obtained after some manipulations as

$$F^{(c)}_{\frac{X_M}{|i_{T_1}|^2}}(x) = \sum_{n=0}^{M-1}\sum_{\Omega(n,N)}\sum_{i=1}^{\rho(\mathbf{D})}\sum_{j=1}^{\tau_i(\mathbf{D})}\sum_{k=0}^{N+\delta_n-1}\frac{\Theta_n\zeta_{i,j}(\mathbf{D})\Gamma(k+j)}{\mu_{<i>}^j(j-1)!}\frac{M\rho^{-k}(N+\delta_n-1)!}{(n+1)^{N+\delta_n-k}\Gamma(N)k!}\frac{x^k}{\frac{x(n+1)}{\rho}+\frac{1}{\mu_{<i>}}}. \quad (7.63)$$

The next step is to calculate the CMGF of the first hop SIR. From (7.7), and using (7.63), along with some basic algebraic manipulations, it follows that

$$M^{(c)}_{\frac{X_M}{|i_{T_1}|^2}}(s) = \sum_{n=0}^{M-1}\sum_{\Omega(n,N)}\sum_{i=1}^{\rho(\mathbf{D})}\sum_{j=1}^{\tau_i(\mathbf{D})}\sum_{k=0}^{N+\delta_n-1}\frac{\Theta_n\zeta_{i,j}(\mathbf{D})\Gamma(k+j)\rho}{(j-1)!\mu_{<i>}\Gamma(N)}\frac{M(N+\delta_n-1)!}{(n+1)^{N+\delta_n+1}}\Psi\left(k+1,2-j,\,s\frac{\rho}{\mu_{<i>}(n+1)}\right). \quad (7.64)$$

Since $M^{(c)}_{\frac{X_M}{|i_{T_1}|^2}}$ is derived in (7.64), the remaining task is to figure out $M^{(c)}_{Z^K}$. In order to derive the latter, one needs the closed-form statistics of

$$\text{SIR}_j^{H_2} = \frac{\lambda|\mathbf{h}_j^R|^2}{\sum_{l=1}^{Q_j}\nu_l|u_{jl}|^2} = \frac{z}{y}, \quad j = 1,\dots,K. \quad (7.65)$$

We assume without loss of generality that u_{jl} are i.i.d over j and also over l and that all users prone equal interference number Q, meaning that $y \stackrel{d}{=} \chi(2Q)$ with pdf

$$f_y(x) = \frac{x^{Q-1}}{\nu^Q\Gamma(Q)}e^{-\frac{x}{\nu}}. \quad (7.66)$$

Since $\mathbf{h}_j^R$ is a vector with i.i.d entries, then

$$f_z(x) = \frac{x^{N-1}}{\lambda^N\Gamma(N)}e^{-\frac{x}{\lambda}}. \quad (7.67)$$

Conditioning on y, the probability distribution function (pdf) of $\text{SIR}_j^{H_2}$, $f_s(x)$, can be written as

$$\begin{aligned}
f_s(x) &= \int_0^\infty y f_z(xy)f_y(y)dy \\
&= \frac{x^{N-1}}{\frac{\lambda^N}{\nu}B(N,Q)}\left(\frac{x\nu}{\lambda}+1\right)^{-(N+Q)}. \quad (7.68)
\end{aligned}$$

We can also calculate the CDF of the per user SIR, $\text{SIR}_j^{H_2}$, as

$$\begin{aligned}
F_s(x) &= \frac{(\frac{x\nu}{\lambda})^N\,{}_2F_1\left(N+Q,N,1+N,-\frac{x\nu}{\lambda}\right)}{NB(N,Q)} \\
&\stackrel{(a)}{=}\frac{(\frac{x\nu}{\lambda})^N\left(1+\frac{x\nu}{\lambda}\right)^{1-Q-N}}{NB(N,Q)}\sum_{k=0}^{Q-1}\frac{(1-Q)_k(-1)^k}{(1+N)_k}\left(\frac{x\nu}{\lambda}\right)^k, \quad (7.69)
\end{aligned}$$

where (a) follows from substituting the gauss hypergeometric function by its finite series expansion [31]. Since $\text{SIR}_j^{H_2}$ for $j = 1, \ldots, K$ are i.i.d. random variables, the CDF of the second hop SIR $Z_K = \max \text{SIR}_j^{H_2}$ is $[F_s(x))^K$. Accordingly, using (7.69), we get

$$F_{Z_K}^{(c)}(x) = 1 - \left(\left(\frac{\frac{x\nu}{\lambda}}{1 + \frac{x\nu}{\lambda}} \right)^{Q+N-1} + \frac{\left(\frac{x\nu}{\lambda}\right)^N}{NB(N,Q)} \left(1 + \frac{x\nu}{\lambda} \right)^{1-Q-N} \sum_{k=0}^{Q-2} \frac{(1-Q)_k(-1)^k}{(1+N)_k} \left(\frac{x\nu}{\lambda}\right)^k \right)^K . \quad (7.70)$$

By repeatedly resorting to the multinomial expansion [21, Eq.(1.111.1)], it follows after some manipulations that

$$F_{Z_K}^{(c)}(x) = \sum_{i=0}^{K(Q+N-1)-1} \binom{K(Q+N-1)}{i} \left(\frac{x\nu}{\lambda}\right)^i \left(1+\frac{x\nu}{\lambda}\right)^{-K(Q+N-1)} - \sum_{n=1}^{K} \sum_{\Omega(n,Q-1)} \frac{\binom{K}{n} n! \prod_{p=0}^{Q-2} \left(\frac{(1-Q)_p(-1)^p}{(1+N)_p}\right)^{n_{p+1}}}{(NB(N,Q))^n \prod_{k=1}^{Q-1} n_k!}$$
$$\left(\frac{x\nu}{\lambda}\right)^{\delta_n + K(Q+N-1)+n(1-Q)} \left(1 + \frac{x\nu}{\lambda}\right)^{-K(Q+N-1)} . \quad (7.71)$$

In the same line of (7.64), substituting (7.71) into (7.7) and resorting to [21, Eq. (9.211.1)] yield the CMGF of Z_K as

$$M_{Z_K}^{(c)}(s) = \sum_{i=0}^{K(Q+N-1)-1} \binom{K(Q+N-1)}{i} \frac{\lambda}{\nu} \Gamma(i+1) \Psi\left(i+1, i+2-K(Q+N-1), \frac{\lambda s}{\nu}\right) - \sum_{j=1}^{K} \sum_{\Omega(j,Q-1)} \binom{K}{j} \frac{\lambda \alpha_j}{\nu}$$
$$\Gamma\left(\delta_j + K(Q+N-1)+j(1-Q)+1\right) \Psi\left(\delta_j + 2 - j(Q-1), \delta_j + K(Q+N-1)+j(1-Q)+1, \frac{\lambda s}{\nu}\right), \quad (7.72)$$

where

$$\alpha_j = \prod_{p=0}^{L-2} \left(\frac{(1-L)_p(-1)^p}{(1+N_r)_p}\right)^{n_{p+1}} \frac{j! B(N,Q)^{-j}}{N^j \prod_{k=1}^{Q-1} n_k!}. \quad (7.73)$$

Appendix B : on extreme value theory

Here we prove a property of the maximum among n i.i.d. RVs $\{x_1, x_2, \ldots, x_n\}$ [19]- [20]. We assume x_i's be positive random variables with continuous and strictly positive distribution function $f_X(x)$ and CDF of $F_X(x)$.

Corollary A : Gnedenko's Sufficient and Necessary Conditions for the Domain of Attraction of Gumbel Distribution : For the parent distribution function $F_X(x)$, let its lower endpoint $\varepsilon(F) = \inf\{x : F_X(x) > 0\}$ be finite. Further define an auxiliary function $H(x) = 1 - F_X(x - \varepsilon(F)), x > 0$. Let restate [20, Eq.(26)] as follows : If $H(x)$ is such $\lim_{x \to \infty} \frac{H(x)}{H(dx)} = x^\beta > 0$, then

$$\lim_{n \to \infty} F^n(c_n + x d_n) = e^{-x^{-\beta}}, \quad x > 0, \quad (7.74)$$

where $c_n = \varepsilon(F)$ and $d_n = \inf\{x : 1 - F_X(x) = 1/n\} - \varepsilon(F)$.

Corollary B : Gnedenko's Sufficient and Necessary Conditions for the Domain of Attraction of Frechet Distribution : Let's define the growth function as $g_X(x) = (1 - F_x(x))/f_X(x)$. We also define a_n to to be the unique solution to $1 - F_X(a_n) = 1/n$. Let restate [19, Eq.(18)] as follows :
If g_X is such $\lim_{x \to \infty} g_X(x) = c > 0$ and $g_X^{(m)} = O(1/a_n^m)$ with $a_n = O(\ln(n))$, then

$$\ln\{-\ln(F^n(a_n + cx))\} = -x + O\left(\frac{e^{-x}}{n}\right). \tag{7.75}$$

Appendix C : derivation of $\phi_0(a, b)$

Recalling that

$$\Phi_0(a, b) = \int_0^\infty e^{-s}\left(1 - e^{-as}\right)\frac{K_1\left(2b\sqrt{s}\right)}{\sqrt{s}}ds. \tag{7.76}$$

Using the fact that [21, Eq. 8.486.15]

$$\frac{d(x^{-\mu}K_\mu(x))}{dx} = -x^\mu K_{\mu+1}(x), \tag{7.77}$$

and integrating by part we obtain

$$\Phi_0(a, b) = 2\int_0^\infty e^{-s}\left(1 + ae^{-as}\right)K_0\left(2b\sqrt{s}\right)ds. \tag{7.78}$$

Finally using [21, Eq. 6.643.6] concludes the proof.

Bibliographie

[1] C.J. Chen and L.C. Wang, "Enhancing coverage and capacity for multiuser MIMO systems by utilizing scheduling," *IEEE Trans. Wireless Commun.* vol. 5, no. 5, pp. 1148-1157, May 2006.

[2] P. Viswanath, D. N. C. Tse, and R. Laroia, "Opportunistic beamforming using dumb antennas," *IEEE Trans. Inform. Theory, vol.* 48, no. 6, pp. 1277-1294, June 2002.

[3] H. Dai, A. Molisch, and H. Poor, "Downlink capacity of interference-limited MIMO systems with joint detection," *IEEE Trans. Wireless Commun.,* vol. 3, no. 2, pp. 442-453, Mar. 2004.

[4] S. Catreux, P. F. Driessen, and L. J. Greenstein, "Attainable capacity of an interference-limited multiple-input multiple-output (MIMO) cellular system," *IEEE Trans. on Communications,* vol. 49, no. 8, pp. 1307-1311, Aug. 2001.

[5] X. Zhang, W. Wang, and X. Ji, "Multiuser diversity in multiuser two- hop cooperative relay wireless networks (TCRN) : system model and performance analysis," textitIEEE Trans. Veh. Technol., vol. 58, pp. 1031-1036, Feb. 2009

[6] H.J. Joung and C. Mun, "Capacity of multiuser diversity with cooperative relaying in wireless networks," *IEEE Commun. Lett.,* vol. 12, pp. 752-754, Oct. 2008.

[7] J.B. Kim and D. Kim, "Comparison of two SNR-based feedback schemes in multiuser dual-hop amplify-and-forward relaying networks," *IEEE Commun. Lett .,* vol. 12, pp. 557-559, Aug. 2008.

[8] W. Xu, X. Dong, W.S. Lu, "Joint precoding optimization for multiuser multi-antenna relaying downlinks using quadratic programming," *IEEE Trans Commun,* vol. 59, no. 5, pp. 12281235, oct. 2011.

[9] L. Yang and W. Liu, "On the capacity of MIMO relay wireless network with receive antenna selection," *IEEE Commun. Lett.,* vol. 15, no. 6, pp. 626-638, June 2011.

[10] G. Zhu, C. Zhong, H. A. Suraweera, Z. Zhang and C. Yuen, "Ergodic capacity comparison of different relay precoding schemes in dual-hop AF systems with co-channel interference," *IEEE Trans. Commun.* , vol. 62, no. 7, pp. 2314-2328, July 2014.

[11] I. Trigui, S. Affes, and A. Stéphenne, "Ergodic capacity of two-hop multiple antenna AF systems with co-channel interference", *IEEE Wireless Commun. Let.*, vol. 4, no. 1, Feb. 2015.

[12] I. Trigui, S. Affes, and A. Stéphenne, "Ergodic capacity analysis for interference-limited AF multi-hop relaying channels in Nakagami-m fading," *IEEE Trans. Commun.,* vol. 61, no. 7, pp. 2726-2734, July 2013.

[13] I. Trigui, S. Affes, and A. Stéphenne, "On the ergodic capacity of amplify-and-forward relay channels with interference in Nakagami-m fading," *IEEE Trans. Commun.*, vol. 61, no. 8, pp. 3136-3145, Aug. 2013.

[14] Huang, F. Al-Qahtani, C. Zhong, Q. Wu, J. Wang, and H. Alnuweiri, "Performance analysis of multiuser multiple antenna relaying networks with co-channel interference and feedback delay," *IEEE Trans. Commun.* , vol. 62, no. 1, pp. 59-73, Jan. 2014

[15] R. W. Heath, S. Sandhu, and A. Paulraj, "Antenna selection for spatial multiplexing systems with linear receivers," *IEEE Commun. Let.*, vol. 5, no. 4, pp. 142-44, Apr. 2001.

[16] H. Weingarten, Y. Steinberg, and S. Shamai, "The capacity region of the Gaussian multiple-input multiple-output broadcast channel," *IEEE Trans. Inf. Theory,* vol. 52, no. 9, pp. 3936-3964, Sep. 2006.

[17] M. Sharif and B. Hassibi, "On the capacity of MIMO broadcast channels with partial side information," *IEEE Trans. Inf. Theory,* vol. 51, no. 2, pp. 506-522, Feb. 2005

[18] R. Blum, "MIMO capacity with interference," *IEEE Journal on Sel. Areas in Communications,* vol. 21, no. 5, pp. 793-801, June 2003.

[19] M. R. Leadbetter and H. Rootzen, "Extremal theory for stochastic processes," *Ann. Probab.,* vol. 16, pp. 431-478, 1988.

[20] Gumbel, "Statistics of Extremes", New York : Columbia University Press, 1968.

[21] I. S. Gradshteyn and I. M. Ryzhik, *Table of Integrals, Series and Products,* 5th Ed., San Diego, CA : Academic, 1994.

[22] R. U. Verma, "On some integrals involving Meijer's G-fucntion of two variables", *Proc. Nat. Inst. Sci. India*, vol. 39, Jan. 1966.

[23] H. Shin and M. Z. Win, "MIMO diversity in the presence of double scattering," *IEEE Trans. Inform. Theory,* vol. 54, no. 7, pp. 2976-2996, July 2008.

[24] I. S. Ansari, S. Al-Ahmadi, F. Yilmaz, M.-S. Alouini, and H. Yanikomeroglu, "A new formula for the BER of binary modulations with dual-branch selection over gereralized-m composite fading channels," *IEEE Trans. Commun.,* vol. 59, no. 10, pp. 2654-2658, Oct. 2011

Conclusions

L'analyse de performances des systèmes de communication sans fil est une tâche très ardue. Elle nécessite souvent l'utilisation de modèles ultra simplifiés au point de sacrifier de sa précision et fiabilité, ou des simulations niveau système extrêmement complexes et exigeantes en temps et argent. Le déploiement de nouvelles technologies émergentes telles que les relais, mobiles soient-ils ou fixes, et les systèmes MIMO rendent, malheureusement, cette tâches encore plus compliquée. Les relais permettent, en fait, aux opérateurs d'étendre considérablement la couverture de leurs réseaux, tandis que les systèmes MIMO améliorent à la fois leurs débit et fiabilité sans toutefois nécessiter des resources (ex :puissance, spectre, etc.) supplémentaires. Cependant, les systèmes de communication sans fil ne pourront jamais profiter pleinement de ces avantages sans une utilisation optimale ou du moins efficace du spectre disponible. La RC est apparue alors comme une solution assurant la bonne gestion de ce spectre. Cette technologie futuriste permet aux usagers secondaires non-autorisés de partager la même bande de fréquences exploitée par les usagers primaires sans pour autant diminuer la qualité de service perçue par ces derniers. Une compréhension des propriétés et du comportement de ces nouvelles techniques de communication est cependant indispensable pour assurer une conception optimale des futures systèmes de communication sans fil.

Cette thèse fournit, à ce titre, une analyse rigoureuse et une étude approfondie des performances des systèmes de communication combinant ces nouvelles technologies et opérant dans des conditions réelles. Afin de résoudre des problèmes de calcul, jusqu'ici insoluble, on a eu recours à de nouvelles transformations novatrices d'intégrales se basant sur la séparation du produit des interférences de chaque saut. Des expressions exactes et précises des paramètres caractérisant les performances à long-termes des systèmes de communications, tel que la capacité érgodique et le taux d'erreur, ont été calculées. Les formules obtenues ont considérablement simplifié l'évaluation des performances des futurs systèmes de communication et la compréhension de leurs compor-

tements et propriétés ; en fournissant soit des expressions analytiques ou des approximations prouvées extrêmement fiables lorsque le nombre d'antennes est très grand. En plus, la nature simple et élégante de ces expressions a permis l'optimisation des performances de ces systèmes par le biais de renseignements importants comme la position optimale de la station de base ou du relai. En outre, Il s'était avéré que les résultats obtenus sont utiles pour de divers scénarios.

Un des systèmes étudiés dans cette thèse est le système à sauts multiples dont le taux d'erreur a été calculé analytiquement, au Chapitre 3, en présence d'un évanouissement Nakagami-m. Une nouvelle expression d'une forme d'intégrale infinie impliquant le produit de fonctions de Bessel a, en fait, rendu possible, pour la première fois, le calcul du taux d'erreur de ce genre de système. Les formules obtenues ont permis d'établir une connexion, jusqu'ici inconnue, entre la probabilité d'erreur relative à différentes modulations et la fonction Lauricella. Ces résultats ne sont autres que la généralisation des travaux pionniers de M.O Hasna sur les systèmes à sauts multiples subissant des évanouissements non-identiques, d'un saut à un autre, avec des paramètres entiers. Au Chapitre 4, les performances d'un système à sauts multiples sont examinées en présence d'interférences co-canal. L'expression de la capacité érgodique, jusque-là insoluble pour un nombre arbitraire d'interférences et de sauts, a été calculée analytiquement avec succès et plusieurs résultats extrêmement intéressants s'en étaient découlés.

Au Chapitre 5, le bruit a été aussi introduit dans l'analyse des performances du système à sauts multiples. La capacité érgodique de ce système a été calculée analytiquement pour la première fois. Pour ce calcul, on a d'abord considéré un évanouissement Nakagami-m puis généralisé le résultat en prenant aussi en compte la présence du phénomène d'ombrage.

Au Chapitre 6, un système de communication MIMO à double sauts a été considéré dans un contexte RC. Contrairement aux anciens travaux qui ont calulé des simples bornes de la capacité érgodique et du taux d'erreur ou imposé des contraintes sévères sur les paramétres du système afin d'obtenir les expressions de ces mesures, ce travail présente pour la première fois leurs expressions exactes pour des configurations arbitraires du systèmes. À partir de ces formules, on a démontré que les réseaux des utilisateurs primaires réduit le taux d'erreur sans affecter l'ordre de diversité du système.

Chapitre 7 a examiné l'impacte des interférences co-canal sur la capacité des systèmes MIMO à double sauts subissant un évanouissement de Rayleigh. L'expression exacte de la capacité de ce système a été calculée en exploitant la fonction génératrice de moments complémentaire du

RSBI du premier saut. La formule obtenue et les résultats qui s'en étaient découlés sont valides pour n'importe quel nombre d'antennes aux relai, source et destination.

Dans les futurs système de communication , tel que LTE-A et 5G, qui utilisent l'accès multi-utilisateurs et le multiplexage OFDM, l'optimisation et l'ordonnancement sont effectués pour améliorer leurs fiabilité tout en assurant un accès équitable aux usagers. Ceci est, en fait, extrêmement important dans un marché en constante expansion qui vise à satisfaire aux maximum ces clients quit à sacrifier un peu de la performance du système. Dans ce contexte, la conception et l'analyse des performances de systèmes MIMO multi-utilisateurs avec relayage employant un ordonnancement opportuniste et opérant en présence non seulement d'évanouissement de Rayleigh, mais aussi des interférences co-canal ont été effectuées au Chapitre 8. L'analyse de ce système à large échelle a permis l'obtention de formules analytiques élégantes et très perspicaces de la capacité érgodique asymptotique. Grâce à ces formules, on a pu démontré que la capacité des systèmes multi-antennes et multi-utilisateurs à double sauts est la moitié de celle du premier saut d'un système MIMO. En plus, il a été prouvé que la perte de capacité à cause de l'accroissement de la dimentionalité des interférences est beaucoup plus prononcée que n'importe quel amélioration grâce à l'augmentation du nombre d'antennes à la source. Finalement, la perte de capacité dû à la croissance du niveau des interférences aux premier et deuxième sauts a été explicitement calculée. Cette dernière information est, en fait, précieuse pour toute conception judicieuse des futurs systèmes de communication mettant en oeuvre ces nouvelles technologies.